# A reconstruction of the mid-to late Pleistocene plant community along the southwestern coast of South Africa using phytolith evidence.

NICOLE JEAN MANN
Supervisor: Dr. Deano Stynder
Department of Archaeology
University of Cape Town



A thesis submitted in fulfillment of the requirements for the degree of Master of Science in Archaeology.

**Department of Archaeology**
**Faculty of Science**
**University of Cape Town**
**26 July 2017**

# Table of Contents

## PLAGIARISM DECLARATION

I declare that the thesis, the results and conclusions, submitted by me at the University of Cape Town, is my own work. Where the work of others has been mentioned, it has been referenced. I have not submitted this thesis at another university or faculty.

Signed,

Nicole Jean Mann
MNNNIC006

**Date:** 26 July 2017

## ACKNOWLEDGEMENTS

- I would like to thank my supervisor, Dr Deano Stynder, for his guidance and supervision.

- I acknowledge financial support from the National Research Foundation (NRF):
  NRF African Origins Platform Grant
  Project title: Archaeological investigations at the Acheulean open-air locality of Duynefontein.
  Grant number: 98821
  This work is based on the research supported by the National Research Foundation. **Any opinion, finding and conclusion or recommendation expressed in this material is that of the author(s) and the NRF does not accept any liability in this regard.**

- I thank Doctor Lloyd Rossouw (Bloemfontein Museum) for his assistance in the project.
- My appreciation to Myra Gohodzi (Bloemfontein Museum) for assisting me with creating my modern plant reference collection.
- I would like to thank Associate Professor Shadreck Chirikure for allowing me access to the microscope and camera equipment housed in the Archaeological Materials Laboratory in the Archaeology Department (UCT).
- I thank my family and friends, whose encouragement and support has been my motivation to finish this thesis.
- Lastly, I would like to thank the examiners fro their valuable reviews.

## ABBREVIATIONS

| | |
|---|---|
| DFT | Duinefontein |
| EFT | Elandsfontein |
| GSSCs | Grass Silica Short Cells |
| HCl | Hydrochloric acid |
| Kya | Thousand years ago |
| LSA | Later Stone Age |
| Ma | Million years ago |
| MSA | Middle Stone Age |
| SPT | Sodium polytungstate |
| STP | Shovel Test Pit |
| WRZ | Winter Rainfall Zone |

# ABSTRACT

The sites of Elandsfontein (EFT) and Duinefontein (DFT) preserve important records of mid-Pleistocene human occupation along South Africa's southwestern coast. In addition to human fossils in the case of EFT, both sites have produced extensive collections of artefacts and faunal remains. Analyses of the latter have provided the broad environmental contexts for mid-Pleistocene human occupation along this coast. Recently, research into landscape use by mid-Pleistocene human populations at EFT and DFT has highlighted the need for more precise palaeoenvironmental data for the region. In response to this need, I analysed plant phytoliths extracted from sediments sampled at EFT and DFT. The results of this analysis are reported and interpreted in this thesis.

To assist with the interpretation of the EFT and DFT phytolith assemblages, I established a modern phytolith reference collection. In addition, pre-existing phytolith collections were examined and literature was consulted. Phytoliths extracted from modern and mid-Pleistocene aged sediments sampled at different localities at EFT and DFT were identified and tallied to determine vegetation composition during the middle Pleistocene. Distinctions were made between "grassier" and "more woody" samples.

Analyses of modern plant samples confirmed that grass species produced abundant phytoliths, whereas the majority of dicotyledons did not produce diagnostic morphotypes. Phytoliths belonging to grass species currently growing in the region were identified in the modern sediment samples, as were non-grass phytoliths that included those from woody dicotyledonous and monocotyledon plants. The majority of the mid-Pleistocene sediment samples from EFT produced varying proportions of grass, woody dicotyledon, monocotyledon, sedge and palm type phytoliths which are characteristic of cool-season growing landscapes. In comparison to EFT, the late mid-Pleistocene sediment samples from DFT contained fewer phytoliths. These results suggest that the conditions at DFT were either not conducive to the preservation of phytoliths or that the vegetation was sparse

and/or did not produce abundant phytoliths. Where sufficient phytoliths were preserved, assemblages suggested landscapes similar to that of EFT. In summary, analyses suggest that during the middle to late Pleistocene, a heterogeneous vegetation community, consisting primarily of $C_3$ grasses, woody dicotyledons and other monocotyledonous plants existed along South Africa's southwest coast. Furthermore, results support the long-term presence of the winter rainfall zone in the region.

This study demonstrates the potential of phytolith analysis as an important proxy in determining the composition of palaeo-vegetation communities in South Africa. Although there were limitations that necessitated the broad classification of phytolith groups, the study nevertheless provided more precise information, particularly about mid-Pleistocene vegetation structure, that was not previously available.

## List of Figures

# List of Tables

## CHAPTER 4

# Chapter 1 : INTRODUCTION

Our species *Homo sapiens* evolved in Africa during the mid-to late Pleistocene, a period of exaggerated climatic fluctuations (Adams & Faure 1997; Potts 1998; Maslin & Christensen 2007; Compton 2011). During this time of climatic upheaval, habitats suitable for hominin occupation diminished, likely leading to the concentration of populations in refugia (Basell 2008; Hetherington *et al.* 2008; Compton 2011). In these refugia, it appears, hominins survived for extended periods, favouring adaptation to new environmental realities rather than relocating when climatic shifts altered habitat structures (Potts 1998). It has been hypothesised that exposure to variable climatic and environmental conditions across space and time, encouraged the development of a high level of adaptability amongst mid-to late Pleistocene hominins. Today, behavioural adaptability is a characteristic feature of *Homo sapiens*. While intriguing, it is difficult to test the hypothesised link between mid-to late Pleistocene hominin adaptability and environmental variability because of (1) the scarcity of Pleistocene-aged archaeological sites, and (2) limited palaeoenvironmental records for the African continent.

Currently our understanding of mid-to late Pleistocene hominin behavioural adaptability is largely based on East African evidence, as this region contains the majority of relevant sites and also has the best palaeoenvironmental records (Partridge *et al.* 1995). Like today, $C_4$ grasslands dominated the mid-to late Pleistocene East African environment. Hominin populations that occupied East Africa at the time would likely have employed adaptive behaviours specifically suited to grasslands. Little is known about the behaviours of human populations that existed in other environments. The way in which hominids adapted to changing environments locally and globally throughout hominid evolution was highly variable. Studying sites outside the East African $C_4$ grasslands will answer a range of questions relating to possible behavioural variation in mid-to late Pleistocene hominins.

Elandsfontein (EFT) and Duinefontein (DFT) represent two extensive mid-to late Pleistocene sites that are not located in East Africa. Previous research has highlighted the potential of these two South African sites as alternative sources of high-resolution archaeological and palaeoenvironmental data for the time period in question. Unfortunately methodological shortcomings in earlier palaeoenvironmental studies and limited recent research have negatively impacted on their usefulness as comparisons with East African sites. As a contribution towards building a more accurate picture of the EFT and DFT mid-to late Pleistocene environments, I analysed the opal phytolith assemblages derived from a series of soil samples collected during excavations at these sites. The results of my analysis are reported and interpreted herein.

Archaeological evidence suggests that the southwestern coast of South Africa, along which EFT and DFT are located, may have been a refugium during the mid-to late Pleistocene (Grine & Klein 1993; Berger & Parkington 1995; Cruz-Uribe *et al.* 2003; Halkett *et al.* 2003; Klein *et al.* 2007; Braun *et al.* 2013). Using taxonomic analogy to reconstruct the diets of fossil ungulates, Klein and colleagues painted a picture of a region dominated by grass (primarily $C_3$) (Klein 1983b; Grine & Klein 1993; Halkett *et al.* 2003). However in recent times, evidence derived from isotope (Luyt *et al.* 2000; Franz-Odendaal *et al.* 2002) and dental mesowear studies (Stynder 2009) have suggested a vegetation community with a much more complex structure. Still, fine-scale palaeoenvironmental data is lacking. By analysing plant phytoliths, this project will generate the fine-scale environmental information required to investigate hominin adaptive versatility in this region. Ultimately, the results from the plant phytolith analysis will provide the first direct evidence of plant families making up the vegetation communities that existed on the southwestern Cape coast during the middle Pleistocene. In contrast to indirect proxies that may provide a broad picture of the environment, phytolith analyses may aid in the identification of plants to the family level. The phytolith analysis should enable a more accurate palaeoenvironmental reconstruction that answers questions relating to plant diversity and the levels of plant productivity.

**Thesis structure**

This thesis consists of six chapters. In chapter two, a brief introduction locates the study within a broad African context before providing the background to EFT and DFT. This includes site locations, past research, geological settings, archaeological ages, as well as present day regional vegetation, climate and fauna. Previous palaeoenvironmental research conducted at EFT and DFT is also discussed briefly and the main reconstructions as proposed by various researchers, highlighted. Chapter three provides a background to phytolith analyses, including its applications and limitations. Chapter four explains the materials and methods used to sample sites and extract phytoliths from extant plants and archaeological/palaeontological sediments. The phytolith morphotypes used in the classification of samples is also described. The tentative association between phytolith morphotypes and grass subfamilies is discussed. Finally, the ways in which the data was analysed and illustrated is discussed. Chapter five provides the discussion and illustration of the modern reference collection as well as the results of the analysis of the sediment samples collected from EFT and DFT. The research results are discussed and compared to previous palaeoenvironmental research in chapter six. Key interpretations are highlighted and final conclusions made.

# Chapter 2 : BACKGROUND

## 2.1 Introduction

There are numerous Pleistocene-aged archaeological sites distributed across Africa that contain significant hominin fossil remains (Fig. 2.1).

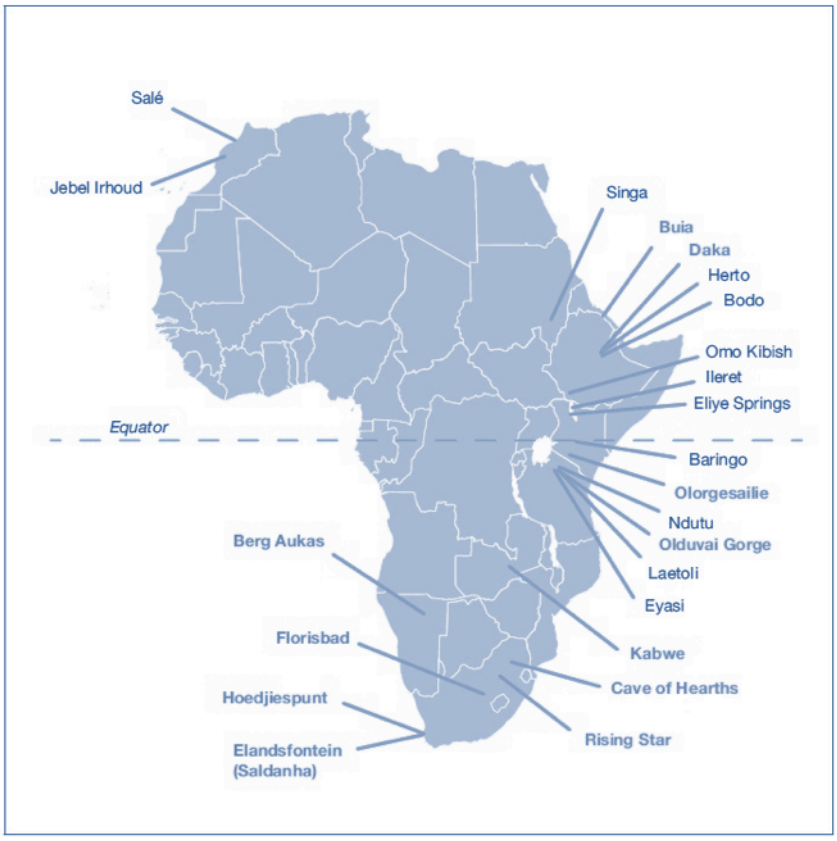


**Fig. 2.1.** *Pleistocene archaeological sites in Africa (modified after: Berger et al. (2017: 4))*

Archaeological sites containing evidence of middle Pleistocene habitation are most abundant in East Africa, a summer rainfall region dominated by $C_4$ grasslands. Due to this skewed distribution, reconstructions of palaeoenvironments occupied by middle Pleistocene hominins and the issue of Acheulean/ early Middle Stone Age (MSA) human adaptability suffer from an East African bias (Partridge *et al.* 1995). Middle Pleistocene hominins were not restricted to East Africa though, as indicated by their archaeological presence in other regions. In the following chapter, I describe the locations of the study sites, as well as climatic, geological and archaeological settings.

## 2.2 Location of Elandsfontein and Duinefontein

Elandsfontein (EFT) is located within the Elandsfontein Private Nature Reserve, situated 95km northwest of Cape Town and 18km inland from the Atlantic Ocean (Fig.2.2). Surveys of the area have identified fossiliferous and artifact-rich Pleistocene sediments covering between six and fifteen km$^2$ (Mabbutt 1956; Besaans 1972). During the 1950s and 1960s, mammalian fossils were unsystematically collected from surfaces exposed by aeolian activity (Klein *et al*. 2007). The site is best known for the discovery of the archaic hominin skullcap, informally known as the Saldanha skull, and a fragment of mandibular ramus (Singer 1954; Rightmire 2001). In addition, vast quantities of late Acheulean artifacts were discovered amongst thousands of middle Pleistocene faunal remains (Klein *et al*. 2007; Braun *et al.* 2013). The accumulation of artifacts and fossils are associated with a calcareous duricrust, which has been labeled Elandsfontein Main (EFTM) (Klein & Cruz-Uribe 1991; Klein *et al.* 2007). The archaeological deposits comprise an extensive record of hominin ecological and behavioral evolution dating to between 1Ma and 600kya (Braun *et al.* 2013).

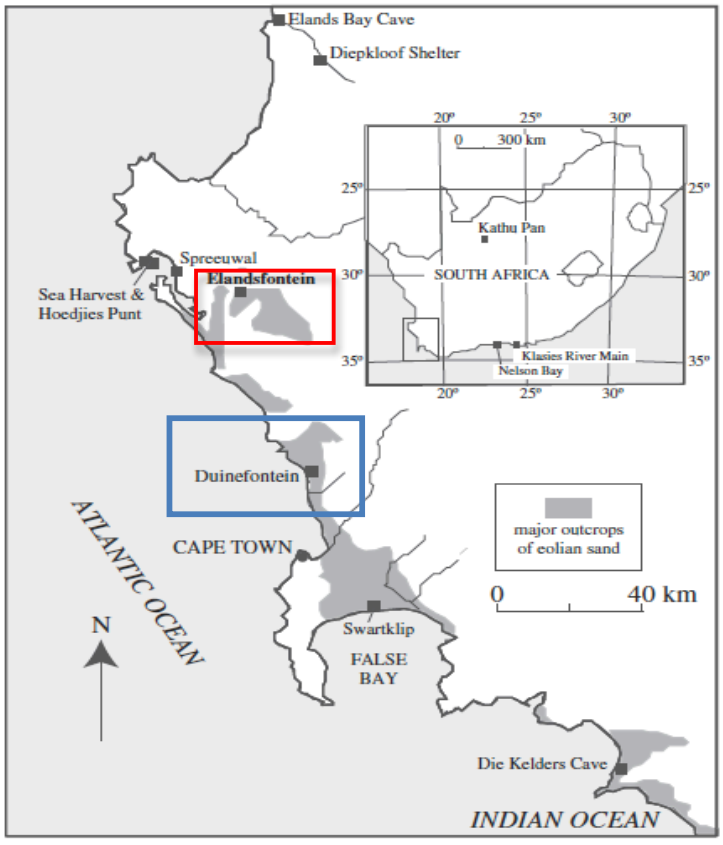


**Fig. 2.2.** *The location of Elandsfontein and Duinefontein (Klein et al. 2007: 165)*

Duinefontein 2 (DFT) is an Acheulean-age site located within the Koeberg Nature Reserve, 35km north of Cape Town and approximately 300m from the Atlantic Coast (Fig.2.2). Today it is adjacent to the Koeberg Nuclear Power station. This fossiliferous multilayer site occurs within a 10m thick dune plume. Since 1956, approximately 2.5km$^2$ of the deflated surface has provided an abundance of wind-and-sand-scoured artifacts and fossilised faunal remains (Hendey 1968). The site contains late Acheulean artifacts and a substantial assemblage of fossil mammalian bones, discovered in ferruginized dune sands (Feathers, 2002).

## 2.3 Previous Research

### 2.3.1 Elandsfontein

People have been finding artefacts and fossils within deflation bays formed by strong southwesterly winds since the early 20$^{th}$ century (Braun *et al.* 2013). Initially artefacts were collected by the general public, while farmers "harvested" fossil bones for the production of fertilizer (Braun *et al.* 2013). The scientific documentation and collection of fossils and artifacts commenced in the 1950s, but was non-systematic. However, following the recovery of the skullcap and mandibular ramus fragment of the archaic human in 1953, local and international researchers began to show a greater interest in the locality (Drennen 1953; Singer & Wymer 1968). It was suggested that the human skullcap bore a resemblance to a more complete skull of *Homo heidelbergensis* that had been discovered at Broken Hill in Zambia in 1921. In the early 1960s, R. Singer, H. J. Deacon and J. Deacon conducted the first systematic excavations at EFT, but found that dune movement hampered the production of reliable maps that could highlight the locations of their excavations within the region. Their work was never fully published (Braun *et al*. 2013). In 1966, Singer and Wymer conducted further excavations at EFT during which a possible butchery site ('Cutting 10') was discovered (Singer & Wymer 1968). The site contained a small but dense accumulation of 456 mammalian fossils and 208 artifacts (Klein 1978; Deacon 1998; Klein *et al*. 2007). Approximately 47 large cutting tools (Acheulean Industry) were uncovered close to fossil faunal remains (Braun *et al.* 2013). These stone tools preserve features that suggest production using the Levallois technique

(Klein 2009). Tools that have intentionally denticulated edges may have been used in the processing of meat (Klein 2009). Research during the 1980s focused on the collection of fossils that were considered to be out of context due to the deflation of the dunefields. This collection, referred to as Elandsfontein Main (EFTM), consists of over 20,000 identifiable fossil specimens (Klein 1988; Klein *et al.* 2007) and is dominated by a diversity of large browsing and grazing ungulates. From 2008 onwards, researchers have conducted numerous systematic excavations with the subsequent creation of large, well-provenanced artefact and fossil fauna collections. Following on from this, attempts have been made to ascertain if a behavioural relationship between assemblages of artefacts and Quaternary faunal remains could be established (contextual link) (Braun *et al.* 2013). In addition, relationships between current surface collections and *in situ* remains were investigated (Braun *et al.* 2013). Efforts have also been made to create an overall image of how hominins may have lived and interacted with the landscape during the middle Pleistocene (Braun *et al.* 2013).

### 2.3.2 Duinefontein

A substantial amount of research has been conducted at DFT, although the greater emphasis has been focused on EFT. In 1956, J. Rudner of the South African Museum began the first collection of artefacts and fossils after wind-scoured fossil fauna remains were exposed on the deflated surfaces between dunes at DFT (Klein 1999). By 1967 the South African Museum had obtained significant archaeological material (contributions from Rudner and private collectors) to justify further research in the region. Based on the descriptions of around 600 surface fossil faunal finds, Hendey (1968) suggested that the fossil faunal remains dated to the late Pleistocene. In August 1973, G. A. Klein and colleagues discovered the first *in situ* bones protruding through a thin layer of yellow cover sand in a deflated area now known as DFT1 (Klein 1976). From September to October 1973, R. G. Klein and colleagues conducted excavations that exposed numerous fossils that were not sand-scoured, but were primarily ungulate and carnivore bones from below the surface at DFT1. The stone artefacts that were recovered from this area were limited and not distinctive enough to be classified (Klein 1999). Following on from this research, R. G. Klein and G. Avery intensified the

research around DFT. In December 1973, Klein identified a new site (DFT2) based on the discovery of an assemblage of stone artefacts and iron-mineralised animal bones. About 200m north of the initial site (DFT1), a 70cm long line of archaeological finds were exposed in the wall of a bulldozer trench (Klein 1999). Following the digging of a $6m^2$ test excavation site, Klein (1999) proposed that the bones and artefacts were vertically restricted to a possible paleosurface.

In March 1975 Leonard Stoch was employed by the South African Museum to map and collect all "endangered" surface finds prior to the construction of a power plant at DFT. Stoch dug five $1m^2$ test pits at DFT2 to establish the extent of the site. Later that year Klein and Stoch initiated a new excavation, expanding on two of the preexisting test pits. Their end goal was to obtain a larger sample of fossils and artefacts to investigate spatial orientation. Within the upper 1.3m of deposit, they identified two vertically separate and distinct "scatters" of stone artefacts and well-preserved bones on presumed paleosurfaces. The height of the water table limited the excavation to a depth of 1.3m.

Research was suspended in the area until 1997 due to the construction of a nuclear power plant in the DFT region. That year, ESCOM and the South African National Monuments Council gave permission for excavations to resume. The procurement of vital funding from the United States National Science Foundation enabled a joint South African-American excavation team to conduct further research at DFT2 (Cruz-Uribe *et al.* 2003). The main goal of their excavation project was to "characterize the spatial arrangement of the bones and artefacts, their types and the numbers of each type, predepositional damage to bones and artefacts, and other variables that will reveal the origin of the bone-artefact association and to ultimately estimate the nature and extent of human influence at DFT2" (Klein 1999: 156).

The current research at DFT2 is being carried out by archaeologists from the University of Cape Town and is focusing on reconstructing landscape use by late middle Pleistocene hominins.

## 2.4 Geological Setting

Elandsfontein and Duinefontein are located in Cenozoic marine and aeolian strata of the Sandveld and West Coast Groups. These groups overlay Proterozoic basement units of the Malmesbury Group, Cape Granite Suite intrusives and Cape Supergroup sedimentary units (Fig.2.3).

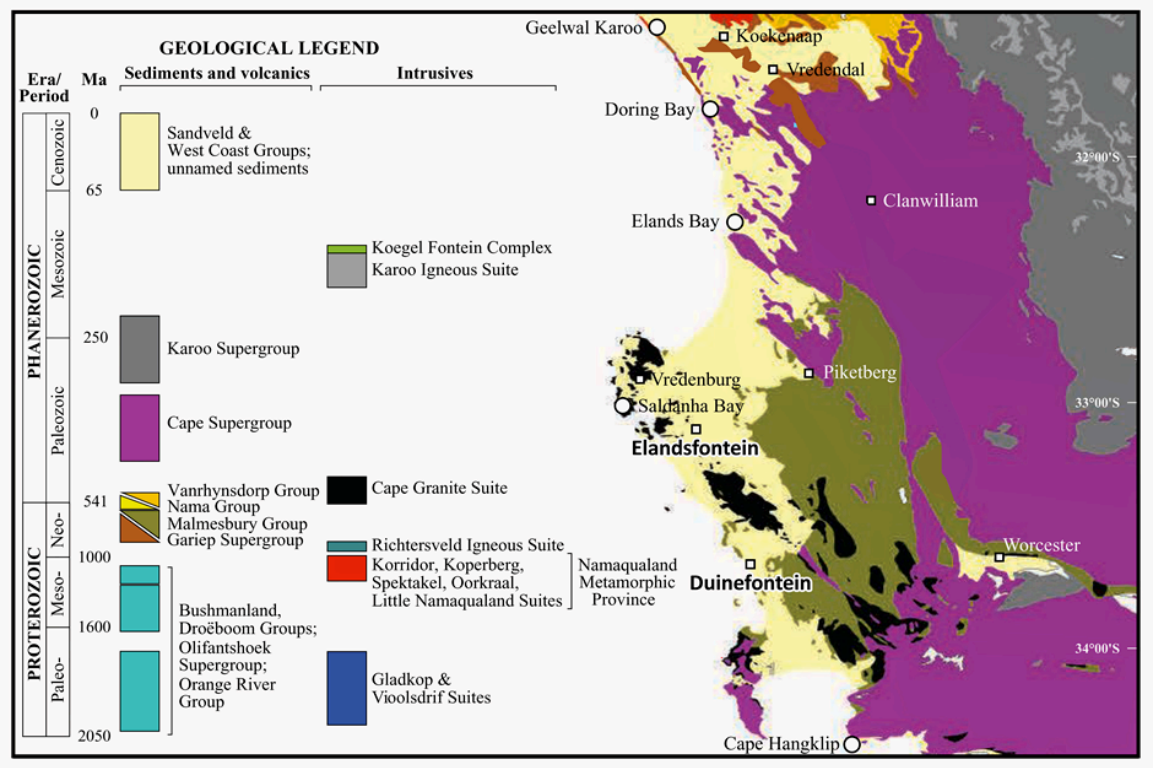


**Fig. 2.3.** *Regional geology and stratigraphy of the area surrounding Elandsfontein and Duinefontein [modified after Philander (2015: Fig.3: pp: 1580)]*

Unconsolidated Cenozoic deposits generally cover the coastal belt. Locally these deposits consist of unconsolidated and semi-consolidated aeolian sands that have been classified as the Sandveld Group. This group extends from Elands Bay southwards towards Cape Hangklip. The Cenozoic deposits that extend in a northerly direction from Elands Bay to Alexander Bay are assigned to the West Coast Group. The Sandveld Group is characterized by a more calcareous and phosphatic component while the West Coast Group are more siliciclastic in nature (Roberts *et al.* 2006).

The aeolian deposits were originally derived from sands that accumulated on the edges of the continental shelf as a result of stream transport, and were further transported along the coast by

longshore currents and wave action to form beach sands. Over a period of time the beach sands have been transported inland by onshore winds to accumulate as dune fields. The development of sand dunes was dependent on numerous interacting factors that include climatic factors such as temperature, rainfall, and prevailing winds that have impacted on the availability of sand to form dunes and vegetation growth, which influenced dune stability. Sea level changes brought on by periods of glaciation combined with eustatic activity have resulted in periods of coastal regression and transgression with the development of multiple generations of aeolian deposits in the Elandsfontein and Duinefontein area. This is confirmed by sedimentological studies of the aeolian dunes in the region, which have indicated that periods of both transgression and regression, representing changes in relative sea level, occurred at or near the modern coast line (Butzer 2004).

Dune types that would likely have formed under these conditions include;

- Transversal dunes comprising relatively straight dune ridges often parallel to the coast.
- Barchan dunes formed where unidirectional wind and small sand supply existed.
- Barchanoid ridge dunes with U and V shaped sand hills with dune ridges consisting of several joined barchan dunes.
- Parabolic dunes, which are similar in shape to the barchan but with dune pointing into the wind.

  Parabolic dunes also develop into blowout dunes. The blowout dunes often develop when vegetation is abundant and stabilises sands and a U-shaped blowout forms between clumps of plants.

Figure 2.4 below highlights the presence of modern barchanoid sand dunes (crests trending east-west) and possibly two older generations of transverse dunes (crests trending 045º and 354º) in the Duinefontein area.

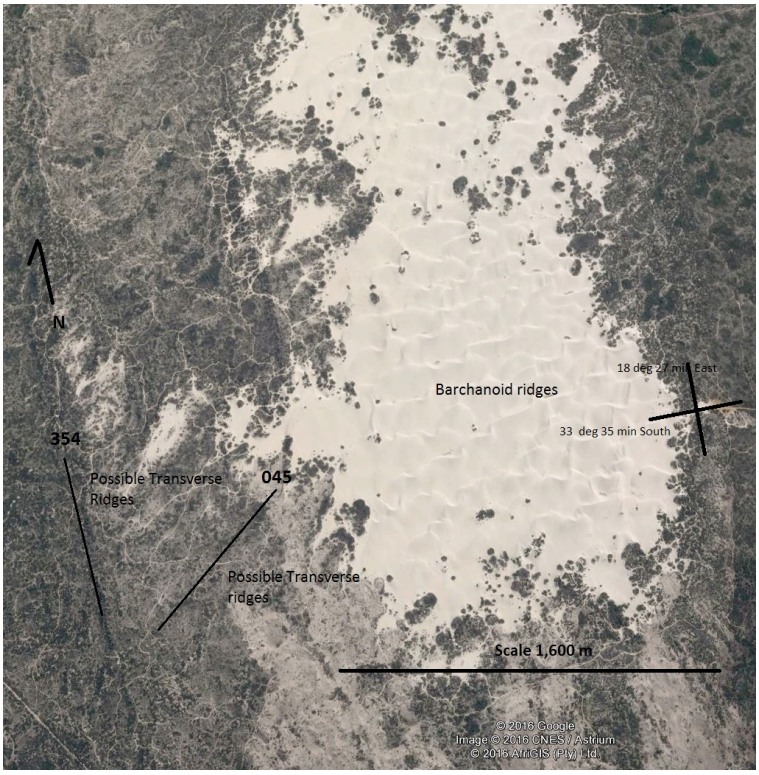


***Fig. 2.4.*** *2016 Satellite image covering a portion of the Duinefontein area showing modern barchanoid sand dunes (crests trending east-west) and possibly two older generations of traverse dunes (crests trending 045° and 354°), (source Google Image 2016).*

In some instances, the sand dunes have become consolidated through the solution and precipitation of carbonate and iron forming resistant calcrete and ferricrete rich units which often form resistant ridges.

Aeolian sand stratigraphic units in the Sandveld Group range in age from the Miocene to Recent (Roberts 2006a, 2006b; Chase & Thomas 2007; Roberts *et al.* 2009). The landscape development and the contemporary sedimentary record are complex and poorly understood. Reconstruction of the sequence of deposition is complicated by repeated periods of erosion and deposition, which has resulted in artefacts and faunal remains being subjected to numerous phases of burial, exposure and erosion. Consequently, assemblages from different time periods may have become mixed. Elandsfontein has a complex geomorphic history, highlighted by periods of dune formation alternating with "periods of soil development or fluvial activity" (Butzer 1973: 234). Despite the active nature of these landscapes, excavations at Elandsfontein and Duinefontein, have revealed that

sediments are not mixed or disturbed as demonstrated by the discovery of fossils preserved in anatomical position which proves that there was minimal post-depositional disturbance (Cruz-Uribe *et al.* 2003; Braun *et al.* 2013). Environmental change through time has influenced the geomorphology of the region. Surface geomorphology has been used to infer the geological context of bones and artifacts, as radiometric dating cannot be applied and there is no external stratigraphy that could be used to give a relative age to the Elandsfontein site (Klein *et al*. 2007).

### 2.4.1 Elandsfontein

Several researchers, including Mabbutt (1956), Needham (1962), Singer and Wymer (1968), Butzer (1973), Roberts (1996), Deacon (1998) and Braun *et al.* (2013) have undertaken geological studies of the fossil and artifact bearing strata at EFT. The common geological features identified by these researchers include:

(i) Indurated calcareous sands which form topographic highs referred to as the **'**Calcrete Ridges**'**,

(ii) Gray sands which contain white nodules

(iii) Ferruginized zones (e.g. iron stained nodules) (Braun *et al.* 2013).

The Quaternary age aeolian sands are interspersed with outcrops of granite and shale (Besaans 1972; Scheepers & Nortje 2000; Chase & Thomas 2007).

Braun *et al*. (2013) have identified three primary sedimentary groups within the EFT strata. These include:

(i) The Upper Pedogenic Sands

(ii) Calcareous Sands and carbonates

(iii) Lag surface deposits

These three units occur at the top of the Sandveld Group (Roberts 2006b). The nodules of the Upper Pedogenic sands are predominantly silica-cemented sand, and may contain minor carbonate components (Braun *et al.* 2013). The oldest geological feature is the 'Calcrete Ridge' (Fig.2.5) that reaches a maximum height of 10m and width of 60m extending over a strike length of

approximately 1km. This ridge was a topographic high during the deposition of the Upper Pedogenic Sands. The ridge is thought to be the indurated core of a dune associated with the early Pleistocene that predates the artifact and bone accumulations (Klein *et al*. 2007).

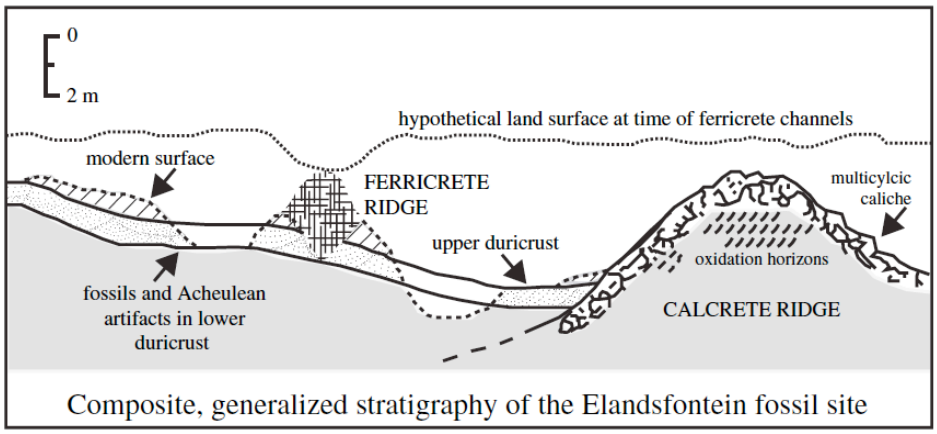


**Fig. 2.5.** *Generalised stratigraphy of Elandsfontein (Klein et al. 2007: 167)*

Two duricrusts postdating the Calcrete Ridge have been identified - a nodular non-calcareous one referred to as Elandsfontein Main (EFTM) and an upper compact ferruginous duricrust that cuts into the sands. A substantially thick fossiliferous horizon is associated with the non-calcareous nodular horizon (nodules ranging in size from 1cm to 15cm in diameter) (Braun *et al*. 2013). Singer and Wymer (1968) have identified artifacts and fossils that were both *in situ* and associated with the white nodular horizon that is below the iron rich (ferricrete) nodular horizon. They have demonstrated that the fossils and artifacts were confined to and associated with the white nodular horizon. Furthermore, Singer and Wymer (1968) show that the sands that are above and below this white nodular horizon were sterile, which is consistent with Braun *et al*.'s (2013) observations. This fossil and artifact horizon is a common feature throughout the dunefield. Fossils are often found enclosed within or close to the nodules. The EFTM material may represent a combination of fossil horizons (Braun *et al*. 2013). The second duricrust, an iron-rich nodular horizon, varies in depth from 2m to 15cm thick across the site and lies above the non-calcareous nodular horizon (Braun *et al*. 2013). Surrounding sands may have been stained a red-brown colour from the iron rich nodules.

### 2.4.2 Duinefontein

Geological research at DFT2 is very limited compared to the studies undertaken at EFT. At DFT, modern dunes have formed as a result of southerly, summer winds that have carried and deposited quartz- and shell-rich sands from nearby beaches (Cruz-Uribe *et al.* 2003). At present the sands are non-calcareous, but Klein *et al*. (1999) believes that in the past the sand contained abundant comminuted shell fragments. Klein *et al*. (1999) recognises two units in the DFT2 area, namely a narrow zone of fine white drift sand of up to approximately 50cm in width which unconformably overlies reddish, iron stained sands, with ferricrete nodules (Fig.2.6).

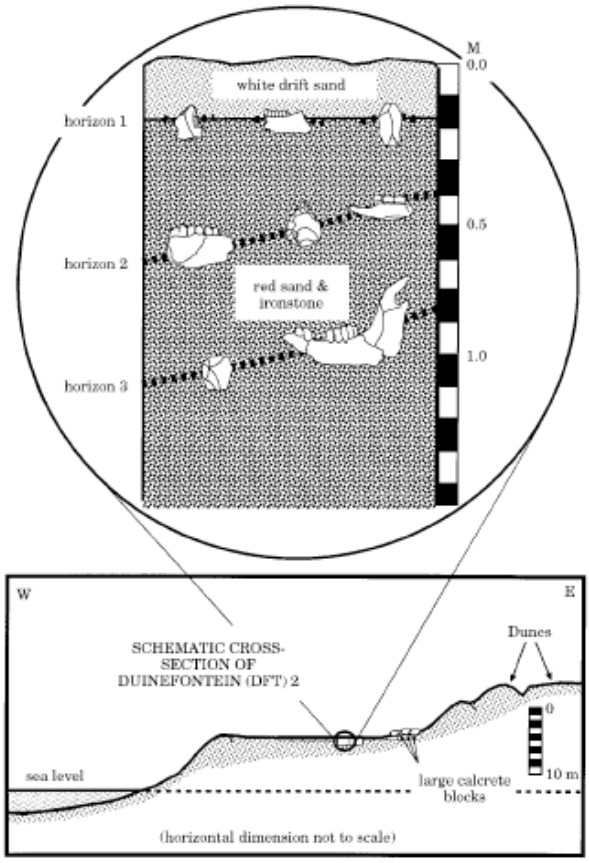


**Fig. 2.6.** *Schematic section through the uppermost deposits at Duinefontein (DFT) 2 and generalised stratigraphy at Duinefontein (from Klein et al. 1999).*

Excavations undertaken by Klein *et al*. (1999) at DFT2 exposed zones where the fine white sands were found to surround calcrete boulders that were interpreted as representing remnants of a late Quaternary duricrust. Duricrust was observed to become increasingly thicker and more continuous towards the east whilst covering the iron stained sands (Cruz-Uribe *et al.* 2003).

In 2001, Cruz-Uribe *et al.* (2003) revealed a calcrete 'ridge' buried within the red sands above Horizon 3 (FIG.2.6). These calcretes and iron stained sands were regarded as being similar to the sediments found at EFTM. Roberts (1996) used aerial photography to show that at both EFT and DFT2, the surficial calcretes that form ridges, are orientated from north to south. This is similar to the elongated arms of active parabolic dunes nearby (Cruz-Uribe *et al.* 2003).

Wind-scoured bones and flaked stone artefacts were found by Klein *et al.* (1999) to be widespread at the white-red sand interface. These finds were associated with an arbitrary Horizon 1. There were no diagnostic Later Stone Age (LSA) artefacts found in the red sands below Horizon 1. Generally the highest red sands are sterile, with the exception of the occasional bone fragment of tortoise carapace and dune molerat bone. Large bones and artefacts are found in a 10-15cm thick band that dips 1-2cm per meter from southeast to northwest (Klein 1999). On the southern and eastern borders of the excavation, the fossiliferous band was found to be near or even intersect the white-red sand interface. Meanwhile to the north and east the band was up to 90cm below the interface. The band was named Horizon 2 and at the end of the 1998 excavation season, the fossil band had been exposed over an area of 262m$^2$ (Klein 1999). Klein (1976) suggested that on the assumption that a higher-lying fossil band had been deflated, the fossil band in question, may have been the remnant of a buried surface. The concentration of bones and artefacts in Horizon 2 may have been associated with a period when the formation of dunes ended, sea level was rather high, and vegetation had stabilised the dune topography (Klein *et al.* 1999). Widespread root action most likely accounts for why the DFT2 sands lack the cross-bedding that frequently charcaterise wind-deposited sands elsewhere (Klein *et al.* 1999). In 1975, two test pits revealed another deeper sealed, sloping band of artefacts and bones 40 to 100cm deeper. Named Horizon 3, this occurrence gradually sloped upwards to the north and to the east (away from the sea) and lay below the local perched water table, making the excavation near impossible at the time of Klein's research in 1975. Cruz-Uribe *et al.* (2003) expanded the excavation between 1997 and 2001, to expose Horizon 2 to approximately 480m$^2$.

## 2.5 Archaeological Age of Sites

### 2.5.1 Elandsfontein

Previous age estimates for the Quaternary deposits at EFT have been based on the biostratigraphy of associated fauna (Klein 1983a; Klein & Cruz-Uribe 1991; Roberts & Brink 2002; Klein *et al*. 2007). The maximum and minimum age estimates for EFT were based on the first and last appearance dates of *Syncerus antiquus* and *Rabaticerus arambourgi*. These age estimates relied on comparisons made between EFT faunal remains with those found in Bed III/IV of Olduvai Gorge, Tanzania (Bishop 2010). Using the EFT biostratigraphy, Klein *et al.* (2007) suggested that EFT fauna must be younger than 1.0 Ma because of the presence of *Syncerus antiquus* and older than 0.6 Ma based on the presence of *Rabaticerus arambourgi*. Evidence now suggests that EFT could in fact predate 1Ma because of the presence of well-provenanced fossils of *Sivatherium* and the Dirk toothed cat *Megantereon whitei* (Braun *et al*. 2013).

### 2.5.2 Duinefontein

A uranium-series analysis of the calcrete overlying red sands in one section of DFT provides a minimum age estimate for underlying red sands with their artefacts and bones, of >150 kya (Klein *et al.* 1999). Feathers (2002) used optically stimulated luminescence (OSL) dating to show that the sands surrounding Horizon 2 accumulated around 270 kya, while sands between Horizons 2 and 3 were accumulating around 290 kya. The fossil fauna found in Horizon 2 suggests an age falling between the more archaic mid-Quaternary fauna from EFTM and the more modern later Quaternary faunas from sites like Klasies River Mouth and Swartklip 1 (Klein 1976). Based on the above statement, Horizon 2 most likely formed between 400 and 200 ka ago. The DFT2 radiometric ages are also consistent with the bovid taxa present in Horizon 2. The artefacts found at DFT2, which include a classic Acheulean handaxe and probable bifacial flakes, further support this age estimate. The DFT2 flake and core types initially suggested an early phase of the MSA (Deacon 1976; Klein 1976), but the 1997 and 1998 excavations provided possible or probable biface shaping and

trimming flakes, and the 1998 excavation produced a classic handaxe. The sum implies that DFT2 belongs to a late phase of the (Early Stone Age) Acheulean Industrial Complex.

To summarise, EFT has been dated to the middle Pleistocene whilst DFT has been dated to the late middle Pleistocene.

### 2.6 Contemporary Environment

The southwestern Cape coast region today, falls within the Winter Rainfall Zone (WRZ) as shown in Figure 2.7. The Mediterranean climate is characterised by short, cool and wet winters, which is brought on by the occurrence of westerly cyclonic fronts (Rutherford & Westfall 1994), and lengthy, warm dry summers, associated with a high frequency of trade winds. The maximum temperature in January is on average 26 °C whilst the maximum average temperature in July is 17 °C (Klein 1999). South-easterly or southerly winds are dominant in summer, while north-westerly or westerly winds prevail in winter. Rain falls in the area primarily in the winter months from April through to September, with an average annual rainfall of 300 mm (Deacon & Lancaster 1988).

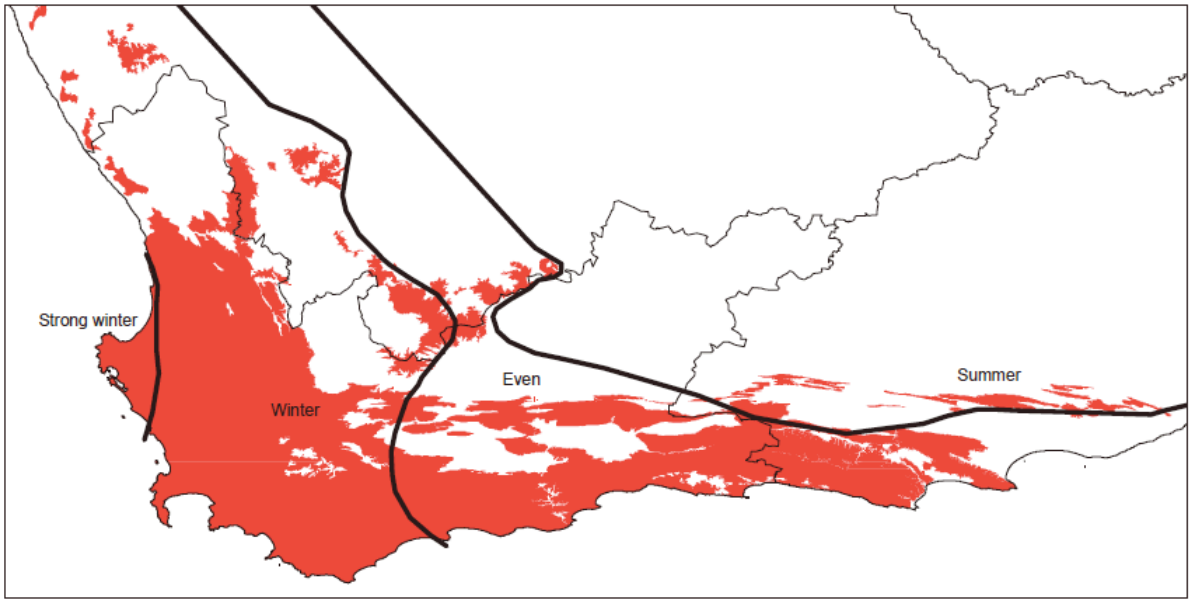


**Fig. 2.7.** *Seasonal rainfall for the Fynbos Biome (Rebelo et al. 2006)*

The two study localities are located within the ecologically rich and unique Fynbos vegetation

biome. The Fynbos biome (Fig.2.8), which is also referred to as the Cape Ecozone (Cape Floristic Region), has one of the highest density of different plant species in the world (more than 9,000 plant species), around 70% of which are endemic to the region (Cowling 1992; Cowling & Lombard 2002; Goldblatt & Manning 2002). The biome covers an area of 87,892 $km^2$ which includes the coastal areas and adjacent Cape Fold Belt Mountains (Cowling & Heijnis 2001). The Fynbos biome is divided into three major vegetation complexes: fynbos, strandveld, and renosterveld (Rebelo *et al.* 2006). With the exception of the alien species such as the Australian wattles (*Acacia mearnsii, Acacia saligna, Acacia cyclops*), introduced by the Europeans to the southwestern region, these complexes comprise mainly of $C_3$ vegetation types in the form of the short, shrubby, drought resistant and fire-adapted fynbos. In addition, very few plant species within the strandveld and renosterveld plant communities utilize the $C_4$ pathway (Cowling 1992; Schulze 1986). Presently, indigenous grasses are a very minor component of this biome, and those present are predominately cool-season growing $C_3$ grasses (Ehrhartoideae, Danthonioideae and introduced species of Pooideae and Arundinoideae; Vogel *et al*. 1978; Gibbs Russell *et al.* 1990; Linder & Ellis 1990; Cowling *et al*. 1997, Goldblatt & Manning 2002, Rebelo *et al.* 2006). According to Rebelo *et al.* (2006), the Restionaceae (restios) and Cyperaceae (sedges) dominate most of the vegetation types of the fynbos in comparison to the Poaceae (grass) family.

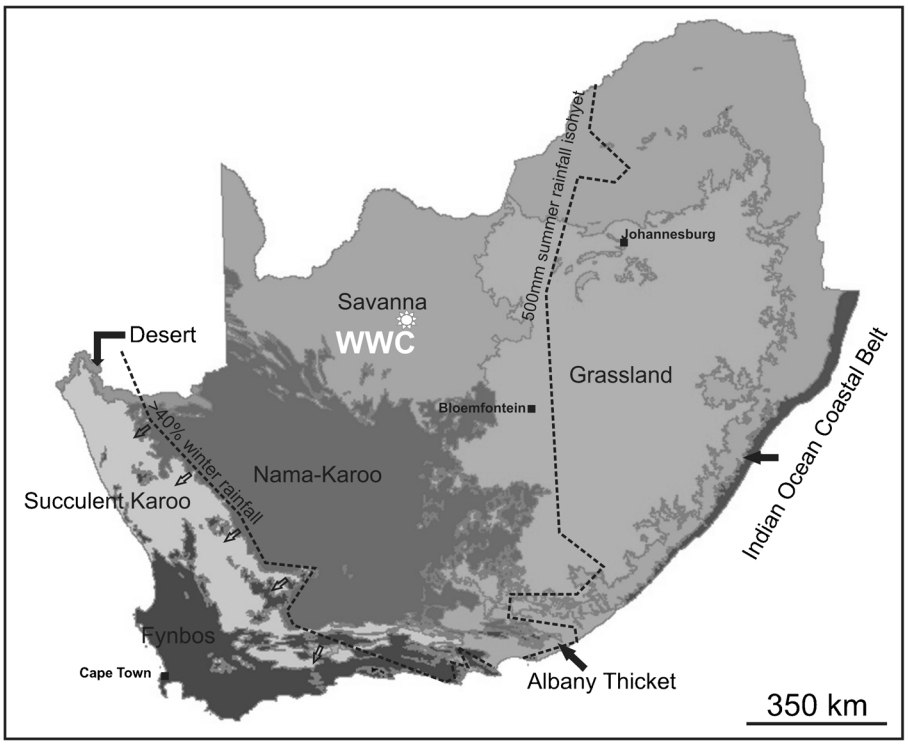


**Fig. 2.8.** *Map of the present day biomes of South Africa (from Rossouw 2016: 253).*

The vegetation of the Duinefontein region has been classified as Cape Flats Dune Strandveld (FS 6) by Rebelo *et al.* (2006). The landscape is characterised by vegetation types that include tall, evergreen, hard-leaved shrubs, grasses and herbs (Rebelo *et al.* 2006). The vegetation of the Elandsfontein region has been classified as Hopefield Sand Fynbos (FFd 3) by Rebelo *et al.* (2006). The landscape in this region is comprised of short, shrubby, drought resistant and fire-adapted fynbos.

The insufficient amount of grass and fresh browse, combined with the low nutritional content of fynbos vegetation and general rarity of surface water, makes the contemporary southwestern Cape coastal environment unsuitable for the maintenance of large herds of large-bodied grazing and browsing mammals (Skead 1980; Klein 1983b; Klein *et al.* 1999). Prior to the onset of widescale farming activities however, historic records indicate that elephant (*Loxodonta africana*), black rhinoceros (*Diceros bicornis*), red hartebeest (*Alcelaphus buselaphus*) and eland (*Taurotragus oryx*) occurred in small numbers, primarily along major river systems. Today, small browsers and mixed feeders such as *Raphicerus melanotis* and *Raphicerus campestris* are the most common naturally

occurring ungulates in the region. The diversity and abundance of the fossil faunas discovered at EFT and DFT however, points to a more productive vegetative community in the past.

## 2.7 Palaeoenvironmental Reconstruction

### 2.7.1 Pre-Pleistocene Paleoenvironment

Research suggests that grasslands were well established in southern Africa by the Late Tertiary (Scott 2002). There is evidence to suggest that fynbos has been present in the southwestern coastal region from at least the middle Miocene (Stynder 2009). In the Langebaanweg region, pollen analysis studies were performed on sediments from the middle Miocene Elandsfontein Formation. Results indicate that subtropical forests, palms and marsh type vegetation with minor fynbos elements were developed in the area (Coetzee & Rogers 1982). The overlying Pliocene Varswater Formation, in the same region, comprised grass and fynbos as confirmed by pollen evidence. This confirms that extensive grasslands and significant amounts of fynbos vegetation had been established during the Pliocene (Tankard & Rogers 1978; Scott *et al.* 1997; Rossouw *et al.* 2009). Results from isotopic studies of tooth enamel from Varswater Formation grazing fauna suggests that $C_3$ grasses were prominent and that the present day wet winter/dry summer (Mediterranean) climatic regime was established before the early Pliocene (Franz-Odendaal *et al.* 2002).

### 2.7.2 Pleistocene Palaeoenvironment

Research into the fossil fauna record from EFT, DFT and other southwestern Cape coast Pleistocene sites such as Hoedjiespunt (Berger & Parkington 1995; Stynder 1997), Sea Harvest (Grine & Klein 1993) and Swartklip (Klein 1975; Klein 1983b) has provided a better understanding of the palaeoenvironments, and specifically the probable climatic conditions and flora, which would have been present to sustain the fauna in the region.

In EFT, a number of different proxies have been implemented in an attempt to reconstruct the middle Pleistocene environment. Research has included the identification of faunal communities (Klein 1983b; Klein *et al*. 2007), studies of wear on ungulate dentition (Stynder 2009) and stable isotopic analysis of faunal remains (Luyt *et al.* 2000; Lehmann *et al.* 2016; Patterson *et al.* 2016). An understanding of dietary patterns (long-term diet; food consumed; seasonal availability of food; selective pressures) and morphological adaptations is gained through the analysis of fossil ungulate teeth. Research has confirmed the mixed nature of the floral environment at EFT, which accounts for the diverse and large fossil mammal fauna (Klein *et al.* 2007; Braun *et al.* 2013). In DFT, a remarkably well-preserved and complete fossil faunal record has been identified by Klein *et al.* (1999) and has been used as the main proxy in the reconstruction of the paleoenvironment.

### 2.7.3 Pleistocene Fauna

#### 2.7.3.1 Elandsfontein

A large and highly diverse sample of late middle Pleistocene mammals has been recovered from EFT. The faunal assemblage is composed of a mix of archaic and modern species (Fig.2.9). In excess of nineteen large mammal species, now extinct, have been discovered in the EFTM faunal remains (Hendey 1974; Klein 1983b). Elandsfontein Main is unique compared to other documented African middle Pleistocene sites due to the large number of African elephant (*Loxodonta*) remains and the lack of Reck's elephant remains (Klein *et al.* 2007). Grazers were diverse and included the gelada baboon (*Theropithecus oswaldi*), zebras (*Equus capensis*, *E. quagga*), the white rhinoceros (*Ceratotherium simum*), two suid species (*Kolpochoerus paiceae, Metridiochoerus andrewsi*), a hippotragine species (*Hippotragus leucophaeus*), the blue antelope, the reedbuck (*Redunca arundinum*), all seven alcelaphine antelopes (*R. arambourgi, D. aff. lunatus, D. niro, D. sp. nov., Parmularius sp. nov., Connochaetes gnou, Megalotragus priscus*), a gazelle (*Gazella sp.),* springboks (*Antidorcas recki, Antidorcas australis*), and the long-horned buffalo (*Pelorovis antiquus*) (Klein *et al.* 2007). Browsers included sivathere (*Sivatherium maurusium*), the greater kudu (*Tragelaphus strepsiceros*), an unnamed "spiral horn" antelope, Cape grysbok (*Raphicerus*

*melanotis*), eland (*Taurotragus oryx*) and black rhinoceros (*Diceros bicornis*). Mixed feeders included the giant hippotragine (*Hippotragus gigas*), Aramburg's hartebeest (*Rabaticeras arambourgi*), and the tsessebe-like antelope (*Damaliscus aff. Lunatus*).

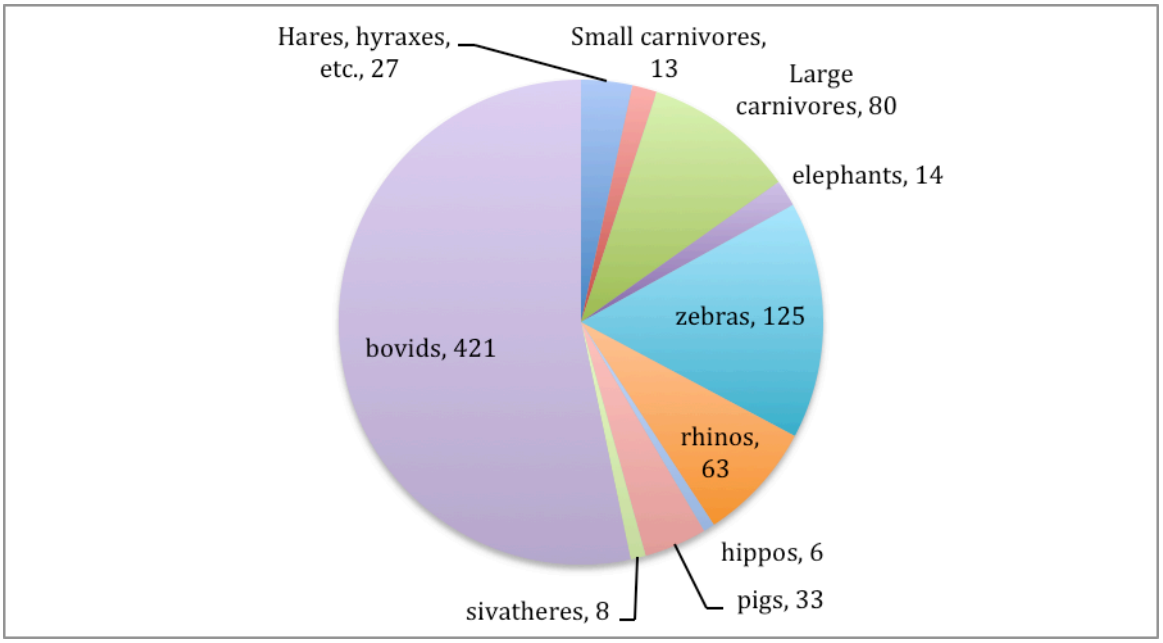


**Fig. 2.9.** *The relative representation of EFTM fauna, based on the MNI (minimum numbers of individuals) represented. The category "Hares, hyraxes etc." represents porcupines, hares, dune mole rats and pangolin. The category "Small carnivores" represents Cape fox, striped polecat, genet, Egyptian mongoose, water mongoose, slender-tailed mongoose. The category "Large carnivores" represents Civet cat, leopard, lion, honey badger, dirk-toothed cat, hyenas, wildcats, caracal and black-backed jackal.*

The diversity in bovids reported from EFT is amongst the highest ever seen in a palaeontological site. Two antelope species unique to EFT have been identified, namely ?*Parmularius* sp. nov. and the unnamed ''spiral horn'' antelope. Extant species identified in the EFTM assemblage are the dune mole rat (*Bathyergus suillus*), Cape fox (*Vulpes chama*), slender-tailed mongoose (suricate; *Suricata suricatta*), gray mongoose (*Herpestes pulverulentus*), brown hyaena (*Parahyaena brunnea*), mountain zebra (*Equus zebra*), quagga (*Equus quagga*), blue antelope (*Hippotragus leucophaeus*), southern reedbuck (*Redunca arundinum*), bontebok/ blesbok (*Damaliscus dorcas*), black wildebeest (*Connochaetes gnou*), Vaalribbok (*Pelea capreolus*), springbok (*Antidorcas sp.*), and Cape grysbok (*Raphicerus melanotis*) (Skinner & Smithers 1990).

### 2.7.3.2 Duinefontein

In contrast to the high levels of taxonomic diversity observed among large herbivore species in the EFTM fossil fauna, it appears that at DFT the diversity of ungulate taxa had decreased significantly (Fig.2.10). DFT2 lacks many of the extinct ungulate species that characterize EFTM. At DFT, browsers include the greater kudu (*Tragelaphus strepsiceros*), black rhino (*Diceros bicornis*) and eland (*Taurotragus oryx*). Grazers include the Cape zebra (*Equus capensis*), white rhino (*Ceratotherium simum*), hippo (*Hippopotamus amphibius*), blue antelope (*Hippotragus leucophaeus*), southern reedbuck (*Redunca arundinum*), long-horned buffalo (*Pelorovis antiquus*) and the black wildebeest (*Connochaetes gnou laticornutus*). Klein *et al.* (1999) in their study of horizon two of the DFT stratigraphy, suggested that the faunal assemblage was dominated by a mix of large grazing and browsing ungulates, which suggested a bush-grass mosaic perhaps broadly resembling the savanna woodland of South Africa. Horizon two has been dated to between 400 and 200 ka ago (Feathers 2002).

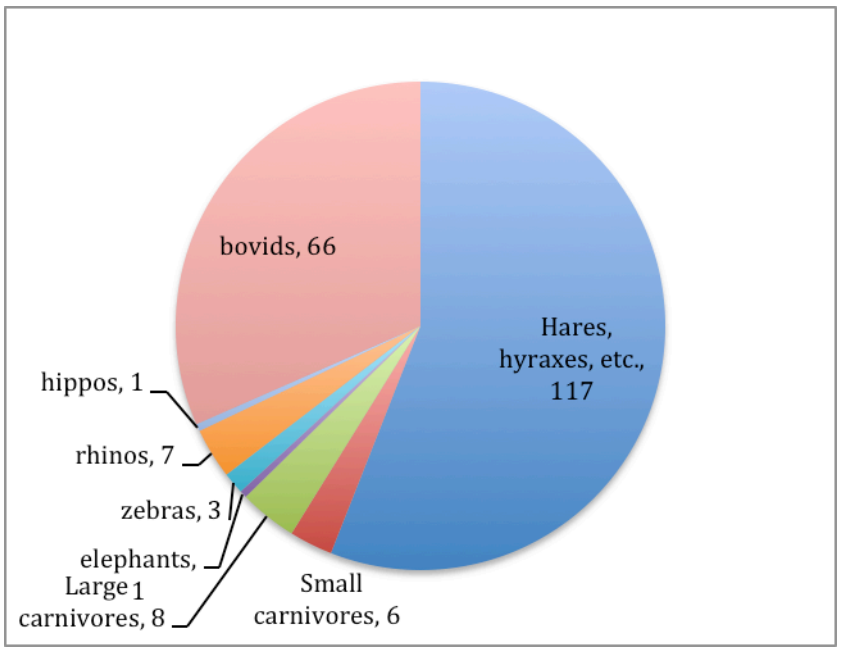


**Fig. 2.10.** *The relative representation of DFT2 fauna, based on the MNI (minimum numbers of individuals) represented. The category "Hares, hyraxes etc." represents porcupines, hares and dune mole rats. The category "Small carnivores" represents striped polecat, genet and Egyptian mongoose. The category "Large carnivores" represents lion, honey badger, hyenas, wildcats, caracal and black-backed jackal.*

### 2.7.4 Paleoenvironmental Reconstruction

#### 2.7.4.1 Elandsfontein

The initial analyses of the EFT fossil faunal remains and the reconstruction of the EFT middle Pleistocene paleoenvironment were executed by Klein (1983b). He argued that the composition of the faunal assemblage indicated that grasses were a significant component of the ancient EFT environment. By employing taxonomic analogies as a proxy, Klein and Cruz-Uribe (1991) and Klein *et al.* (2007) suggested that the vegetation, which grew in the middle Pleistocene EFT environment, was capable of supporting the abundant grazing species observed in the EFTM assemblage. They proposed that this scenario was possibly due to an increase in grasslands that were replacing the fynbos vegetation (Klein & Cruz-Uribe 1991). According to Klein (1983b) the EFT environment also contained a tree component as implied by the remains of giraffid (*Sivatherium maurusium*) and civet cat (*Viverra civetta*). Klein's (1983b) theoretical reconstruction of the EFT middle Pleistocene environment as interpreted through the EFT faunal community thus suggests a vegetation mosaic comprised of grass and bush, which is in contrast to the late Quaternary 'glacial' faunas, which were supported by open grassland with limited bush or thicket. However, applying taxonomic analogy to fossil faunas and extinct species is problematic (Schubert *et al.* 2006) as many modern ungulate taxa have flexible diets (Sponheimer *et al*. 2003).

The presence of water dependent species such as hippopotamus and reedbuck indicates that moist conditions and significant amount of surface water most likely existed in the EFT palaeoenvironment (Luyt *et al*. 2000). Spring-fed environments like those at EFT may have provided crucial resources for fauna in the mid-Pleistocene within an increasingly arid African ecosystem. The EFT Main fossil assemblage may have accumulated when people and animals, attracted by the various water sources in the landscape, died naturally or due to predation. The paleovegetation included fynbos shrubland and grassland mosaic, which was interspersed with trees and broad-leafed bush. This illustration strongly contrasts the dry, wind scoured landscapes that are prevalent in the present day southwestern coastal region of South Africa, where the nearest major

water source is the Great Berg River, which lies 20km north of EFT (Luyt *et al*. 2000; Franz-Odendaal *et al.* 2002; Stynder 2009; Braun *et al.* 2013).

Two theories have been applied to explain the presence of water in the EFT paleoenvironment. One theory suggests that the rise in sea level during the Pleistocene may have accounted for the higher water table and presence of springs in the area and for the formation of spring carbonates and the accumulation of faunal remains. The concentration of surface carbonates may reflect multiple events of spring activity, which would have been associated with an elevated water table (Braun *et al*. 2013). This theory, supported by Pickering *et al.* (2013) in their studies of sea levels along the southern Cape coast prior to 1.11 Ma, suggests that the sea level was 19-20m higher than the current sea level. Taxonomic composition, geomorphic setting, and pollen taken from coprolites also suggested that marshes, or bodies of water would have existed in the region if there had been a higher water table (Klein *et al*. 2007).

A second theory proposed by Klein and Cruz-Uribe (1991) and Klein *et al*. (2007) suggests that this type of environment probably resulted from a higher level of rainfall than present day that may have continued into the summer months, although this has yet to be confirmed. According to Klein *et al.* (2007), an abundance of water combined with mild temperatures, as indicated by the small average size of the EFTM jackals (*Canis mesomelas*), suggests accumulation during one of the mid-Pleistocene interglacial periods. It is possible that as a result of the higher levels of rainfall in summer months, an abundance of palatable browse and graze may have grown on nutrient-rich calcareous soils, which are no longer present in the region (Luyt *et al.* 2000, Braun *et al.* 2013). Additionally, warm season $C_4$ type grasses may have been common during the middle Pleistocene. A predominance of $C_4$ phytoliths over $C_3$ would support this hypothesis. Luyt *et al*. (2000) however proposed that there is no evidence to suggest that there was anything but a winter rainfall regime present at EFT. Pollen studies indicate that fynbos was present along the southwestern coast of South Africa since the middle Miocene (Stynder 2009).

### 2.7.4.2 Duinefontein

A limited amount of palaeoenvironmental work has been undertaken at DFT, in comparison to EFT. Research undertaken by Cruz-Uribe et al. (2003) on the DFT2 sediments and the fossil fauna have been the only bases for environmental reconstruction in DFT. They consider the coarse nature of the sediments detrimental to the preservation of pollen for the identification of specific flora. Hyaena coprolites may possibly contain pollens that could be used in the reconstruction of the paleoenvironment.

Fossil remains of reedbuck (*R. arundinum*), hippopotamus (*Hippopotamus amphibius*), swamp rat (*Dasymys incomtus*), Saunder's vlei rat (*Otomys saundersiae*) and some amphibian taxa (Sampson 2003) located in the DFT region suggest that shallow water bodies were present when fauna bones and artifacts accumulated within horizon 2 and horizon 3 (Cruz-Uribe *et al.* 2003). Sampson's (2003) research into the DFT2 region located abundant amphibian remains from the late mid-Quaternary fossil site. The distribution of amphibian remains indicated the presence of shoreline lags and interdunal ponds in the area. As with the EFT paleoenvironment, the existence of ponds in the region would have required a higher water table than present, and this in turn implies that a high, interglacial sea level may have been influencing the vegetational composition of the later Pleistocene DFT environment. The presence of a higher sea level has also been supported by the identification of bones from sea birds (Cormorant, Penguin) that imply that the coastline was closer to the site when the bones accumulated (Klein 1999).

### 2.7.4.3 Hoedjiespunt (Late middle Pleistocene, 350-200kya)

Fossils from the Hoedjiespunt Peninsula (Fig.2.11) were first analysed by Klein (1983b). Since 1993, further research has been conducted by scientists and students from the University of Cape Town and the University of the Witwaterstrand (Berger & Parkington 1995; Stynder 1997; Stynder *et al.* 2001). The palaeontological assemblage was most likely accumulated by hyaenas and this

accounted for the relatively high number of black-backed jackal bones (Stynder 1997). Grazing ungulates such as the black wildebeest (*Connochaetes gnou*) and red hartebeest (*Alcelaphus buselaphus*) dominated the assemblage, which suggested that the palaeoenvironment had comprised of widespread open grasslands. There was evidence that "glacial" conditions had existed during the accumulation of the palaeontological assemblage (Klein 1983b; Stynder 1997). Browsers were scarce and the largest herbivore recorded was the white rhino (*Cerototherium simum*). Lastly, the small number of marine animals (dolphin, Cape fur seal, cape clawless otter) present in the assemblage may have been an indication of the existence of lowered sea levels during a "glacial" period (Stynder 1997).

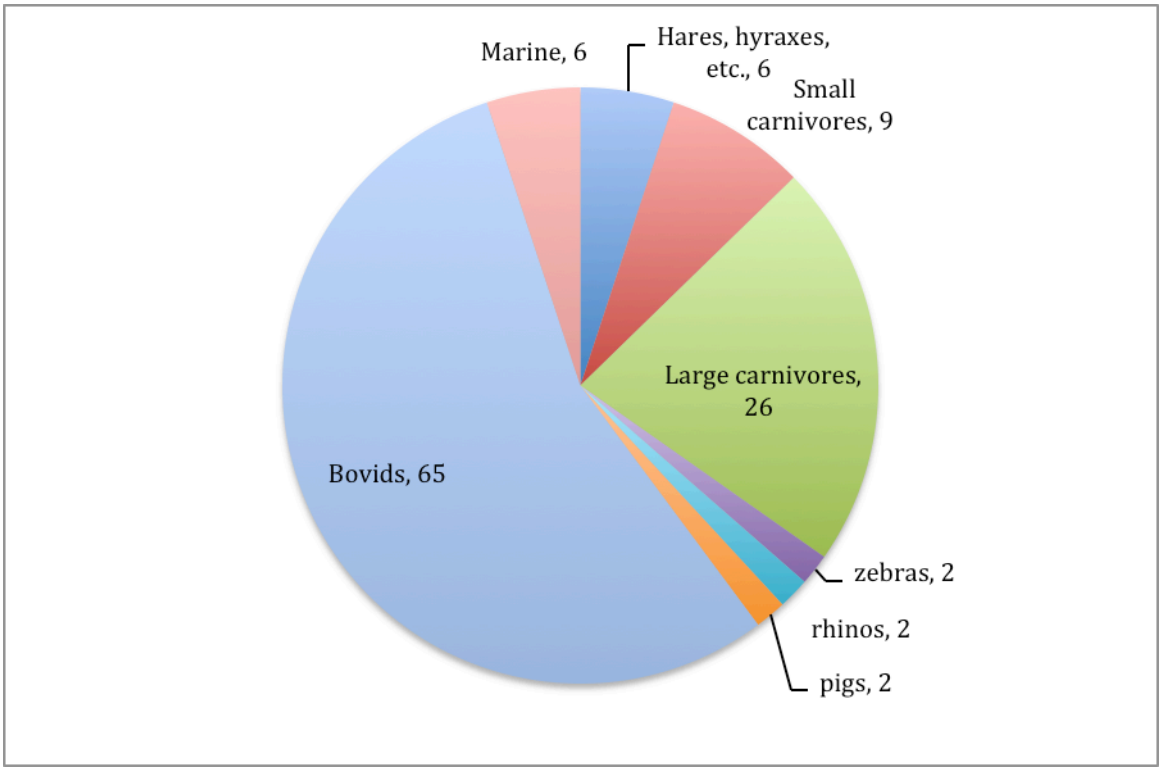


**Fig. 2.11.** *The relative representation of Hoedjiespunt fauna, based on the MNI (minimum numbers of individuals) represented. The category "Hares, hyraxes etc." represents porcupines, hares, rock hyrax and dune mole rats. The category "Small carnivores" represents Cape fox, striped polecat, genet, water mongoose, Egyptian mongoose, slender-tailed mongoose and small spotted cat. The category "Large carnivores" represents lion, leopard, honey badger, hyenas, wildcats, caracal, serval, hunting dog and black-backed jackal. The category "Marine" represents dolphin, crabeater seal, brown fur seal and Cape clawless otter.*

### 2.7.4.4 Sea Harvest (Late Pleistocene, 128-74kya)

Grine and Klein (1993) identified fossil remains of mammals, birds, tortoises, snakes and fish from

the site that was considered to be an ancient hyaena den, (Fig.2.12). They suggested that the abundance of grazing ungulates (zebra, white rhino, warthog, blue antelope, southern reedbuck, black wildebeest, bontebok and springbok) was an indication that the ancient vegetation was considerably grassier. In addition, the analysis of jackals and dune molerat bones suggested cooler and wetter conditions. The large amount of small mammals remains in the faunal assemblage was thought to be associated with small carnivores or owls.

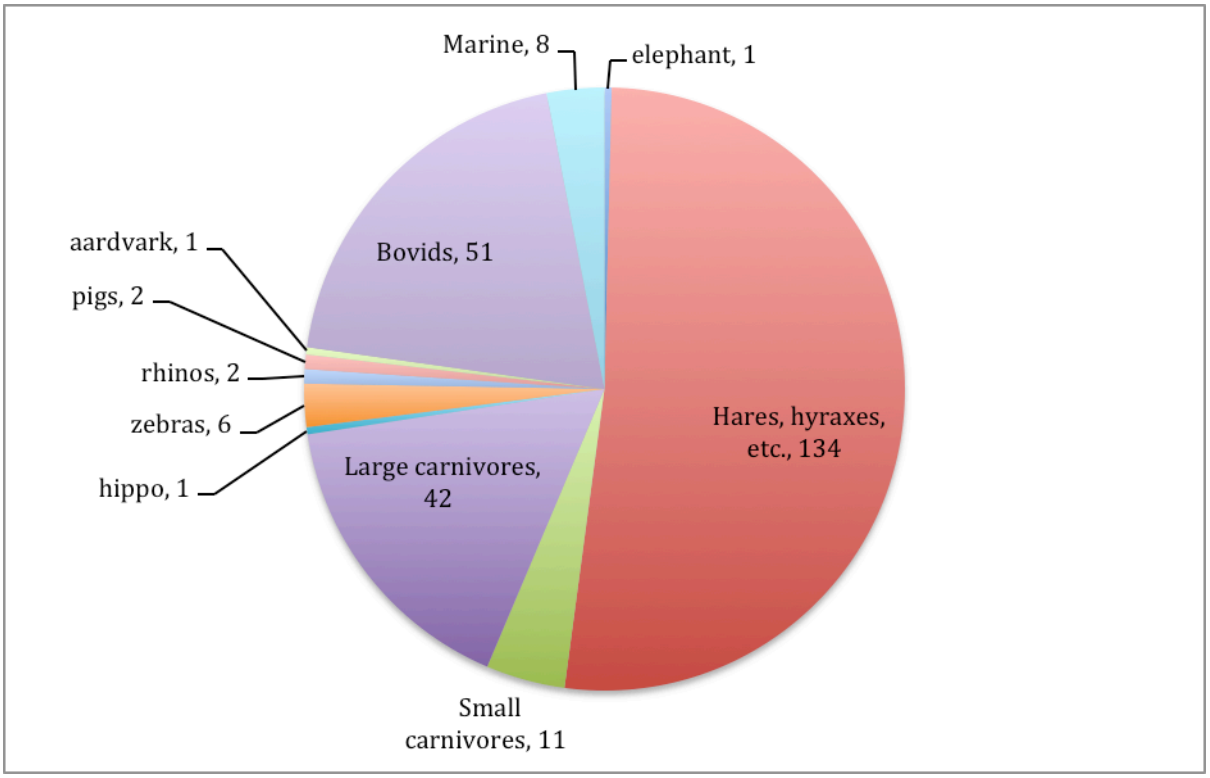


Fig. 2.12. *The relative representation of Sea Harvest fauna, based on the MNI (minimum numbers of individuals) represented. The category "Hares, hyraxes etc." represents porcupines, hares, rock hyrax and dune mole rats. The category "Small carnivores" represents Cape fox, striped polecat, genet, grey mongoose and Egyptian mongoose. The category "Large carnivores" represents cheetah, lion, leopard, honey badger, hyenas, wildcats, serval, hunting dog and black-backed jackal. The category "Marine" represents dolphin, crabeater seal, brown fur seal and Cape clawless otter.*

### 2.7.4.5 Swartklip 1 (Late Pleistocene, 117ka-105kya)

Klein (1975) collected and analysed the majority of the fossil remains from Swartklip (Fig.2.13). Like the Sea Harvest site, the faunal remains (ungulate, carnivore and other animal bones) at Swartklip were collected by hyaenas (Klein 1975). There were no Cape fur seal remains as during this time period, the sea level was much lower (Avery *et al.* 2008). According to Klein (1975;

1983b) the abundance of black wildebeest (*Connochaetes gnou*), white rhino (*Ceratotherium simum*), southern reedbuck (*Redunca arundinum*), the extinct giant buffalo (*Pelorovis antiquus*), and the extinct giant Cape zebra (*Equus capensis*) bones, suggested that the ancient vegetational environment was relatively open and grassy. Water dependent species such as the otter (*Aonyx capensis*), water mongoose (*Atilax palundinosus*), hippo (*Hippopatamus amphibious*) and reedbuck (*Redunca arundinum*) suggested that standing water had been present and that the ancient environment was wetter than at present. Klein (1983b) believed that the climatic conditions were essentially 'glacial'.

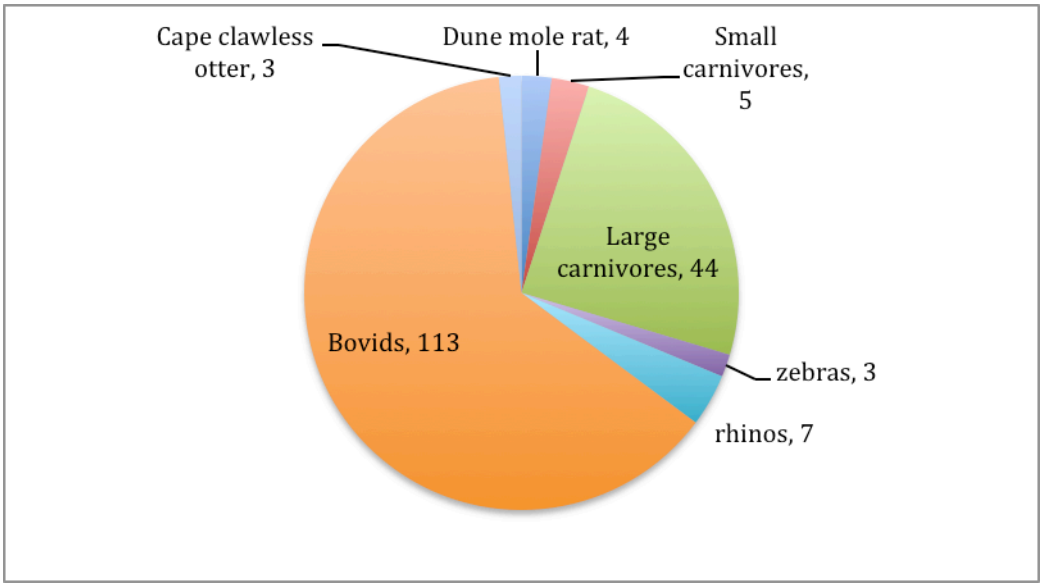


**Fig. 2.13.** *The relative representation of Swartklip fauna, based on the MNI (minimum numbers of individuals) represented. The category "Small carnivores" represents Cape fox, striped polecat, Egyptian mongoose and water mongoose. The category "Large carnivores" represents lion, leopard, honey badger, hyenas, wildcats, serval, caracal, hunting dog and black-backed jackal.*

### 2.7.4.6 Comparing Ungulate Diversity Between Sites

As observed in Figures 2.9 to 2.13, it appears that the ungulate diversity and thus vegetation diversity decreased over time. The fossil fauna from Elandsfontein Main exhibits high levels of taxonomic diversity among large herbivore species, suggesting greater primary productivity of the regional plant community at the time. Ungulate taxa became less diverse over time though, as seen in the faunal communities of sites such as Duinefontein, Hoedjiespunt, Sea Harvest and Swartklip.

This suggests that there had been a decrease in the primary productivity of the region's vegetation community.

### 2.7.5 Stable Isotope Studies

Stable isotope studies on faunal remains have been used to identify $C_3$ or $C_4$ signatures of plants consumed by the fossil fauna along the southwestern Cape coast. $C_3$ and $C_4$ plants are readily distinguishable isotopically. The enamel from faunal teeth can preserve the $C_3$ and $C_4$ isotope signatures for periods of an excess of a million years (Lee-Thorp & Van der Merwe 1987) and can be used to differentiate which plant types were being consumed by the animals (Vogel 1978). The carbon isotope ratios in fossil grazing animals can also be utilised to provide information on seasonal rainfall under certain conditions (Lee-Thorp & Beaumont 1995). Warm season grasses use the $C_4$ pathway, whereas cool season grasses, shrubs and trees use the $C_3$ pathway (Luyt *et al*. 2000).

Stable carbon isotope ratios from a range of fossil EFT grazers and browsers were first analysed by Luyt *et al*. (2000). Luyt *et al.* (2000) confirmed that the stable carbon isotope ratios analysed from EFT faunal tooth enamel showed that the majority of animals consumed predominantly $C_3$ flora, although small amounts of $C_4$ plants were also identified in a number of grazing species. Their results also indicated that cool growing seasons and persistent winter rainfall existed during this period. The high grassy component was interpreted as possibly being the result of the region experiencing extended summer rainfall periods. Luyt *et al*. (2000) confirm that the faunal and isotopic data is indicative of a productive biome with both significant tree/shrub and grassy elements being present during the period in which the Main and Bone Circle assemblages were deposited. The combination of significant tree/shrub and grassy vegetation does not exist in the fynbos biome today. It is likely that the favorable growing conditions disappeared during the course of the last glacial cycle. Luyt *et al.* (2000) suggest that the winter rainfall regime, characteristic of the region today, existed throughout the middle Pleistocene till present day. This hypothesis is

supported by stable carbon isotope studies on faunal remains (predominately grazers) from Hoedjiespunt 1 conducted by Hare and Sealy (2013). The results from the stable isotope analysis suggested that the large grazer species had predominantly $C_3$ diets ($C_3$ grasses). These grazing species would have inhabited an environment experiencing glacial climatic conditions, where grasslands were extensive and the sea levels were lower. Therefore it appears that the results from both stable isotope studies (Luyt *et al.* 2000; Hare & Sealy 2013) suggest that $C_3$ grasses dominated and that the WRZ on the West Coast had existed throughout the Pleistocene.

Lehmann *et al.* (2016) synthesized carbon and oxygen data of the teeth from large mammals at Langebaanweg (~5 Ma), Elandsfontein (1.0–0.6 Ma), and incorporated data from Hoedjiespunt 1 (0.35–0.20 Ma) obtained by Hare and Sealy (2013), with the aim of investigating possible environmental change between the Pliocene and Pleistocene along the southwestern coast of South Africa. Most of the herbivore fossils from these sites yielded enamel δ13C values that are associated with a pure $C_3$ diet (winter rainfall conditions). However some of the taxa were found to have enamel δ13C values which suggest the presence at times, of small amounts of $C_4$ grasses (limited summer rainfall) during the Pleistocene. Their research also indicates that the winter rainfall zone may in fact have been in place for the past 5 million years. In addition, the variable periods of winter rainfall seen in the modern winter rainfall zone was in fact active during the mid-Pleistocene. Therefore, during periods of increased winter rainfall, there would have been an increase in $C_3$ vegetation

Isotope studies undertaken by Patterson *et al.* (2016) discovered that δ13C values of the micromammal, Cape dune mole-rat (*B. suillus*), was remarkably different compared to those of contemporaneous large mammals from EFT. These results suggest that there was a notable presence of $C_4$ plants during the mid-Pleistocene, compared to the present day $C_3$ dominated ecosystems along the west coast of South Africa. This suggests that there may have been patches of $C_4$ vegetation (microhabitats) within a predominantly $C_3$ paleoenvironment.

### 2.7.6 Mesowear Analysis

Mesowear analysis has been used for palaeoenvironmental reconstructions. Stynder (2009) analysed mesowear patterns of 15 EFTM ungulate species to differentiate vegetation types and the long-term dietary behaviour of the fauna in the EFT region. He confirmed the distinct difference between the mesowear patterns of grazers (consumed abrasive foods such as grass), browsers (consumed less abrasive foods like leaves) and mixed feeders. The results suggested that there were more browsing faunal species in the EFTM environment than proposed originally by researchers such as Klein and Cruz-Uribe (1991) and Klein *et al.* (2007). Stynder (2009) suggested that there were the same amount of browser or specialist grazer ungulate species based on the dental wear. The mesowear results also suggested that browse (fynbos) was more abundant and prominent than what previous research by Klein and Cruz-Uribe (1991) had proposed. Stynder (2009) stated that during the middle Pleistocene, fynbos, substantial $C_3$ grasslands, trees and broadleaved bush would have provided adequate vegetational diversity to account for the extraordinary diversity of EFTM ungulates. The proposed flora rich productive EFTM environment is not seen in the modern Fynbos Biome, as grasses (generally $C_3$ species) are not common in the current EFT environment. Presently in the southern and eastern sections of the Fynbos Biome, $C_4$ grasses are more common (Cowling 1984; Campbell 1985; Moll *et al.* 1984). In contrast to the modern day Fynbos Biome where trees are not present, pollen analysis from the EFTM environment suggests that large trees were present (e.g. Acacia sp. and Schlerocarya sp.) in the palaeoenvironment (Moll et al. 1980; Stynder 2009). The vegetational diversity that had existed in the EFTM environment would have required wetter climatic conditions than those observed today. The soils, which supported trees and broad-leaved bush, had to have been more nutritionally rich. Overall the depiction of the EFTM environment represents an interesting time period in the evolution of the Fynbos Biome.

### 2.7.7 Concluding Remarks

A number of indirect proxies have been used at sites along the southwestern Cape coast in the aim of reconstructing Pleistocene palaeoenvironments. It appears that research into the identification of faunal communities (e.g., Klein 1983b; Klein *et al*. 2007) has highlighted the taxonomic diversity at various sites. Furthermore, studies of wear on ungulate dentition (Stynder 2009) and stable isotopic analysis of faunal remains (Luyt *et al.* 2000; Lehmann *et al.* 2016; Patterson *et al.* 2016) have provided some level of understanding of the diets of palaeo-fauna. What is apparent throughout the studies is that the palaeoenvironment was both different compared to historic and present day environments. When observing the transition from the oldest to the youngest site, it is noted that there has been a decrease in taxonomic diversity. This evidence suggests that the primary productivity of the vegetational environment must have been decreasing through time. Currently there is still a debate on the composition of the middle Pleistocene vegetation community and whether widespread grasslands or mixed vegetation had prevailed during this time period.

This phytolith study will provide direct evidence of the palaeo-flora and as such, will contribute to a greater understanding of the paleoenvironments of EFT and DFT during the Pleistocene. Decreasing ungulate diversity suggests that trees and broadleaved bush may have been disappearing over time, leaving behind a plant community composed of a mosaic of $C_3$ grasses (and occasionally $C_4$ grasses), fynbos, strandveld and renosterveld species. This phytolith analysis will hopefully answer the question of whether there was a significant reduction in the productivity of the region's vegetation community that in turn may have led to a reduction in faunal diversity.

# Chapter 3 : PHYTOLITH ANALYSIS AS A PALAEOENVIRONMENTAL TOOL

This chapter provides a background to phytolith analysis as a means of reconstructing ancient plant communities. In addition to providing a general review, I also address phytolith studies within the South African context.

## 3.1 Introduction

Phytoliths are microscopic silica bodies that are formed in living plants. Plant phytoliths are also referred to as opal phytoliths, grass opal or opaline silica (Runge 1999). They are formed when dissolved silica (soluble monosilicic acid; $Si(OH)_4$) is absorbed through plant roots along with groundwater and other minerals, then transported by transpiration via the vascular tissue (xylem) before being deposited as amorphous silica gel within or between specific plant cells (Piperno 1988; 2006). The shape and size of the phytoliths is determined by the space in which the silica is deposited as silica dioxide ($SiO_2$). Plant species such as grasses, sedges, palms, woody and herbaceous dicots may produce different quantities and forms of phytolith morphotypes (Twiss *et al.* 1969; Piperno 1988, 2006; Bozarth 1992; Ollendorf 1992; Rosen 1992; Berlin *et al.* 2003).

In 1675, Loeuwenhoek identified phytoliths during his research of plant anatomy and physiology. Since the 1970s phytoliths have successfully been used as an environmental proxy (Piperno 1988). Phytolith analyses have been used in research to provide information on the types of plants that occurred (e.g., Alexandre *et al.* 1997, 1999), and the climate that prevailed during certain time periods in the history of a region (e.g., Fredlund & Tieszen 1997; Alexandre *et al.* 1999; Baker *et al.* 2000).

Phytoliths will accumulate in soils and sediments as plant tissue decays. The accumulation of these phytolith assemblages can be used to reconstruct the local vegetation types developed within a

paleoenvironment (Piperno 2006). Phytoliths are inorganic, composed of resistant silica and are likely to remain relatively stable and intact in variable and/or oxidized environments (Rovner 1983), as opposed to pollen which can be broken down by microorganisms (Pearsall 2015). Phytoliths tend to be sturdier than pollens and are likely to survive soil pressures and the affects of shrinking and swelling of clay soils (Pearsall 2015.). Pollens are easily transported by water and wind and therefore more likely to be randomly deposited. As such, pollen assemblages are more prone to reflect macro-environmental vegetation (Rovner 1983; Pearsall 2000). Pollens are also more likely to decompose in moist environments as opposed to phytoliths (Rovner 1988; Pearsall 1982; Piperno 2006; Mulholland 1989). This phenomenon has enabled scientists to investigate past vegetation structures at the local level, based on sediments extracted from archaeological sites (Barboni *et al.* 2010). Potentially, phytoliths, which are classified as plant microfossils, may be invaluable tools for obtaining palaeoenvironmental information when plant macrofossils and pollen are not preserved in sediments.

One of the main limitations in phytolith analyses is that not all plant species produce phytoliths (Piperno 2006). However, Grass Silica Short Cell phytoliths (GSSCs) are produced in large numbers and are easily identified, thus their distribution may provide a reliable tool for reconstructing palaeoenvironments in southern Africa (Mclean and Scott 1999; Grab *et al.* 2005; Scott & Rossouw 2005; Norstrom *et al.* 2009; Rossouw *et al.* 2009; Cordova & Scott 2010; Rossouw & Scott 2011; Cordova 2013).

In phytolith analyses, ‘multiplicity’ and ‘redundancy’ have to be taken into account. Rovner (1971) recognised methodological limitations in using phytoliths due to problems in the identification of phytolith morphotype shapes. As a result of ‘redundancy’ and ‘multiplicity’ in phytolith morphotype shapes (Rovner 1971; Fredlund & Tieszen 1994), one phytolith morphotype can seldom be associated with one plant taxon. To allow for an accurate reconstruction of a palaeoenvironment, phytolith morphotypes must be examined as an assemblage rather than as a

singular entity. In the case of grass phytoliths, rather than being diagnostic at the species level, the morphotypes instead can be linked to different grass subfamilies (Barboni *et al.* 2007).

### 3.2 Preservation Of Phytoliths

The mainly inorganic silica composition of phytoliths makes them extremely durable and resistant to a range of chemical decaying processes (e.g. oxidation in well-drained soils) (Baker 1959; Retallack 1990; Pearsall 2000). Consequently, phytoliths may preserve in ancient soils and sediments as old as the Miocene and Pliocene (Wolde Gabriel *et al.* 2009). A number of factors determine the composition of phytolith assemblages that are preserved in sediments (see Fig.3.1 below). These factors can be separated into two major groups, namely original plant input and pre- and post-depositional taphonomy (Zurro *et al.* 2016).

Phytoliths are incorporated in sediments through a set of processes (Dodd & Stanton 1990; Osterrieth *et al.* 2009; see Fig.3.1) that comprise:

1) Necrolysis, which refers to the decaying and disaggregation of the plant at the time of "death";
2) Biostratinomy, which is the processes that occur once the plant has died but before the phytoliths are buried;
3) Fossil diagenesis, which refers to the combined effects of the biological (bioturbation; termites), chemical and physical processes that may destroy or change the phytolith fossil record.

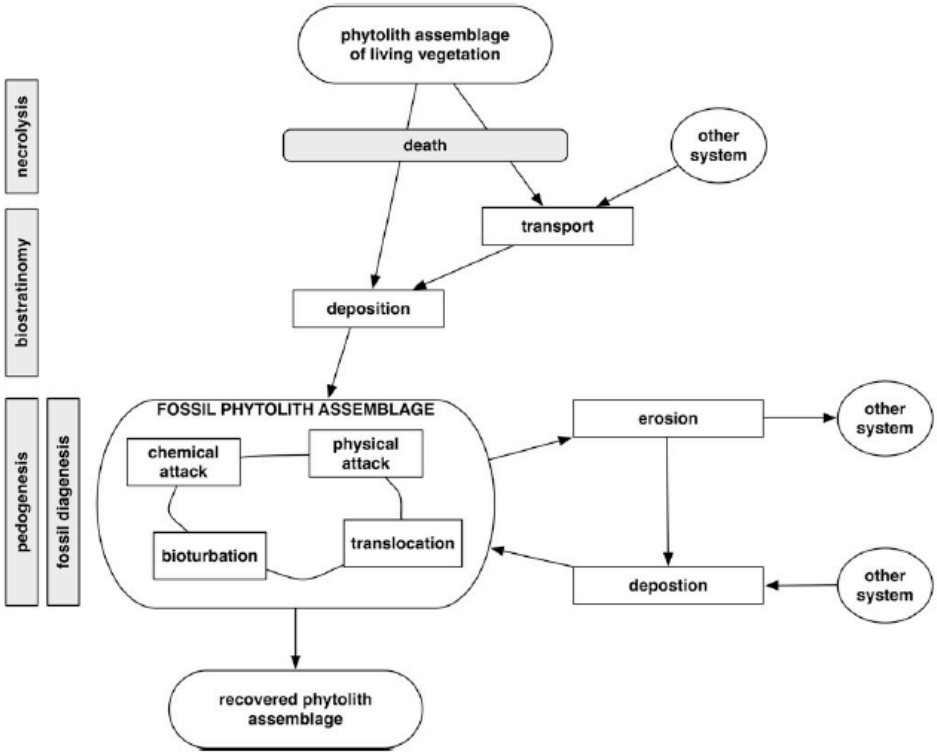


**Fig. 3.1.** *Theoretical diagram of the depositional process of phytoliths in natural deposits (Figure 1 from Osterrieth et al. 2009: 71).*

When analysing phytolith assemblages then, the taphonomy of the research site should be taken into consideration if possible biases are to be identified. The preservation of phytoliths is dependent on shape, surface area, and degree of silicification (Piperno 2006). Large phytolith morphotypes may be subject to degradation due to soil/sediment pressures (Pearsall 2015). Although phytoliths may be present in most soil conditions (e.g. loess (Lu *et al.* 1996), lake mud (Carter 2002) and sand dunes (Horrocks *et al.* 2000)), there are a number of factors that can affect their preservation. Phytolith production and preservation may be influenced to some extent by the environment in which the plant grows, the nature of the soil, the level of concentrations of monosilicic acid in the groundwater, the temperature and moisture (water) content of soils, the pH, the climate (wind), fire, animal and human activities, the maturity of the plant and the rate of plant litter decomposition (Piperno 1988; Bowdery 1999). The alkalinity of sediments may affect the rate of phytolith decay (dissolution), especially if the climate is hot and humid. At pH values of eight or less, the phytoliths are highly insoluble. If the pH is alkaline (pH>=9) for prolonged periods, the rate of dissolution is often accelerated, and phytoliths may partially or completely dissolve (Albert *et al.* 2003; Piperno

2006). For example, research by Albert *et al.* (2003) demonstrated that phytoliths that were exposed to pH values above eight and associated with calcite rich sediments had etched surfaces compared to phytoliths occurring in more acidic sediments.

The interpretation of phytolith assemblages may also be influenced by the high mobility of phytolith morphotypes within the sediments (Dunn 1983; Fishkis *et al*. 2009; 2010; Osterrieth *et al.* 2009). The transport rate of phytoliths can vary depending on the sediment's physical characteristics (Fishkis *et al.* 2010). Lighter pollen particles will also be transported further than heavier phytoliths (Madella & Lancelotti 2012). The phytoliths contained within the sediments are therefore less randomly deposited than pollen (Pearsall 2000), which may travel distances over 100km (Okubo & Levin 1989). Phytolith assemblages may behave differently in dry environments with sparse vegetation and strong winds (e.g. deserts, loess plateaus) as opposed to environments with heavy precipitation and runoff.

### 3.3 The Scope of Phytolith Research

Phytolith analyses have been applied across the world in various research projects. These include applications such as the reconstruction of palaeoenvironments, the study of the domestication of wild plant types (e.g. Piperno 2006), the extraction of phytoliths from dental remains, or coprolites to determine plant types consumed in diets (e.g., Gobetz & Bozarth 2001; Horrocks *et al.* 2004), to identify plant types processed using stone tools (e.g., Kealhofer *et al.* 1999), the types of plants that were processed/stored in ceramics (e.g., Saul *et al.* 2013), and also in the identification of plant fuels used at archaeological sites (e.g., Albert & Marean 2012). More specifically, phytoliths have been used to identify vegetation types growing under specific climatic conditions. Some examples of phytolith research are summarised below.

In China, Lu *et al.* (1996) used phytolith assemblages collected from a loess sequence to demonstrate the possible evolution of vegetation over the last 150 000 years for the region. In their study of the plant phytoliths, they were able to link climatic variations to the phytolith record. They were also able to relate vegetation types to variations in temperature and precipitation.

In Central America, Piperno and Jones (2003) used phytolith records from the Pacific coastal plain of Panama, to show landscape changes and climatic variations during the late Pleistocene. Using phytoliths, they were able to demonstrate how the landscape changed from tropical deciduous forest through to dry savanna-like vegetation type.

Parolin, Rasbold and Pessenda (2014) carried out a palaeoenvironmental reconstruction of peat deposits in the State of Parana, Brazil. They utilised grass phytoliths (climatic index, Ic%; aridity index, Iph% and water stress index, Bi%) combined with carbon and nitrogen stable isotope analyses to establish environmental changes from the late Pleistocene through to the middle Holocene. Their research enabled them to demonstrate the climate changes from drier through to more humid conditions.

In New Zealand, Carter (2002) used phytoliths extracted from a sediment core in Hawkes Bay to demonstrate changes in the vegetation types from the last interglacial through to present day. Carter was able to show that the phytolith record reflected that during warmer periods grasses and sedges were present, and that during the colder periods woody taxa dominated the phytolith assemblages.

In the context of Africa, numerous studies conducted across the continent have emphasised the value of using phytoliths for reconstructing paleoenvironments (e.g. Alexandre *et al*. 1997; Runge 1999; Albert *et al.* 2006; Bamford *et al.* 2008; Fahmy 2008; Neumann *et al.* 2009; Rossouw 2009; Barboni *et al.* 2010; Mercader *et al.* 2010; Albert & Marean 2012; Garnier *et al.* 2012; Novello *et al.* 2012, 2015). Two significant studies that relate to this study are outlined below.

Of major significance is the research undertaken by Albert *et al.* (2006), who analysed phytolith assemblages from Pliocene and Pleistocene sediment samples taken from Olduvai Gorge in Tanzania. They examined modern and fossil phytolith assemblages present in the sediment samples and were able to establish that wood/bark phytoliths were more resistant to degradation than those of sedges and grasses. They were able to highlight the significance of soil chemistry in the preservation of phytoliths. High alkalinity soils tended to result in the degradation of phytolith assemblages over time. Understanding the above relationships is important in drawing conclusions about the palaeo-vegetation.

Mercader *et al.* (2010) examined grass phytolith assemblages found in modern sediments in the Niassa Rift region of Northern Mozambique. They examined the amount of silica production in the $C_3$ and $C_4$ type grasses and highlighted the potential for the long term preservation of phytoliths in sediments, which made them a useful tool in reconstructing ancient plant communities and plant-human interactions. The concentration and preservation of phytoliths in modern and ancient sediments was examined. They noted the decrease in the number of phytoliths preserved in fossil sediments and that this should be taken into account when reconstructing palaeoenvironments. They emphasised that the absence of certain phytoliths may not relate to the presence or absence of vegetation plant types.

In South Africa, fossil grass phytoliths were used as a proxy for palaeoenvironmental reconstruction at the Langebaanweg E Quarry (Rossouw *et al.* 2009), Tswaing crater (McLean & Scott 1999) and at Florisbad (Scott & Rossouw 2005). Rossouw (2009) created the first plant reference collection that mainly focused on Poaceae (grass) species from South Africa and developed a standardized model for interpretating GSSC phytolith assemblages. In addition, Cordova and Scott (2010) examined the potential of diagnostic phytoliths in the Poaceae, Cyperaceae and Restionaceae family. Albert and Marean (2012) included a phytolith analysis in their research into the interpretation of modern human evolution in the Greater Cape Floristic Region (GCFR) (Pinnacle

Point). Cordova (2013) highlighted the potential of using graminoid phytolith morphotypes as proxies for reconstructing past winter rainfall in South Africa. Esteban et al. (2016) showed that modern plant phytolith concentration was related to the dominant vegetation types rather than to the type of soils that occurred along the south coast of South Africa. Short summaries of the results from some of the South African research projects are provided below.

Langebaanweg E Quarry:

A phytolith analysis was initiated by Rossouw *et al*. (2009) on the Langebaanweg E Quarry Varswater Formation in an attempt to reconstruct the palaeoenvironment of the area during the Miocene-Pliocene transition. Four diagnostic grass phytolith morphologies were recognised in the sediment samples, namely bilobates, saddles, rondels and trapeziform phytoliths. Restionaceae (Cape reed grasses) and Areceaceae (palms) phytoliths were also identified. Three units within the Varswater formation supported the theory that $C_3$ grasses already prevailed during Late Miocene/Early Pliocene times at Langebaanweg. Whilst the fourth (last) unit sampled, yielded saddle-shaped grass phytoliths characteristic of $C_4$ grasses (Gibbs Russell 1988). This $C_4$ phytolith evidence confirmed that there had been major changes in the characteristics of the grassland composition, which may have occurred towards the end of the Miocene when climatic conditions changed from tropical to cooler conditions (Scott 1995). The identification of Restionaceae phytoliths confirmed that South Africa's southwestern coast was becoming drier and more open during the Early Pliocene (Franz-Odendaal & Kaiser 2003).

Pretoria Saltpan:

McLean and Scott (1999) showed that the proportions of different phytolith morphotypes from sediments could be used as a proxy to interpret past environmental processes, including seasonal changes such as rainfall and temperature that had affected the Pretoria saltpan. Due to the scarcity of organic matter such as pollen, their phytolith research had filled in gaps in the understanding of the history of the vegetation in the surroundings of the crater (McLean & Scott 1999). In addition to

the complications in determining the source of the phytoliths and the consequent regional interpretations, there was a low count of grass phytoliths, which made the analysis less reliable. The identification of a high concentration of phytolith morphotypes associated with the Festucoideae (Pooideae) grass subfamily however, was an indication that cooler growing seasons for grasses were actually more common in the study area during the middle to late Pleistocene.

Florisbad:

A pilot study was undertaken using grass phytoliths extracted from the dental cavities of fossil bovid teeth (Rossouw 1996), fossilized hyaena coprolites and soil samples, to assist in the reconstruction of the late Quaternary period grassland ecology at Florisbad. This late middle Pleistocene site consisted of an abundance of fauna and the fossilised remains of an archaic human that supported the existence of a $C_4$ grass-dominated environment. However, there was evidence that contamination of the fossil teeth from the surrounding organic matrix ($C_3$ grasses) currently found in the area had occurred. More recent research by Scott and Rossouw (2005) suggested that the available pollen and phytolith data together with the identification of the Xanthoxylum wood emphasised the need for more extensive research into the palynology, phytolith assemblages and isotope analysis of the site.

Central and western South Africa:

The assessment of phytoliths from central and western South Africa by Cordova and Scott (2010) showed that the geographic variability in selected grass silica short cells, sedge and restio phytoliths had the potential to indicate summer temperatures, total annual precipitation, rainfall seasonality and variability. This research established a general classification of diagnostic Restionaceae and Cyperaceae phytoliths from identified plant specimens.

Cordova (2013) attempted to create a proxy for reconstructing past winter rainfall in the Cape region of South Africa by identifying graminoid phytolith morphotypes. Phytolith assemblages

were extracted from sediment samples collected along two transects across the winter, all-year (ARZ), and summer (SRZ) rainfall zone of South Africa. The results demonstrated that the highest frequencies of the diagnostic $C_3$ GSSC morphotypes increased with winter rainfall. Despite certain limitations, Cordova (2013) demonstrated that $C_3$ type GSSCs and Restionaceae phytolith could potentially be used to reconstruct the extent of winter rainfall during the colder stages of the Pleistocene, especially if a study area had a larger number of reference material and tighter geographical sampling.

South coast of South Africa (Greater Cape Floristic Region):

At Pinnacle Point 13B Cave (Mossel Bay), Albert and Marean (2012) used phytoliths to identify the types of plants used as fuel in hearths by Early *Homo sapiens* at the MSA. The phytolith analysis was also used to identify the different parts of the plants used by the early *Homo sapiens* as fuel in their hearths for fires, or other fire-related activities such as cooking.

Esteban *et al*. (2016) studied phytoliths extracted from modern surface soil samples from a study area within an area in the Greater Cape Floristic Region to characterise Fynbos vegetation types on the south coast of South Africa. Their study showed the potential and limitations for using these phytolith assemblages. Grass phytoliths were found to be present in the modern soil samples despite being a minor component in the modern day vegetation types. Fynbos vegetation was found to have distinctive phytoliths. However, if grasses were growing with the fynbos, it was not possible to identify Fynbos vegetation accurately.

More recently, Esteban (2016) studied phytolith assemblages from the MSA site of Pinnacle Point 5-6 (Mossel Bay) to investigate how the first modern humans exploited plants as well as to reconstruct the palaeoenvironmental conditions on the south coast of South Africa.

Finally, the first modern plant reference collection of geophytes and eudicotyledonous plants from the GCFR was created by Esteban *et al*. (2017).

### 3.4 Summary And Conclusion

This chapter has provided a short history of the first application of phytolith research, the process of phytolith formation and factors that affect phytolith preservation. The value of phytolith analyses as a tool in palaeoenvironmental reconstructions has been demonstrated in a number of regional settings. In drawing conclusions from phytolith assemblages and analyses, one needs to take into account the degree to which types of phytoliths are preserved (e.g. wood/bark versus grass phytolith preservation). Soil geochemistry, specifically pH that will influence the degree to which phytoliths will be preserved in sediments, is an important consideration. Therefore the absence or presence of certain phytoliths may not be related to the presence or absence of vegetation plant types.

# Chapter 4 : MATERIALS AND METHODS

## 4.1 Introduction

There are several processes involved in the extraction of phytoliths from sediment samples through to microscopic analysis. Specific methods used by researchers are dependent on the ecosystem and the information required about that environment. This research project entails an investigation of the phytolith assemblages of EFT and DFT, with the intention of reconstructing the vegetation community that existed along the South African southwest coast during the middle to late middle Pleistocene. The analytical process will involve the identification, quantification and interpretation of the phytolith assemblages occurring in sediment samples collected from various localities at EFT and DFT. In the following sections, the field sampling, extraction and analytical techniques will be discussed.

## 4.2 Sample Materials

Sample materials included modern plant specimens used for the construction of a reference collection, and sediment samples from modern and fossil-bearing contexts. These samples were collected and analysed as set out below.

### 4.2.1 Modern Reference Collection

The production and abundance of plant phytoliths varies amongst angiosperms, gymnosperms and pteridophytes. Plants can either be silica accumulators, thereby producing phytoliths, or non-accumulators that are void of phytoliths (Piperno 2006). Research has shown that plant species belonging to the same family tend to have a similar pattern of phytolith production (Blinnikov *et al.* 2002; Piperno 2006). Monocotyledons are considered to be the best accumulators of phytoliths, whilst dicotyledons are regarded as poor silica accumulators. Therefore in general, within the same environments, dicotyledons will produce less phytoliths than monocotyledons (Piperno 2006). The

Poaceae (grass) family in particular, produces large numbers of distinctive phytoliths, which can be identified beyond family level (Twiss *et al.* 1969; Piperno 2006).

In addition to the modern reference collection that was created for this study, other reference material was used to assist in the identification of grass phytoliths in the sediment samples from EFT and DFT (e.g., Bremond *et al.* 2008; Barboni & Bremond 2009; Neumann *et al.* 2009; Rossouw *et al.* 2009; Blinnikov *et al.* 2013; Garnier *et al.* 2012). Several grass silica short cell (GSSC) phytolith images from Rossouw's (2009) dissertation, as well physical reference material stored at the National Bloemfontein Museum, were also used in the identification of fossil phytolith assemblages. With reference to the non-grass vegetation component, the study used published pictures of phytolith morphotypes (Rovner 1971, 1983; Bozarth 1992; Blinnikov 1999; Runge 1999; Barboni *et al.* 1999, 2007; Albert *et al.* 1999, 2000, 2003, 2006, 2009, 2015; Albert & Weiner 2001; Albert & Bamford 2012; Blinnikov *et al.* 2002; Stromberg 2004; Madella *et al.* 2005; Piperno 2006; Gu *et al.* 2008; Mercader *et al.* 2009, 2011; Nuemann *et al.* 2009; Messager *et al*. 2010; Stromberg & McInerney 2011; Albert & Marean 2012; Novello *et al*. 2012; Das *et al*. 2013; Aleman *et al.* 2014; Watling *et al.* 2015; Collura & Neumann 2016; Esteban *et al.* 2016).

#### 4.2.1.1 Sampling Procedures

To aid with the identification of EFT and DFT phytolith assemblages, I created a reference collection derived from plants currently growing along the southwestern Cape coast, as well as a number of plants from the modern savanna woodland biome. I identified several plant taxa from the fynbos region that are palatable to browsers (see Table 4.1; Njenga 2005; City of Cape Town (CoCT) 2011). The website (www.plantzafrica.com) contains relevant information that aided this study. The American Society of Mammalogists' website (www.mammalsociety.org) was also useful due to the fact that it listed articles that focused on the diets of a large number of faunal species (Van Zyl 1965; Grunow 1980; Owen-Smith & Cooper 1987; MacLeod *et al*. 1996; Ganqa

*et al.* 2005). Additionally, a number of commonly browsed plant taxa (tree and broadleaved bush taxa) consumed by browsers in modern South African savannah woodland environments were also identified and sampled.

Research was conducted into the patterns of phytolith production and the taxonomic significance in modern plant species throughout the world (Piperno 2006). The plant families analysed in this study were classified in the following groups:

1. Plant families that are known to produce large numbers of phytoliths and that have distinct family and subfamily characteristics:
   - Monocotyledons: Poaceae (grass)
   - Eudicots: Asteraceae (daisy)

2. Plant families that are known to produce fewer phytoliths but are family-specific in shape and/or have specific shapes diagnostic of a specific growth habitat:
   - Eudicots: Euphorbiaceae

3. Plant families in which phytolith production varies greatly among the different subfamilies and tribes with limited diagnostic shapes:
   - Eudicots: Fabaceae (legumes), Malvaceae (mallows)

4. Plant families in which phytoliths have not been identified or where their development is uncommon and non-diagnostic:
   – Eudicots: Apocynaceae, Solanaceae, Anacardiaceae, Myricaceae

Piperno (2006) has not reported the occurrence of phytoliths in the plant families Gerniaceae, Santalaceae, and Asphodelaceae that form part of the modern reference collection.

The main objective of the current research was to establish which modern plants in the reference collection produced phytoliths and if possible, to identify diagnostic forms in the sediment samples

collected from DFT and EFT. Plants were included in the modern reference collection if they grow in the region of the sites today. In addition, a sample of extant savanna-woodland species were selected to investigate Klein *et al*.'s (1999, 2007) suggestion that the EFT and DFT vegetation community in some ways resembled extant savanna-woodland vegetation communities. Samples were obtained from plant nurseries and DFT field locations.

Plant identification was confirmed by literature references (Van Oudtshoon 1992; Manning 2007) and communication with Biology students from the Botany Department of the University of Kwazulu Natal (Doarsamy, S., Mtshali, H., Lansdowne, A. and Scholfied, J., Personal communication, July 2016). Twenty different plant species were collected from the study area and nearby coastal region as well as from the savannah woodland of the Kruger National Park.
A list of the plant species included in the modern reference collection is given in Table 4.1. The plant species that produced phytoliths are discussed further in section 5.2 of the results chapter.

**Table 4.1** *Plant species analysed, from which phytoliths were extracted, and habitats in which the species are found in South Africa.*

| Sample No. | Taxon | Common Name | Food Type | Habitat | Plant Part Sampled |
|---|---|---|---|---|---|
| 1-2 | *Lessertia (Sutherlandia) frutescens* (Fabaceae family) | Balloon Pea (Kankerbos) | Palatable browse shrub | Dry areas (West Coast) | Leaf and stem |
| 3-4 | *Carissa macrocarpa* (Apocynaceae family) | Natal Plum | Shrub eaten by bushbuck | Coastal bush, forests and sand dunes (East Coast) | Leaf and stem |
| 5-6 | *Osteospermum (Chrysanthemoides) moniliferum subsp. monilifera* (Asteraceae family) | Brother-berry (Boetabessie) | Semi-succulent shrub; palatable browse for Bushbuck | Fynbos and strandveld | Leaf and stem |
| 7-9 | *Acacia karroo* (Fabaceae family) | Sweet Thorn | Tree; palatable to blesbok, Blue gnu, White-tailed gnu, buffalo, | From Western Cape through to Zambia and Angola; low lying areas to Highveld | Leaf, branch stem and seed pod |

| | | | | | |
|---|---|---|---|---|---|
| | | | Burchell's zebra, springbok, Greater kudu, and Giraffe | -Kruger | |
| 10-13 | *Lycium afrum* (Solanaceae family) | Kraal honey thorn | Shrub | Sandy, coastal flats and Shale Renosterveld | Leaf, stem, fruit and flowers |
| 14-15 | *Metalasia muricata* (Asteraceae family) | White Bristle Bush | Shrub, palatable browse | Coastal to mountainous regions. Tolerant to poor sandy soils. (West Coast) | Leaf and stem |
| 16-17 | *Grewia occidentalis* (Malvaceae family) | Cross-berry | Shrub eaten by blesbok, Blue gnu, White-tailed gnu, buffalo, Burchell's zebra, springbok, Greater kudu, and Giraffe | Western Cape up to Zimbabwe and Mozambique; drought-hardy | Leaf and stem |
| 18-20 | *Eriocephalus punctulatus* (Asteraceae family) | Wild Rosemary (Kapokbos) | Shrub eaten by wild animals | WRZ, Greater Cape Floristic Region | Leaf, stem and flowers |
| 21-23 | *Dichrostachys cinerea* (Fabaceae family) | Sickle Bush | Tree; blesbok, Blue gnu, White-tailed gnu, buffalo, Burchell's zebra, springbok, Greater kudu, and Giraffe | Warm, dry savannas.<br><br>-Kruger | Leaf, branch stem and seed pod |
| 24-25 | *Acacia nigrescens* (Fabaceae family) | Knob Thorn | Tree; blesbok, Blue gnu, White-tailed gnu, buffalo, Burchell's | Savannah regions; drought resistant.<br><br>-Kruger | Leaf and branch stem |

| | | | | | |
|---|---|---|---|---|---|
| | | | zebra, springbok, Greater kudu, and Giraffe | | |
| 26-28 | *Grewia flavescens* (Malvaceae family) | Sandpaper raisin | Tree | Bushveld, open woodland and thicket; temperate climates with moderate summer rainfall. -Kruger | Leaf, stem and seed pod |
| 29-31 | *Acacia (Vachellia) nilotica* (Fabaceae family) | Scented-pod Acacia | Tree | Wooded grassland and scrub escarpment, forests and low-lying forest, in deep soil and along rivers. -Kruger | Leaf, branch stem and seed pod |
| 32-33 | *Acacia (Vachellia) tortilis* (Fabaceae family) | Umbrella Thorn | Tree; blesbok, Blue gnu, White-tailed gnu, buffalo, Burchell's zebra, springbok, Greater kudu, and Giraffe | Tolerate high alkalinity, drought, high temperatures, sandy & stony soils. Savanna woodland -Kruger | Leaf and branch stem |
| 34-35 | *Pelargonium spp. (P.capitatum)* (Gerniaceae family) | rose-scented pelargonium, | Shrub | Sand dunes or low hillsides near the coast. Also found growing in disturbed areas. | Leaf and stem |
| 36-38 | *Metalasia densa* (Asteraceae family) | Blombos | Shrub | Coastal to mountainous regions. Tolerant to poor sandy soils. | Leaf, stem and flowers |
| 39-40 | *Searsia spp. (S. lucida)* (Anacardiaceae family) | glossy crowberry (blinktaaibos) | Shrub | Coastal dunes, bush and along watercourses, it is also found inland | Leaf and stem |

| | | | | | |
|---|---|---|---|---|---|
| | | | | among fynbos vegetation. | |
| 43-44 | *Morella cordifolia* (Myricaceae family) | Dune waxberry | Shrub | Coastal sands and dunes, and sandy flats | Leaf and stem |
| 45-46 | *Thesium spp.* (Santalaceae family) | | Shrub | Coastal dune thicket | Leaf and stem |
| 47-48 | *Trachyandra divaricate* (Asphodelaceae family) | False Onion Weed (Duinekool) | Geophyte | Coastal sand dune | Leaf and root |
| 49-50 | *Ehrharta villosa* var. villosa (Poaceae family) | Dune Ehrharta | | Grows on coastal sand dunes and up to 1km inland | Leaf |

*Samples 41 and 42 were excluded from this study

#### 4.2.1.2 The Extraction Of Phytoliths From Modern Plants

Within an individual plant, the morphology of the phytoliths it contains will vary depending on the part of the plant (Albert *et al.* 1999, 2000, 2003; Albert & Weiner 2001). As a result, each part of the plant was analysed separately where possible. Phytoliths were extracted from leaves, woody stems, pods, fruit and flower material.

The plant parts were subjected to standard dry-ashing procedures in order to extract phytoliths (Parr *et al.* 2001). This process was completed in a laboratory at the National Museum in Bloemfontein. Dry-ashing procedures were chosen over wet oxidation methods, as the former process does not require the use of hazardous chemicals and/or fume hood (Piperno 2006). The dry-ashing procedures leave less residual plant matter compared to the wet oxidation method (Parr *et al.* 2001).

**Dry-ashing Procedure**

The plant parts were rinsed with distilled water to remove soil and possible contaminants. Plant parts were placed into labeled 200ml (25x49mm) glass vials. Vials were then placed into an electric furnace and subjected to a temperature of 500°C for approximately seven hours over the course of four days, after which the samples were suitable for further processing. While the furnace was on,

temperatures were maintained at a constant 500°C to ensure that no morphological changes in phytoliths occurred. It has been noted that morphological changes take place when temperatures approached 600°C (Parr *et al.* 2001, Piperno 2006).

The vials of burnt plant residue were placed on a warmed up hot plate after which 10% HCl was added to each sample. Changes in colour were recorded. The samples were transferred to 15ml test tubes. The test tubes were weighed and distilled water added to ensure centrifuge equilibrium was established. The samples were centrifuged at 2500rpm for three minutes. The supernatant was discarded, after which the test tubes were weighed and centrifuged again. The process was repeated for a total of three times to ensure that the HCl had been removed from the samples.

Samples that were too dark in colour were treated with hydrogen peroxide. This was to ensure that the samples could be viewed under a microscope using transmitted light. Where samples had to be treated with hydrogen peroxide, the sample was transferred from the test tube into a beaker, which was then placed on a warmed up hot plate. A small amount of hydrogen peroxide was added to the beaker. The samples were removed from the hot plate when the colour had lightened. The hydrogen peroxide then had to be washed out of the samples. These samples were then centrifuged at 2500rpm for three minutes, re-suspended in distilled water and centrifuged a further three times.

The supernatant was then discarded from the test tubes and a small amount of distilled water was added. A pipette was used to transfer the silica residue onto microscope slides. (Note: a separate pipette was used for each sample to eliminate contamination.) The remaining sample was transferred to a vial for future examination.

### 4.2.2 Sediment Samples

In order to ensure the highest possible confidence level in collection of the sediment samples, attention was paid to the sediment structure and stratigraphy within the deposit being interpreted. Care was taken in extracting the samples from the sediment profile, ensuring that the specific sediment layers (characterised by colour, texture and composition) were not mixed. This was to ensure that the extracted phytolith assemblage was representative of the specific stratigraphic layer.

#### 4.2.2.1 Collection of Sediment Samples

Samples were collected from 2-meter deep shovel test pits (STPs), where recognizable stratigraphic layers were identified and recorded (see geology section 2.4 in Chapter Two). To limit contamination within the pits, the exposed walls of the stratigraphic level were scraped using a clean trowel to remove possible modern wind-blown phytoliths.

A representative sample was collected from each homogenous stratigraphic layer using a 45mm (inner diameter) PVC tube that was driven approximately 200mm horizontally into the sediment layer. Precautions were taken to ensure that samples were not taken from areas where there was evidence of possible contamination caused by plant root and animal activity. When working on the samples in the laboratory, the first 50mm of the sample was discarded to avoid contamination after which a 50g sample was collected from the proceeding portion of the sample.

In total, nineteen samples were collected from EFT during 2014 and 2016 (Table 4.2). Nine samples were collected from DFT in 2016 (Table 4.3). A description of the sediment samples and their associated stratigraphic layer is provided below.

Four modern surface samples were collected from EFT and one modern surface sample from DFT. The modern surface samples were collected adjacent to the shovel test pit sites. This entailed taking

a surface scraping of the uppermost sediment layer. The modern samples were collected to compare the modern surface phytoliths with the fossil sediment phytoliths.

#### 4.2.2.1.1 Elandsfontein Sediment Sampling

The locations of the EFT sediment sampling bays are given in the figure below (Fig.4.1). Sampling "bays" refer to deflation hollows between large modern dune crests (Braun *et al.* 2013). Table 4.2 lists the sample numbers, bay number, extraction information and the stratigraphic context of the sediment samples from EFT. Photographs and diagrams of the EFT STP sample sites are shown in Figures 4.2-4.5.

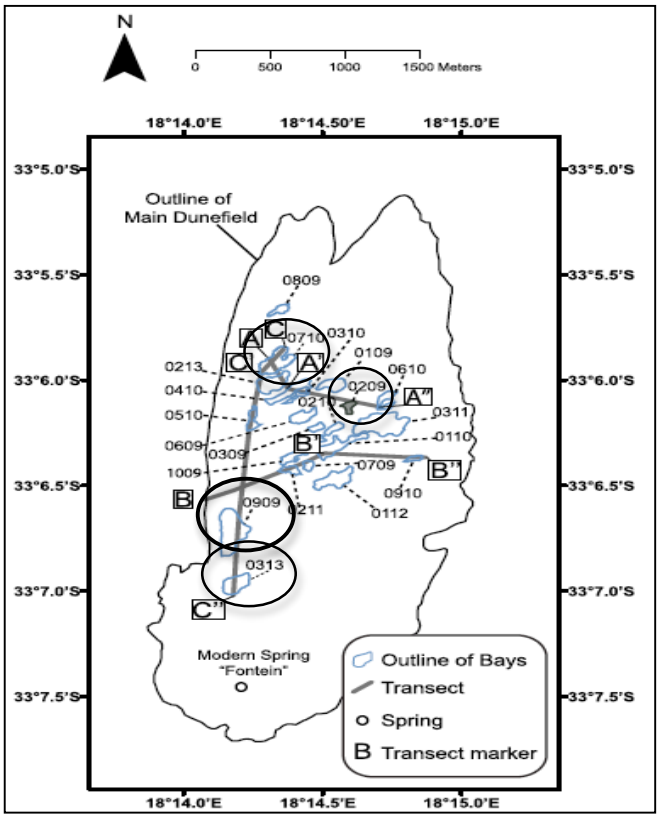


**Fig. 4.1.** *Site map shows the location of bays. Black circles outline Bay 0209, Bay 0909, Bay 0710 and Bay 0313 (Braun et al. 2013: 148).*

**Table 4.2** *Sediment samples from EFT.*

| Lab Sample Number | Bay | Extraction Information | Stratigraphic Context |
|---|---|---|---|
| EFT1.1 | 0209 | STP 527 (# 9837) | Above white nodular area |
| EFT1.2 | 0209 | STP 527 (# 9836) | In lower nodular layer |
| EFT1.3 | 0209 | STP 527 (#9835) | In upper nodular layer |
| EFT1.4* | 0209 | STP 527 (#9850) | Modern |
| EFT2.1 | 0909 | STP 530 (#9757) | Higher in artefact horizon |
| EFT2.2 | 0909 | STP 530 (#9756) | Lower in artefact horizon |
| EFT2.3* | 0909 | STP 530 (#9758) | Modern |
| EFT3.1 | 0710 | STP 528 (# 9754) | Taken from locality where artifacts had been recovered |
| EFT3.2* | 0710 | STP 528 (# 9753) | Modern sample |
| EFT4.1 | 0313 | STP 650 (#61063) | Coarse sand above white nodular layer |
| EFT4.2 | 0313 | STP 650 (#61064) | Calcareous sand below white nodular layer |
| EFT4.3 | 0313 | STP 652 (#61065) | Within white nodular layer |
| EFT4.4 | 0313 | STP 522 (# 9703) | Above nodular layer |
| EFT4.8 | 0313 | STP 522 (# 9704) | In upper nodular layer |
| EFT4.9 | 0313 | STP 522 (# 9705) | In lower nodular area |
| EFT4.10* | 0313 | STP 522 (# 9702) | Modern sample |

**Note:** The sediment samples EFT4.5- EFT4.7 were removed due to uncertainty of location.

**Bay 0209**

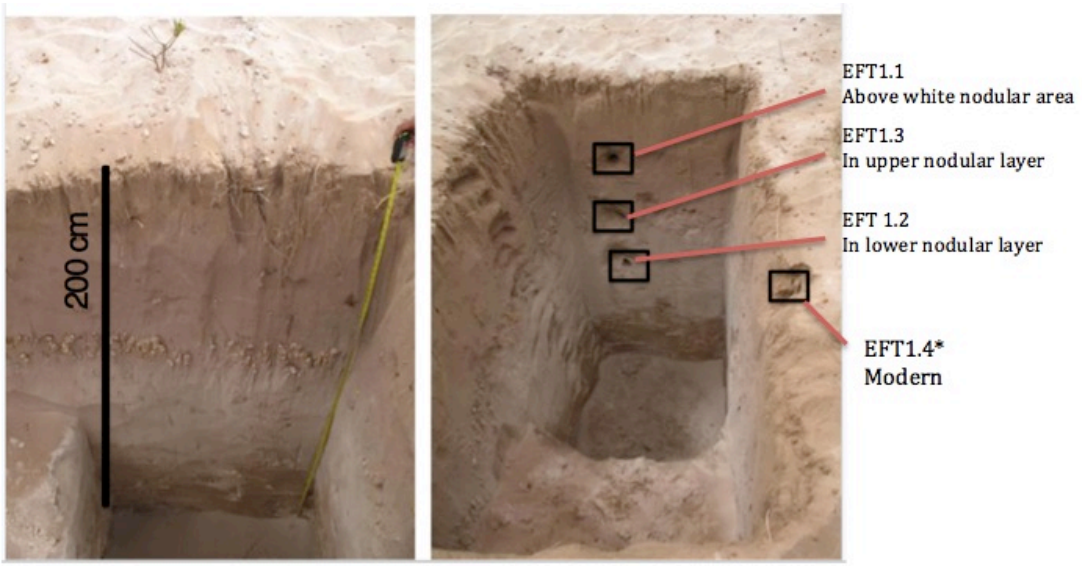


**Fig. 4.2**. *Photograph of STP 527 from Bay 0209 highlighting the location of the phytolith sediment samples.*

**Bay 0909**

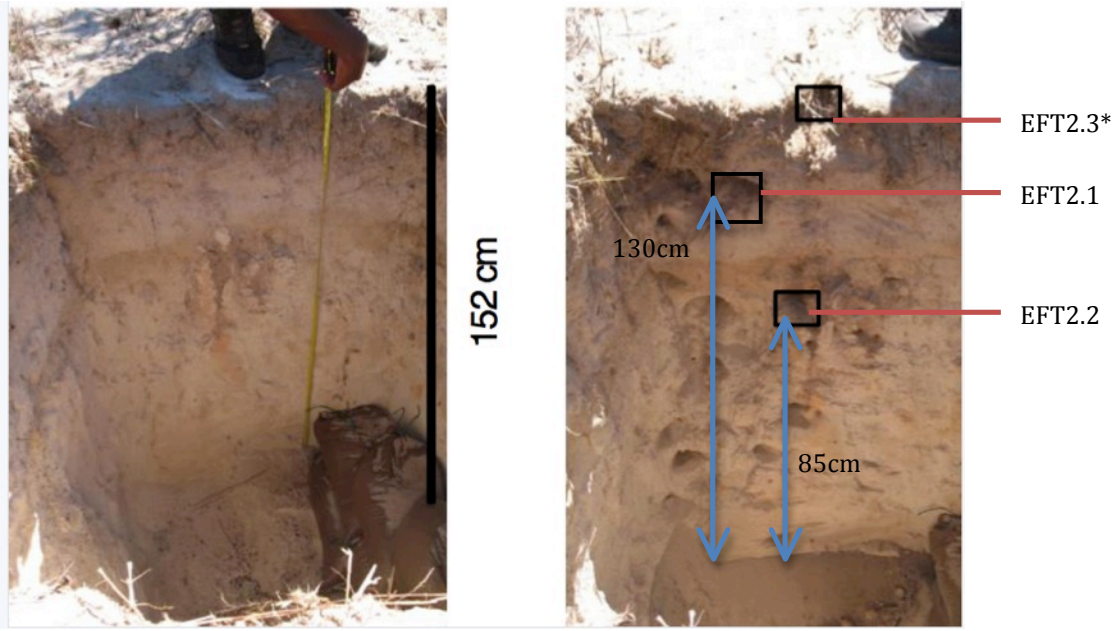


**Fig. 4.3.** *Photograph of STP 530 from Bay 0909 highlighting the location of the phytolith sediment samples.*

**Bay 0710**


**Fig. 4.4.** *Photograph of STP 528 from Bay 0710 highlighting the location of the phytolith sediment samples.*

**Bay 0313**


**Fig. 4.5.** *Photograph of STP 522 from Bay 0313 highlighting the location of the phytolith sediment samples.*

**EFT Stratigraphic Horizons**

1. Modern Sediment Horizon

Modern sediment samples were collected from Bay 0209 (EFT1.4), Bay 0909S (EFT2.3), Bay 0710 (EFT3.2) and Bay 0313NW (EFT4.10).

2. Coarse Upper Pedogenic (Ferruginous) Sand Horizon (above white nodular horizon)

Two samples were collected from Bay 0313NW (EFT4.1; EFT4.4) and one sample from Bay 0209 (EFT1.1).

3. White Nodular (Calcrete) Horizon

One sample was collected from Bay 0313NW (EFT4.3).

4. Artefact/Fossil Horizon Within White Nodular Horizon

One sample was collected from Bay 0710N (EFT3.1).

5. Higher in artefact/fossil horizon (associated with white nodular horizon)

One sample was collected was collected from Bay 0209S (EFT1.3), one sample from Bay 0909S (EFT2.1) and one sample was collected from Bay 0313NW (EFT4.8).

6.) Lower in artefact/fossil horizon (associated with white nodular horizon)

One sample was collected from Bay 0209 (EFT1.2), one sample was collected from Bay 0909S (EFT2.2) and one sample was collected from Bay 0313NW (EFT4.9).

7.) Calcareous quartz sand (carbonate cemented quartz sand) below white nodular horizon

One sample was collected from Bay 0313NW (EFT4.2).

#### 4.2.2.1.2 Duinefontein Sediment Sampling

Table 4.3 lists the sample numbers, sample locality, extraction information and the stratigraphic context of the sediment samples from DFT. A diagram of the general stratigraphy of a DFT STP is shown in Figure 4.6.

**Table 4.3.** *Sediment samples from DFT*

| Lab Sample Number | Sample Locality | Extraction Information | Stratigraphic Context |
|---|---|---|---|
| DFT1.1 | DFT1 | North wall of STP | In leached out orange horizon; below calcareous fossil/artefact horizon |
| DFT1.2 | DFT1 | West wall of STP | Within calcrete horizon |
| DFT2.1 | DFT2, West of current excavation | North wall of STP | In pale yellow/orange sediment |
| DFT2.2 | DFT2 | South wall of STP | In orange sediment (in Klein excavation) |
| DFT2.3 | DFT2 | South wall of STP | Below orange sediment, within yellow sediment |
| DFT2.4 | DFT2, North of current excavation | North wall of STP | Ferricrete horizon |
| DFT2.5 | DFT2, North of current excavation | North wall of STP | Below red sediment; in yellow sediment |
| DFT2.6 | DFT2, North of current excavation | North wall of STP | Within red sediment |
| DFT2.7 | DFT2, West of current excavation | Taken from surface near sample DFT2.1 | White modern surface sand |

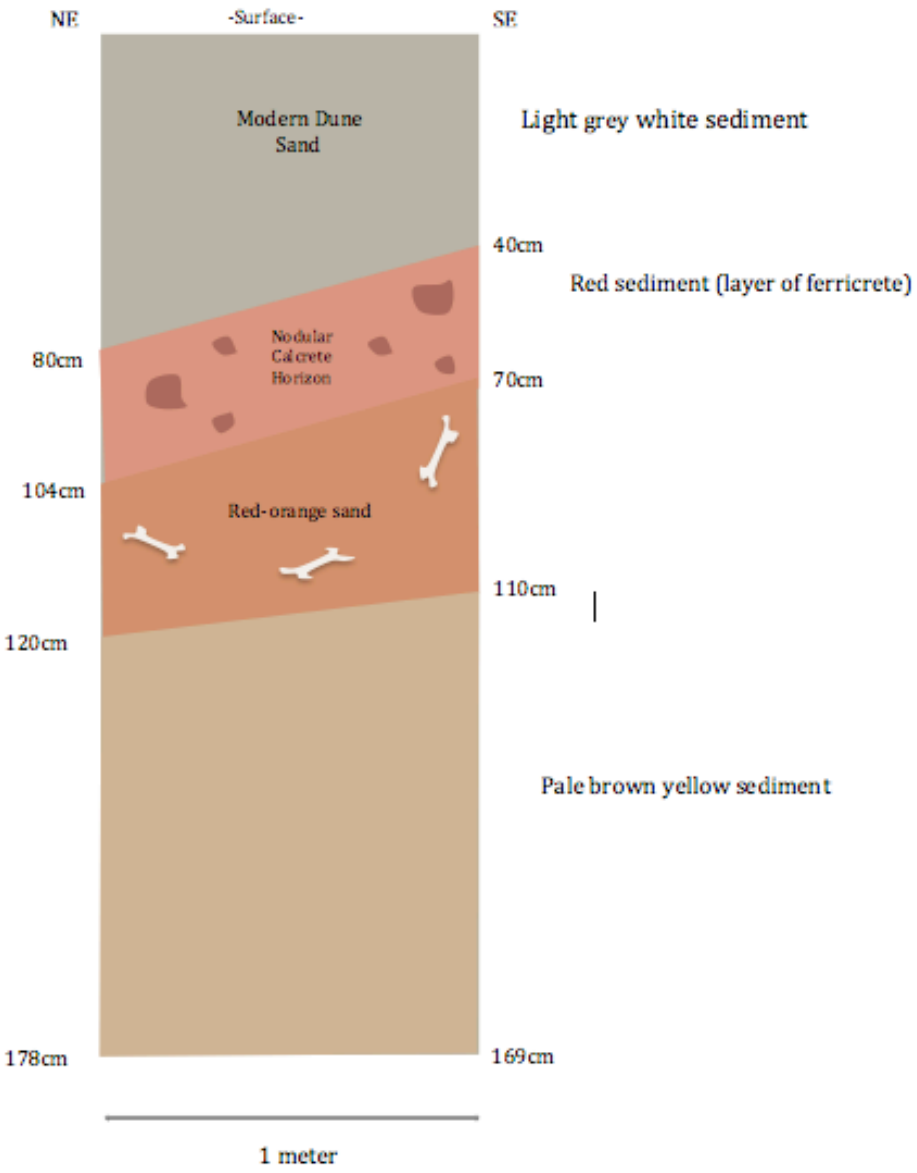


**Fig. 4.6.** *DFT stratigraphy schematic.*

**DFT Stratigraphic Horizons**

1. Modern Sediment

One modern sediment sample was taken to the west of sample DFT2.1 (DFT2.7).

2. White Nodular Horizon (Calcareous Sand)

One sample was taken from DFT1 (DFT1.2).

3. Ferricrete Horizon

One sample was collected from DFT2 (DFT2.4).

4. Red Sediment

One sample was collected from DFT2 (DFT2.6).

5. Pale yellow-orange horizon below calcareous horizon (associated artefact/fossil horizon; possible leaching).

One sample was collected from DFT1 (DFT1.1) and one sample was collected from DFT2 (DFT2.1).

6. Orange-red horizon (minimal leaching)

One sample was collected from DFT2 (DFT2.2).

7. Below orange-red horizon in yellow sediment

Two samples were collected from DFT2 (DFT2.3; DFT2.5).

#### 4.2.2.2 Phytolith Extraction From Sediment Samples

Sediment samples contain phytoliths, soil particles, organic materials and minerals. As a result, the identification and quantification of phytoliths extracted from soils tends to be a lengthy process. Specific procedures are required to be able to separate phytoliths from soil prior to them being grouped together as a phytolith assemblage (Piperno 2006). A series of steps to isolate the phytoliths from the sediment sample were followed that were dependent on the type and condition of the sediment samples. A number of processes were carried out to ensure that the phytoliths were released from the soil matrix, and other materials such as carbonates and organics were removed from the sample. This enabled clearer identification of phytolith morphotypes.

The technique used in this study is based on published techniques (Lentfer & Boyd 2000; Horrocks 2005). Guidance on extraction methods was also provided by Dr Lloyd Roussouw. By using standard laboratory procedures and ensuring that human error was kept to a minimum, the resulting phytolith assemblages should be unbiased or at least affected by the same errors. To ensure that samples were not contaminated, each lab sample was processed using separate, clean and labeled beakers, test tubes and glass rods. A description of the steps used in this study to extract the phytoliths from the sediment samples is provided below.

**Extractions Technique:**

Sediment cleaning:

Fifty grams of each sediment sample was weighed and placed into a 100ml labeled beaker. In order to break up the lumps and aggregated soil, diluted liquid detergent was added to the beaker. The samples were stirred with a clean glass rod, after which the beakers were covered with cling wrap to ensure that dust particles did not contaminate the samples. The samples were then left to stand for a twelve-hour period.

Removal of detergent from sediment samples:

Limitations in the size of the centrifuge necessitated the processing of samples in batches of four. Using a clean glass rod and distilled water, samples were transferred from the 100ml beaker into a labeled 50ml test tube. The test tube was weighed and additional distilled water added to ensure equilibrium when centrifuging. The test tubes were then manually shaken before being transferred into the centrifuge (four test tubes per batch). They were then centrifuged at 2000rpm for three minutes after which the soapy liquid (supernatant) was discarded leaving the sediment at the base of the test tube.

Sufficient distilled water was added to the sediment remaining in the test tube to ensure that the sample was fully rinsed. The test tubes were once again agitated, weighed and additional distilled water added to the test tube to ensure equilibrium when centrifuging. The test tubes were then centrifuged at 2000rpm for a further three minutes. The washing process was repeated until all the soapsuds/detergent were removed from the samples. This process was repeated five to six times for each sediment sample.

Removal of carbonates from sediment samples:

Following the cleaning process, the supernatant was discarded from the centrifuged sample. The solid matter from the test tubes was flushed out into a calibrated 600ml beaker with the aid of a clean glass rod and a dilute (10%) HCl solution. Dilute (10%) HCl was added to the beaker until the 100ml calibrated mark was reached. The sample was stirred using a clean glass rod after which the beaker was covered with cling film. Samples were stirred (clean glass rod) every fifteen minutes over a one-hour period. A record was kept of those samples that reacted (effervesced) with the HCl. The contents of the beaker were agitated and approximately 50ml of the slurry carefully poured into a test tube. The test tube was then weighed and additional distilled water added to ensure equilibrium when centrifuging. The test tubes were centrifuged at 2500rpm for three minutes to consolidate sediments at the bottom. The sediment plug was retained and the supernatant discarded. The remaining content of the beaker was processed in a similar manner.

Removal of HCl from sediment samples:

Distilled water was added to the test tubes. They were then agitated, and additional distilled water added to ensure equilibrium when centrifuging. The test tubes were then centrifuged at 2500rpm for three minutes. The remaining supernatant was carefully poured out. A total of three water washes was performed to remove the HCl from the samples. The samples were then transferred to 15ml test tubes using distilled water to flush out the sediment plug. The samples were once again centrifuged at 3000rpm for five minutes.

Addition of Hydrogen peroxide to sediment samples:

Hydrogen peroxide was added to the samples to make each one more transparent. Distilled water was used to flush out the 15ml test tube samples into 50ml beakers to which concentrated hydrogen peroxide was added. The beakers were left to stand until the samples became clearer. The sample was transferred into a 15ml test tube to which distilled water was added. The tubes were agitated and additional distilled water added to ensure equilibrium when centrifuging. The test tubes were then centrifuged at 2500rpm for three minutes. This process was repeated three times in order to remove the hydrogen peroxide from the samples. The sediment plug was retained each time for heavy liquid floatation treatment.

Phytolith Extraction Using Heavy Liquid Solution Of Sodium Polytungstate:

The phytoliths were separated from the clastic silica using a heavy liquid floatation solution of sodium polytungstate (Twiss et al., 1969; Rovner, 1971; Piperno, 2006). Approximately 250g of crystal sodium polytungstate (SPT) was mixed with 100ml of distilled water to form a solution with a specific density of 2.3.

The calibrated test tube containing the sediment plug was vortexed after which an SPT solution was added until the 12ml mark was reached. Plastic tubing was bent into a U-shape and placed into a 50ml test tube. The contents of the 15ml test tube were agitated before being poured into U-shaped plastic tubing (Fig.4.7). The 50ml test tube was weighed and distilled water added (not into the U-shaped tube) to ensure equilibrium when centrifuging. The samples were centrifuged at 2500rpm for 10 minutes.

Piperno (2006) notes that the specific gravity of phytoliths range from about 1.5 to 2.3. By adding SPT with a density of 2.3, the phytoliths are forced to move to the top of the sample tubing.

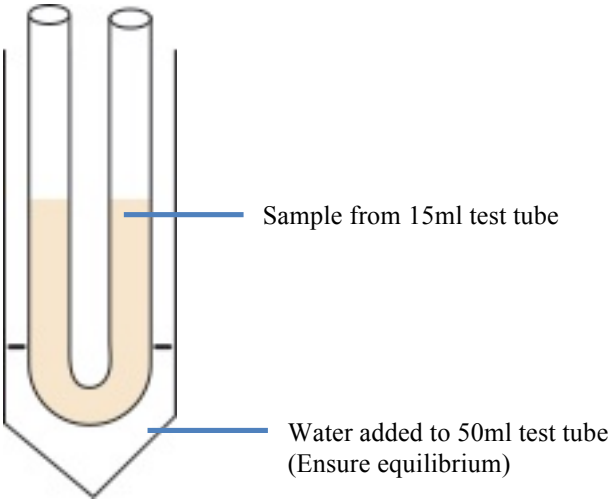


**Fig. 4.7.** *Illustration of U-shaped tubing.*

The U-shaped tubing was clamped (using pliers) at the contact between the floating matter and the more dense solution. The supernatant with the floating matter was poured into a 100ml beaker. Distilled water was used to flush out all the supernatant into the beaker. The sample from the 100ml beaker was then transferred using distilled water into a 15ml test tube. The sample was weighed and additional distilled water added to the test tube to ensure equilibrium when centrifuging. The samples were centrifuged at 3000rpm for five minutes. This water washing process was repeated three times to flush out the SPT.

Transfer sample to microscope slide:

The test tubes were vortexed to dislodge samples from the base. Sufficient distilled water was added to them in order to facilitate the transfer of the sample onto the microscope slide. Using a pipette, 0.05ml of the sample solution was placed onto a microscope slide resting on a warm hot plate (a new pipette was used each time a sample slide was made). A clean spiked rod was used to spread the liquid sample across the slide while it was being heated. When the sample had dried, the slide was taken off the hot plate and a clean glass rod was used to place a drop of rapid mounting medium (‘Entellan New’) onto the slide. Finally a cover slip was placed over the mountant, so as to minimise the development of air bubbles and ensure an even spread of the sample on the slide.

### 4.3 Microscope Equipment And Process

Phytolith identification and counting of phytolith morphotypes was undertaken using a Celestron Professional Biological Microscope at a total magnification of 400x and 600x. Slides were scanned in a linear manner, from top to bottom, and phytoliths present on the entire slide counted. Morphological analyses were undertaken in order to determine the form and structure of the phytoliths present on the slides. Where possible, phytoliths were identified at a subfamily and/or family level. The contribution of each plant group phytolith (assemblage of morphotypes) was calculated as a percentage of the total phytolith count. Photographic images of the phytolith slides were taken using an Olympus BX51 microscope and an Olympus SC30 digital camera, connected via the C-mount adapter (Stream Basic software) housed in the Archaeological Materials Laboratory of the Department of Archaeology at the University of Cape Town. Images were transferred and stored as TIFF/JPEG files. Notes were made of phytolith samples that had been subjected to post-depositional processes such as dissolution, which is reflected by pitting and erosion on the phytolith surface.

#### 4.3.1 Morphological Phytolith Classification

##### 4.3.1.1 Introduction

The morphological descriptions employed in this study follow the guidelines provided by the International Code for Phytolith Nomenclature 1.0 (Madella *et al*. 2005). The fossil phytolith taxonomic identification was complex and was carried out using published photographs and descriptions (references to follow in sections 4.3.1.2 and 4.3.1.3), standard literature (Twiss *et al*. 1969; Mulholland & Rapp, 1992; Piperno 1988, 2006), and modern soil phytolith reference data (Lloyd Rossouw, National Museum, Bloemfontein).

**Phytolith Morphologies**

Phytolith morphologies were grouped into six categories. These include:

1. Grass silica short cell phytoliths (GSSCs)
2. Woody dicotyledons phytoliths
3. Family Specific phytoliths
4. Monocots
5. Other grass phytoliths (refered to as “Poaceae”)
6. Non-diagnostic phytoliths

Categories 2-5 were grouped into non-GSSC phytoliths described below (4.3.1.3).

#### 4.3.1.2 GSSC Phytoliths

Grass silica short cells (GSSC; Fig.4.8) are derived from grass leaf epidermal cells (Twiss *et al*. 1969).

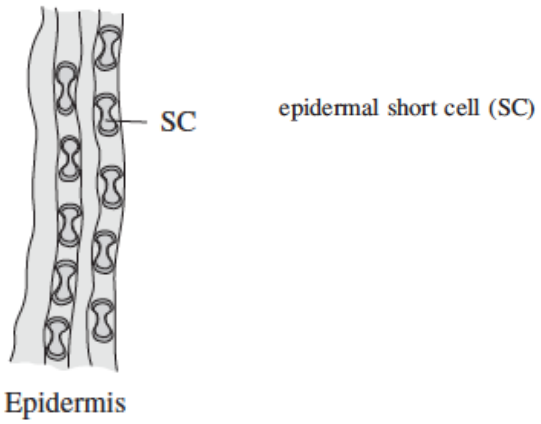


**Fig. 4.8.** *Descriptors for anatomical terms (Madella et al. 2005).*

The observed types of grass phytoliths are classified based on eight phytolith morphotypes, that include bilobates (Twiss *et al.* 1969; Rossouw 2009), crosses (Piperno 2006; Rossouw 2009), polylobates (Rossouw 2009), saddles (Twiss *et al.* 1969; Rossouw 2009), trapezoids (Rossouw 2009), rondels (Rossouw 2009), reniform (Rossouw 2009) and oblong phytoliths (Rossouw 2009). These morphotypes are subdivided into Lobate, Saddle and Trapeziform classes.

#### 4.3.1.2.1 Lobate Class

Bilobates (ICPN; dumbbells) form between the elongated epidermal cells of grass leaves (Twiss *et al.* 1969). These cells are made up of two distinct lobes separated by a central portion (also referred to as the shank) of varied length and thickness (Ellis 1979; Mulholland 1989; Madella *et al.* 2005). The lobes are generally rounded, however the terminal margins may have notches on the edge or surface (indentations). According to Rossouw (2009), there are three basic bilobate variants (B1, B2, B3), which are classified based on the size of the shank, and the outline of the planar surface. Polylobates have more than two lobes and distinctive central portions between the lobes, while the crosses (ICPN; quadra-lobate) have four lobes.

**Bilobate variant 1** (B1; Fig.4.9. #1-2)

The central portion is relatively elongated, and is defined as measuring more than one third of total length of the phytolith body. The rounded lobes are symmetrical in planar (2-D) view. The B1 morphotype equates to types 3c and 3e observed in Twiss *et al.* (1969) (Fig.4.14) and Twiss (1992).

**Bilobate variant 2** (B2; Fig.4.9. #3-12)

The central portion is relatively short, and is defined as being equal or less than one third of total length of the phytolith body. The lobes range from a rounded to ovate shape that are symmetrical in planar view. The B2 morphotype equates to types 3b, 3d and 3f in Twiss *et al.* (1969) (Fig.4.14) and Twiss (1992). The Stipa-type bilobate, a mainly Pooideae morphotype, is included in this category (Mulholland 1989; Fredlund & Tieszen 1994).

**Bilobate variant 3** (B3; Fig.4.9. 13-16)

The bilobate is asymmetrical in planar view. The length of its central portion is less than one third of total length of the phytolith body. In the lateral (side) view, the shape of the phytolith is either tabular or trapezoidal. The B3 morphotype equates to the irregular complex dumbbell recognized by Twiss *et al*. (1969) (Fig.4.14).

**Polylobate (**Fig.4.9. #17-20)

This morphotype has more than two lobes and unique central portions between the lobes, which differentiate it from sinuate trapeziform phytoliths. When viewed along their length polylobates are tabular and elongate in outline (Rossouw 2009). This morphotype equates to type 3i in Twiss *et al*. (1969) (Fig.4.14).

**Cross (**Fig.4.9. #21-26)

In planar view the cross morphotype, which is comprised of four lobes (symmetrical or irregular shape), is essentially equidimensional in shape (Rossouw 2009). The lobes of this short cell can be rounded or pointed and the central portion fairly well defined. This morphotype equates to the type 3a in Twiss *et al*. (1969) (Fig.4.14).


**Fig. 4.9.** *The Lobate Class. Bilobate: 1-16. Polylobate: 17-20. Cross: 21-26. (Rossouw 2009: 52).*

#### 4.3.1.2.2 Saddle Class

Equidimensional bodies represent the Saddle class. Saddle short cells have concave outer surfaces that are differentiated for the most part by their planar outlines. There are two saddle variants. Variant 1's 2-D shape is like a concave saddle, whereas variant 2 is more square and/or rectangular.

**Saddle Variant 1** (Fig.4.10 #1-10**)**

The body of this short cell is trapezoidal in side view and has a concave base and plateau that differs from square to rectangular when observed in the planar view. The plateau has rounded corners, with one to two medially constricted margins, which are crescent in shape. The two sides

are generally convex shaped (Rossouw  2009; Fig.4.11).

**Saddle Variant 2** (Fig.4.10 #11-15**)**

The body of this short cell is trapezoidal in side view and has a concave base and plateau that differ from square to rectangular when observed in the planar view. The plateau generally has rounded corners with margins that are not constricted (Rossouw 2009; Fig.4.12).

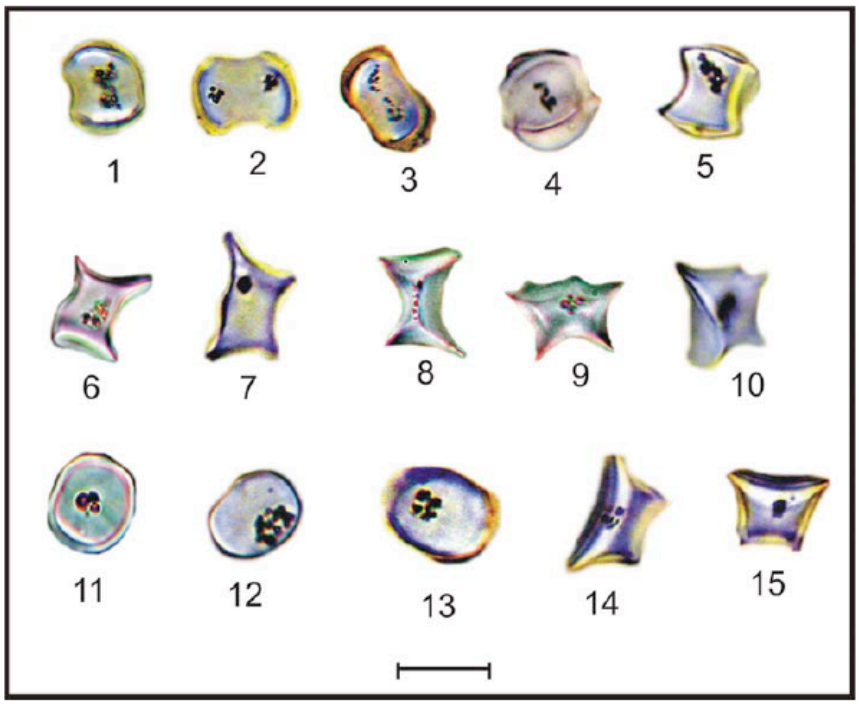


**Fig. 4.10.** *The Saddle Class. Variant one (1-10) and variant two (11-15) (Rossouw 2009: 53).*

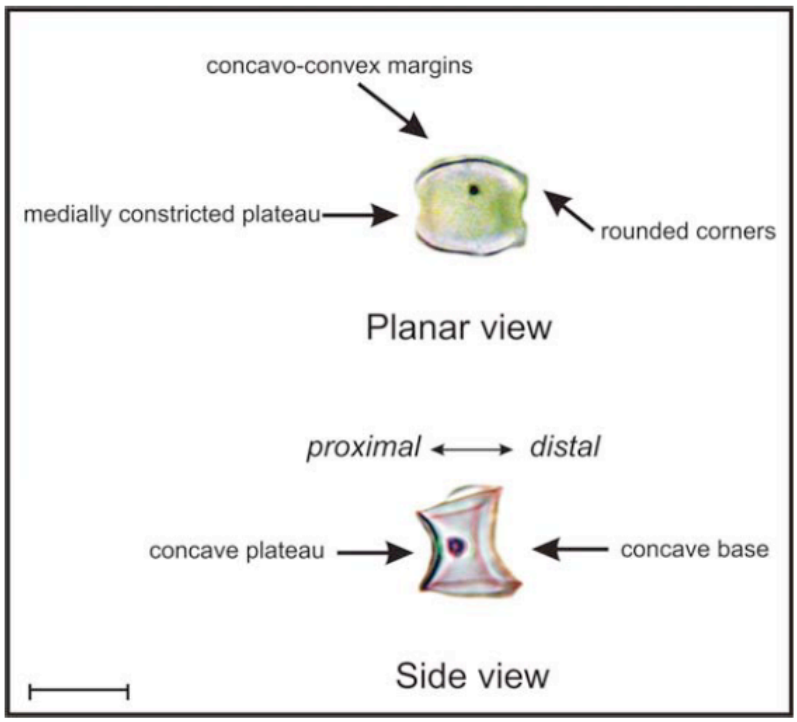


**Fig. 4.11.** *The morphological features of saddle Var.1 (Rossouw, 2009: 54).*

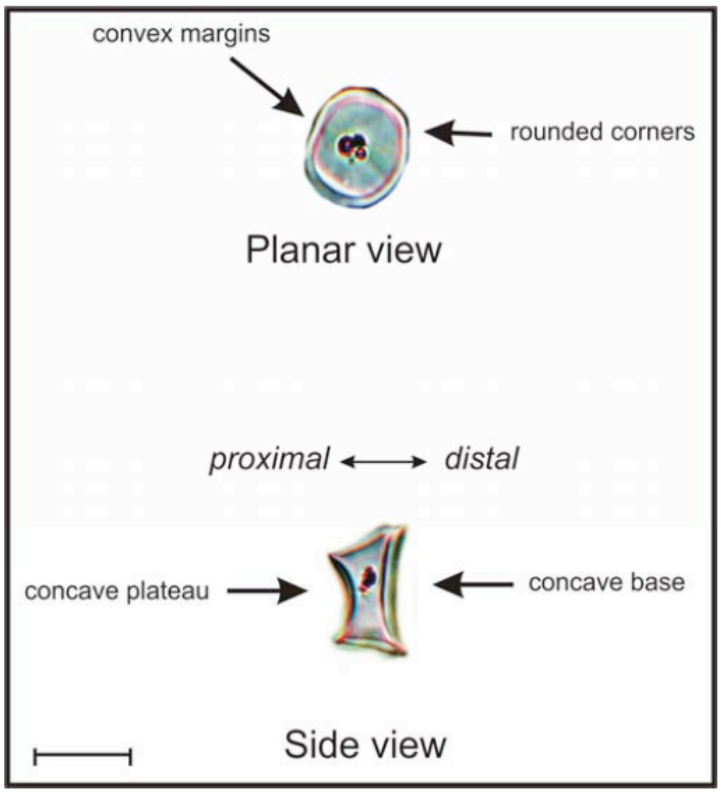


**Fig. 4.12.** *The morphological features of saddle Var.2 (Rossouw, 2009: 54).*

#### 4.3.1.2.3 Trapeziform Class

This class includes a more diverse range of morphotypes that are also regarded as geometrically straight forward (Mulholland 1989). Trapezoids (ICPN, square or rectangular) are six-sided, tabular in shape, with sides that are generally not parallel to each other. The Rondel (ICPN; orbicular or ovate) is cylindrical or semi-cylindrical in shape, and may look like a shortened cone (Mulholland 1989). The Oblongs (ICPN; elongated, rectangular) are six-sided, and are twice as long as wide, with essentially parallel sides. This morphotype has smooth, sinuous or polylobate edges. The Reniform (ICPN; Crescentic) morphotype is a crescent-shaped trapezoid.

**Trapezoid** (Fig.4.13 #1-12)

Trapezoids are six-sided, tabular silica bodies generally with non-parallel sides.

This morphotype equates to types 1b, 1d and 1f in Twiss et al (1969) (Fig.4.14), and the rondel types that were described by Mulholland (1989).

**Rondel** (Fig.4.13 #13-18)

Circular or Rondel morphotypes resemble a truncated cone and as the name suggests can be circular, or semi-cylindrical in form (Mulholland 1989). In planar view the short cell is observed as circular, elliptical or acicular. This morphotype equates to type 1a in Twiss et al. (1969) (Fig.4.14) and the conical type described by Fredlund and Tieszen (1994).

**Oblong** (Fig.4.13 #19-27)

This category includes six sided phytoliths that are elongate, generally twice as long as they are wide with sides that tend to parallel to each other. (Rossouw 2009). Oblong short cells have smooth, sinuous or crenate planar edges. This category equates to types 1c, 1g and 1h in Twiss et al. (1969) (Fig.4.14).

**Reniform** (Fig.4.13 #28-31)

This morphotype is described as being a crescent "bean-shaped" trapezoid. The margins of this phytolith type tend to be angular planar with one concave edge (Rossouw 2009). The reniform equates to type 1e in Twiss et al. (1969) (Fig.4.14).

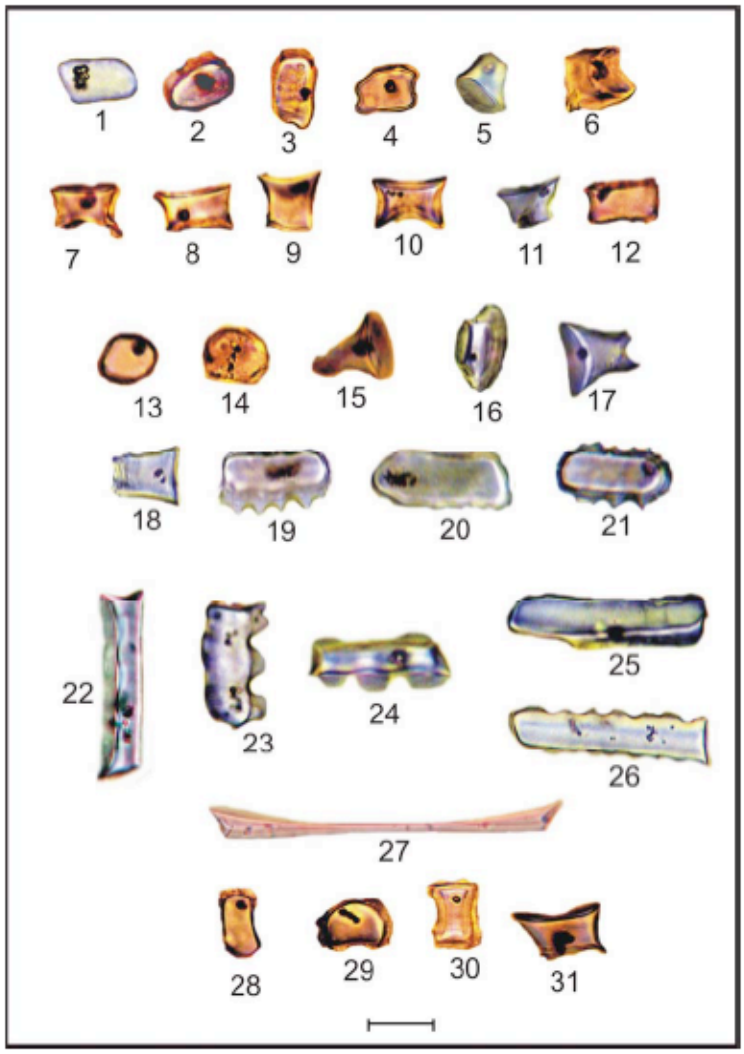


**Fig. 4.13.** *The Trapeziform Class. Trapezoids (1-12); Rondel (13 – 18); Oblongs (19 – 27); Reniform (28 – 31). (Rossouw 2009: 55).*


CLASSIFICATION OF GRASS PHYTOLITHS

I) Festucoid Class
1a. Circular
1b. Rectangular
1c. Elliptical
1d. Acicular, variable focus
1e. Crescent, variable focus
1f. Circular crenate
1g. Oblong
1h. Oblong, sinuous

II) Chloridoid Class
2a. Chloridoid
2b. Thin Chloridoid

III) Panicoid Class
3a. Cross, thick shank
3b. Cross, thin shank
3c. Dumbbell, long shank
3d. Dumbbell, short shank
3e. Dumbbell, long shank, straight or concave ends
3f. Dumbbell, short shank, straight or concave ends
3g. Dumbbell, nodular shank
3h. Dumbbell, spiny shank
3i. Regular, complex dumbbell
3j. Irregular, complex dumbbell
3k. Crenate

IV) Elongate Class (no subfamily characteristics)
4a. Elongate, smooth
4b. Elongate, sinuous
4c. Elongate, spiny
4d. Elongate, spiny with pavement
4e. Elongate, concave ends

**Fig. 4.14.** *Classification of grass phytoliths according to Twiss et al. (1969: 111).*

### *4.3.1.3 Non-GSSC Phytoliths*

Non-GSSC phytoliths are often derived from leaves, woody matter, fruits and flowers. Examples of some of these include long cells, bulliform cell and stomata phytoliths (Fig.4.15).

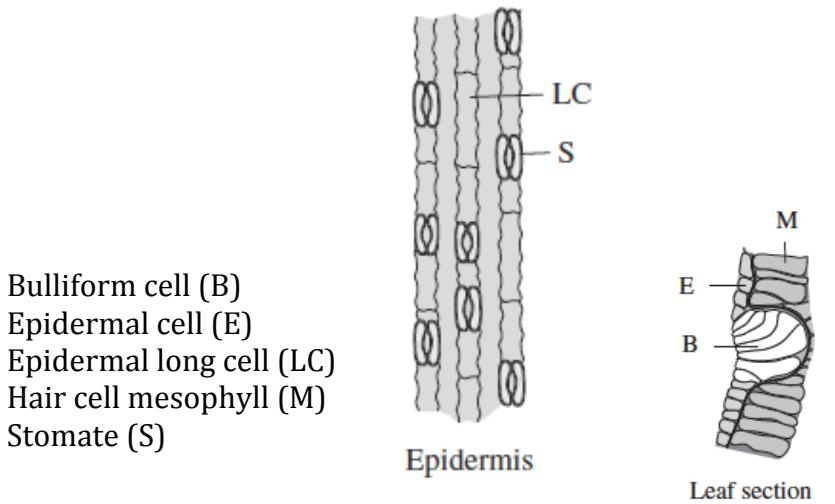


**Fig. 4.15.** *Descriptors for anatomical terms (Madella et al. 2005).*

Phytolith morphotypes are often described using palynological terms (ICPN, Madella *et al*. 2005) as shown in Table 4.4.

**Table 4.4.** *Palynological terms, which have been used to describe phytolith morphotypes (Madella et al. 2005).*

| Texture and ornamentation | Definition |
|---|---|
| Psilate | Smooth or sub-smooth surface |
| Facetate | Several flat areas form the surface |
| Granulate | Granular surface |
| Echinate | Covered with prickles |
| Dendriform | Dendritic: has many finely branched processes |
| Sinuate | Sinuous: has a margin with alternating uneven concavities and convexities |

It should be noted that the morphotypes of woody herbs, shrubs and trees have not been differentiated and are listed as "Woody Dicotyledons" phytoliths in this study. Additionally the category "Monocots" was used to list morphotypes, which may have been associated with herbaceous monocots, grasses, sedges and/or restios (Restionaceae) (as proposed by Albert & Marean 2012). The non-GSSC phytoliths observed in this study are described in the following table.

**Table 4.5.** *Descriptions of the non-GSSC phytoliths included in this study.*

| Plant Group | Name | Morphotype description | Figure No. | Origin | Equivalents/ References |
|---|---|---|---|---|---|
| *Woody Dicotyledons* | Blocky faceted | Usually smooth blocky elongates which are transparent and faceted | 4.16 | Mesophyll of leaves | Elongate faceted (Runge 1999; Mercader *et al.* 2009; Neumann *et al*. 2009) |
| | Blocky Polyhedron | A polygon having more than five sides with smooth surface; relatively plate-like bodies | 4.17 | Dicotyledons leaves and wood | Blocky polyhedral (Rovner 1971; Piperno 1988; Blinnikov 1999; Blinnikov *et al.* 2002; Stromberg 2004; Neumann *et al.* 2009; Collura & Neumann |

| | | | | | |
|---|---|---|---|---|---|
| | | | | | 2016) |
| | Globular decorated (includes globular granulate) | Spherical, with various surface decorations | 4.18 | Leaves, Wood/bark dicotyledons | Globular/Spheroid granulate/verrucate decoration (Piperno 2006; Neumann *et al*. 2009; Novello *et al*. 2012) |
| | Globular small faceted | Faceted, usually spherical body, edges are scalloped | 4.19 | Epidermal cell | (Runge 1999; Madella *et al*. 2005; Neumann *et al.* 2009) |
| | Parallelepiped blocky | Four-sided geometrical figure with parallel opposite sides (width is greater than length) | 4.20 | Wood/bark dicotyledons | Parallelepipedal (Albert 1999; Albert & Weiner 2001; Madella *et al.* 2005; Mercader *et al*. 2010; Novello *et al*. 2012; Esteban *et al*. 2016) |
| | Sclerenchyma (Sclereid) | A variably shaped cell with a central spine or ridge, usually spherical | 4.21 | Dicotyledons leaves | Cylindrical sclereid; thin-branched sclereid (Runge 1999; Gu *et al*. 2008; Mercader *et al.* 2009; Neumann *et al*. 2009; Aleman *et al*. 2014) |
| | | | | | |
| *Family Specific* | Globular echinate (Arecaceae) | Globular to sub-globular with conical spines | 4.22 | Arecaceae | Spheroid echinate (Piperno 2006; Novello *et al.* 2012; Garnier *et al*. 2012; Watling *et al*. 2015). |
| | Opaque perforated platelet (Asteraceae) | Opaque platelet with holes | 4.23 | Asteraceae epidermal cell | (Mercader *et al*. 2000; Gu *et al*. 2008; Watling *et al*. 2015; Bozarth 1992) |
| | Cyperaceae type | Polyhedrons, pentagonal or hexagonal, with central rounded cone | 4.24 | Cyperaceae leaves | (Runge 1999; Piperno 2006; Gu *et al*. 2008; Neumann *et al.* 2009; Novello *et al*. 2012) |
| | | | | | |
| *Monocots (herbaceous monocots, grasses and sedges)* | Cylindroid | Morphologies with smooth and rugose margins. | 4.25 | monocotyledons | Elongate, cylindric (Albert *et al.* 2015) |

| | | | | | |
|---|---|---|---|---|---|
| | Parallelepiped elongate psilate | Four-sided geometrical figure with parallel opposite sides. Smooth surface | 4.26 | monocotyledons | Elongate (Albert 1999) |
| | Parallelepiped elongate faceted | Elongate with several flat areas forming the surface | 4.27 | Monocotyledons | Elongate facetated (Madella *et al*. 2005); Parallelepiped elongate facetated (Albert & Marean 2012) |
| | Stomata cells | Monocot stomata are usually arranged in parallel arrays | 4.28 | Monocotyledons (in this case) | (Rovner 1971, 1983; Stromberg 2004; Piperno 2006) |
| | Silica skeleton long cells psilate | | 4.29 | Monocotyledons leaves/stems | Silica skeleton long cell smooth margin (Albert & Marean 2012); Epidermis long cell psilate (Madella *et al.* 2005) |
| | | | | | |
| *Poaceae* | Bulliform (fan/pillow shape) | Keystone-shaped and other Bulliform cells | 4.30 | Grass leaves | Parallelepipedal and cuneiform Bulliform cell |
| | Long cell dendriform/echinate | | 4.31 | Grass inflorescences | Epidermal long cell |
| | Parallelepiped thin psilate | Thin four sided figure with all sides parallel to the opposite side; smooth surface | 4.32 | Grass leaves | Tabular psilate (Madella *et al*. 2005); (Albert & Bamford 2012) |
| | | | | | |
| *Non-diagnostic, grasses and other (monocotyledons, trees etc)* | Blocky | Block shaped | 4.33 | May occur in all plant parts and types | Novello *et al.* 2012 |
| | Elongate echinate | Elongate with spiny edges | 4.34 | Leaves and roots of grasses, woody dicotyledons, sedges and palms | Elongate spiny; Elongate echinate long cell; Piperno 1988; Stromberg 2004; Madella *et al.* 2005; Neumann *et al*. 2009; Barboni *et al*. 1999; Esteban *et al.* 2016. |
| | Elongate sinuous | Elongate with | 4.35 | Leaves and roots | Piperno 1988; Stromberg |

| | | | | | |
|---|---|---|---|---|---|
| | | sinuous edges | | of grasses, woody dicotyledons, sedges and palms | 2004; Madella *et al*. 2005; Barboni *et al*. 1999, 2007. |
| | Ellipsoid psilate/rugose | | 4.36 | Wood/bark dicotyledons and monocotyledons | (Madella *et al.* 2005; Albert *et al*. 2000, 2003, 2006, 2009; Albert & Marean 2012) |
| | Globular psilate | Globular to sub-globular, smooth surface | 4.37 | Leaf/wood dicotyledons and observed in monocotyledons | Globular/Spheroid smooth (Albert *et al.* 2000; 2009; Runge 1999; Stromberg 2004; Madella *et al*. 2005; Barboni *et al*. 2007; Gu *et al.* 2008; Mercader *et al*. 2009; Neumann *et al.* 2009) |
| | Honeycombed plate | Partially opaque plate with perforations in a honeycomb-like structure | 4.38 | | Madella *et al.* 2005 |
| | Mesophyll | Infilled mesophyll cells | 4.39 | Leaves and roots of woody dicotyledons and monocotyledons | mesophyll aggregate; (Rovner 1971;Stromberg 2004) |
| | Perforated platelet | Platelet with perforations (not opaque) | 4.40 | | |
| | | | | | |
| | Trichome/ Hair | Point shaped | 4.41 | Leaves and roots of grasses, sedges and various other taxa | Acicular hair cell, prickle (Runge 1999; Stromberg 2004; Piperno 2006; Albert & Marean 2012) |
| | Vessels/Tracheids | Cylindric, with spiral thickenings often with slanting ends. | 4.42 | Treachery elements (leaves, roots) of palms, sedges, grasses, woody dicotyledons | Vascular elements; Trachary elements; Cylindric sulcate tracheid (Runge 1999; Stromberg 2004; Madella *et al*. 2005; Neumann *et al*. 2009; Messager *et al.* 2010; Albert & Marean 2012; Das *et al.* 2013; Aleman *et al.* 2014) |

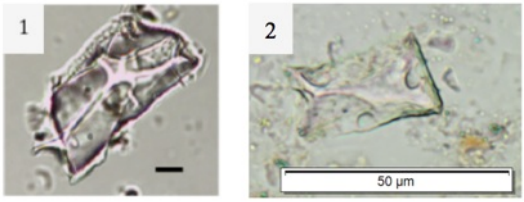


**Fig. 4.16.** Blocky faceted phytoliths: (1) Aleman *et al.* (2014), scale: 10µm; (2) Observed in this research project, scale: 50µm.

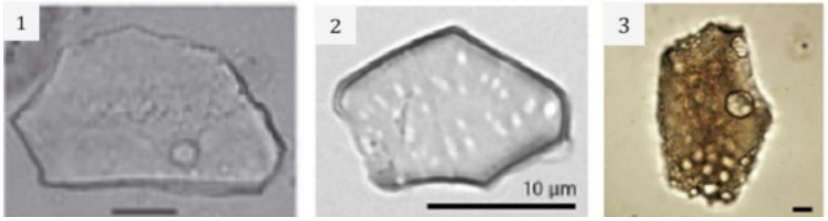


**Fig. 4.17.** Blocky polyhedron phytoliths: (1) Gu *et al.* (2008), scale: 10µm; (2) Collura & Neumann (2016), scale: 10 µm; (3) Neumann et al., 2009, scale: 10µm.

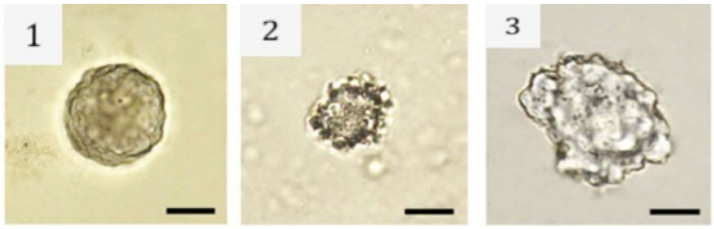


**Fig. 4.18.** Globular decorated phytoliths: (1-3) Neumann *et al. (*2009), scale: 10µm.

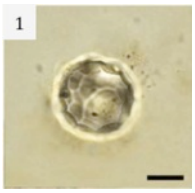


**Fig. 4.19.** Globular faceted phytolith: (1) Neumann *et al.* (2009), scale: 10µm.

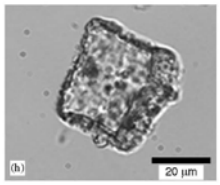


**Fig. 4.20.** Parallelepiped blocky phytolith: (1) Albert *et al*. (2006), scale: 20µm.

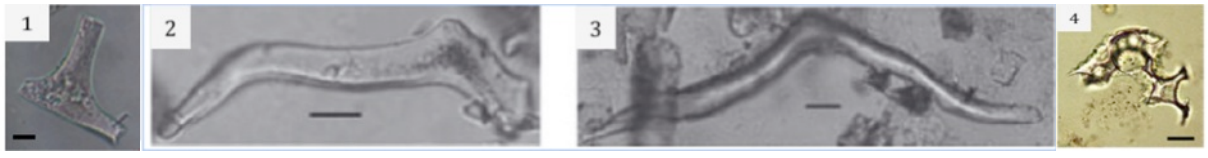

**Fig. 4.21.** Sclereid phytoliths: (1) Alemann *et al*. (2014), scale: 10µm; (2-3) Gu *et al*. (2008), scale: 10µm; (4) Neumann *et al.* (2009), scale: 10µm.

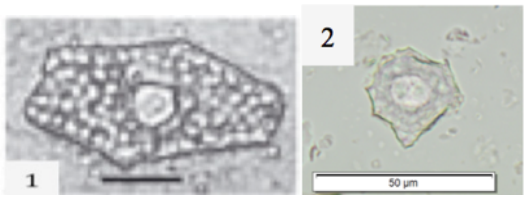


**Fig. 4.22.** Cyperaceae type phytoliths: (1) Gu *et al.* (2008), scale: 10µm; (2) Observed in this research project, scale: 50µm.

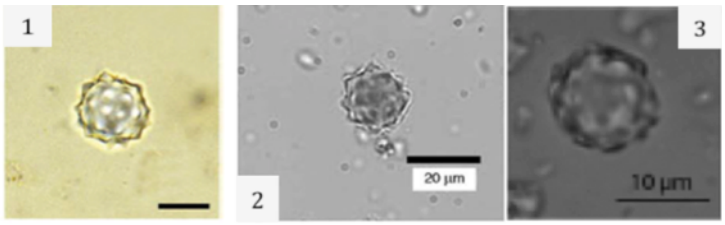


**Fig. 4.23.** Arecaceae - Globular echinate phytoliths: (1) Neumann *et al*. (2009), scale: 10µm; (2) Albert *et al.* (2006), scale: 20µm; (3) Messager *et al*. (2010), scale: 10µm.

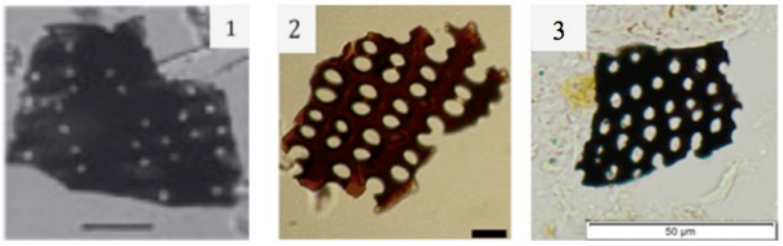


**Fig. 4.24.** Asteraceae- Opaque perforated platelet: (1)Gu *et al*. (2008), scale: 10µm; (2) Yost, 2008, scale: 10µm; (3) Observed in this research project, scale: 50µm.

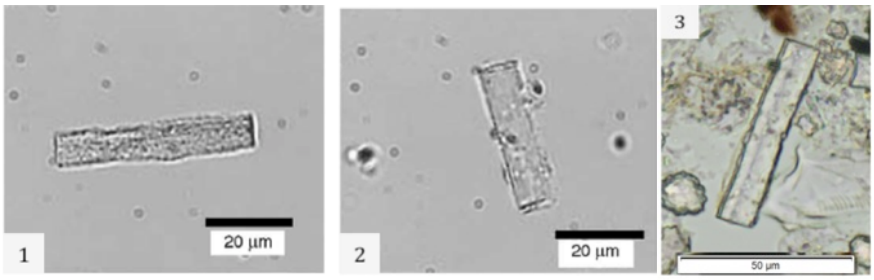


**Fig. 4.25.** Cylindroid phytoliths: (1-2) Albert *et al.* (2006), scale: 20µm; (3) Observed in this research project, scale: 50µm.

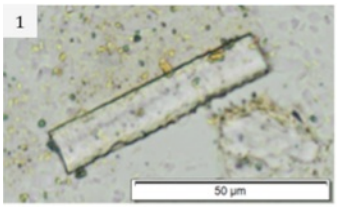


**Fig. 4.26.** Parallelepiped elongate psilate phytolith: (1) Observed in this research project, scale: 50µm.

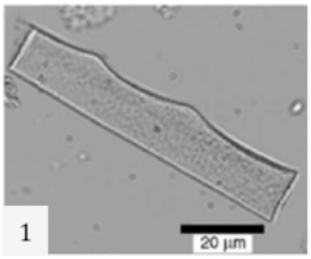


**Fig. 4.27.** Parallelepiped elongate facetated phytolith: (1) Albert *et al*. (2006), scale: 20µm.


**Fig. 4.28.** Stomata cell: (1) Observed in this research project, scale: 50µm.

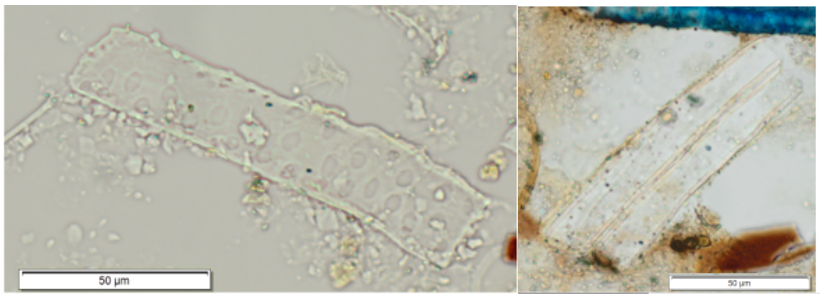


**Fig. 4.29.** Silica skeleton long cells psilate: (1-2) Observed in this research project, scale: 50µm.

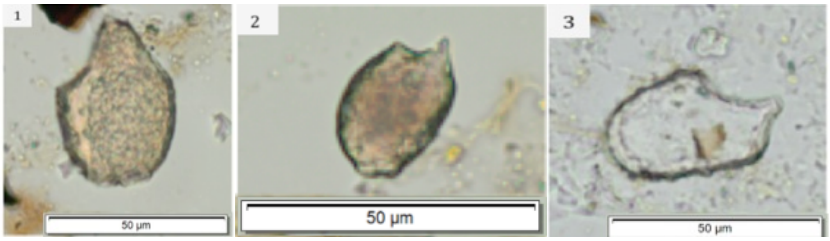


**Fig. 4.30.** Bulliform cells: (1-3) Observed in this research project, scale: 50µm.


**Fig. 4.31.** Long cell dendriform/echinate phytoliths: (1-2) Observed in this research project, scale: 50µm.

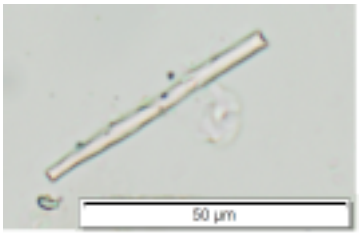


**Fig. 4.32.** Parallelepiped thin psilate phytoliths: (1) Observed in this research project, scale: 50µm.

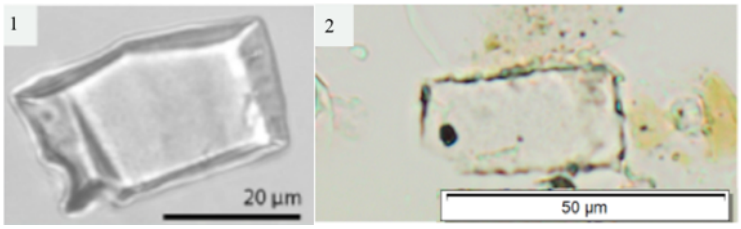


**Fig. 4.33.** Blocky phytoliths: (1) Collura & Neumann (2016); (2) Observed in this research project, scale: 50µm.

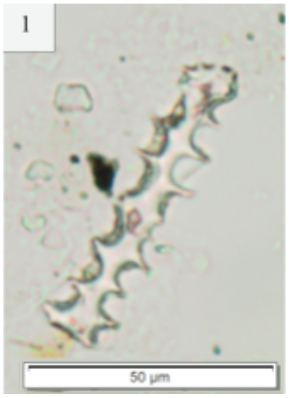


**Fig. 4.34.** Elongate echinate phytoliths: (1) Observed in this research project, scale: 50µm.


**Fig. 4.35.** Elongate sinuous phytoliths: (1) Observed in this research project, scale: 50µm.

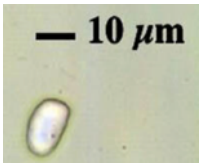


**Fig. 4.36.** Ellipsoid phytolith: (1) PhytCore DB (2014), scale: 10µm.

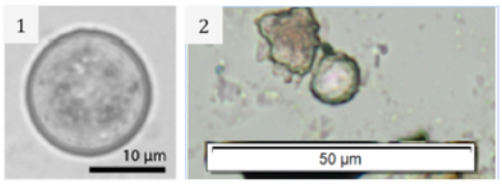


**Fig. 4.37.** Globular psilate phytoliths: (1) Collura & Neumann (2016), scale: 10µm; (2) Observed in this research project, scale: 50µm.

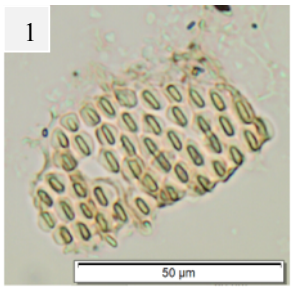


**Fig. 4.38.** Honeycombed plate phytoliths: (1) Observed in this research project, scale: 50µm.

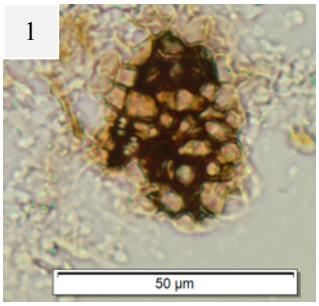


**Fig. 4.39.** Mesophyll: (1) Observed in this research project, scale: 50µm.

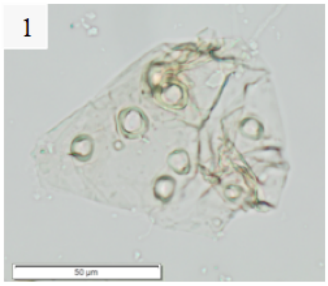


**Fig. 4.40.** Perforated platelet: (1) Observed in this research project, scale: 50µm.

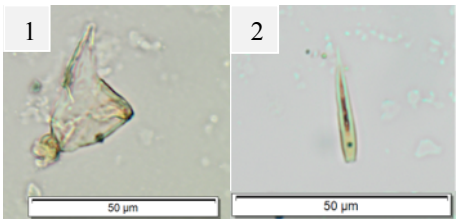


**Fig. 4.41.** Trichome/ Hair cell: (1-2) Observed in this research project, scale: 50µm.

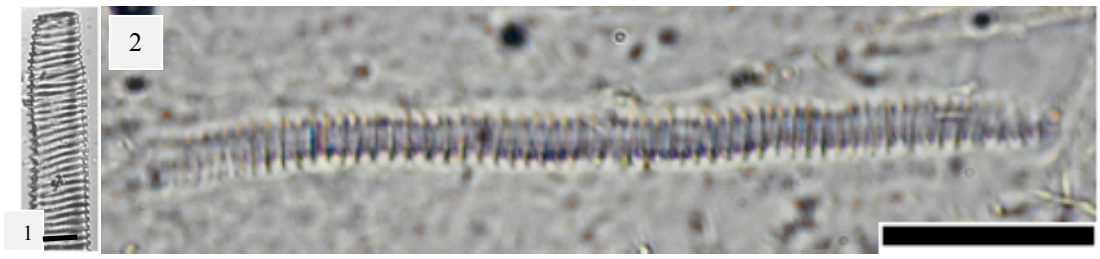


**Fig. 4.42.** Vessels/tracheids: (1) Runge (1999), scale: 10µm; (2) Xiao-Hong (2015), scale: 20µm.

### 4.3.2 Phytolith Association Between Grass Subfamilies And GSSC Morphotypes

The development of $C_3$ and $C_4$ grasses will vary significantly depending on their location within the winter, summer and year-round rainfall regions (Vogel *et al.* 1978; Gibbs Russell 1988). As a result, the expected relative abundance of GSSC phytolith morphotypes produced by $C_3$ and $C_4$ grasses will also vary in winter, summer and year-round rainfall regions. Consequently, the distribution of grasses in southern Africa is primarily linked to growing season temperature where elevated temperatures during the growing season favour the $C_4$ photosynthetic pathway in grasses and cooler temperatures the $C_3$ photosynthetic pathway (Vogel *et al.* 1978; Ellis *et al.* 1980; Gibss Russell *et al.* 1990; Ehleringer *et al*. 1991, 1997; Cerling *et al.* 1997).

Temperature, rainfall and altitude determine the distribution of plant species that belong to the different subfamilies. Eight grass subfamilies have been identified in southern Africa and these include Aristidoideae, Arundinoideae, Bambusoideae, Chloridoideae, Danthonioideae, Ehrhartoideae, Panicoideae and the Pooideae subfamily (Ellis 1984; GPWG 2001**)**. The Arundinoideae subfamily consists of $C_3$ type grasses, which grow in temperate and tropical habitats (Fig.4.43). The Bambusoideae subfamily ($C_3$ grasses) grows in temperate and tropical forests, near riverbanks, in high mountainous grassland and savanna biomes (Fig.4.44). The Danthonioideae subfamily ($C_3$ grasses) only grows in the southern hemisphere, in mesic and xeric open habitats (Fig.4.45). The Ehrhartoideae subfamily ($C_3$ grasses) grows in forests, on open hillsides and in aquatic environments (Fig.4.46). The Pooideae ($C_3$) grasses are common in cool, moist temperate and boreal regions (Fig.4.47). They can also grow in high elevation environments, where available soil moisture is high during the growing season (Tieszen *et al.* 1979; GPWG 2001; Gibson 2009; Aleman *et al.* 2014). The Chloridoideae subfamily consists of only short $C_4$ type grasses which are adaptable to warm, dry (arid; low available soil moisture; xeric environments) tropical and subtropical climates, as well as a wide variety of other environmental conditions for example high pH and saline soils (Vogel *et al.* 1978; Tieszen *et al.* 1979) (Fig.4.48). These grasses are found in

dry tropical and subtropical regions (Gibson 2009). The Aristidoideae subfamily is comprised of both $C_3$ and $C_4$ type grasses and often grows in tropical or xerophytic temperate zones and in open habitats (Gibson 2009) (Fig.4.49). The Panicoideae grass subfamily includes both $C_3$ ad $C_4$ type grasses (Gibson 2009) as well as species with $C_3/C_4$ intermediary pathways (Fig.4.50). Panicoideae grasses are tall grasses that are adapted to warm climate (tropical and subtropical) regions and they are often encountered in savannah habitats (Tieszen *et al.* 1979). They are also adaptable to shady and moist (mesic) environments (Aleman *et al.* 2014) however they are not as adaptable as plants belonging to the Pooideae subfamily. In Africa, 21% of the grass species in this subfamily (which are classified as $C_3$) mostly grow under tropical forest canopies (Tieszen *et al.* 1979).

Establishing the presence and frequencies of various GSSC phytoliths may be used in the identification of $C_3$ or $C_4$ grass subfamilies and the environment. Researchers such as Twiss *et al.* (1969) and Rossouw (2009) have shown that certain GSSCs correspond to particular grass subfamilies. Twiss (1992) provided the first synthesis in the world of the distribution of grasses and the potential use of phytolith assemblages to interpret climatic and environmental conditions. Twiss *et al.* (1969) and Rossouw (2009) consider the grass subfamily Panicoideae to have abundant simple form bilobate morphotypes. However bilobates are also found in smaller amounts in the other grass subfamilies such as Bambusoideae, Chloridoideae, Danthonoideae, Ehrhartoideae and Aristidoideae (Fredlund & Tieszen 1994; Piperno & Pearsall 1998; Mercader *et al.* 2010). In addition, Bilobates are associated with moisture-loving grasses that favour shade and/or mesic to wet habitats (Barboni *et al.* 2010). The cross and polylobate morphotypes have been mainly identified in Panicoideae grasses (Twiss *et al.* 1969; Fredlund & Tieszen 1994). Stipa-type bilobates, rondels, trapezoids, oblongs and polylobate morphotypes are associated with the Pooideae grass subfamily **(**Twiss *et al.* 1969; Fredlund & Tieszen 1994; Bremond *et al.* 2008; Rossouw 2009; Mercader *et al.* 2010). Rossouw (2009), Cordova and Scott (2010) and Cordova (2013) have identified trapezoids and rondel morphotypes in the South African Danthionoideae and Ehrhartiodeae grass subfamilies. The variant S1 morphotype (squat saddles) and variant S2

(elongated saddle) phytolith variants occur in the Chloridoideae subfamily (Rossouw 2009). Variant 2 type saddle morphotypes are also associated with the Aristidoideae subfamily (Rossouw 2009). Saddles are associated with sun-loving grasses that prefer open and dry habitats (Barboni *et al.* 2010).

According to Bamford *et al*. (2006) and Piperno and Pearsall (1998), the division of $C_3$ and $C_4$ grass phytolith morphotypes can be problematic. In their study of modern plants, Bamford *et al.* (2006) observed that some $C_4$ type grasses were producing more $C_3$ type morphotypes than the $C_4$ characteristic short cells. Therefore, the grass subfamily classifications that are based on observed phytolith assemblages in the sediment samples, should take this possibility into consideration.

**Fig. 4.43.** *Some of the phytolith morphotypes associated with the Arundinoideae grass subfamily (Rossouw 2009). Additional reference material for the subfamily was obtained from the reference collections stored in one of the labs at the National Bloemfontein Museum.*

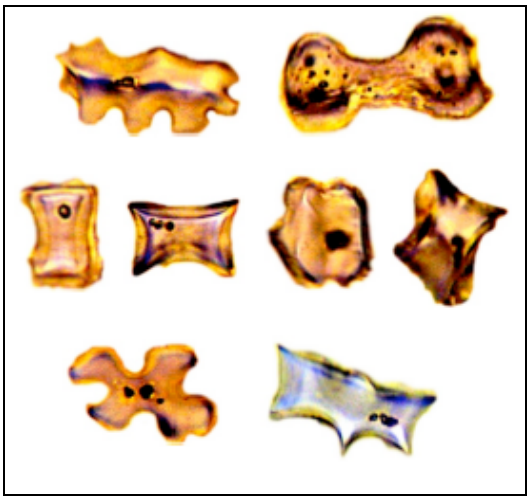

**Fig. 4.44.** *Some of the phytolith morphotypes associated with the Bambusoideae grass subfamily (Rossouw 2009). Additional reference material for the subfamily was obtained from the Bloemfontein stored in one of the labs at the National Bloemfontein Museum.*

**Fig. 4.45.** *Some of the phytolith morphotypes associated with the Danthonioideae grass subfamily (Rossouw 2009). Additional reference material for the subfamily was obtained from the Bloemfontein stored in one of the labs at the National Bloemfontein Museum.*

**Fig. 4.46.** *Some of the phytolith morphotypes associated with the Ehrhartoideae grass subfamily (Rossouw 2009). Additional reference material for the subfamily was obtained from the Bloemfontein stored in one of the labs at the National Bloemfontein Museum.*

**Fig. 4.47.** *Some of the phytolith morphotypes associated with the Pooideae grass subfamily (Rossouw 2009). Additional reference material for the subfamily was obtained from the Bloemfontein stored in one of the labs at the National Bloemfontein Museum.*

**Fig. 4.48.** *Some of the phytolith morphotypes associated with the Chloridoideae grass subfamily (Rossouw 2009). Additional reference material for the subfamily was obtained from the Bloemfontein stored in one of the labs at the National Bloemfontein Museum.*

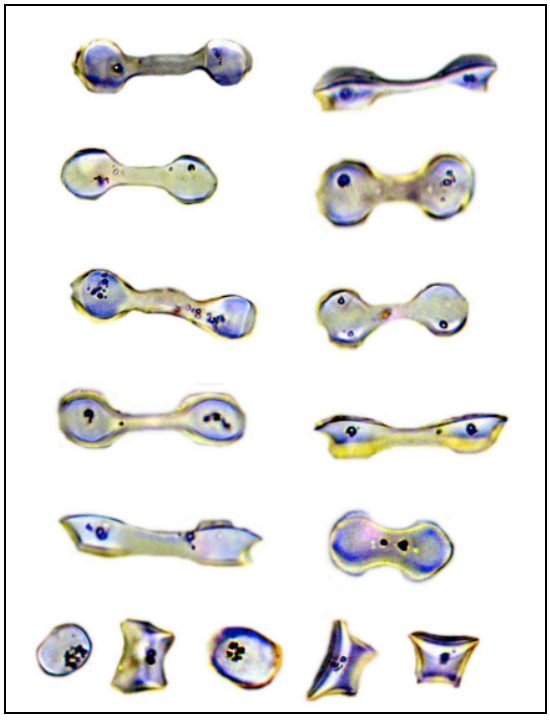

**Fig. 4.49.** *Some of the phytolith morphotypes associated with the Aristidoideae grass subfamily (Rossouw 2009). Additional reference material for the subfamily was obtained from the Bloemfontein stored in one of the labs at the National Bloemfontein Museum.*

**Fig. 4.50.** *Some of the phytolith morphotypes associated with the Panicoideae grass subfamily (Rossouw 2009). Additional reference material for the subfamily was obtained from the Bloemfontein stored in one of the labs at the National Bloemfontein Museum.*

### 4.4. Data Analysis And Interpretation

Phytolith analysis has been used to identify the middle to late middle Pleistocene vegetation community at EFT and DFT. The analysis relies on the quantitative comparison between phytolith assemblages at particular sites. The comparison of morphotype counts and classes of morphotypes (plant groups) is made in order to interpret the phytolith assemblages extracted from sediment samples. The value of interpretation of a phytolith assemblage may differ if there is an insufficient amount of diagnostic phytoliths. According to Stromberg (2009) vegetation inference is statistically robust for assemblages with a clearly skewed morphotype distribution. For example 90% woody dicotyledons phytoliths vs. 10% Poaceae phytoliths.

Albert and Weiner (2001) determined that a phytolith sample population of 194 with consistent morphology gave an error margin of 23% whereas for 265 phytoliths the error margin was 12%.

They noted that rare phytolith morphotypes were unlikely to be identified where total counts were below 200.

In this study, where possible, a minimum of 200 diagnostic phytoliths were counted per sample. In cases where the count of 200 diagnostic phytoliths was not possible, a minimum count of 50 diagnostic phytoliths was considered in the interpretation. Albert and Weiner (2001) regarded this a minimum number for data to be included in the study without the loss of information. It was accepted that these low count samples used in the interpretation would have high error margins of 40% compared to those with a 200 diagnostic phytolith count.

Simple statistical analyses using bar graphs and pie charts were created to illustrate the phytolith morphotype patterns observed across the sites. Total phytolith count for each sample, the contribution patterns of each plant group (set of morphotypes), and presence of more grassy or woody samples were calculated, and results illustrated in the results chapter. Data were interpreted and compared to determine whether the GSSCs in the samples were more diverse or less diverse.

The Ic phytolith index (C3/C4 grass composition index Ic [%] = trapeziform short cells/[trapeziform short cells + saddle + cross + bilobates])and Iph phytolith index (humidity-aridiy index Iph[%] =saddle/[cross+ bilobates + saddle]) were not used in this research, as the main implementation of these indices has been based on East and West African samples (e.g. Alexandre *et al*. 1997; Bremond *et al*. 2005; Bremond *et al*. 2008). There has also been evidence to suggest that in some environments, the indices may not be relevant indicators and may need to be regionally validated before application (Bremond *et al.* 2008).

# Chapter 5 : RESULTS

## 5.1 Introduction

The first section of this chapter is dedicated to describing the types of phytoliths extracted from the modern plant specimens. In the second section, I will present the results of the phytolith analysis of the modern sediment samples, followed by the results from the analysis of the fossil sediment samples.

## 5.2 Comparative Collection

A selection of modern fynbos plants were collected from the Duinefontein site, while examples of plants growing in other regions of the southwestern Cape coast were obtained from the Kirstenbosch National Botanical Garden nursery. Plant samples representing savannah-woodland plant types were obtained in the Kruger Park region. Images of the modern plants sampled are available in Appendix I. Phytoliths were extracted from the stems, leaves, pods, fruit and flowers of these plant species. A description and photographs of the modern plant phytoliths are provided below.

### 5.2.1 Modern South-West Cape Coast Fynbos Plants

Plant Name: *Carissa macrocarpa*

The leaves and the stems of the *Carissa macrocarpa* (Natal Plum) plant were studied. Only the leaves were found to contain phytoliths, which comprised cylindroid psilate phytoliths (Fig.5.1.a) together with spheroid psilate phytoliths (Fig.5.1.b), hair phytoliths (Fig.5.1.c) and blocky phytoliths (Fig.5.1.d).

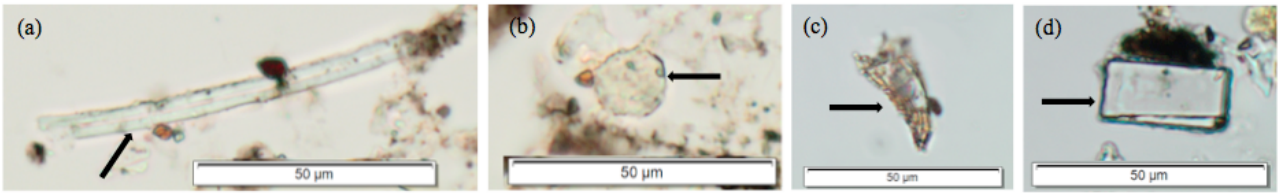


**Fig. 5.1.** *Carissa macrocarpa* phytolith types: (a) Cylindroid psilate, from leaf material; (b) Spheroid psilate, from leaf material; (c) Hair, from leaf material; (d) Blocky, from leaf material. Scale: 50µm.

Plant Name: *Ehrharta villosa* var. villosa

*Ehrharta villosa* var. villosa (Dune Ehrharta) grasses were observed throughout the EFT and DFT sites. During microscope examination, only the inflorescence was found to contain stomata cell phytoliths (Fig.5.2.a) and short cell rondel phytoliths (Fig.5.2.b-e).

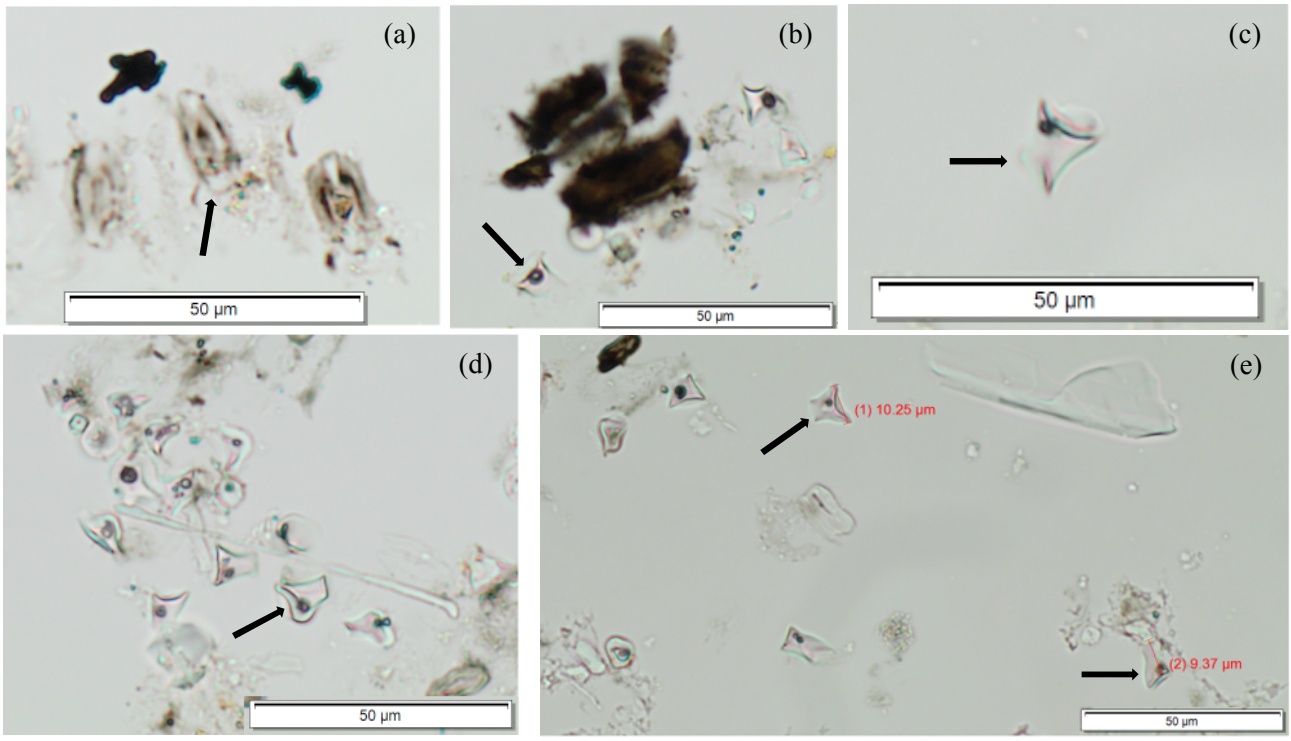


**Fig. 5.2.** *Ehrharta villosa* var. villosa phytolith types: (a) Stomata cells; (b-e) Short cell rondel. Scale: 50µm.

Plant Name: *Eriocephalus punctulatus*

There were no phytoliths present in the leaves, stem or flower of the *Eriocephalus punctulatus* (Wild Rosemary) plant. This is unusual as the Asteraceae family generally produce an abundance of

phytoliths. The fact that the plant sample was not mature may account for the non-development of phytoliths.

Plant Name: *Lessertia (Sutherlandia) frutescens*

The *Lessertia frutescens* (Balloon Pea) leaves were found to contain hair phytoliths (Fig.5.3.a). Irregular phytoliths (Fig.5.3.b) were observed in the plants stems.

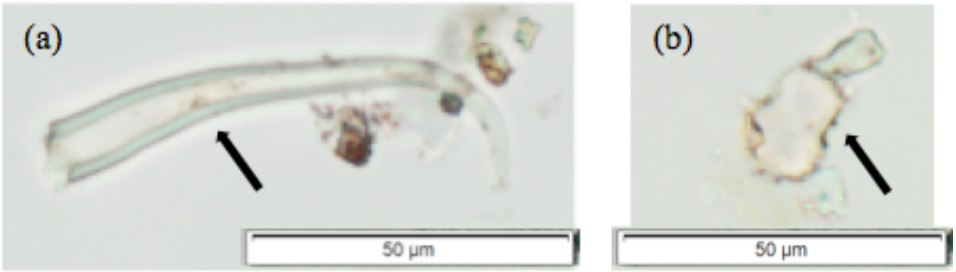


**Fig. 5.3.** *Lessertia frutescens* phytolith types: (a) Hair, from leaf material; (b) Irregular phytolith, from stem material. Scale: 50µm.

Plant Name: *Lycium afrum*

The distribution of *Lycium afrum* (Kraal honey thorn) was found to be sparse at DFT. The leaves, stems, berries and flowers were studied. No phytoliths were observed in *Lycium afrum*.

Plant Name: *Metalasia densa*

*Metalasia densa* (Blombos) was found to be endemic in the DFT area. The leaves and stems contained phytoliths but none were observed in the flowers. Silica skeleton phytoliths (Fig.5.4.a) were identified in the leaf sample and spheroid psilate phytoliths (Fig.5.4.b) were observed in the plant stems.

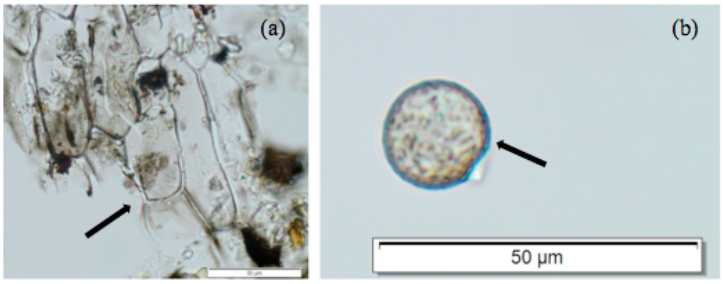


**Fig. 5.4.** *Metalasia densa* phytolith types: (a) Silica skeleton, from leaf material; (b) Spheroid psilate, from stem material. Scale: 50µm.

Plant Name: *Metalasia muricata*

Only the leaves of the *Metalasia muricata* (White Bristle Bush) contained hair phytoliths (Fig.5.5.a). No phytoliths were observed in the other parts of the plant.

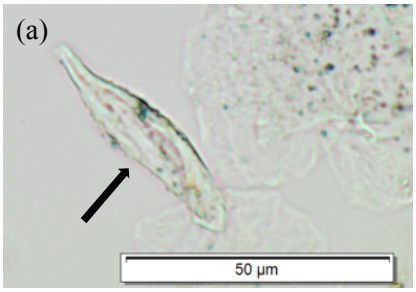


**Fig. 5.5.** *Metalasia muricata* phytolith types: (a) Hair, from leaf material. Scale: 50µm.

Plant Name: *Morella cordifolia*

No phytoliths were observed in the leaves and stems of the *Morella cordifolia* (Dune waxberry) plant.

Plant Name: *Osteospermum (Chrysanthemoides) moniliferum subsp. monilifera*

The *Osteospermum moniliferum subsp. monilifera* (Brother berry) leaves were found to contain polyhedral assemblage phytoliths (Fig.5.6.a), mesophyll phytoliths (Fig.5.6.b) and tracheid phytoliths (Fig.5.6.c). Opaque perforated plate phytoliths (Fig.5.6.d) were observed in the plant stems.

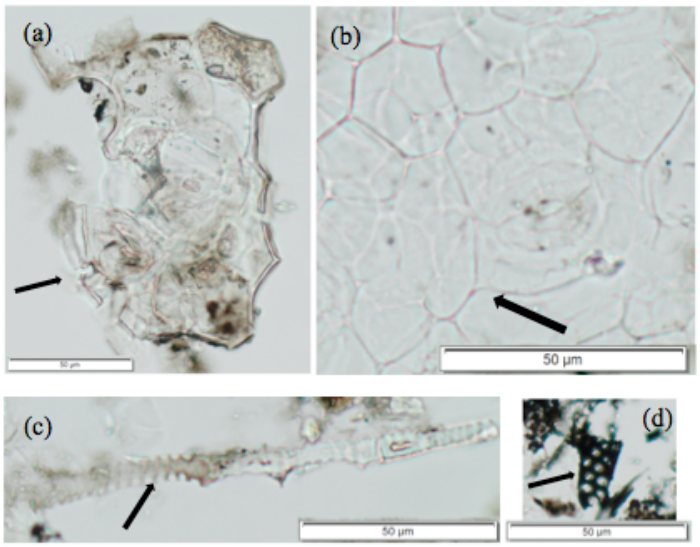


**Fig. 5.6.** *Osteospermum moniliferum subsp. monilifera* phytolith types: (a) Polyhedral assemblage, from leaf material; (b) Mesophyll, from leaf material; (c) Tracheid, from leaf material; (d) Opaque perforated plate, from stem material. Scale: 50µm.

Plant Name: *Pelargonium spp. (P.capitatum)*

The leaves of *Pelargonium spp.* phytoliths were found to contain irregular phytoliths (Fig.5.7.a) and cylindroid psilate phytoliths (Fig.5.7.b). Irregular phytoliths (Fig.5.7.c-d), cylindroid bulbous phytoliths (Fig.5.7.e-f) and blocky phytoliths (Fig.5.7.g) were noted in the plant stems.

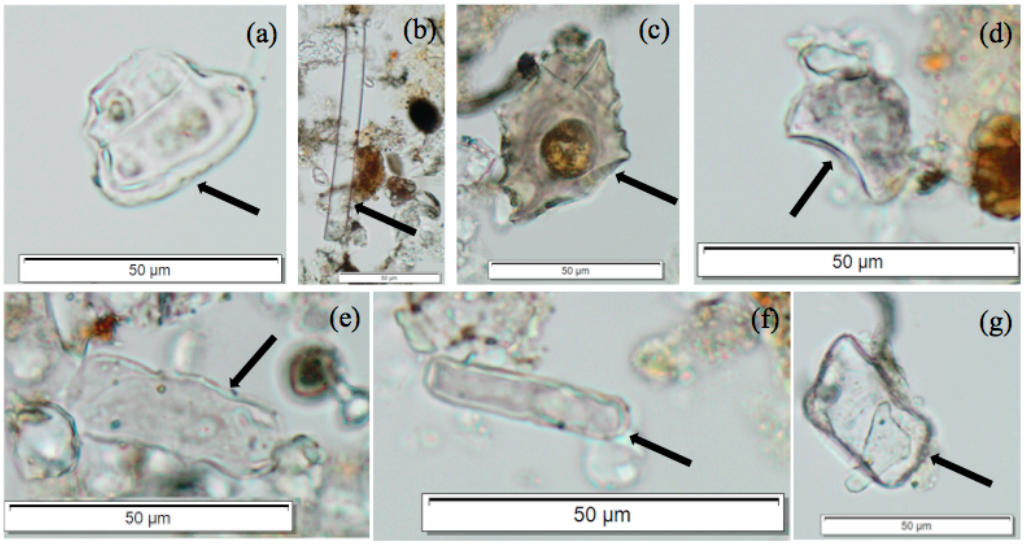


**Fig. 5.7.** *Pelargonium spp.* phytolith types: (a) Irregular, from leaf material; (b) Cylindroid psilate, from leaf material; (c-d) Irregular, from stem material; (e-f) Cylindroid bulbous, from stem material; (g) Blocky, from stem material. Scale: 50µm.

Plant Name: *Searsia spp*.

A Searsia spp. was observed growing in association with the *Metalasia densa* in the DFT region. Trichome phytoliths (Fig.5.8.a), spheroid psilate phytoliths (Fig.5.8.b), cylindroid bulbous phytoliths (Fig.5.8.c-d; Fig.5.8.f) and cylindroid psilate phytoliths (Fig.5.8.e) were observed in the leaves, but the stem of the plant was found to be devoid of phytoliths.

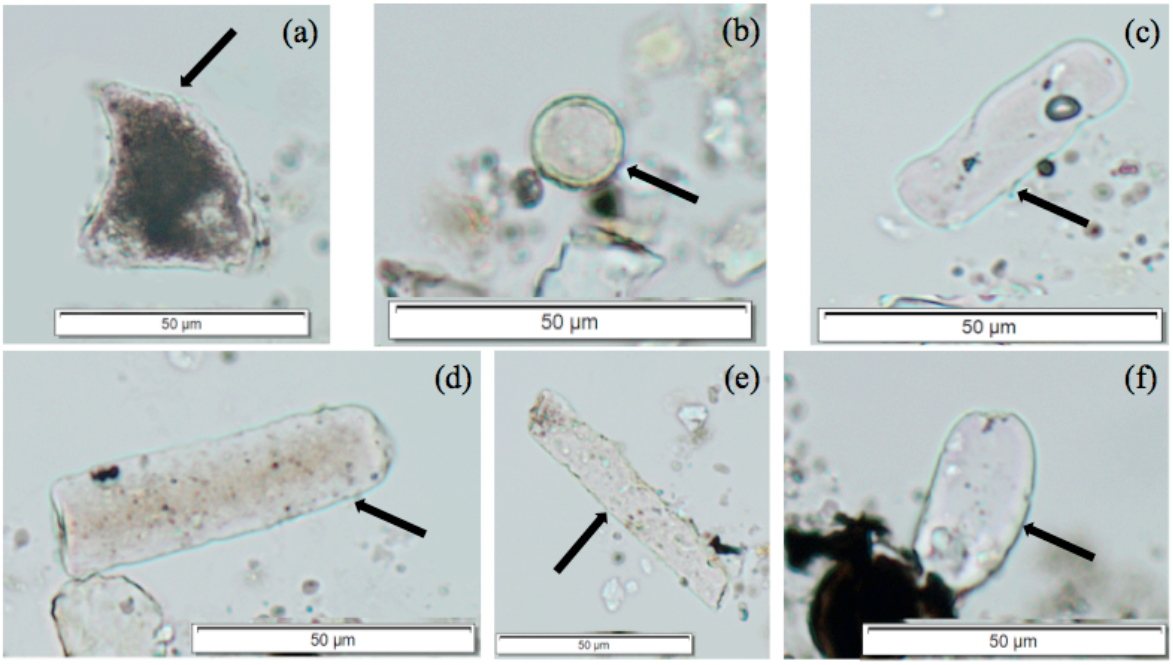


**Fig. 5.8.** *Searsia spp.* phytolith types: (a) Trichome, from leaf material; (b) Spheroid psilate, from leaf material; (c-d, f) Cylindroid bulbous, from leaf material; (e) Cylindroid psilate, from leaf material. Scale: 50µm.

Plant Name: *Thesium spp.*

Only the leaves of *Thesium spp* were found to contain phytoliths. These comprised of cylindroid psilate phytoliths (Fig.5.9.a).

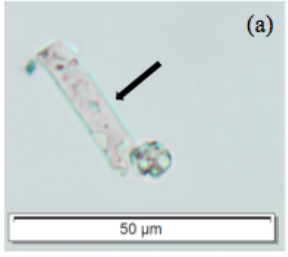


**Fig. 5.9.** *Thesium spp.* phytolith types: (a) Cylindroid psilate, from leaf material. Scale: 50µm.

Plant Name: *Trachyandra divaricata*

*Trachyandra divaricata* (False onion weed) was observed growing on the sandy dunes throughout the DFT area. Irregular phytoliths (Fig.5.10.a) were observed in the leaves and cylindroid psilate phytoliths (Fig.5.10.b) were identified in the root material.

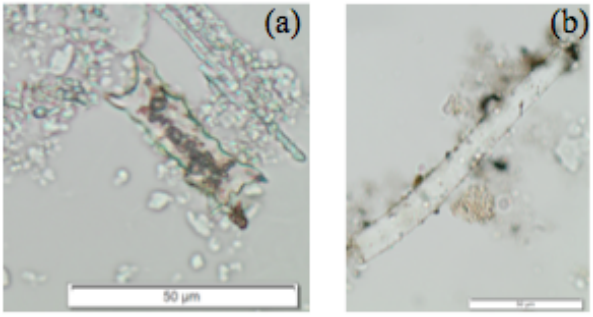


**Fig. 5.10.** *Trachyandra divaricata* phytolith types: (a) Irregular, from leaf material; (b) Cylindroid psilate, from root material. Scale: 50µm.

### 5.2.2 Woodland-Savannah Plants

Plant Name: *Acacia karroo*

Phytoliths were observed in the leaves, branch stems and seedpods of *Acacia karroo* (Sweet Thorn). During microscope examination, blocky phytoliths (Fig.5.11.a) and spheroid psilate phytoliths (Fig.5.11.b) were found in the leaves, spheroid psilate phytoliths (Fig.5.11.c) and trichome phytoliths (Fig.5.11.d) were found in the plant stems and parallelepipedal thin rugose phytoliths (Fig.5.11.e) were observed in the seedpods. Additional reference material slides for this plant species was obtained from Lloyd Roussouw's reference collection in Bloemfontein.

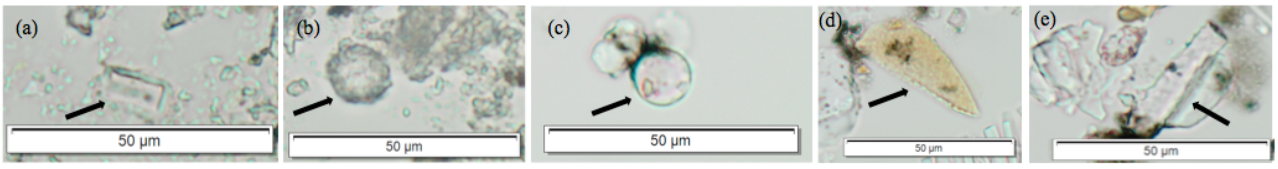


**Fig. 5.11.** *Acacia karroo* phytolith types: (a) Blocky, from leaf material; (b) Spheroid psilate, from leaf material; (c) Spheroid psilate, from branch stem material; (d) Trichome, from branch stem material; (e) Parallelepipedal thin rugose, from pod material. Scale: 50µm.

Plant Name: *Acacia nigrescens*

In *Acacia nigrescens* (Knob Thorn), phytoliths were identified in leaves and branch stems. Hair base phytoliths (Fig.5.12.a; top), blocky phytoliths (Fig.5.12.a; bottom) and silica skeleton phytoliths (Fig.5.12.b) were observed in the leaves. The branch stems contained spheroid psilate phytoliths (Fig.5.12. c).

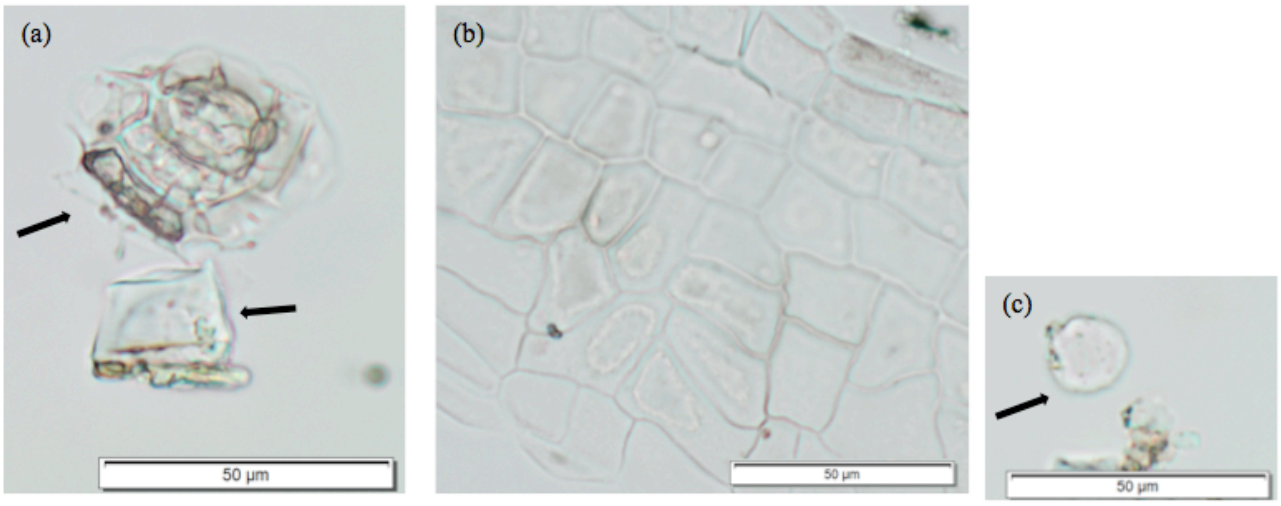


**Fig. 5.12.** *Acacia nigrescens* phytolith types: (a) hair base; top and blocky; bottom, from leaf material; (b) Silica skeleton, from leaf material; (c) Spheroid psilate, from branch stem material. Scale: 50µm.

Plant Name: *Acacia nilotica*

The *Acacia nilotica* (Scented-pod Acacia) leaves were found to contain spheroid psilate phytoliths (Fig.5.13.a-b), parallelepipedal thin rugose phytoliths (Fig.5.13.c) and irregular phytoliths (Fig.5.13.d). Parallelepipedal thin rugose phytoliths (Fig.5.13.e) and irregular phytoliths (Fig.5.13.f) were observed in the branch stems. No phytoliths were observed in the seedpods.

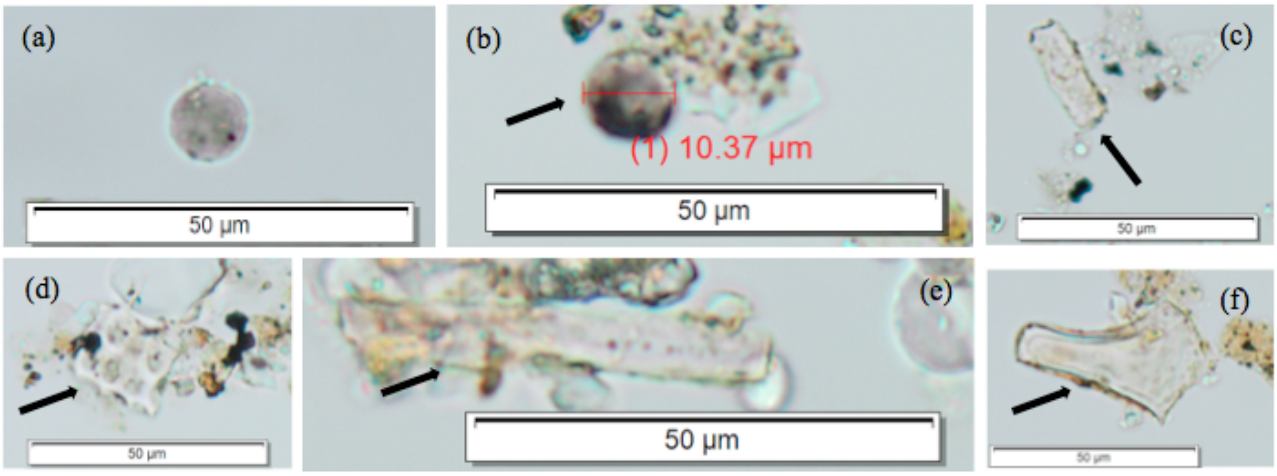


**Fig. 5.13.** *Acacia nilotica* phytolith types: (a-b) Spheroid psilate, from leaf material; (c) Parallelepipedal thin rugose, from leaf material; (d) Irregular, from leaf material; (e) Parallelepipedal thin rugose, from branch stem material; (f) Irregular, from branch stem material. Scale: 50µm.

Plant Name: *Acacia tortilis*

In *Acacia tortilis* (Umbrella thorn) leaves, irregular phytoliths (Fig.5.14.a-c) and trichome phytoliths (Fig.5.14.d) were observed. The branch stems contained irregular blocky phytoliths (Fig.5.14.e), cylindroid psilate phytoliths (Fig.5.14.f-g) and cylindroid bulbous phytoliths (Fig.5.14.h). Additional reference literature for this plant species was obtained from Mercader et al. (2009) and the website www.phytcore.org.

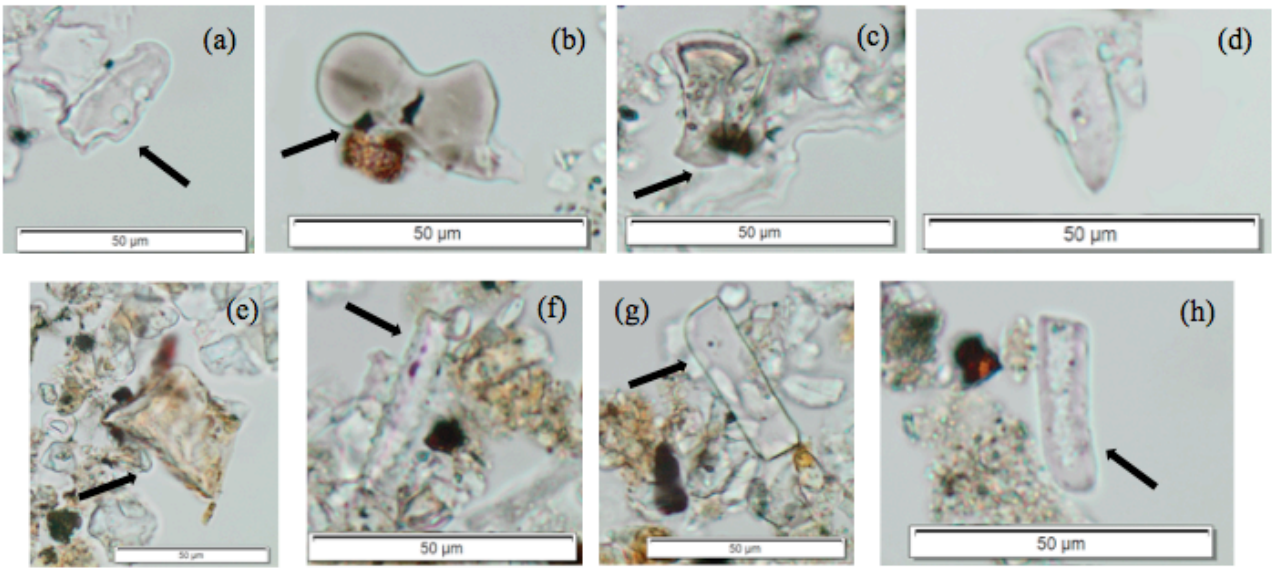


**Fig. 5.14.** *Acacia tortilis* phytolith types: (a-c) Irregular, from leaf material; (d) Trichome, from leaf material; (e) Irregular blocky, from branch stem material; (f-g) Cylindroid psilate, from branch stem material; (h) Cylindroid bulbous, from branch stem material. Scale: 50µm.

Plant Name: *Dichrostachys cinerea*

*Dichrostachys cinerea* (Sickle Bush) leaves contained honeycombed spheroid assemblage phytoliths (Fig.5.15.a) and the branch stems contained spheroid psilate phytoliths (Fig.5.15.b). In the seedpods, spheroid psilate phytoliths (Fig.5.15.c) were observed.

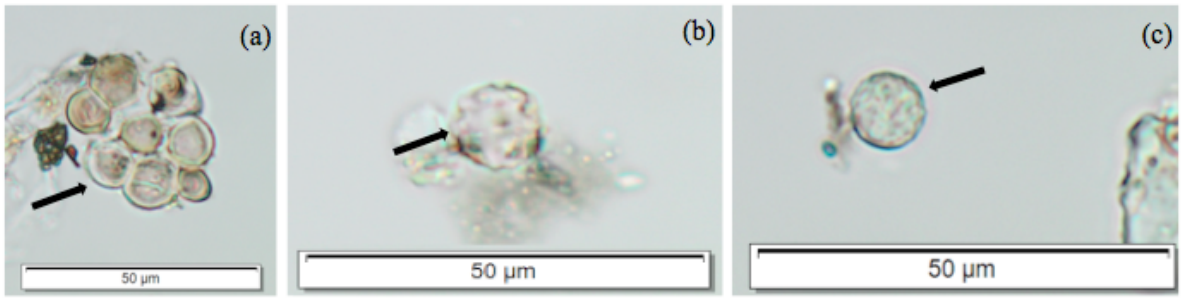


**Fig. 5.15.** *Dichrostachys cinerea* phytolith types: (a) Honeycombed spheroid assemblage, from leaf material; (b) Spheroid psilate, from branch stem material; (c) Spheroid psilate, from pod material. Scale: 50µm.

Plant Name: *Grewia flavescens*

The microscope examination of the *Grewia flavescens* (Sandpaper raisin) revealed that the leaves contained cylindroid sinuous irregular end phytoliths (Fig.5.16.a), stomata cell phytoliths (Fig.5.16.b) and irregular phytoliths (Fig.5.16.c). Irregular phytoliths (Fig.5.16.d) were observed in the stems of the plant and the seedpods contained spheroid psilate phytoliths (Fig.5.16.e), cylindroid psilate phytoliths (Fig.5.16.f) and irregular phytoliths (Fig.5.16.g).

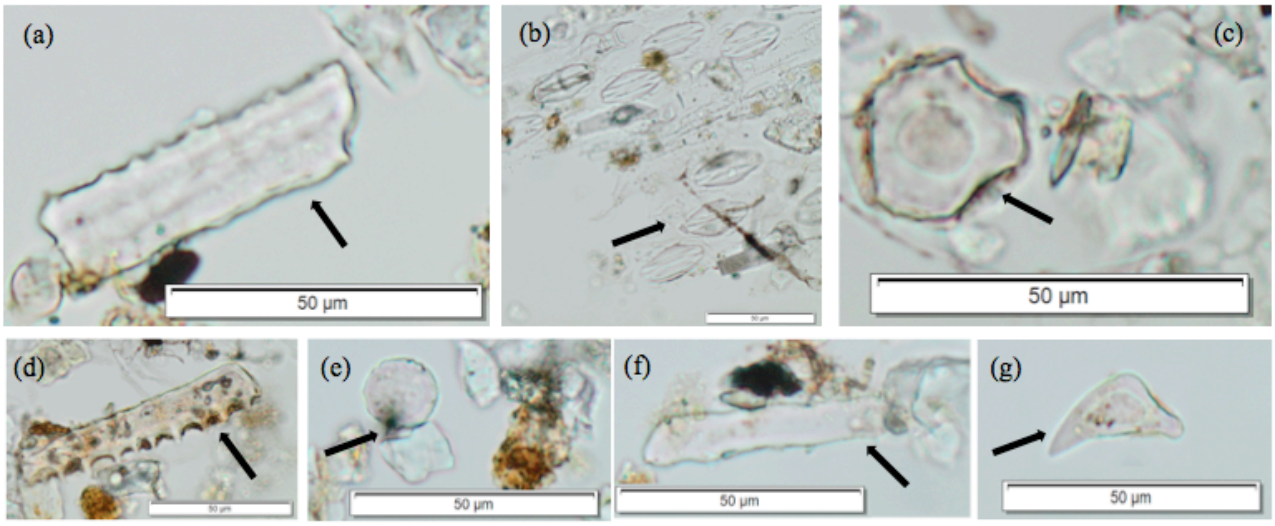


**Fig. 5.16.** *Grewia flavescens* phytolith types: (a) Cylindroid sinuous irregular ends, from leaf material; (b) Stomata cells, from leaf material; (c) Irregular, from leaf material; (d) Irregular, from stem material; (e) Spheroid psilate, from pod material; (f) Cylindroid psilate, from pod material; (g) Irregular, from pod material. Scale: 50µm.

Plant Name: *Grewia occidentalis*

No phytoliths were observed in the leaves or plant stems of *Grewia occidentalis* (Cross-berry).

## 5.3 Phytoliths In The EFT And DFT Soils

In this section, the results of the phytolith analysis of each sediment sample by site are presented. Modern soils collected from the top of the sampling sites may be representative of the vegetation present in the area for the last years/decades. Therefore the modern sediment samples were used for comparison with the phytolith assemblages observed in the fossil record in order to detect changes in the vegetation composition of the region at a local scale. The archaeological samples are interpreted chronologically, with the oldest sample being described first. As the weight of the original sample was not recorded during collection and processing, it was not possible to quantify precisely the phytolith numbers in these samples. Refer to Appendix II for the tables that record the phytolith counts, types and frequencies in the EFT and DFT samples.

The criteria of Albert and Weiner (2001), described in section 4.4 (Data Analysis And Interpretation) were used to validate the reliability and representatively of phytolith assemblages within the sediment samples. A minimum number of 200 phytoliths with consistent morphology was considered necessary in order to obtain a reliable analysis of the phytoliths present in a sediment sample. Below this number some morphologies present in lower amounts could be missed. A count of less than 50 phytoliths was considered an unreliable representation of the phytolith population and was excluded.

#### 5.3.1.1 Elandsfontein Bay 0209

Sample EFT1.3 yielded a total phytolith count of 167 of which 124 were regarded as being diagnostic. However the sample was considered an unreliable representation of the phytolith assemblage compared to sample EFT1.1. EFT1.1 yielded a total phytolith count of 435 of which

340 were regarded as being diagnostic and a reliable representation of the phytoliths types within the sediment sample. The modern sample EFT1.4 yielded a total phytolith count of 114 of which 86 were regarded as being diagnostic.

#### 5.3.1.1.1 Bay 0209 Plant Groups And Phytolith Morphologies

Phytolith morphotypes for each sediment sample were identified and associated with specific plant groups. These included woody dicotyledons, grasses, Cyperaceae, Arecaceae and monocotyledons.

Sample EFT1.3:

Sample EFT1.3 was taken from the sediment section that was representative of the upper nodular layer. The largest percentage of phytoliths recorded in this sample was from the woody dicotyledons group (30.5%), followed by phytoliths from grasses (22.8%), Cyperaceae (1.2%), monocotyledons (13.2%) and other non-diagnostic types (32.3%) (Fig.5.17.)

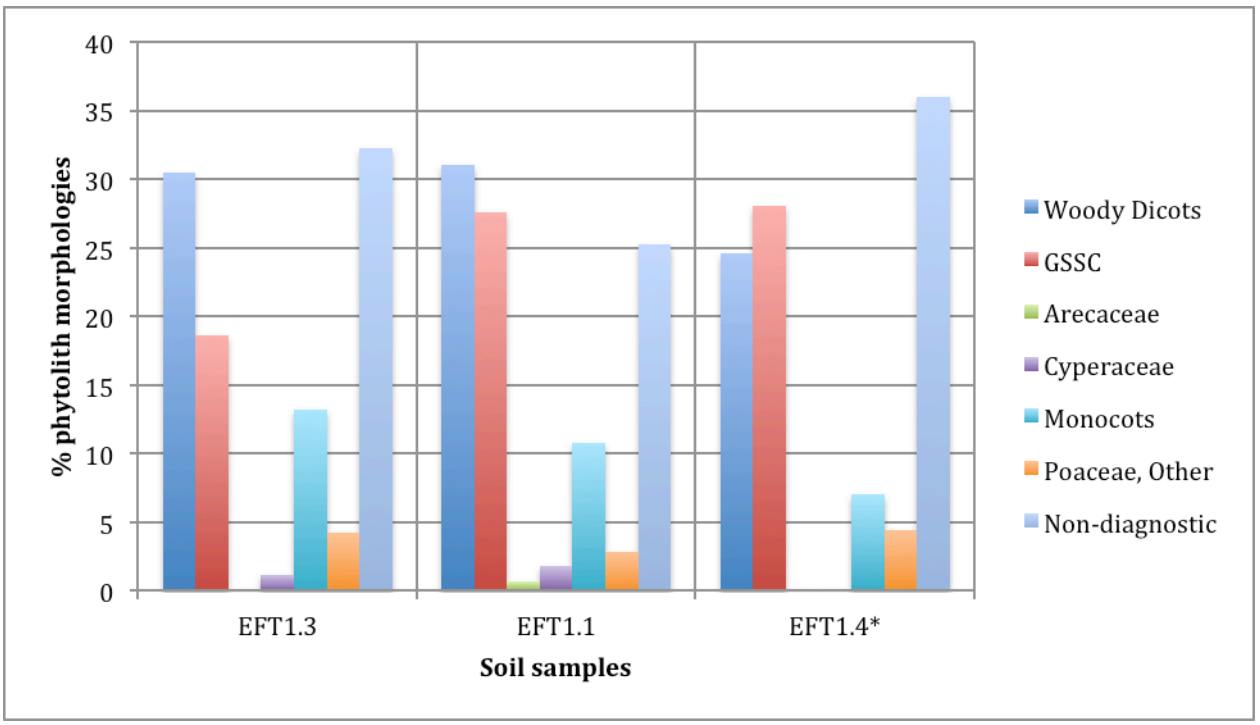


**Fig. 5.17.** EFT Bay 0209, Samples EFT1.3, EFT1.1 and EFT1.4 plant group phytolith morphotypes (samples listed from left to right in decreasing age).

Sample EFT1.1:

Sample EFT1.1 was taken from the sediment section that was representative of the unit above the white nodular layer. The dominant phytoliths in this sample were from woody dicotyledons (31%). These were followed by the grass group (30.4%), the monocotyledons (10.8%), Cyperaceae (1.8%), Arecaceae (0.7%) and other non-diagnostic types (25.3%) (Fig.5.17.)

Globular decorated phytoliths were diagnostic of woody dicotyledons (Fig.5.18.a). Bulliform cell phytoliths from other grass types were recognised in the sample (Fig.5.18.b) as well as trichome phytoliths representing non-diagnostic plant types (Fig.5.18.c).

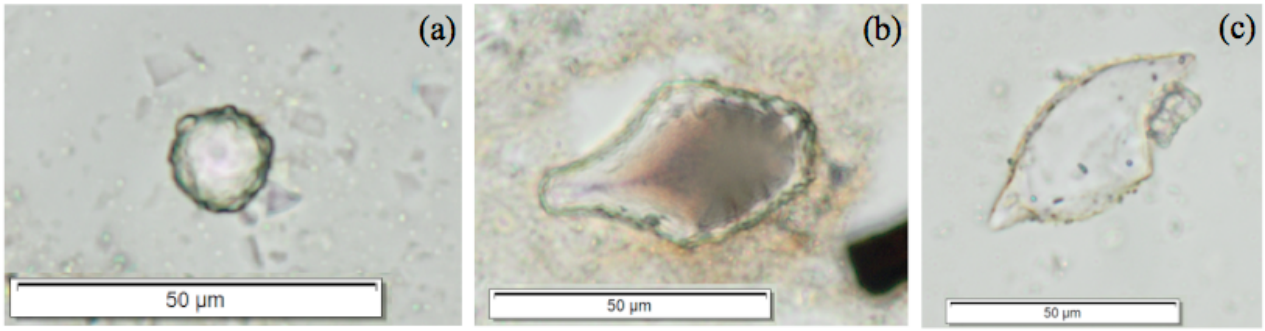


**Fig. 5.18.** EFT1.1 phytolith types: (a) Globular decorated phytolith (woody dicotyledon); (b) Bulliform cell (grass type); (c) Trichome (non-diagnostic type). Scale: 50µm.

Sample EFT1.4:

The largest percentage of phytoliths recorded in this modern sample were from the grass groups (32.5%), followed by phytoliths from woody dicotyledons (24.6%) with the remainder being derived from monocotyledons (7%) and other non-diagnostic types (36%) (Fig.5.17.)

**5.3.1.1.2 Bay 0209 GSSC Phytoliths**

The presence and frequencies of various GSSC morphotypes were used to charcaterise the grass phytoliths. Modern grass reference collections and published literature were used to aid in the identification of the GSSC phytoliths. These included bilobate variant 1 (Var.1), bilobate variant 2

(Var.2), cross, saddle variant 1 (Var.1), saddle variant 2 (Var.2), trapezoid, rondel, oblong and reniform phytoliths (Fig.5.19.)

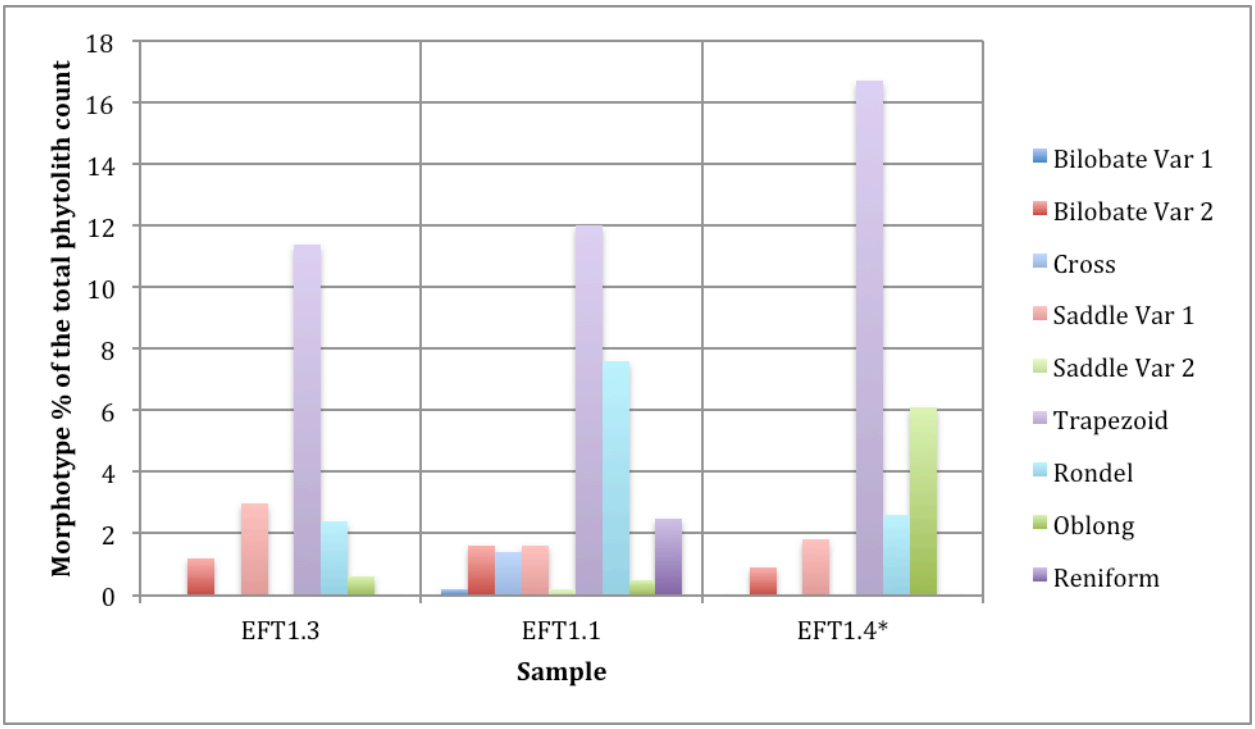


**Fig. 5.19.** EFT Bay 0209, Samples EFT1.3, EFT1.1 and EFT1.4 GSSC phytoliths (samples listed from left to right from the oldest to youngest sample).

Sample EFT1.3:

The most abundant GSSC phytolith morphotype within this sample was the trapezoid (11.4%) followed by the saddle Var.1 (3%) and rondel (2.4%). Other minor phytolith morphotypes included the bilobate Var.2 (1.2%) and the oblong (0.6%) (Fig.5.19).

**Note**: The GSSC morphotype percentages listed represent a proportion of the total phytolith population (including woody dicotyledons, grasses, Cyperaceae, Arecaceae and monocotyledons) in each sediment sample.

Examples of some of the trapezoid and oblong morphotypes are provided below in Fig.5.20.

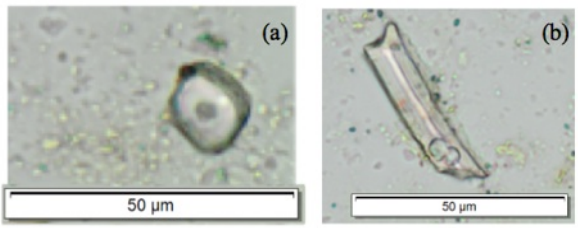


**Fig. 5.20.** EFT 1.3 phytolith types: (a) Trapezoid; (b) Oblong (Trapeziform smooth). Scale: 50µm.

Sample EFT1.1:

The trapezoid phytolith (12%) was the most observed morphotype in this sample, followed by the rondel (7.6%). Other minor morphotypes included the reniform (2.5%), the bilobate Var.2 (1.6%), the saddle Var.1 (1.6%) and cross (1.4%). The oblong, bilobate Var.1 and saddle Var.2 morphotypes were observed, but their abundance was not noteworthy (<1%) (Fig.5.19).

Examples of saddle Var.1, bilobate Var.2, oblong and trapezoid morphotypes are provided in Fig.5.21.

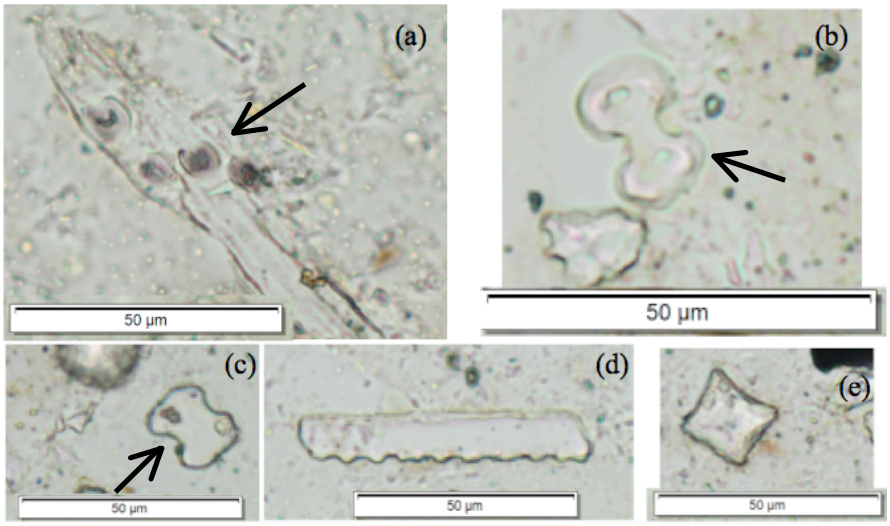


**Fig. 5.21.** EFT1.1 phytolith types: (a) Saddle Var.1; (b-c) Bilobate Var.2; (d) Oblong (Trapeziform sinuous); (e) Trapezoid. Scale: 50µm.

Sample EFT1.4:

The most abundant GSSC phytolith morphotype in this sample was the trapezoid (16.7%), followed by the oblong (6.1%) and rondel (2.6%). Other minor morphotypes included the saddle Var.1 (1.8%) and bilobate Var.2 (0.9%) phytoliths (Fig.5.19).

#### 5.3.1.1.3 Bay 0209 Grass Subfamily Phytoliths

The characterisation of $C_3$ and $C_4$ type grasses using GSSC phytoliths is recognised as being problematic because some $C_4$ type grasses are known to produce more $C_3$ type morphotypes than the characteristic $C_4$ short cells. The composition of GSSC assemblages can give an indication of grass species that grew in palaeoenvironments. The grass subfamilies identified in sediment

samples from Bay 0209, include Chloridoideae, Danthonioideae, Ehrhartoideae, Panicoideae and Pooideae (Fig.5.22).

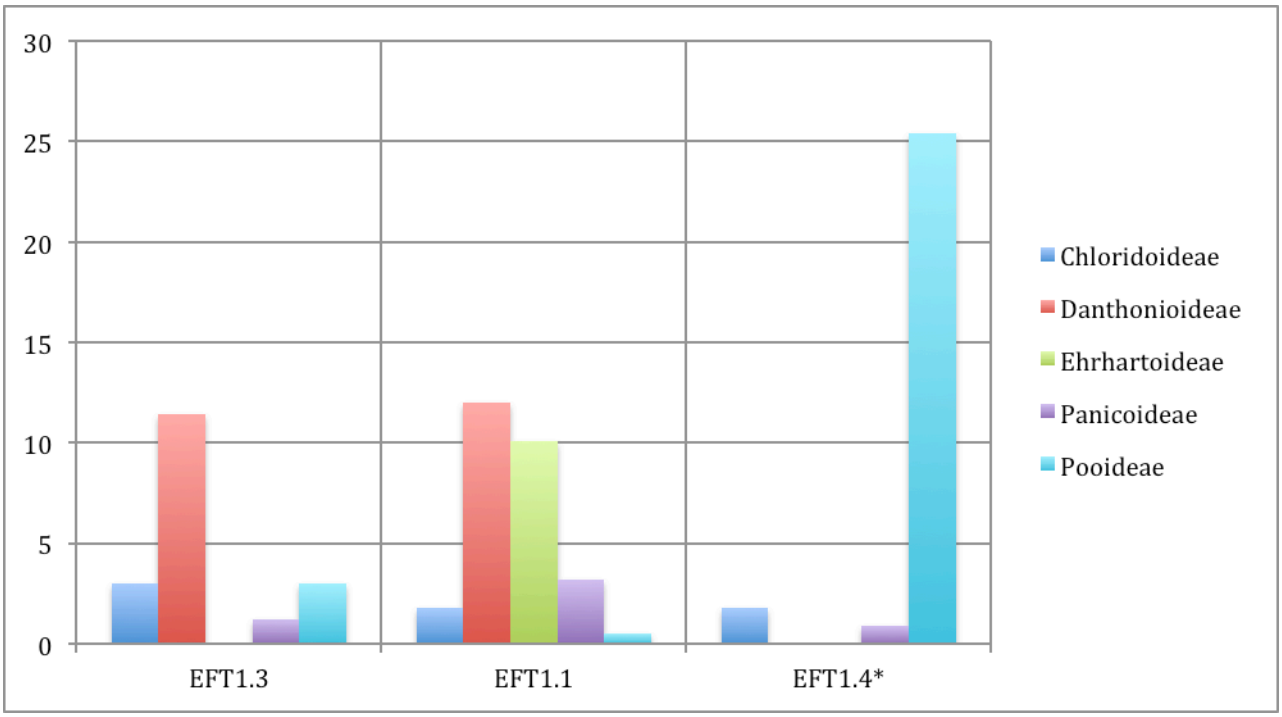


**Fig. 5.22.** EFT Bay 0209, Samples EFT1.3, EFT1.1 and EFT1.4 grass subfamily phytolith morphotypes (samples listed from left to right are from the oldest to youngest).

Sample EFT1.3:

The most abundant GSSC morphotypes in this sample were associated with the $C_3$ grass subfamily Danthonoideae (11.4%), followed by the $C_4$ Chloridoideae (3%), $C_3$ Pooideae (3%) and $C_4$ Panicoideae (1.2%) subfamilies (Fig.5.22). The composition of this phytolith assemblage suggests that C3 type grasses (14.4%) were dominant at the time that the upper portion of the nodular layer was deposited.

Sample EFT1.1:

Within this sample, the largest percentage of GSSC morphotypes were associated with the $C_3$ grass subfamilies Danthonoideae (12%) and Ehrhartoideae (10.1%), followed by $C_4$ grass subfamilies Panicoideae (3.2%) and Chloridoideae (1.8%), and lastly by the $C_3$ grass subfamily Pooideae (0.5%) (Fig.5.22). The composition of this phytolith assemblage suggests that $C_3$ type grasses

(22.6%) were dominant at the time that the section of sediment above the nodular layer was laid down.

Sample EFT1.4:

The most abundant GSSC morphotypes in this sample belongs to the $C_3$ grass subfamily Pooideae (25.4%), followed by the $C_4$ Chloridoideae (1.8%) and Panicoideae (0.9%) (Fig.5.22). The composition of this modern sediment phytolith assemblage reflects the current situation in the winter rainfall region where $C_3$ type grasses are dominant over $C_4$ type grasses.

#### 5.3.1.1.4 Bay 0209 Monocotyledon-Dicotyledon Phytolith Comparison

The percentages of phytoliths associated with samples EFT1.3, EFT1.1 and EFT1.4 are provided in Fig.5.23.

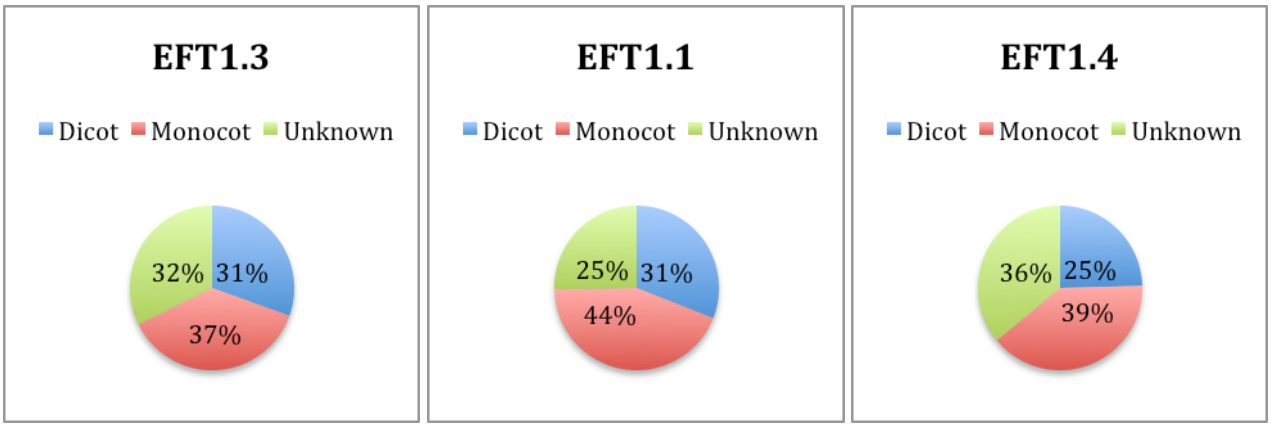


**Fig. 5.23**. EFT Bay 0209, EFT1.3, EFT1.1 and EFT1.4, Monocotyledon-Dicotyledon phytolith comparison pie charts.

The phytolith assemblages associated with the fossil samples EFT1.3 and EFT1.1 from Bay 0209, suggest that the vegetation was comprised of a more or less even percentage of herbaceous monocots, grasses and woody/shrubby plants, if the non-diagnostic phytoliths are excluded. The phytolith assemblages ascribed to the modern sample EFT1.4 is similar to the fossil samples, but represents a disturbed surface affected by modern human activity and by the introduction of alien plants.

#### 5.3.1.2 Elandsfontein Bay 0909

Sample EFT2.2 yielded a total phytolith count of 301, of which 225 were regarded as diagnostic and a reliable representation of the phytolith types within the sediment sample. EFT2.1 yielded a total phytolith count of 204 of which 168 were regarded as diagnostic, however this sample is not considered to be as reliable a representation of the phytolith assemblage as sample EFT2.2. The modern sample EFT2.3 yielded a total phytolith count of 286 of which 172 were regarded as diagnostic.

##### 5.3.1.2.1 Bay 0909 Plant Groups And Phytolith Morphologies

Phytolith morphotypes were identified and associated with specific plant groups for every sediment sample. The plant groups included woody dicotyledons, grasses, Arecaceae and monocotyledons.

Sample EFT2.2:

Sample EFT2.2 was taken from the sediment section representative of the lower portion of the artefact/fossil horizon. The largest percentage of phytoliths recorded in this sample was from the grass groups (47.5%) followed by monocotyledons (13.3%), with the remainder from woody dicotyledons (6.6%), Arecaceae (1.7%) and other non-diagnostic types (30.9%) (Fig.5.24).

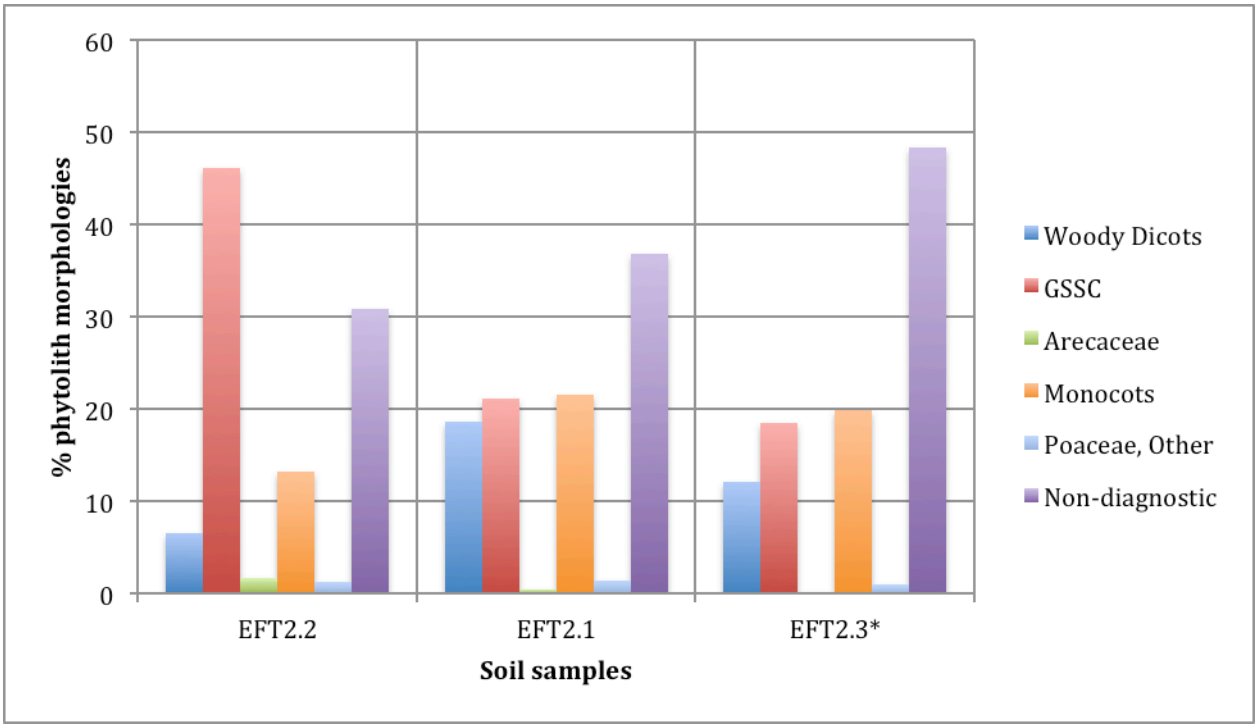


**Fig. 5.24.** EFT Bay 0909, Samples EFT2.2, EFT2.1 and EFT2.3 plant group phytolith morphotypes (samples listed from left to right in decreasing age).

Sample EFT2.1:

Sample EFT2.1 was taken from the sediment section representative of the higher portion of the artefact/fossil horizon. The dominant phytoliths in this sample were from the grass group (22.6%). These were followed by monocotyledons (21.6%), woody dicotyledons (18.6%), Arecaceae (<1%) and other non-diagnostic types (36.8%) (Fig.5.24).

Sample EFT2.3:

The largest percentage of phytoliths recorded in this modern sample was from the grass group (19.5%), followed by monocotyledons (19.9%), woody dicotyledons (12.2%) and other non-diagnostic types (48.3%) (Fig.5.24).

#### 5.3.1.2.2 Bay 0909 GSSC Phytoliths

The GSSC phytoliths identified in the sediment samples included bilobate variant 2 (Var.2), polylobate, cross, saddle variant 1 (Var.1), saddle variant 2 (Var.2), trapezoid, rondel and oblong morphotypes (Fig.5.25).

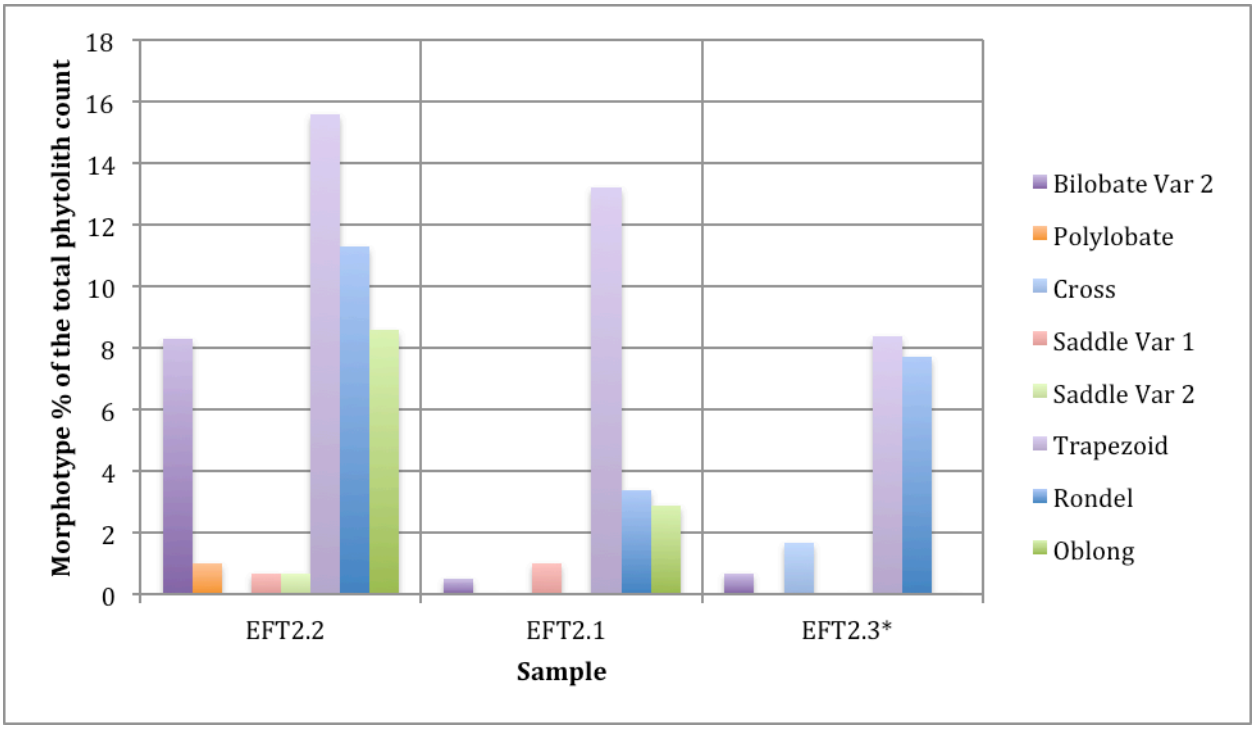


**Fig. 5.25.** EFT Bay 0909: Samples EFT2.2, EFT2.1 and EFT2.3 GSSC phytoliths (samples listed left to right from the oldest to youngest sample).

Sample EFT2.2:

The most abundant GSSC phytolith morphotype was the trapezoid (15.6%), followed by the rondel (11.3%), oblong (8.6%) and lastly the bilobate Var.2 (8.3%). Other minor morphotypes included the polylobate (1%), saddle Var.1 (0.7%) and saddle Var.2 (0.7%) (Fig.5.25).

Examples of bilobate Var.2, saddle Var.2, rondel and oblong morphotypes are provided in Fig.5.26.

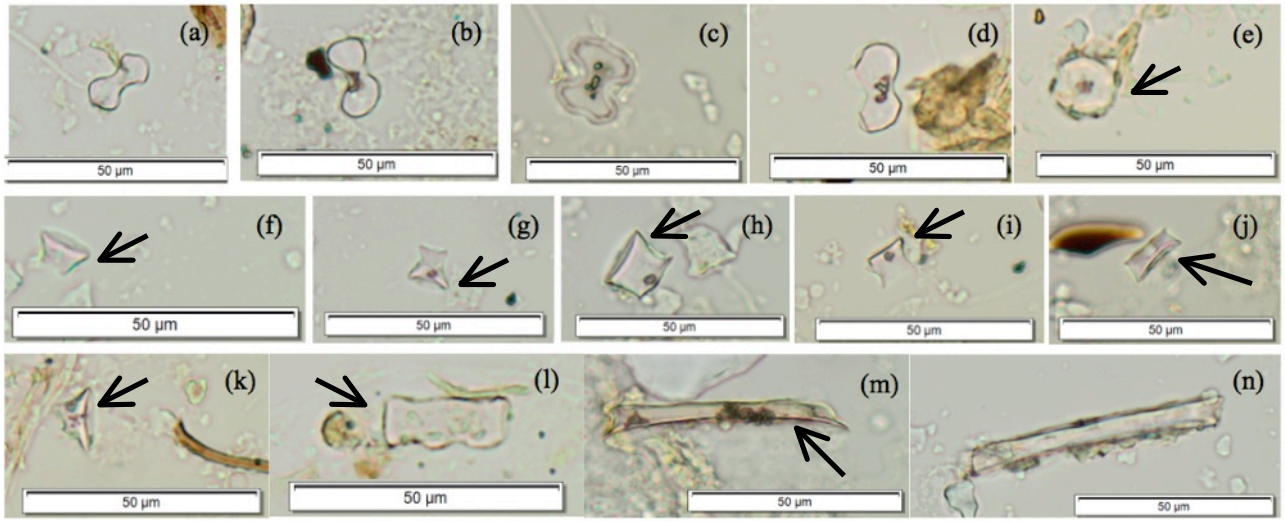


**Fig. 5.26.** EFT2.2 phytolith types: (a-d) Bilobate Var.2; (e-f) Saddle Var.2; (g-k) Rondel; (l-n) Oblong. Scale: 50µm.

Sample EFT2.1:

The most observed morphotype in this sample were the trapezoid (13.2%). Other minor morphotypes included the rondel (3.4%), the oblong (2.9%) and the saddle Var.1 (1%). The bilobate Var.2 morphotypes were observed but their abundance was not noteworthy (<1%) (Fig.5.25). Examples of rondel, trapezoid and saddle Var.1 morphotypes present in sample EFT2.1 are depicted in Fig.5.27.

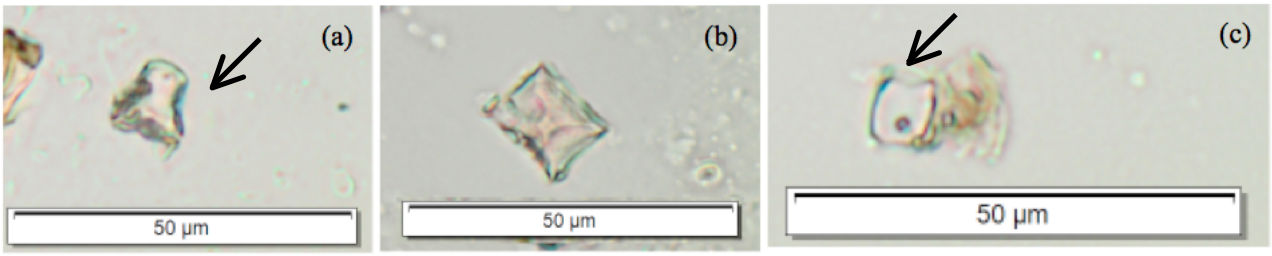


**Fig. 5.27.** EFT2.1 phytolith types: (a) Rondel; (b) Trapezoid; (c) Saddle Var.1. Scale: 50µm.

Sample EFT2.3:

The most abundant GSSC morphotypes were the trapezoid (8.4%) and rondel (7.7%). Other minor morphotypes included the cross (1.7%) and bilobate Var.2 (0.7%) (Fig.5.25).

#### 5.3.1.2.3 Bay 0909 Grass Subfamily Phytoliths

The grass subfamilies identified in sediment samples from Bay 0909 include Chloridoideae, Danthonioideae, Ehrhartoideae, Panicoideae and Pooideae (Fig.5.28).

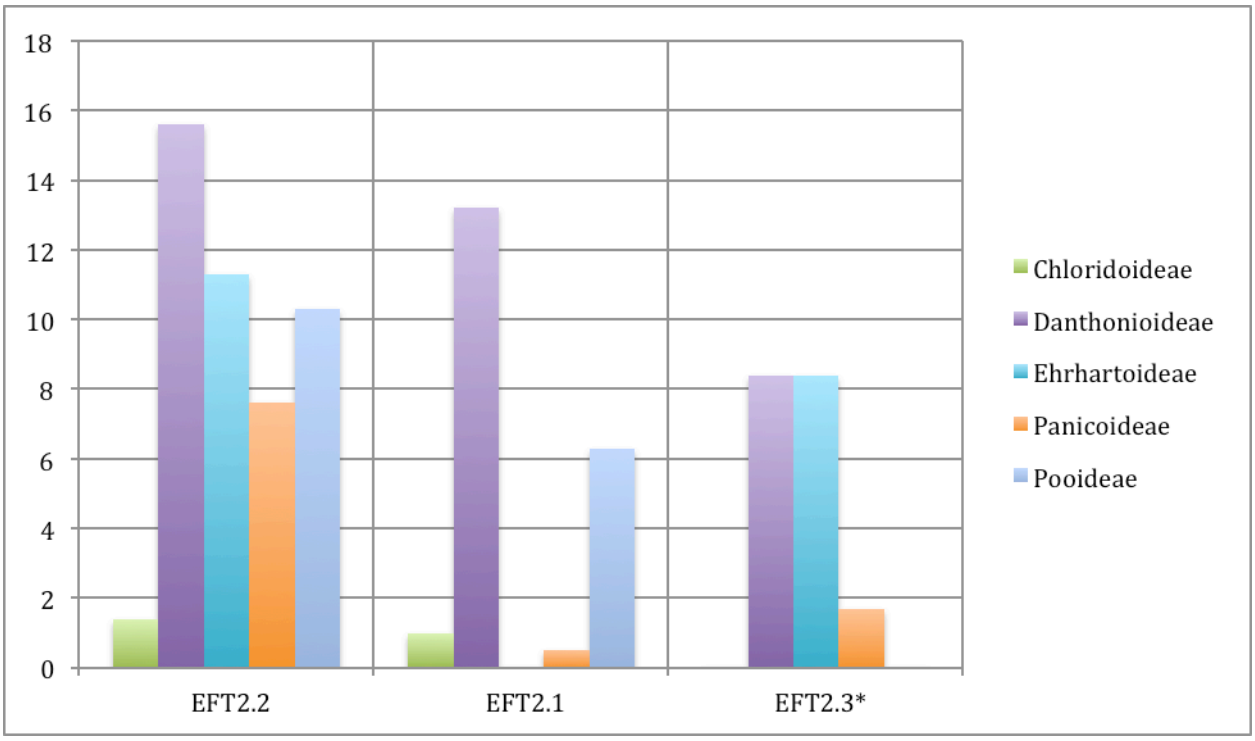


**Fig. 5.28.** EFT Bay 0909, Samples EFT2.2, EFT2.1 and EFT2.3 grass subfamily phytolith morphotypes (samples listed left to right in decreasing age).

Sample EFT2.2:

Within this sample, the largest percentage of GSSC morphotypes belonged to the $C_3$ grass subfamilies Danthonoideae (15.6%), Ehrhartoideae (11.3%) and Pooideae (10.3%), followed by $C_4$ subfamilies Panicoideae (7.6%) and Chloridoideae (1.4%) (Fig.5.28). The composition of this phytolith assemblage suggests that $C_3$ type grasses (37.2%) were dominant at the time that the lower section of sediment within artefact/fossil horizon was laid down.

Sample EFT2.1:

The most abundant GSSC morphotypes in this sample belonged to the $C_3$ grass subfamilies Danthonoideae (13.2%) and Pooideae (6.3%), followed by $C_4$ grass subfamilies Chloridoideae (1%)

and Panicoideae (0.5%) (Fig.5.28). The $C_3$ type grass phytoliths (19.5%) were the dominant grass type at the time that the upper portion of the artefact/fossil horizon was deposited.

Sample EFT2.3:

The most abundant GSSC morphotypes in this sample belonged to the $C_3$ subfamilies Danthonioideae (8.4%) and Ehrhartoideae (8.4%), followed by the $C_4$ Panicoideae (1.7%) subfamily (Fig.5.28). The composition of this modern sediment phytolith assemblage reflects the current situation in the winter rainfall region where $C_3$ type grasses are dominant over $C_4$ type grasses.

#### 5.3.1.2.4 Bay 0909 Monocotyledon- Dicotyledon Phytolith Comparison

The percentages of phytoliths associated with samples EFT2.2, EFT2.1 and EFT2.3 are provided in Fig.5.29.

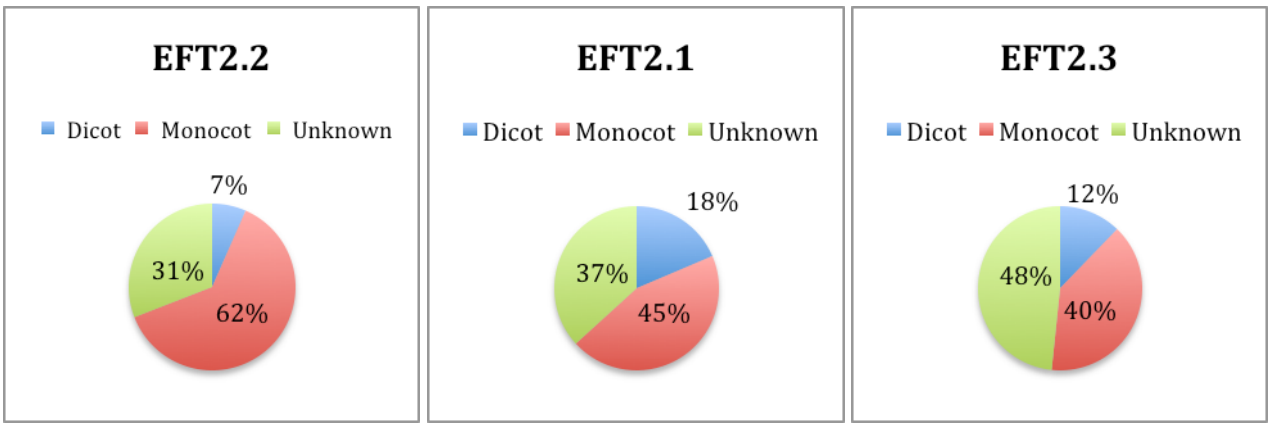


**Fig. 5.29.** EFT Bay 0909, EFT2.2, EFT2.1 and EFT2.3, Monocotyledon-Dicotyledon phytolith comparison pie charts.

The phytolith assemblages associated with the fossil samples EFT2.2 and EFT2.1 from Bay 0909, suggest a vegetation community comprised of a substantially higher percentage of herbaceous monocots and grasses than woody/shrubby plants. The phytolith assemblages associated with the modern sample EFT2.3 is similar to the fossil samples but represents a disturbed surface affected by modern human activity and by the introduction of alien plants.

### 5.3.1.3 Elandsfontein Bay 0710

Sample EFT3.1 yielded a total phytolith count of 294, of which 246 were regarded as being diagnostic and a reliable representation of the phytolith types within the sediment sample. The modern sample EFT3.2 yielded a total phytolith count of 300, of which 264 were regarded as being diagnostic.

#### 5.3.1.3.1 Bay 0710 Plant Groups And Phytolith Morphologies

The plant groups identified through the analysis of phytolith morphotypes in these sediment samples included woody dicotyledons, grasses, Arecaceae, Cyperaceae and monocotyledons.

Sample EFT3.1:

This sample was taken from the fossil/artefact layer. The largest percentage of phytoliths recorded in this sample was from the grass group (29.6%) followed by phytoliths from woody dicotyledons (26.9%), monocotyledons (11.6%), Cyperaceae (7.1%), Arecaceae (0.7%) and other non-diagnostic types (24.1%) (Fig.5.30).

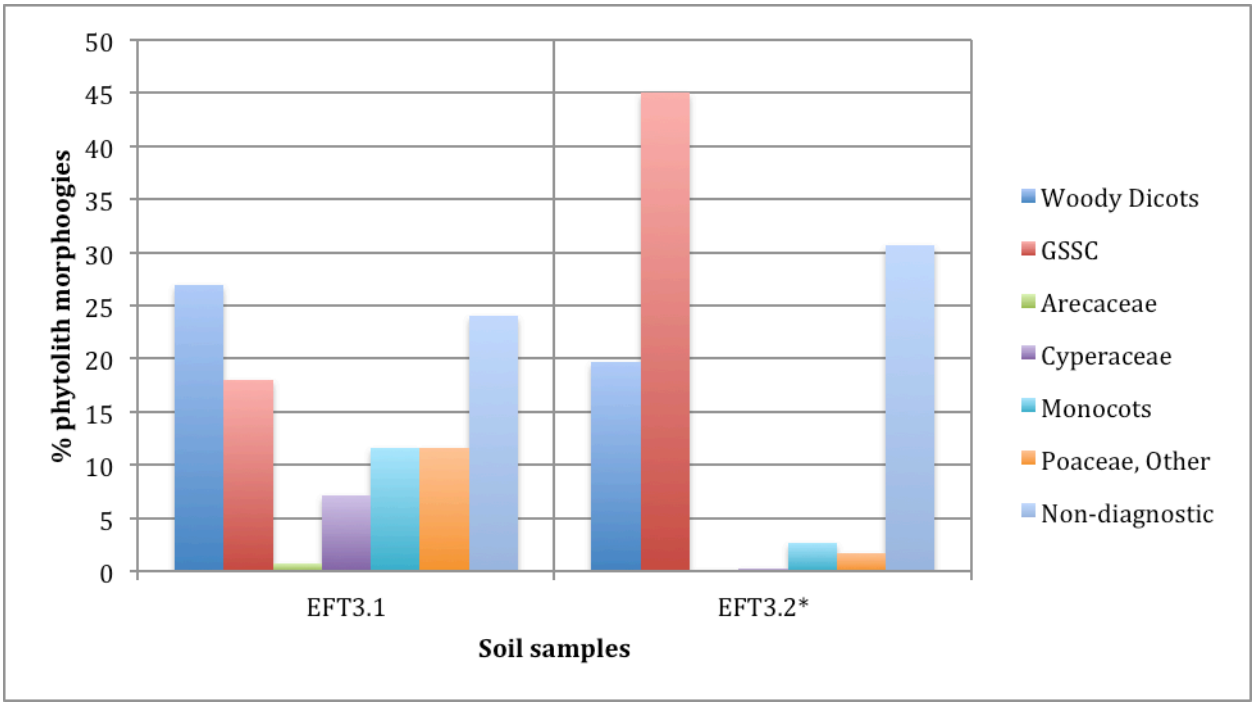


**Fig. 5.30.** EFT Bay 0710, Samples EFT3.1 and EFT3.2, plant group phytolith morphotypes (samples listed left to right in decreasing age).

Sample EFT3.2:

The largest percentage of phytoliths recorded in this modern sample was from the grass groups (46.7%), followed by phytoliths from woody dicotyledons (19.7%) with the remainder being derived from monocotyledons (2.7%) and non-diagnostic types (30.7%). In this sample, less than 1% of Cyperaceae type phytoliths were recorded (Fig.5.30).

**5.3.1.3.2 Bay 0710 GSSC Phytoliths**

The phytolith morphotypes observed in these samples included the bilobate variant 2 (Var.2), cross, saddle variant 1 (Var.1), trapezoid, rondel, oblong and reniform phytoliths (Fig.5.31).

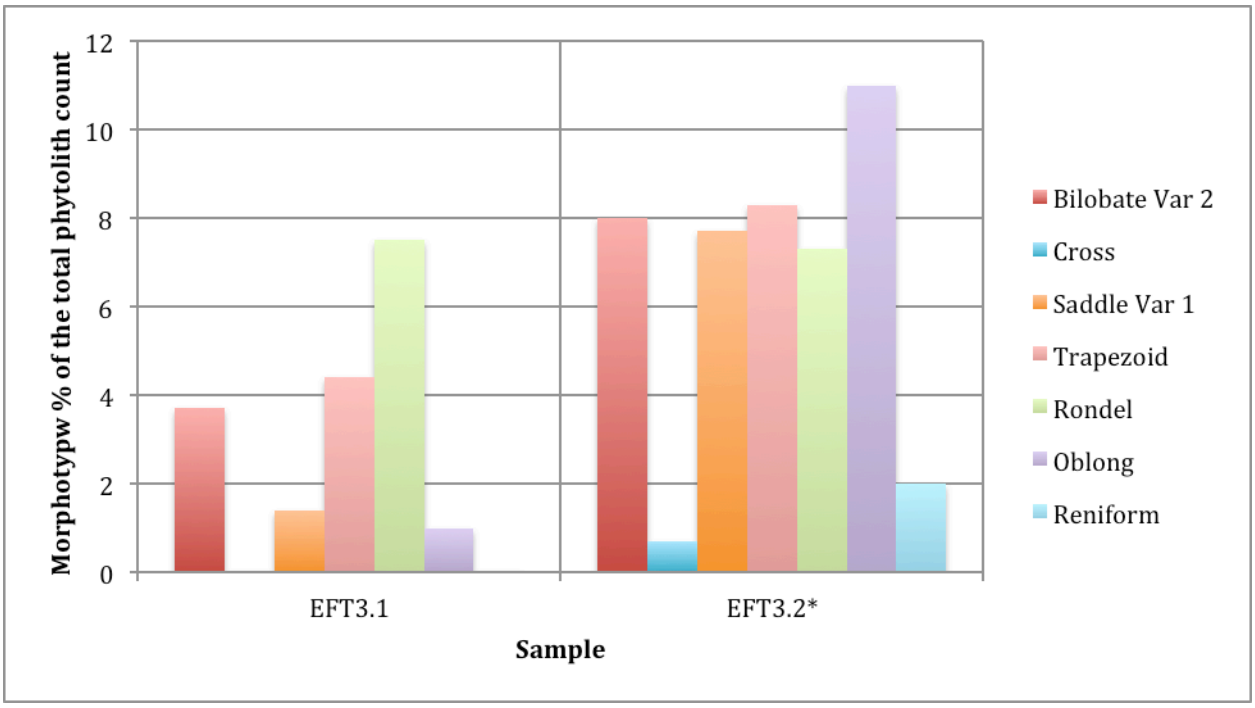


**Fig. 5.31.** EFT Bay 0710, Samples EFT3.1 and EFT3.2 GSSC phytoliths (samples listed left to right from the oldest to youngest).

Sample EFT3.1:

The most abundant GSSC phytolith morphotype was the rondel (7.5%) followed by the trapezoid (4.4%) and then the bilobate Var.2 (3.7%). Other minor morphotypes include the saddle Var.1 (1.4%) and oblong (1%) phytoliths (Fig.5.31).

An example of a bilobate Var.2 morphotype is provided below in Fig.5.32.

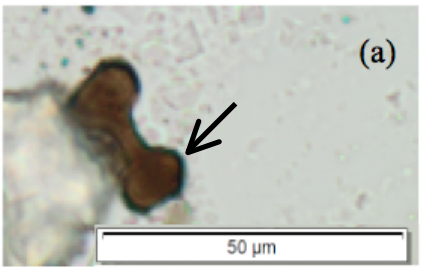


**Fig. 5.32.** EFT3.1 Bilobate Var.2 phytolith. Scale: 50µm.

Sample EFT3.2:

The oblong phytoliths (11%) were the most observed morphotype in this sample followed by the trapezoid (8.3%), bilobate Var.2 (8%), saddle Var.1 (7.7%) and rondel (7.3%). Other minor morphotypes included the reniform (2%) and cross (0.7%) (Fig.5.31).

Examples of oblong, rondel, bilobate Var.2 and saddle Var.1 morphotypes are provided below in Fig.5.33.

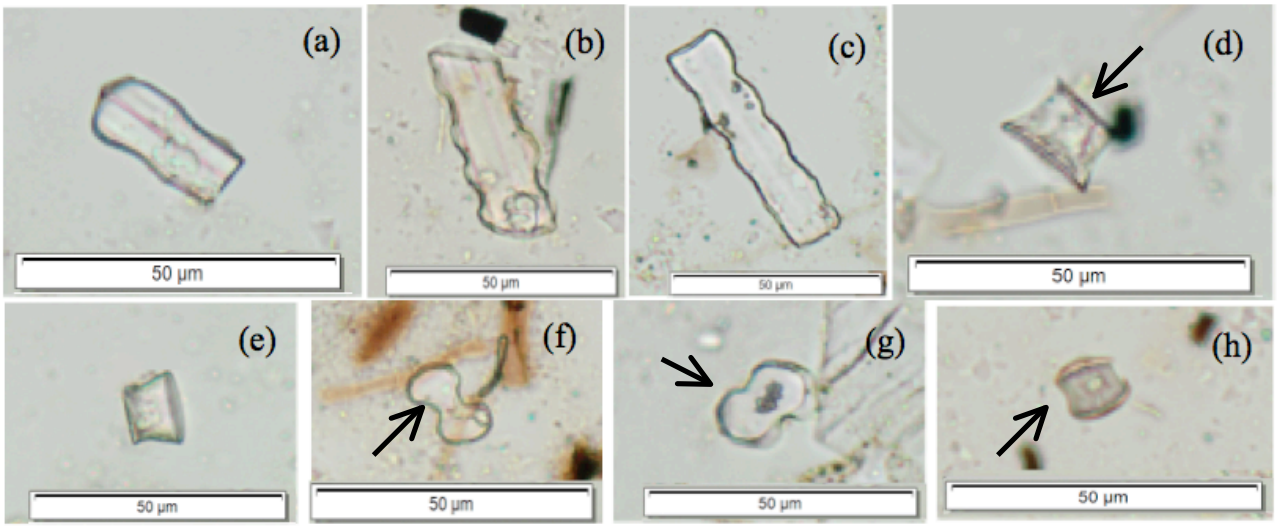


**Fig. 5.33.** EFT3.2 phytolith types: (a-c) Oblong; (d-e) Rondel; (f-g) Bilobate Var.2; (h) Saddle Var.1. Scale: 50µm.

### 5.3.1.3.3 Bay 0710 Grass Subfamily Phytoliths

The grass subfamilies identified in sediment samples from Bay 0710, include Chloridoideae, Danthonioideae, Ehrhartoideae, Panicoideae and Pooideae (Fig.5.34).

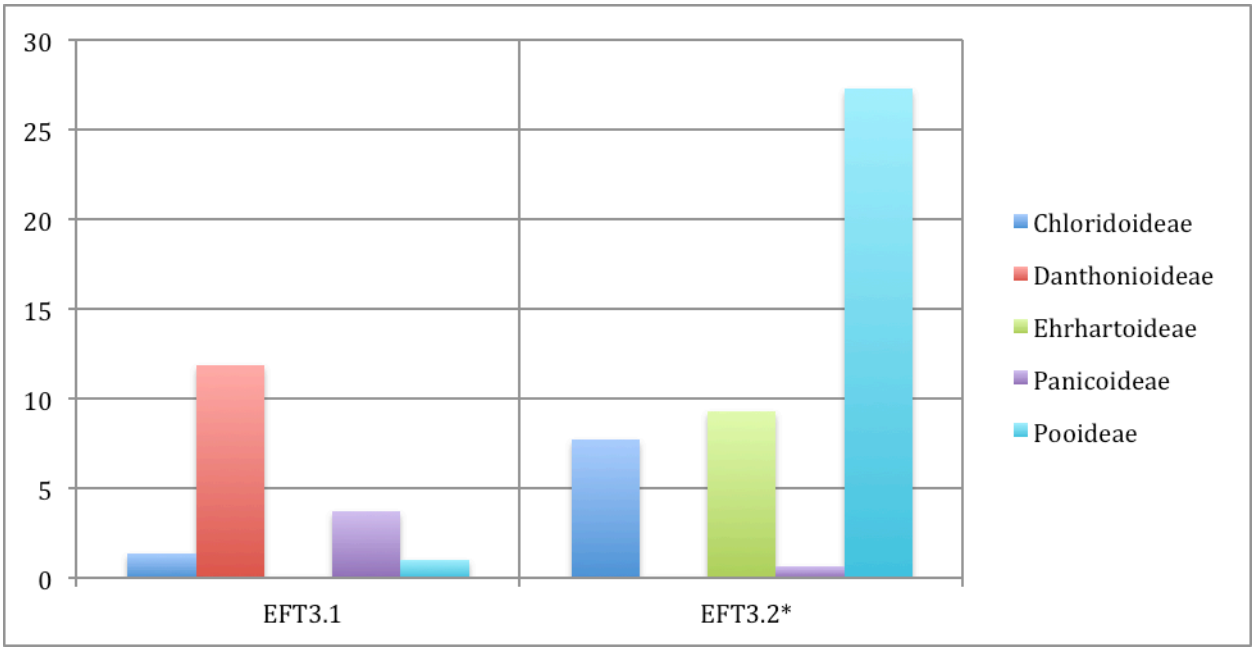


**Fig. 5.34.** EFT Bay 0710, Samples EFT3.1 and EFT3.2 grass subfamily phytoliths morphotypes (samples listed left to right from the oldest to youngest sample).

Sample EFT3.1:

The most abundant GSSC morphotypes in this sample were associated with the $C_3$ grass subfamily Danthonioideae (11.9%) followed by the $C_4$ Panicoideae (3.7%), Chloridoideae (1.4%) and lastly by the $C_3$ grass subfamily Pooideae (1%), refer to Fig.5.34. The composition of this phytolith assemblage suggests that C3 type grasses (12.9%) were dominant at the time that the section of sediment representing the fossil/artefact layer was laid down.

Sample EFT3.2:

Within this modern sample, the largest percentage of GSSC morphotypes belonged to the $C_3$ grass subfamilies Pooideae (27.3%) and Ehrhartoideae (9.3%), followed by the $C_4$ grass subfamilies Chloridoideae (7.7%) and Panicoideae (0.7%) (Fig.5.34). This phytolith assemblage reflects the contemporary environment where $C_3$ type grasses dominant over $C_4$ type grasses.

**5.3.1.3.4 Bay 0710 Monocotyledon-Dicotyledon Phytolith Comparison**

The percentages of phytoliths associated with samples EFT3.1 and EFT3.2 are provided in Fig.5.35.

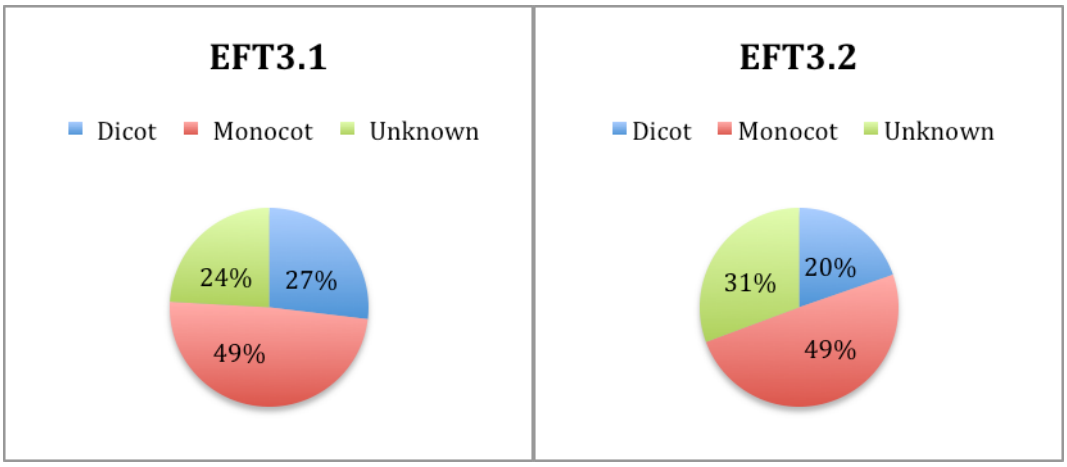


**Fig. 5.35.** EFT Bay 0710, EFT3.1 and EFT3.2, Monocotyledon-Dicotyledon phytolith comparison pie charts.

The phytolith assemblages associated with the fossil sample EFT3.1 from Bay 0710, suggest that the vegetation community was comprised of a higher percentage of herbaceous monocots and grasses compared to the woody/shrubby plants if the non-diagnostic phytoliths are excluded.

The phytolith assemblages associated with the modern sample EFT3.2 are similar to the fossil samples but represent a disturbed surface affected by modern human activity and by the introduction of alien plants.

#### 5.3.1.4 Elandsfontein Bay 0313

Sample EFT4.2 yielded a total phytolith count of 172 of which 129 were regarded as diagnostic, however the sample is considered to be not as reliable as the phytolith assemblage in sample EFT4.4.

EFT4.9 yielded a total phytolith count of 246 of which 195 were regarded as being diagnostic and a reliable representation of the phytoliths types within the sediment sample.

EFT4.8 yielded a total phytolith count of 151 of which 115 were regarded as diagnostic, however the sample is considered not as reliable as the phytolith assemblage in sample EFT4.4.

EFT4.4 yielded a total phytolith count of 254 of which 211 were regarded as being diagnostic and a reliable representation of the phytoliths types within the sediment sample.

EFT4.1 yielded a total phytolith count of 200 of which 156 were regarded as diagnostic, however the sample is considered not as reliable as the phytolith assemblage in sample EFT4.4. The modern sample EFT4.10 yielded a total phytolith count of 541 of which 470 were regarded as diagnostic.

#### 5.3.1.4.1 Bay 0313 Plant Groups And Phytolith Morphologies

The specific plant groups observed in these samples included woody dicotyledons, grasses, Arecaceae, Cyperaceae and monocotyledons.

Sample EFT4.2:

Sample EFT4.2 was taken from the calcareous sand layer below the white nodular layer. The largest percentage of phytoliths recorded in this sample was from the grass groups (38.3%), followed by phytoliths from woody dicotyledons (15.1%), monocotyledons (8.1%) and other non-diagnostic types (38.4%) (Fig.5.36).

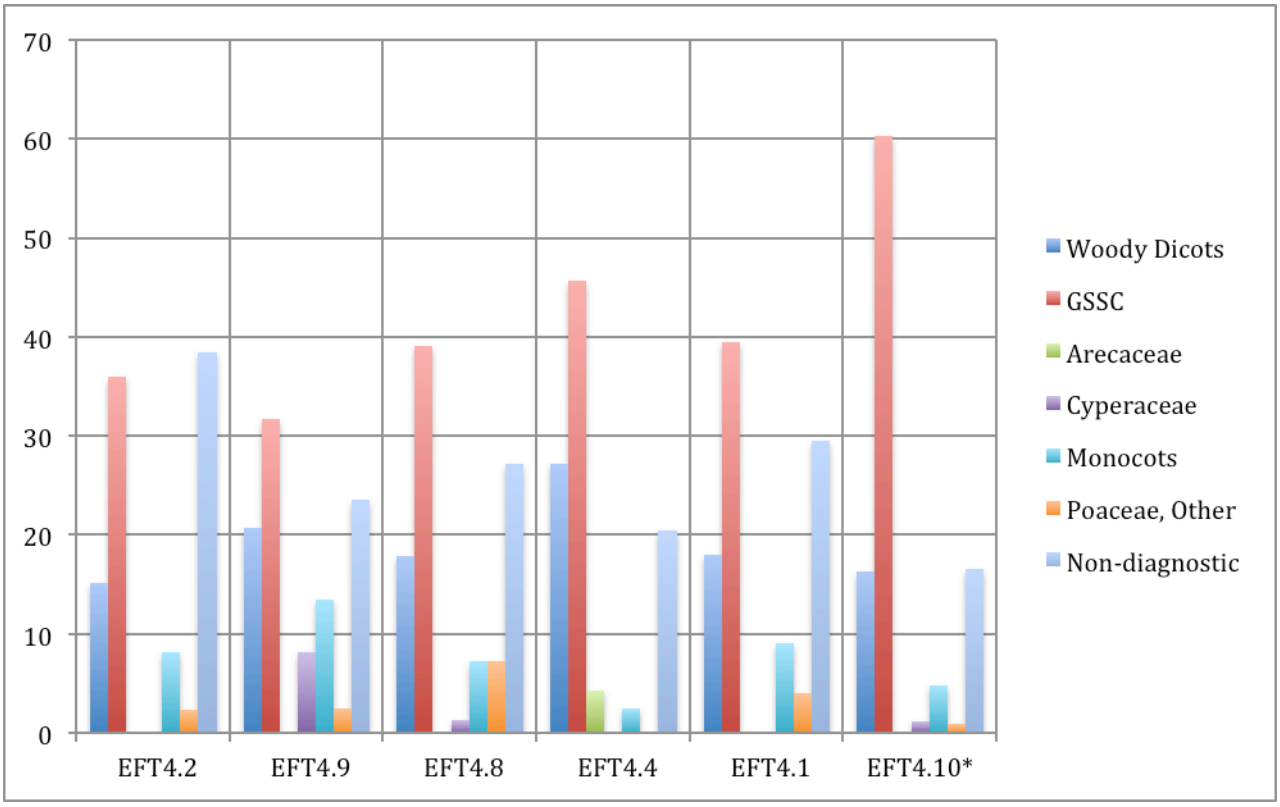


**Fig. 5.36.** EFT Bay 0313, Samples EFT4.2, EFT4.9, EFT4.8, EFT4.4, EFT4.1 and EFT4.10 plant group phytolith morphotypes (samples are listed left to right from the oldest to youngest).

Sample EFT4.9:

Sample EFT4.9 was taken from the lower unit of the nodular layer. The dominant phytoliths in this sample were from the grass groups (34.1%). These were followed by phytoliths from woody dicotyledons (20.7%), monocotyledons (13.4%), Cyperaceae (8.1%) and other non-diagnostic types (23.6%) (Fig.5.36).

Sample EFT4.8:

Sample EFT4.8 was taken from the upper section of the nodular layer. The largest percentage of phytoliths recorded in this sample was from the grass groups (46.4%), followed by phytoliths from woody dicotyledons (17.9%), monocotyledons (7.3%), Cyperaceae (1.3%) and other non-diagnostic types (27.2%) (Fig.5.36).

Sample EFT4.4:

Sample EFT4.4 was taken from the sediment above the nodular layer. The dominant phytoliths in this sample were from the grass groups (45.7%). These were followed by phytoliths from woody dicotyledons (27.2%), Arecaceae (4.3%), monocotyledons (2.4%) and other non-diagnostic types (20.5%) (Fig.5.36).

Sample EFT4.1:

Sample EFT4.1 was taken from the coarse sand above the white nodular layer. The largest percentage of phytoliths recorded in this sample was from the grass groups (43.5%), followed by phytoliths from woody dicotyledons (18%), monocotyledons (9%) and other non-diagnostic types (29.5%) (Fig.5.36).

Sample EFT4.10:

The dominant phytoliths in this modern sample were from the grass groups (61.2%). These were followed by phytoliths from woody dicotyledons (16.3%), monocotyledons (4.8%), Cyperaceae (1.1%) and other non-diagnostic types (16.6%) (Fig.5.36).

#### 5.3.1.4.2 Bay 0313 GSSC Phytoliths

The phytolith morphotypes observed in these samples included the bilobate variant 2 (Var.2), bilobate variant 3 (Var.3), polylobate, cross, saddle variant 1 (Var.1), saddle variant 2 (Var.2), trapezoid and rondel types (Fig.5.37).

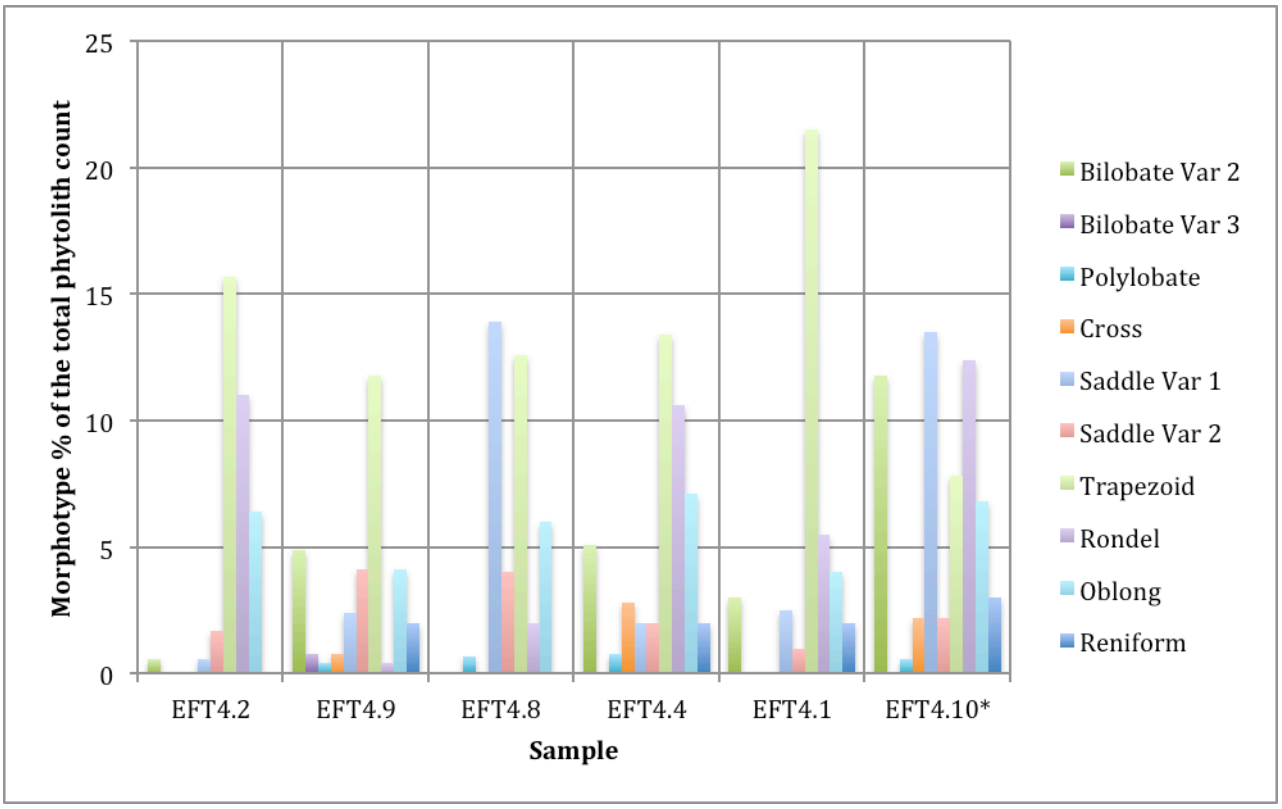


**Fig. 5.37.** EFT Bay 0313, Samples EFT4.2, EFT4.9, EFT4.8, EFT4.4, EFT4.1 and EFT4.10 GSSC phytoliths (samples listed left to right from the oldest to youngest).

Sample EFT4.2:

The most abundant GSSC phytolith morphotype was the trapezoid (15.7%) followed by the rondel (11%) and oblong (6.4%). Other minor morphotypes included the saddle Var.1 (0.6%), saddle Var.2 (1.7%) and the bilobate Var.2 (0.6%) (Fig.5.37).

Sample EFT4.9:

The trapezoid (11.8%) was the most observed phytolith morphotype, followed by the bilobate Var.2 (4.9%), oblong (4.1%), saddle Var.2 (4.1%), saddle Var.1 (2.4%), reniform (2%), bilobate Var.3 (0.8%), and cross (0.8%). Other minor morphotypes included the polylobate (0.4%) and rondel (0.4%) (Fig.5.37).

Examples of bilobate Var.2, cross and polylobate morphotypes are provided below in Fig.5.38.

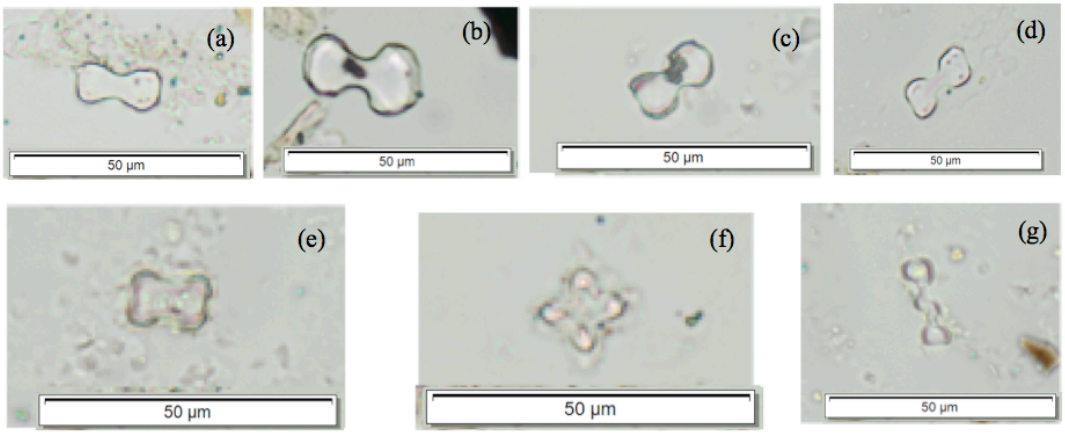


**Fig. 5.38.** EFT4.9 phytolith types: (a-d) Bilobate Var.2; (e-f) Cross; (g) Polylobate. Scale: 50µm.

Sample EFT4.8:

The most abundant morphotype was the saddle Var.1 (13.9%) followed by the trapezoid (12.6%) and the oblong (6%). Other minor morphotypes included the saddle Var.2 (4%), rondel (2%) and the polylobate (0.7%) (Fig.5.37).

Examples of saddle Var.1 morphotypes are provided below in Fig.5.39.

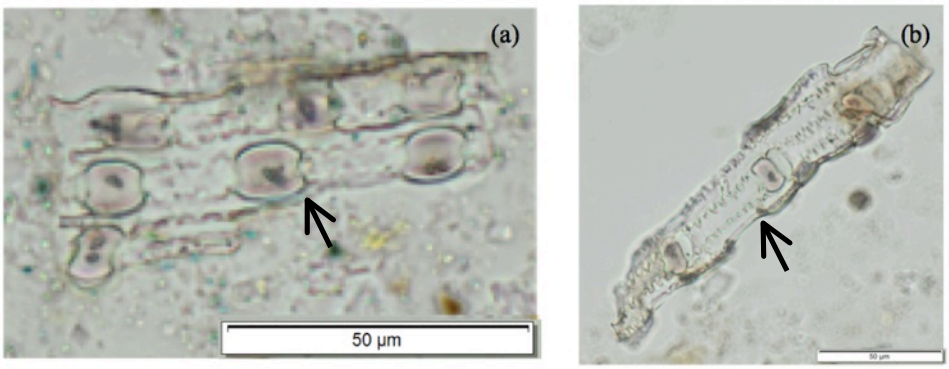


**Fig. 5.39.** EFT4.8 phytolith types: (a-b) Articulated saddle Var.1 cells with several long cell echinate phytoliths. Scale: 50µm.

Sample EFT4.4:

The trapezoid (13.4%) was the most observed phytolith morphotype, followed by the rondel (10.6%), oblong (7.1%) and bilobate Var.2 (5.1%). Other minor types included the cross (2.8%), saddleVar.1 (2%), saddle Var.2 (2%), reniform (2%) and polylobate (0.8%) (Fig.5.37).

Examples of rondel, bilobate Var.2, oblong and polylobate morphotypes are provided in Fig.5.40.

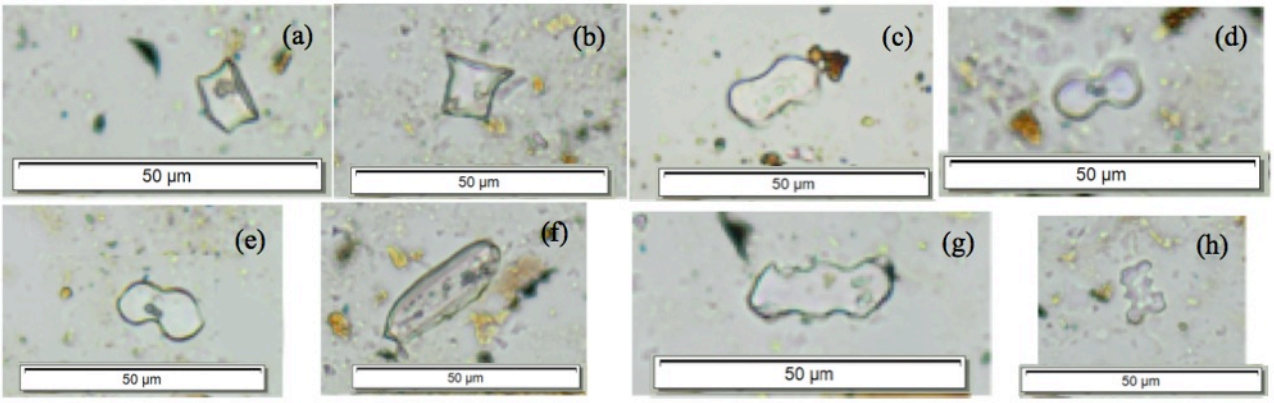


**Fig. 5.40.** EFT4.4 phytolith types: (a-b) Rondel; (c-e) Bilobate Var.2; (f-g) Oblong; (h) Polylobate. Scale: 50µm.

Sample EFT4.1:

The most abundant phytolith morphotype was the trapezoid (21.5%) followed by the rondel (5.5%), oblong (4%), bilobate Var.2 (3%), saddle Var.1 (2.5%), reniform (2%) and saddle Var.2 (1%) (Fig.5.37).

Examples of the saddle Var.1 and rondel morphotypes are provided in Fig.5.41.

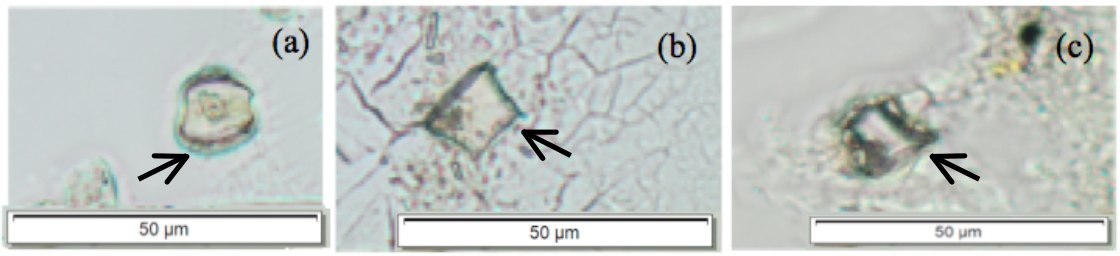


**Fig. 5.41.** EFT4.1 phytolith types: (a) Saddle Var.1; (b-c) Rondel. Scale: 50µm.

Sample EFT4.10:

The saddle Var.1 (13.5%), rondel (12.4%) and bilobate Var.2 (11.8%) were the most observed phytolith morphotypes in this sample, followed by the trapezoid (7.8%), oblong (6.8%), reniform (3%), saddle Var.2 (2.2%), cross (2.2%) and polylobate (0.6%) (Fig.5.37).

Examples of the bilobate Var.2, rondel, cross, oblong and polylobate morphotypes are provided in Fig.5.42.

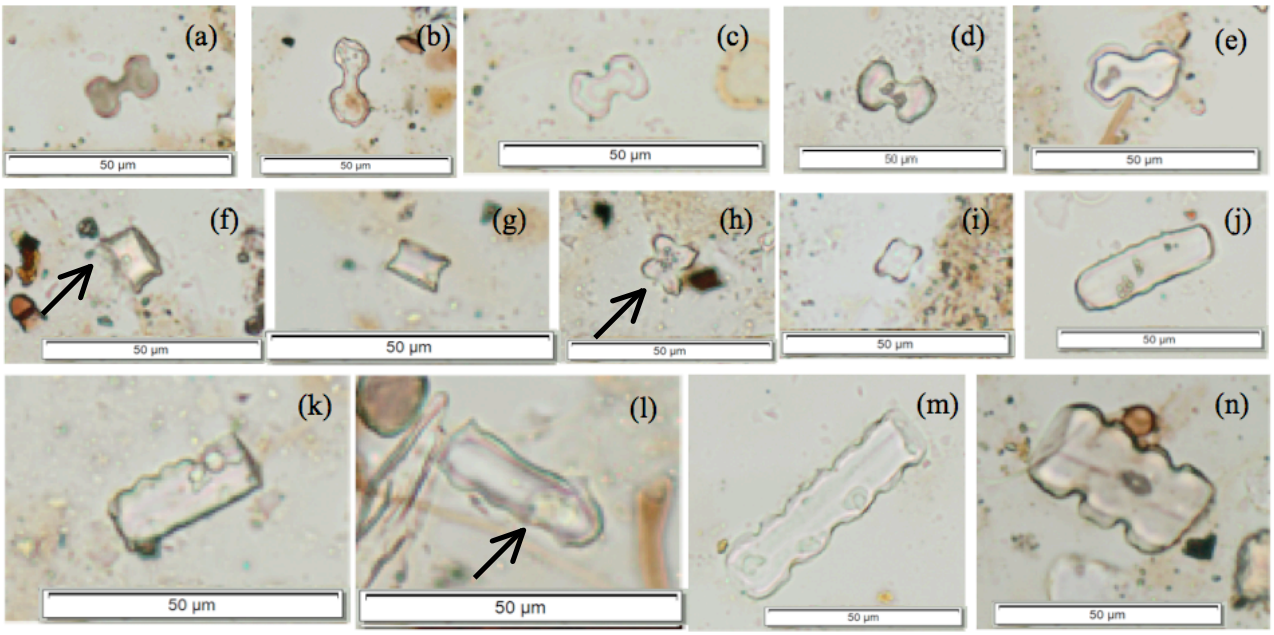


**Fig. 5.42.** EFT4.10 phytolith types: (a-e) Bilobate Var.2; (f-g) Rondel; (h-i) Cross; (j-m) Oblong. (n) Polylobate. Scale: 50µm.

#### 5.3.1.4.3 Bay 0313 Grass Subfamily Phytoliths

The grass subfamilies identified in the sediment samples from Bay 0313 include the Chloridoideae, Danthionoideae, Ehrhartoideae, Panicoideae and Pooideae (Fig.5.43).

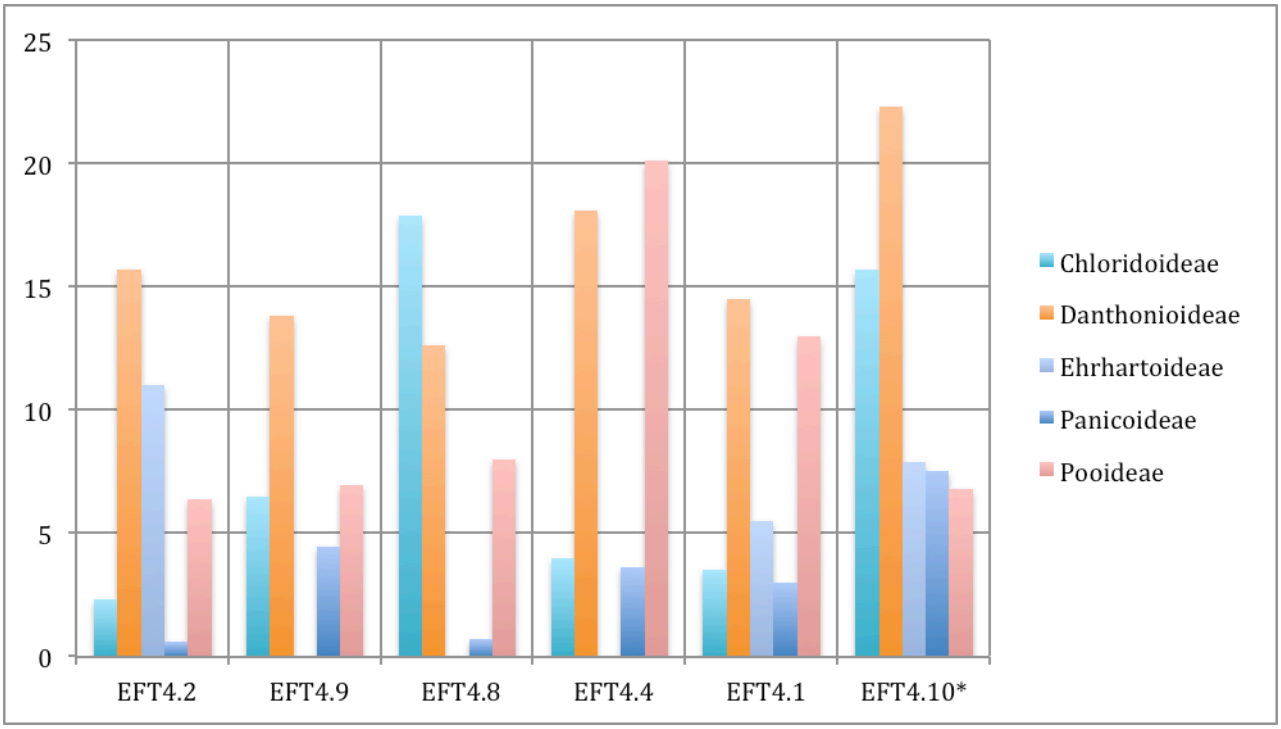


**Fig. 5.43.** EFT Bay 0313, Samples EFT4.2, EFT4.9, EFT4.8, EFT4.4, EFT4.1 and EFT4.10 grass subfamily phytolith morphotypes (samples listed left to right from the oldest to youngest).

Sample EFT4.2:

The most abundant GSSC morphotypes in this sample belonged to the $C_3$ grass subfamilies Danthonoideae (15.7%), Ehrhartoideae (11%) and Pooideae (6.4%), followed by the $C_4$ Chloridoideae (2.3%) and Panicoideae (0.6%) subfamilies (Fig.5.43). The $C_3$ type grasses (33.1%) dominated this sample at the time that the calcareous sand below the white nodular layer was deposited.

Sample EFT4.9:

Within this sample, the largest percentage of GSSC morphotypes were belonged to the $C_3$ grass subfamilies Danthonoideae (13.8%) and Pooideae (6.95%), followed by $C_4$ grass subfamilies Chloridoideae (6.5%) and Panicoideae (4.45%) (Fig.5.43). The composition of this phytolith

assemblage suggests that $C_3$ type grasses (20.75%) were dominant at the time that the lower section of the white nodular layer was laid down.

Sample EFT4.8:

The most abundant GSSC morphotypes in this sample belonged to the $C_4$ grass subfamily Chloridoideae (17.9%) and the $C_3$ grass subfamily Danthonoideae (12.6%), followed by the $C_3$ subfamily Pooideae (8%) and lastly by the $C_4$ grass subfamily Panicoideae (0.7%) (Fig.5.43). The composition of this phytolith assemblage suggest that nearly the same amount of $C_4$ type grasses (18.6%) and C3 type grasses (20.6%) grew at the time that the upper section of the white nodular layer was deposited.

Sample EFT4.4:

Within this sample, the largest percentage of GSSC morphotypes belonged to the $C_3$ grass subfamilies Pooideae (20.1%) and Danthionoideae (18.1%), followed by the $C_4$ grass subfamilies Panicoideae (3.6%) and Chloridoideae (4%) (Fig.5.43). The composition of this phytolith assemblage suggests that the $C_3$ type grasses (38.1%) were dominant at the time that this section of sediment above the white nodular layer was laid down.

Sample EFT4.1:

The most abundant GSSC morphotypes in this sample belonged to the $C_3$ grass subfamilies Danthonoideae (14.5%), Pooideae (13%) and Ehrhartoideae (5.5%), followed by the $C_4$ grass subfamilies Chloridoideae (3.5%) and Panicoideae (3%) (Fig.5.43). The composition of this phytolith assemblage suggests that $C_3$ type grasses (27.5%) were dominant at the time that the coarse sand above the white nodular layer was deposited.

Sample EFT4.10:

Within this modern sample, the largest percentage of GSSC morphotypes belonged to the $C_3$ grass subfamily Danthonioideae (22.3%), followed by the $C_4$ grass subfamily Chloridoideae (15.7%), the $C_3$ grass subfamily Ehrhartoideae (7.9%), the $C_4$ grass subfamily Panicoideae (7.5%) and lastly the $C_3$ grass subfamily Pooideae (6.8%) (Fig.5.43). This phytolith assemblage reflects the contemporary environment where $C_3$ type grasses (37%) are dominant over $C_4$ type grasses (23.2%).

#### 5.3.1.4.4 Bay 0313 Monocotyledon-Dicotyledon Phytolith Comparison

The percentages of phytoliths associated with samples EFT4.2, EFT4.9, EFT4.8, EFT4.4, EFT4.1 and EFT4.10 are provided in Fig.5.44.

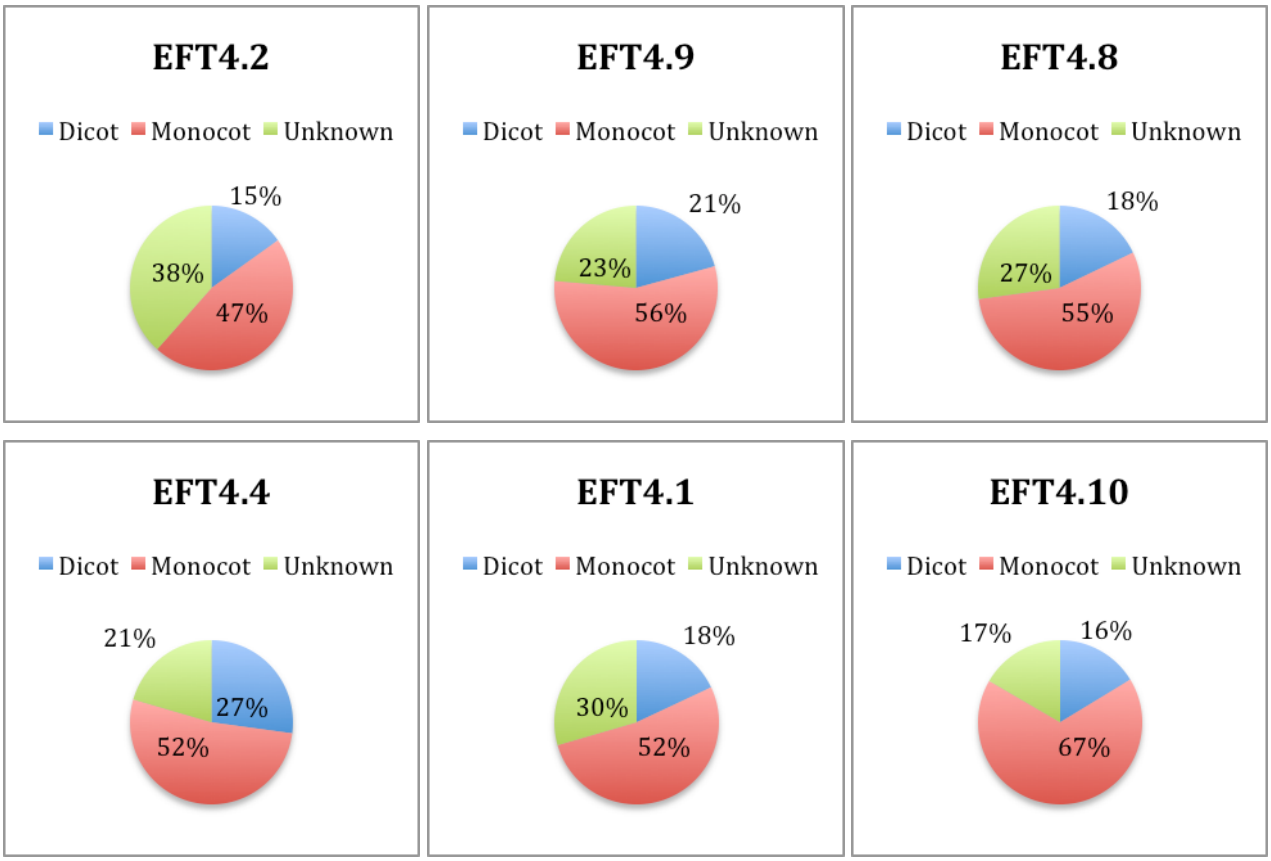


**Fig. 5.44.** EFT Bay 0313, EFT4.2, EFT4.9, EFT4.8, EFT4.4, EFT4.1 and EFT4.10, Monocotyledon-Dicotyledon phytolith comparison pie charts.

The phytolith assemblages associated with the fossil samples EFT4.2, EFT4.9, EFT4.8, EFT4.4, EFT4.1 from Bay 0313, strongly suggests that the vegetation was comprised of a higher percentage

of herbaceous monocots and grasses compared to woody/shrubby plants. Once again the phytolith assemblages associated with the modern sample EFT4.10 is similar to the fossil samples, but represents a disturbed surface affected by modern human activity and by the introduction of alien plants.

### 5.3.2 Duinefontein

Sample DFT2.5 yielded a total phytolith count of 90 of which 76 were regarded as diagnostic, however the sample is not considered to be a reliable representation of the phytolith assemblage compared to sample DFT2.3.

DFT2.3 yielded a total phytolith count of 478 of which 351 were regarded as diagnostic and a reliable representation of the phytolith types within the sediment sample.

DFT2.2 yielded a total phytolith count of 300 of which 217 were regarded as diagnostic and a reliable representation of the phytolith types within the sediment sample.

DFT2.1 yielded a total phytolith count of 200 of which 163 were regarded as diagnostic and a reliable representation of the phytolith types within the sediment sample.

DFT1.1 yielded a total phytolith count of 124 of which 60 were regarded as diagnostic, however the sample is considered not as reliable a representation of the phytolith assemblage compared to sample DFT2.3.

The modern sample DFT2.7 yielded a total phytolith count of 463 of which 411 were regarded as diagnostic.

#### 5.3.2.1 DFT Plant Groups And Phytolith Morphologies

Phytolith morphotypes for each sediment sample were identified and associated with specific plant groups. These included woody dicotyledons, grasses, Asteraceae and monocotyledons.

Sample DFT2.5:

This sample was taken from the yellow sediment (below the red sediment). The largest percentage of phytoliths recorded was from the grass groups (51.1%), followed by phytoliths from woody dicotyledons (24.4%), monocotyledons (5.6%) and other non-diagnostic (18.9%) types (Fig.5.45).

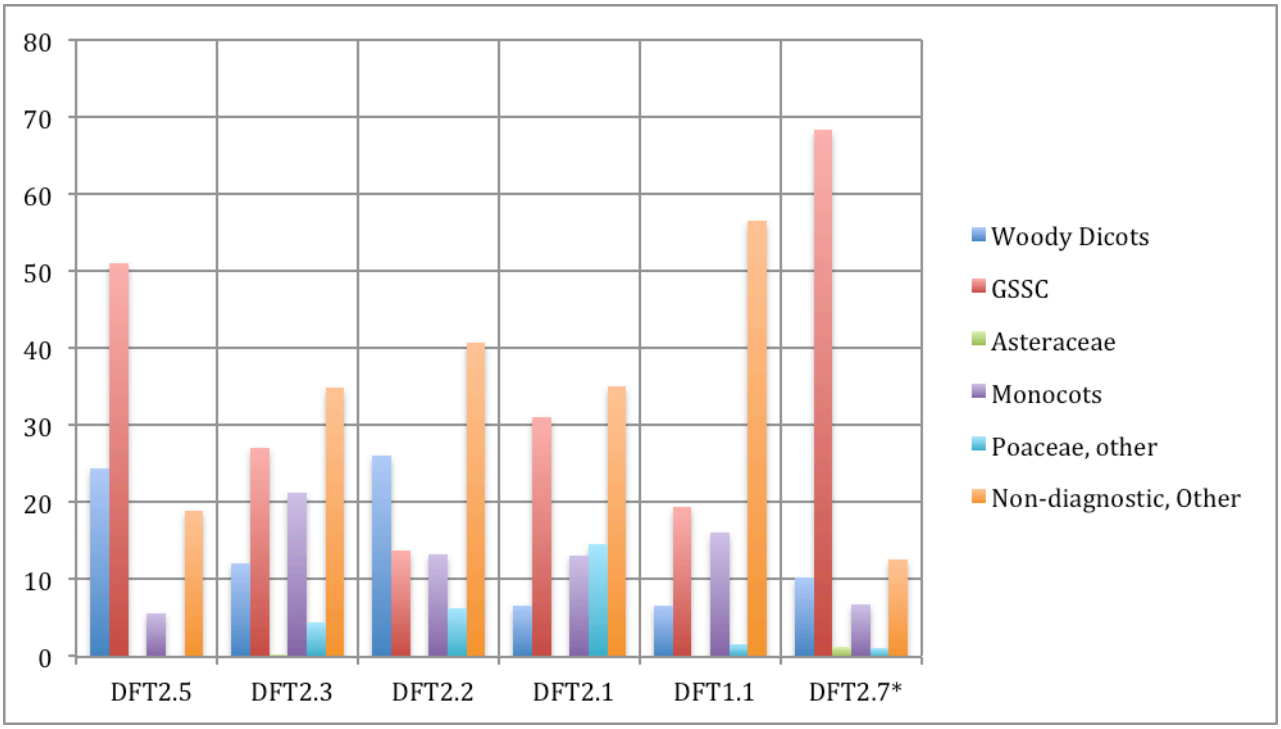


**Fig. 5.45.** DFT, Samples DFT2.5, DFT2.3, DFT2.2, DFT2.1, DFT1.1 and DFT2.7 plant group phytolith morphotypes (samples listed from left to right from the oldest to youngest).

Sample DFT2.3:

Sample DFT2.3 was taken from the yellow sediment (below the orange sediment). The dominant phytoliths were from the grass groups (31.4%) followed by monocotyledons (21.3%), woody dicotyledons (12.1%), Asteraceae (<1%) and other non-diagnostic types (34.9%) (Fig.5.45).

Sample DFT2.2:

Sample DFT2.2 was taken from the orange sediment. The largest percentage of phytoliths was from the woody dicotyledons group (26%), followed by grasses (20%), monocotyledons (13.3%) and other non-diagnostic types (40.7%) (Fig.5.45).

Sample: DFT2.1:

This sample was taken from the pale yellow/orange sediment. The dominant phytoliths were from the grass groups (45.5%), followed by monocotyledons (13%), woody dicotyledons (6.5%) and other non-diagnostic types (35%) (Fig.5.45).

Sample DFT1.1:

Sample DFT1.1 was taken from the leached out orange horizon, below the calcareous "fossil" horizon. The largest percentage of phytoliths was from the grass groups (21%), followed by monocotyledons (16.1%), woody dicotyledons (6.5%) and other non-diagnostic types (56.5%) (Fig.5.45).

Sample DFT2.7:

The dominant phytoliths in this modern sample were from the grass groups (69.4%). These were followed by phytoliths from woody dicotyledons (10.2%), monocotyledons (6.7%), Asteraceae (1.3%) and other non-diagnostic types (12.5%) (Fig.5.45).

**5.3.2.2 DFT GSSC Phytoliths**

The phytolith morphotypes observed in these samples included the bilobate variant 1 (Var.1), bilobate variant 2 (Var.2), bilobate variant 3 (Var.3), polylobate, cross, saddle variant 1 (Var.1), saddle variant 2 (Var.2), trapezoid, rondel, oblong and reniform types (Fig.5.46).

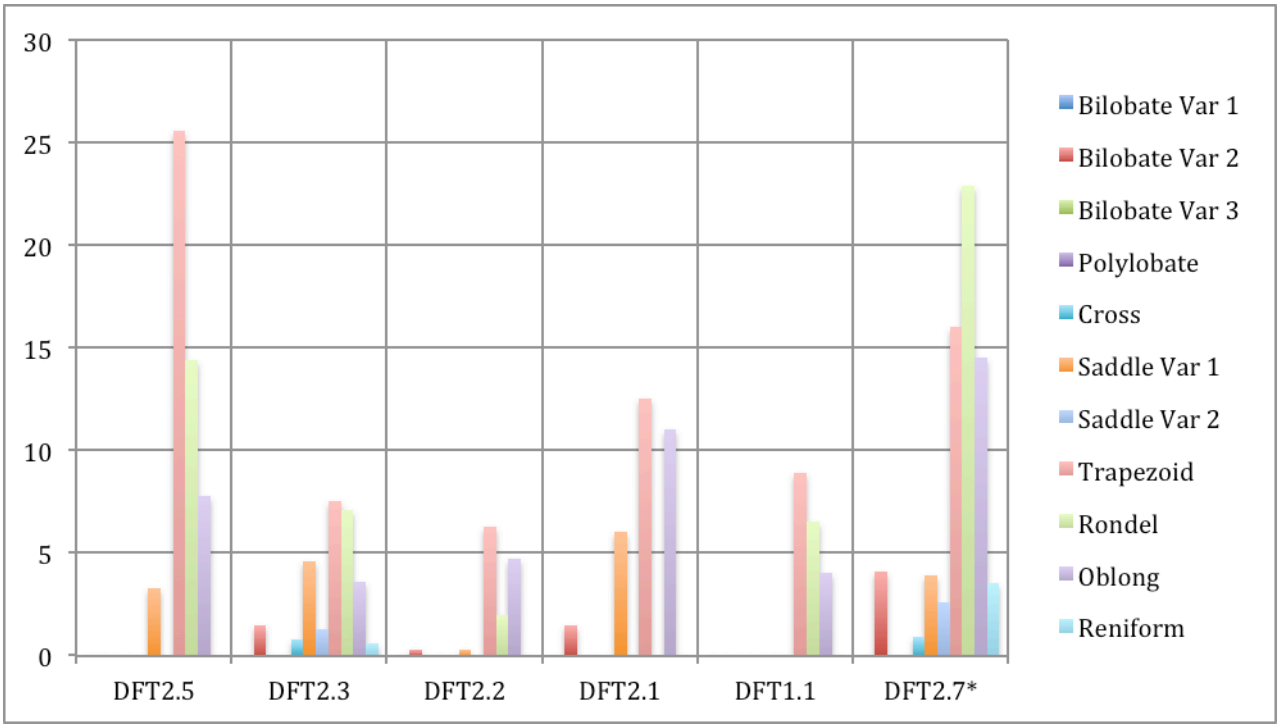


**Fig. 5.46.** DFT, Samples DFT2.5, DFT2.3, DFT2.2, DFT2.1, DFT1.1 and DFT2.7 GSSC phytoliths (samples listed from left to right from the oldest to youngest).

Sample DFT2.5:

The most abundant GSSC phytolith morphotype was the trapezoid (25.6%), followed by the rondel (14.4%), oblong (7.8%) and saddle Var.1 (3.3%) (Fig.5.46).

Examples of saddle Var.1 and rondel morphotypes are provided below in Fig.5.47.

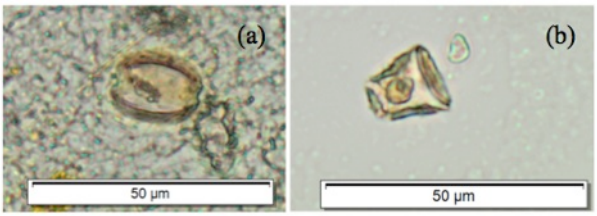


**Fig. 5.47.** DFT2.5 phytolith types: (a) Saddle Var.1; (b) Rondel. Scale: 50µm.

Sample DFT2.3:

The most abundant morphotype was the trapezoid (7.5.%) followed by the rondel (7.1%) and saddle Var.1 (4.6%). Other minor morphotypes included the oblong (3.6%), bilobate Var.2 (1.5%), saddle Var.2 (1.3%), cross (0.8%) and reniform (0.6%) (Fig.5.46).

Examples of bilobate Var.2, rondel, cross and saddle Var.1 morphotypes is provided below in Fig.5.48.

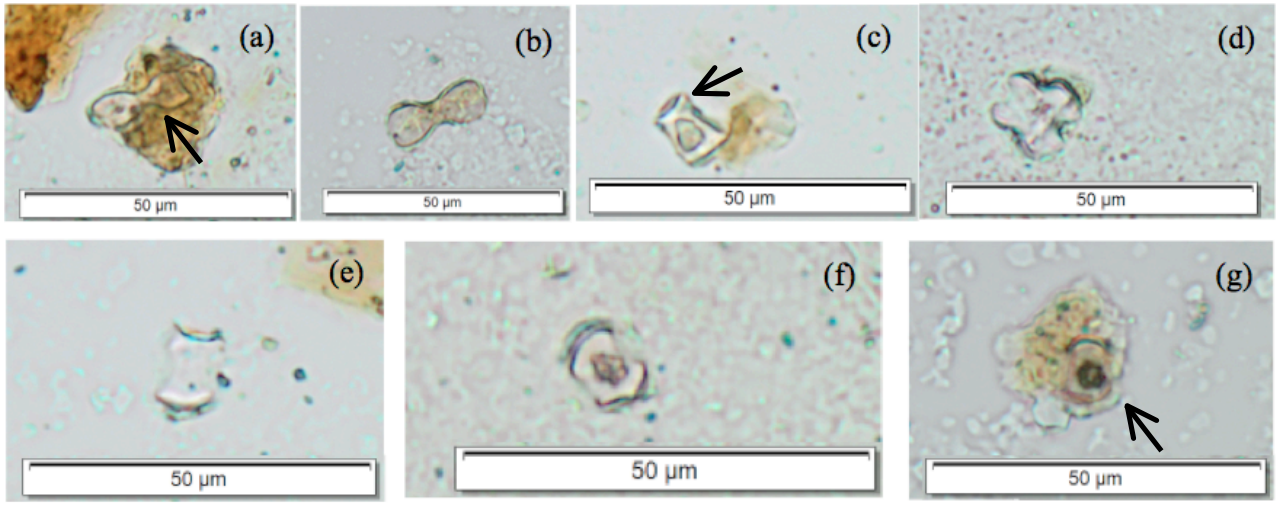


**Fig. 5.48.** DFT2.3 Phytolith types: (a-b) Bilobate Var.2; (c) Rondel; (d) Cross; (e-g) Saddle Var.1. Scale: 50µm.

Sample DFT2.2:

The trapezoid (6.3.%) and oblong (4.7%) phytoliths were the most observed morphotypes in this sample, followed by the rondel (2%), bilobate Var.2 (0.3%) and saddle Var.1 (0.3%) (Fig.5.46).

Sample DFT2.1:

The most abundant phytolith morphotypes were the trapezoid (12.5%) and oblong (11%). Other phytoliths included the saddle Var.1 (6%) and bilobate Var.2 (1.5%) (Fig.5.46).

An example of a bilobate Var.2 morphotype is provided in Fig.5.49.

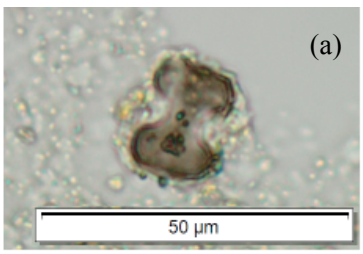


**Fig. 5.49.** DFT2.1 Bilobate Var.2 phytolith. Scale: 50µm.

Sample DFT1.1:

The trapezoid (8.9%) was the most observed phytolith morphotype in this sample, followed by the rondel (6.5%) and oblong (4%) (Fig.5.46).

Sample DFT2.7:

The most abundant morphotypes present in the modern sample were the rondel (22.9%), trapezoid (16%) and oblong (14.5%; FIG. 6.91), followed by the bilobate Var.2 (4.1%), saddle Var.1 (3.9%), reniform (3.5%), saddle Var.2 (2.6%) and cross (0.9%) (Fig.5.46).

Examples of trapezoid, rondel, bilobate Var.2, oblong, cross and saddle Var.1 morphotypes are provided below in Fig.5.50.

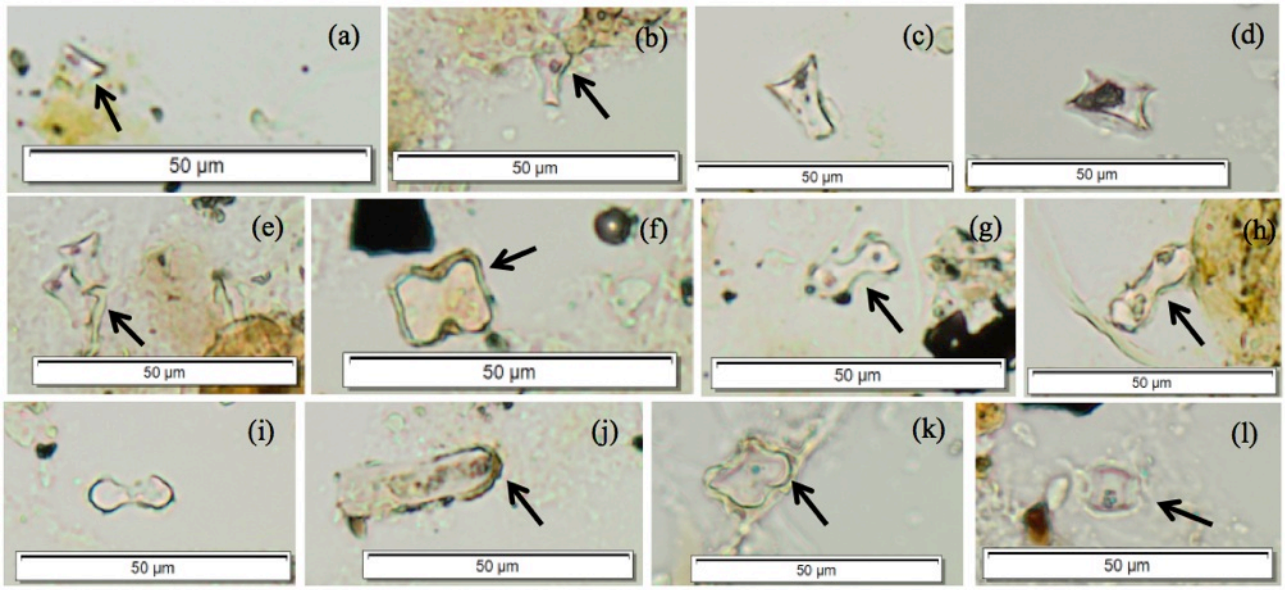


**Fig. 5.50.** DFT2.7 phytolith types: (a) Trapezoid; (b-e) Rondel; (f-i) Bilobate Var.2; (j) Oblong; (k) Cross; (l) Saddle Var.1. Scale: 50µm.

### 5.3.2.3 DFT Grass Subfamily Phytoliths

The grass subfamilies identified in the sediment samples from DFT, include the Chloridoideae, Danthionoideae, Ehrhartoideae, Panicoideae and Pooideae (Fig.5.51).

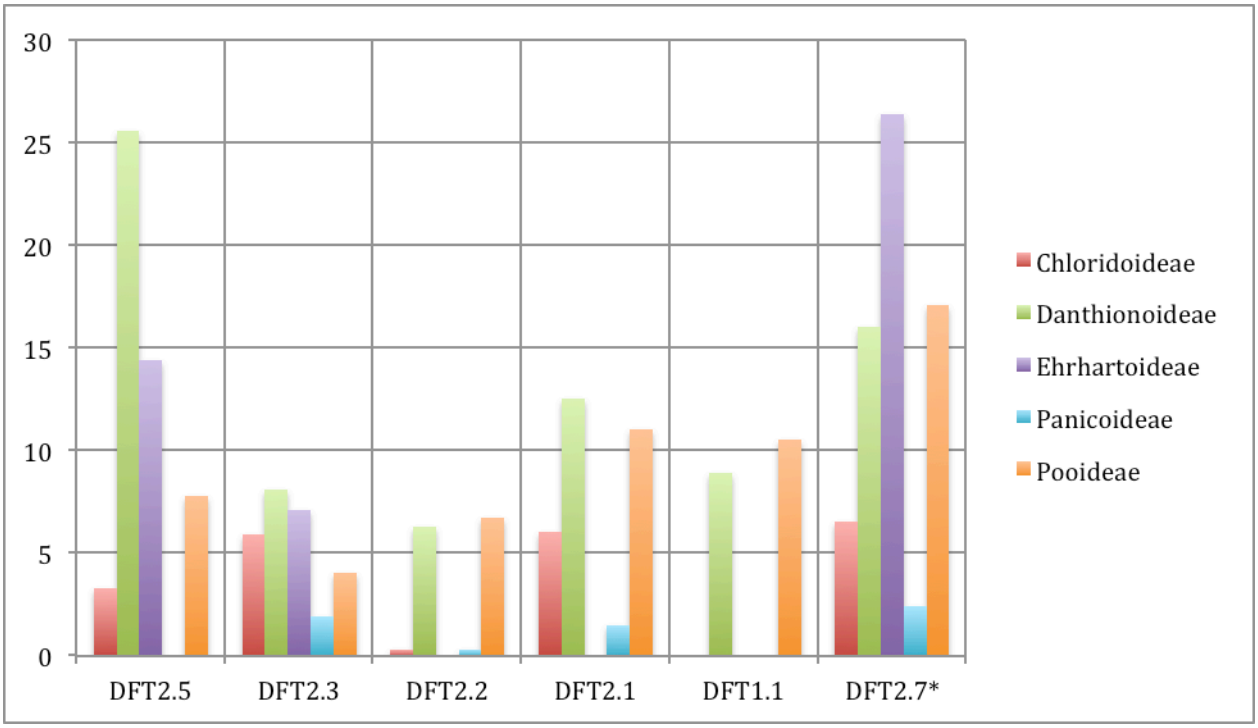


**Fig. 5.51.** DFT, Samples DFT2.5, DFT2.3, DFT2.2, DFT2.1, DFT1.1 and DFT2.7 grass subfamily phytolith morphotypes (samples listed from left to right from the oldest to youngest).

Sample DFT2.5:

The most abundant GSSC morphotypes in this sample belonged to the $C_3$ grass subfamilies Danthionoideae (25.6%), Ehrhartoideae (14.4%) and Pooideae (7.8%), followed by the $C_4$ Chloridoideae (3.3%) subfamily (Fig.5.51). The composition of this phytolith assemblage suggests that $C_3$ type grasses (47.8%) were the dominant grass type present at the time that the section the yellow sediment (below the red sediment) was deposited.

Sample DFT2.3:

Within this sample, the largest percentage of GSSC morphotypes belonged to the $C_3$ grass subfamilies Danthonoideae (8.1%) and Ehrhartoideae (7.1%), followed by $C_4$ grass subfamilies Chloridoideae (5.9%), the $C_3$ grass subfamily Pooideae (4%) and lastly the $C_4$ grass subfamily Panicoideae (1,9%) (Fig.5.51). The composition of this phytolith assemblage suggests that $C_3$ type grasses (19.2%) were dominant at the time that the section of yellow sediment (below the orange sediment) was laid down.

Sample DFT2.2:

The most abundant GSSC morphotypes in this sample belonged to the $C_3$ grass subfamilies Pooideae (6.7%) and Danthionoideae (6.3%), followed by the $C_4$ grass subfamilies Panicoideae (0.3%) and Chloridoideae (0.3%) (Fig.5.51). The composition of this phytolith assemblage suggests that $C_3$ type grasses (13%) were dominant at the time that the section of orange sediment was deposited.

Sample DFT2.1:

Within this sample, the largest percentage of GSSC morphotypes belonged to the $C_3$ grass subfamilies Danthionoideae (12.5%) and Pooideae (11%), followed by the $C_4$ Chloridoideae (6%) and Panicoideae (1.5%) grass subfamilies (Fig.5.51). The composition of this phytolith assemblage suggests that $C_3$ type grasses (23.5%) were dominant at the time that the section of pale yellow/orange sediment was laid down.

Sample DFT1.1:

The GSSC morphotypes in this sample belonged to the $C_3$ grass subfamilies Pooideae (10.5%) and Danthionoideae (8.9%) (Fig.5.51). The composition of this phytolith assemblage suggests that $C_3$ type grasses (19.4%) were dominant at the time that the section of the leached out orange sediment horizon below the calcareous "fossil" horizon was deposited.

Sample DFT2.7:

Within this modern sample, the largest percentage of GSSC morphotypes was belonged to the $C_3$ grass subfamilies Ehrhartoideae (26.4%), Pooideae (17.1%) and Danthonioideae (16%), and lastly the $C_4$ Chloridoideae (6.5%) and Panicoideae (2.4%) grass subfamilies (Fig.5.51). This phytolith assemblage reflects the contemporary environment where $C_3$ type grasses (59.5%) dominant $C_4$ type grasses (8.9%).

### 5.3.2.4 DFT Monocotyledon-Dicotyledon Phytolith Comparison

The percentages of phytoliths associated with samples DFT2.5, DFT2.3, DFT2.2, DFT2.1, DFT1.1 and DFT2.7 are provided in Fig.5.52.

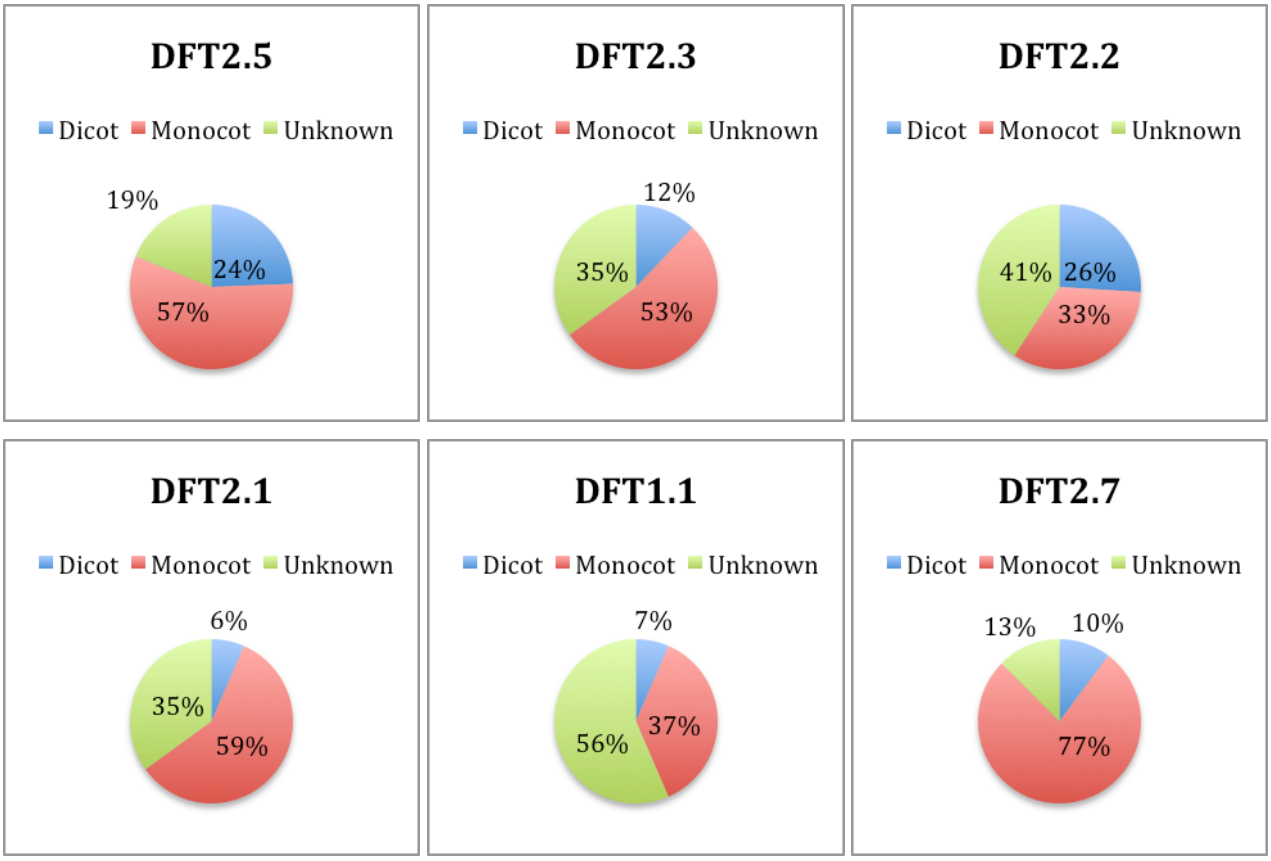


**Fig. 5.52.** DFT, Samples DFT2.5, DFT2.3, DFT2.2, DFT2.1, DFT1.1 and DFT2.7, Monocotyledon-Dicotyledon phytolith comparison pie charts.

The phytolith assemblages associated with the fossil samples DFT2.5, DFT2.3, DFT2.1, DFT1.1 from DFT, suggest that the vegetation was comprised of a higher percentage of herbaceous monocots and grasses compared to woody/shrubby plants. These fossil samples differ from the phytolith assemblage of fossil sample DFT2.2 that implies the vegetation was comprised of a more or less even percentage of herbaceous monocots, grasses and woody/shrubby plants. The modern sample DFT2.7 has a high percentage of monocotyledonous plants but the sample represents a disturbed surface affected by modern human activity and by the introduction of alien plants.

# Chapter 6 : DISCUSSION AND CONCLUSIONS

## 6.1 Introduction

Isotopic analyses undertaken on a range of EFT ungulate taxa indicate that $C_3$ plants, which may have included $C_3$ grasses, persisted along the South African southwestern coast when $C_4$ grasses dominated most African plant communities. The results of the current phytolith study agree with the findings of previous isotopic work and provide the first direct evidence of the presence of significant amounts of $C_3$ grass in the EFT and DFT middle to late middle Pleistocene environment.

## 6. 2 Modern Plant Phytolith Reference Collection

Firstly the modern plant phytolith reference collection was created in order to establish whether the modern plants, which included selected modern plants occurring in the fynbos and savanna woodland biomes, produced phytoliths. A number of the species studied either did not produce phytoliths or when they did, the phytoliths that they produced were not diagnostic to family level. The fynbos biome plants that produced phytoliths include the grass species *Ehrharta villosa var. villosa*, *Carissa macrocarpa, Lessertia frutescens, Lycium afrum, Metalasia muricata, Osteospermum moniliferum subsp. monilifera, Pelargonium spp., Searsia spp*., *Thesium spp.* and *Trachyandra divaricate.* The fynbos biome plants that did not produce phytoliths include *Eriocephalus punctulatus* and *Morella cordifolia.* The woodland-savanna plants that produced phytoliths include *Acacia karroo*, *Acacia nigrescens, Acacia nilotica, Acacia tortilis, Dichrostachys cinerea* and *Grewia flavescens.* The woodland-savanna plant that did not produce phytoliths was *Grewia occidentalis.* It should be noted that the lack of phytolith production in some of these plants might have been influenced by the maturity of the individual plant. Secondly, the modern reference collection would confirm whether similar plant types were present in the fossil record.

## 6.3 Modern Sediment Phytolith Assemblages

### 6.3.1 Introduction

A range of factors may affect the deposition and accumulation of phytoliths within modern sediments (Piperno 2006). These include the amount of vegetation cover, the stage of the plant life cycle, varied phytolith production by different plant species and the influence of wind and fire on phytolith accumulation (Esteban *et al.* 2016). Esteban *et al.* (2016) in their study of modern soil phytolith assemblages in the southern Cape coast fynbos soils, demonstrated that both restios and the wood of dicotyledonous plants were more likely to produce fewer phytoliths per gram of plant material compared to grasses. Their research indicated that South African grasses produced more phytoliths than trees, shrubs, restios and most geophytes (Iridaceae family). Trees have a longer life cycle and will not contribute as much organic matter as grasses and herbaceous plants which have a shorter life cycle (Esteban e*t al.* 2016). Apart from the grass species *Ehrharta villosa var. villosa*, none of the dicotyledonous phytoliths from the modern plant collection were recognisable in the modern sediment samples.

### 6.3.2 Elandsfontein

The vegetation of the Elandsfontein region has been classified as Hopefield Sand Fynbos (FFd 3) by Rebelo *et al.* (2006). The modern vegetation of this region consists of short, woody, shrubby, drought resistant and fire-adapted fynbos, alien species such as the Australian wattles (*Acacia mearnsii, Acacia saligna, Acacia cyclops*), $C_3$ Ehrhartoideae grasses and introduced species of Chloridoideae and Pooideae grasses.

#### 6.3.2.1 Bay 0209

The type of vegetation that is reflected in the phytolith assemblage does appear to reflect the current EFT plant community. This modern phytolith assemblage consisted of 32.5% grass, 24.6% woody dicotyledonous, 7% monocotyledonous and 36% non-diagnostic type phytoliths. In terms of links

between GSSCs and grass subfamilies, $C_3$ Pooid grasses appeared to be well represented in the sample. The high percentage of the woody dicotyledonous phytoliths in this sample is a reflection of the dominance of these plants in the landscape. Furthermore, the absence of Cyperaceae (sedge) type phytoliths in this modern sediment sample also reflects the modern day conditions that are more arid than humid.

#### 6.3.2.2 Bay 0909

This sample appears to be a reliable reflection of the current regional vegetation as it contains phytoliths from the locally occurring grass species *Ehrharta villosa var. villosa.* This modern assemblage consisted of 19.5% grass, 12.2% woody dicotyledonous, 19.9% monocotyledonous and 39.9% non-diagnostic type phytoliths. In terms of links between GSSCs and $C_3$ grass subfamilies, Danthonioideae and Ehrhartoideae grasses dominate the sample. Irrespective of the non-diagnostic type phytoliths, the analysis suggests that there are more monocotyledons (grasses, herbaceous monocots) present than woody/shrubby (dicotyledonous) vegetation. However, the lower concentration of woody dicotyledonous phytoliths may be due to the fact that woody plants produce few phytoliths per gram of plant material compared to grasses. In addition, the absence of Cyperaceae type phytoliths in this sample reflects the arid conditions in the region.

#### 6.3.2.3 Bay 0710

The vegetation reconstruction based on this samples phytoliths appears to be reflecting the current vegetation as it contains phytoliths from the grass species *Ehrharta villosa var. villosa* (Ehrhartoideae) and *Cynodon dactylon* (Chloridoideae) that have been recorded in this somewhat sparsely vegetated region. The modern sample EFT3.2 consisted of 46.7% grass, 19.7% woody dicotyledonous, 27% monocotyledonous, 0.7% sedge (Cyperaceae) and 30.7% non-diagnostic type phytoliths. In terms of links between GSSCs and $C_3$ grass subfamilies, Pooideae and Ehrhartoideae grasses appeared to dominate the sample. Chloridoid ($C_4$) phytoliths (7.7%) were also present.

Irrespective of the amount of non-diagnostic type phytoliths, the analysis suggests that there are more monocotyledons (grasses, herbaceous monocots) than woody/shrubby (dicotyledons) vegetation. As mentioned previously, the observed phytolith pattern may be influenced by a range of factors such as the presence of shrubby vegetation that does not necessarily produce an abundance of phytoliths.

#### 6.3.2.4 Bay 0313

The type of vegetation that is reflected in the phytolith assemblage does appear to reflect the current EFT plant community. The modern assemblage consisted of 61.2% grass, 16.3% woody dicotyledonous, 5% monocotyledonous, 1.1% sedge (Cyperaceae) and 16.6% non-diagnostic type phytoliths. In terms of making possible links between GSSCs and grass subfamilies, Danthonioideae ($C_{3)}$ and Chloridoid ($C_4$) grasses appeared to dominate the sample. With regards to GSSCs, the phytolith assemblage was diverse. In terms of the high percentage of Chloridoid type phytoliths present in the sample, the grass species *Cynodon dactylon* has been observed growing in this region. The assemblage appears to be dominated by monocotyledons rather than woody/shrubby (dicotyledons) vegetation. This phytolith pattern may represent the presence of 'poor' phytolith producing dicotyledons. However, it is more likely that the somewhat dense understory of monocotyledons present at the site is responsible.

### 6.3.3 Duinefontein

The vegetation of the Duinefontein region has been classified as Cape Flats Dune Strandveld (FS 6) by Rebelo *et al.* (2006). The landscape is characterised by vegetation types that include tall, evergreen, hard-leaved shrubs, grasses and herbs (Rebelo *et al.* 2006).

The type of vegetation that is reflected in the phytolith assemblage does appear to reflect the current DFT plant community. The modern sample DFT2.7 consisted of 69.4% grass, 11.5% woody

dicotyledonous (of which 1.3% was comprised of Asteraceae), 6.7% monocotyledonous and 12.5% non-diagnostic type phytoliths. The $C_3$ Ehrhartoideae, Pooideae and Danthonioideae grass subfamilies made up the bulk of the GSSCs. These results give a clear reflection of the grass subfamilies present in the modern environment. Presently, indigenous grasses are a very minor component of the Fynbos biome, and those present are predominately cool-season growing $C_3$ grasses. The presence of the Ehrhartoideae (rondel) type phytoliths in the sample correlate with the grass species *Ehrharta villosa var. villosa* that has been observed growing in this region (see modern reference collection). In addition, the grass subfamily Danthionoideae and introduced species of Pooideae have also been identified within the modern sediment sample and recorded as growing in the area. The dominance of the monocotyledon type phytoliths in the modern sediment sample is likely due to the fact that the dicotyledons (woody/shrubby plants) in the region produce fewer phytoliths as observed in the modern reference collection.

## 6. 4 Fossil Phytolith Assemblages

### 6.4.1 Introduction

Phytoliths similar to the modern sample of *Ehrharta villosa var. villosa* were observed in the modern and fossil sediment samples. However, no phytoliths associated with the modern woody plant taxa (fynbos/woodland-savannah plants) were observed in the fossil sediment samples. The same factors influencing the accumulation and preservation of phytoliths in modern sediment samples could apply to the fossil sediment samples. In addition, the influence of pH conditions in the sediments could have had a greater influence on the preservation of phytoliths in the fossil sediments. The pH levels of the sediments were tested to account for this preservation factor. Indications of partial dissolution of phytoliths were noted in some of the samples as evidenced by the presence of surface pitting and holes. Furthermore, according to Esteban *et al.* (2017) the vegetation composition might also be responsible for the variations in the phytolith concentration.

The sediment samples from recognizable stratigraphic layers developed during the middle Pleistocene at EFT are grouped together and discussed from the youngest to the oldest sample. The late middle Pleistocene DFT fossil sediment samples are discussed separately.

### 6.4.2 Elandsfontein – Upper Pedogenic Sand Horizon (Above White Nodular Layer)

Samples EFT1.1 (Bay 0209) Bay, EFT4.1 (Bay 0313) and EFT4.4 (Bay 0313) were taken across the Upper Pedogenic Sand Horizon. Samples EFT1.1 and EFT4.4 had a reliable representation of phytolith types within the sediment sample however the representation of phytoliths in sample EFT4.1 was less reliable.

The fossil sediment assemblages consisted of 18% - 31% woody dicotyledonous, 30% - 46% grass, 2 - 11% monocotyledonous, 1.8% sedge (Cyperaceae), 0.7% - 4.3% palm (Arecaceae) and 21% - 30% non-diagnostic phytoliths. The most dominant grass subfamilies recognised were the $C_3$ Danthonioideae, Ehrhartoideae and Pooideae and to a lesser extent $C_4$ Panicoideae and Chloridoideae. The GSSC assemblages are likely to reflect a diverse assemblage of grasses. In the present day the Danthonioideae, Ehrhartoideae and Pooideae grass subfamilies grow in moist cool conditions. Furthermore, the presence of Cyperaceae phytoliths may be interpreted as representative of humid conditions, with the presence of riparian vegetation, with grasses dominating but woody dicotyledonous plants also well represented. Based on the percentage of plant types defined by the phytolith assemblages an assumption can be made that a mosaic plant community existed, taking into account that the woody dicotyledons are likely to be underrepresented due to their lower rate of phytolith production.

### 6.4.3 Elandsfontein - White Nodular Horizon (Cemented)

Phytoliths were not observed in the fossil sediment sample EFT4.3 (Bay 0313) from the White Nodular Horizon. Vegetation composition may have also been responsible for the lack of

phytoliths. In addition to this factor that may habe affected the deposition and accumulation of phytoliths, the formation of the calcareous nodular layers contributed to the high pH level (8-9) that may have resulted in the dissolution of phytoliths.

### 6.4.4 Elandsfontein - Artefact/Fossil Horizon (Within The Nodular Horizon)

Sample EFT3.1 (Bay 0710) from the artefact/fossil horizon had a reliable representation of phytolith types within the sediment sample. The fossil sediment assemblage consisted of 29.6% grass, 26.9% woody dicotyledonous, 7.1% sedge (Cyperaceae), 0.7% palm (Arecaceae), 11.6% monocotyledonous and 24.1% non-diagnostic phytoliths. The $C_3$ Danthonioideae grasses were the most dominant grass subfamily recognised in the sediment sample with minor quantities of the grass subfamilies Panicoideae ($C_4$), Chloridoideae ($C_4$) and Pooideae ($C_3$). The GSSC assemblages are likely to reflect a less diverse assemblage of grasses. In the present day the Danthonioideae grass subfamily grows in moist cool conditions. Furthermore, the relatively high percentage (7.1%) of Cyperaceae type phytoliths is an indication of the presence of humid conditions, and the presence of swampy, wetland or riparian type vegetation. Once again taking into account the percentage of plant types defined by the phytolith assemblages, an assumption can be made that a mosaic plant community existed, but whether the monocotyledons were the dominant vegetation type is not conclusive. Woody plants produce fewer phytoliths per gram of plant material and the high concentration of these phytoliths as observed in this sample may in fact be a reflection of the dominance of woody plants in the landscape.

### 6.4.5 Elandsfontein - Higher In The Artefact/Fossil Horizon (Within The Nodular Horizon)

Samples EFT1.3 (Bay 0209) Bay, EFT2.1 (Bay 0909) and EFT4.8 (Bay 0313) were taken across the upper section of the artefact/fossil horizon. Sample EFT2.1 had a moderate degree of confidence in terms of the representation of phytolith types within the sediment sample. The representation of phytoliths in samples EFT1.3 and EFT4.8 however, was less reliable. The fossil

sediment assemblages consisted of 19% - 31% woody dicotyledonous, 23% - 47% grass, 7 - 22% monocotyledonous, 1% sedge (Cyperaceae), 0.5% palm (Arecaceae) and 33% - 37% non-diagnostic phytoliths. The dominant grass subfamilies recognised in samples EFT1.3 and EFT2.1 were $C_3$ Danthonioideae and Pooideae and to a lesser extent $C_4$ Panicoideae and Chloridoideae. In sample EFT4.8 Chloridoideae was the dominant grass subfamily followed by Danthonioideae and Pooideae with minor amounts of Panicoideae. The GSSC assemblages are likely to reflect a less diverse assemblage of grasses. In present day environments, the Danthonioideae and Pooideae grass subfamilies grow in moist cool conditions. Compared to the younger stratigraphic layer (sample EFT 3.1) mentioned above, it appears that the conditions represented by these samples were less humid based on the small percentage of Cyperaceae type phytoliths. An assumption can be made that a mosaic plant community existed, but whether the monocotyledons were the dominant vegetation type is not conclusive.

### 6.4.6 Elandsfontein - Lower In The Artefact/Fossil Horizon (Within The Nodular Horizon)

Less than 50 diagnostic phytoliths were counted in sample EFT1.2 (Bay 0209) and as a result, this sample was not included in the analysis. In some of the phytoliths pitting and/or dissolution (weathering) of phytolith morphotypes was observed which may have been due to the high alkaline conditions in the sediment.

Samples EFT2.2 (Bay 0909) and EFT4.9 (Bay 0313) taken across the lower section of the artefact/fossil horizon had a reliable representation of phytolith types within the sediment sample. The fossil sediment assemblages comprised 34% - 48% grass, 7% - 21% woody dicotyledonous, 1.7% palm (Arecaceae), 8.1% sedge (Cyperaceae), 13% monocotyledonous and 24% - 31% non-diagnostic phytoliths. In EFT4.9, $C_3$ Danthonioideae grasses dominated with minor amounts of $C_3$ Pooideae and $C_4$ Chloridoideae grasses. In EFT2.2 Danthonioideae, Ehrhartoideae ($C_3$), Pooideae and Panicoideae ($C_4$) grasses dominated with minor amounts of Chloridoideae grasses.

The GSSC assemblages are likely to reflect a more diverse assemblage of grasses. In present day environments, the Danthonioideae, Ehrhartoideae and Pooideae grass subfamilies are observed to grow in moist cool conditions. It should be noted that Panicoideae grasses can grow in shady and moist environments, but have also been observed to grow in regions with warm climates (tropical and subtropical) and they are often encountered in savanna habitats. Sample EFT4.9 had the highest frequency of Cyperaceae (8.1%) and monocot type phytoliths compared to younger sediment samples. These results may be interpreted as representative of humid conditions, with the presence of riparian or swampy type vegetation, with grasses dominating but dicotyledonous plants also well represented.

### 6.4.7 Elandsfontein -Below The White Nodular Horizon

The representation of phytoliths in sample EFT4.2 (Bay 0313) from the sediment below the white nodular horizon was not totally reliable due to the fact that the phytolith count was low. The fossil sediment assemblage consisted of 38.3% grass, 15.1% woody dicotyledonous, 8.1% monocotyledonous and 38.4% non-diagnostic phytoliths. $C_3$ Danthonioideae and Ehrhartoideae grasses dominated the sample, with minor quantities of Pooideae ($C_3$), Chloridoideae ($C_4$) and Panicoideae ($C_4$).

### 6.4.8 Elandsfontein - Summary

Taking into account the phytolith assemblages observed in the sediment samples, the following assumptions can be made with regards to the palaeoenvironment in EFT. Based on the percentage of plant types defined by the phytolith assemblages, an assumption can be made that a mosaic plant community likely existed throughout the different stratigraphic layers. Within the sediment samples, the GSSC assemblages generally reflected a diverse range of grasses but in some of the samples there was less variation. Overall, the $C_3$ Danthionoideae, Ehrhartoideae and Pooideae grasses were the most dominant grass subfamilies recognised in the sediment samples with minor

quantities of $C_4$ Panicoideae and Chloridoideae. In the present day Fynbos Biome the Danthonioideae, Ehrhartoideae and Pooideae grass subfamilies grow in moist cool conditions. There were varitations in the presence (percentage) of Cyperaceae type phytoliths through time in each sample bay. This was clearly seen in Bay 0313 where the oldest stratigraphic layers had higher frequencies of these phytolith morphotypes compared to younger stratigraphic layers. This may be interpreted as representative of humid conditions occurring in the past that were becoming more arid through time. Woody plants, which produce few phytoliths per gram of plant material, were represented in the phytolith record in relatively high concentrations, throughout the stratigraphic layers, which reflects their strong presence in the landscape.

### 6.4.9 Duinefontein -White Nodular Horizon

Phytoliths were not observed in the fossil sediment sample DFT1.2 from the White Nodular Horizon. In addition to the factors affecting the deposition and accumulation of phytoliths, the formation of the calcareous nodular layers contributed to the high pH level (tested to be 8-9) that may have resulted in the dissolution of phytoliths.

### 6.4.10 Duinefontein - Ferricrete Horizon

Phytoliths were not observed in the fossil sample DFT2.4 from within the ferricrete horizon. The lack of phytoliths may have been due to dissolution in the sediment as a result of the high pH (tested to be 8-9) and the presence of iron oxides (reviewed in Piperno, 1988).

### 6.4.11 Duinefontein - Red Sediment

Less than 50 diagnostic phytoliths were counted in sample DFT2.6 from within the red sediment and as a result this sample was not included in the analysis. In addition to the factors affecting the deposition and accumulation of phytoliths, the high pH level (tested to be 8-9) may have resulted in the dissolution of the phytoliths.

### 6.4.12 Duinefontein - Pale Yellow/Orange Sediment Below Calcareous Horizon

Sample DFT1.1 and DFT2.1 were taken from within the pale yellow sediment below the calcareous horizon. DFT2.1 had a moderate degree of confidence in terms of the representation of phytolith types within the sediment sample. The phytolith count in sample DFT1.1 however was less reliable. The fossil sediment assemblages consisted of 21% - 46% grass, 6.5% woody dicotyledonous, 13% - 16% monocotyledonous and 35% - 57% non-diagnostic phytoliths. The most dominant grass subfamilies recognised were the $C_3$ Danthonioideae and Pooideae and to a lesser extent, $C_4$ Chloridoideae and Panicoideae. The GSSC assemblages are likely to reflect a less diverse assemblage of grasses. In the present day environments the Danthonioideae and Pooideae grass subfamily grow in moist cool conditions. An assumption can be made that a mosaic plant community existed. The fact that woody dicotyledons are likely to be underrepresented due to their lower rate of phytolith production should be taken into account when considering dominant vegetation types. Noticeable however, was the lower percentage of dicotyledons compared to those observed in the fossil EFT sediment samples.

### 6.4.13 Duinefontein - Orange-Red Horizon

Sediment sample DFT2.2 taken from within the orange-red sediment horizon_had a reliable representation of phytolith types. The fossil sediment assemblage comprised 26% woody dicotyledonous, 20% grass, 13.3% monocotyledonous and 40.7% non-diagnostic phytoliths. The $C_3$ Pooideae and Danthonioideae grasses were the most dominant grass subfamilies recognised in the sample, which also had minor quantities of $C_4$ Chloridoideae and Panicoideae type phytoliths. The GSSC phytoliths reflect a less diverse assemblage of grasses. The Danthonioideae and Pooideae grass subfamilies are observed to grow in moist cool conditions in present day environments. The assumption is made that a mosaic plant community existed, but whether the monocotyledons were the dominant vegetation type is not conclusive. However, compared to the younger samples (DFT1.1 and DFT21.), the woody plant phytoliths were represented in the phytolith record in higher

concentrations and is therefore a reflection of the dominance of these plants in the landscape associated with this stratigraphic layer.

### 6.4.14. Duinefontein - Below Orange-Red Sediment in Pale Yellow Sediment

Samples DFT2.3 and DFT2.5 were taken from the pale yellow sediment below the orange-red sediment. Sample DFT2.3 had a reliable representation of phytolith types, however the representation of phytoliths in sample DFT2.5 was less reliable. The fossil assemblages consisted of 31%-51% grass, 12% - 24% woody dicotyledonous, 6% - 21% monocotyledonous, 0.2% daisy (Asteraceae) and 19% - 41% non-diagnostic phytoliths. In DFT2.3, Danthonioideae ($C_3$), Ehrhartoideae ($C_3$) and Chloridoideae ($C_4$) grasses dominated with minor amounts of Pooideae and Panicoideae grasses. The most dominant grass subfamilies recognised in DFT2.5 were the Danthonioideae, Ehrhartoideae and Pooideae and to a lesser extent Pooideae and Chloridoideae. The GSSC assemblages reflect a more diverse assemblage of grasses. In present day environments the Danthonioideae, Ehrhartoideae and Pooideae grass subfamilies are to be observed growing in moist cool conditions. It should be noted that Chloridoideae grasses generally grow in warm and dry tropical and subtropical environments. The assumption is made that a mosaic plant community existed, but once again the high concentrations of woody dicotyledonous type may be in fact be a reflection of the dominance of these plants in the landscape.

### 6.4.15 DFT Summary

Taking into account the phytolith assemblages observed in the sediment samples, the following assumptions can be made with regards to the palaeoenvironment in DFT. The sediment samples from DFT were more alkaline than those from EFT. In some of the DFT fossil samples, the pH of the sediment may have been alkaline (pH>=9) for prolonged periods, which may in turn have partially or completely dissolved phytoliths (Albert et al., 2003; Piperno, 2006). It has been found that phytolith assemblages with a high number of long cells versus short cells should emphasise a

higher degree of preservation, as long cells are more often less silicified and offer wider surface area to chemical and physical attack (Madella 1997; Lancelotti 2010). In the samples that have been observed as showing poor phytolith preservation, there are less long cells preserved.

Based on the percentage of plant types defined by the phytolith assemblages, the assumption is made that a mosaic plant community existed throughout the different stratigraphic layers. Within the sediment samples, the GSSC assemblages generally reflected a diverse range of grasses, but in some of the samples there was less variation in grass types. Overall, the $C_3$ Danthionoideae, Ehrhartoideae and Pooideae grasses were the most dominant grass subfamilies recognised in the sediment samples, with minor quantities of $C_4$ Panicoideae and Chloridoideae phytoliths preserved. In the present day Fynbos Biome of the southwestern Cape coast, the Danthonioideae, Ehrhartoideae and Pooideae grass subfamilies are observed growing in moist cool conditions. Due to the lack of phytolith preservation in some of these samples, the paleoenvironmental reconstruction for DFT cannot be considered as reliable as that for EFT. Having said that, when the woody dicotyledonous phytoliths are represented in the phytolith record in such high concentrations, as seen in the older stratigraphic layers, it is a reflection of the dominance of these plants in the region. The absence of Cyperaceae type phytoliths in the fossil record may be due to poor preservation and as a result there is no further evidence to support the presence of wetlands, swamps or riparia vegetation communities in the past.

### 6.5 Paleoecological Implications Of The EFT And DFT Phytolith Samples

In both EFT and DFT, the frequency of plant types defined by the phytolith assemblages, suggests that mosaic/heterogeneous plant communities existed throughout the different stratigraphic layers. Based on the high frequencies of grass phytoliths it may appear that grasses dominated the ancient landscade, however woody dicotyledonous phytoliths were well represented in the phytolith record. The EFT samples associated with the oldest stratigraphic layers suggest that the woody plants may

have dominated the landscapes whereas the youngest stratigraphic layers at DFT suggest that woody dicotyledonous plants were not as well represented in the landscape.

The $C_3$ Danthionoideae, Ehrhartoideae and Pooideae grasses were the most dominant grass subfamilies recognised in the sediment samples. Minor amounts of $C_4$ Panicoideae and Chloridoideae grasses were observed. The older fossil sediment samples from EFT exhibited a diverse mixture of grass subfamilies. The variability of grass subfamilies increases with age of the sediment samples. The higher diversity of grass types in the modern sediments from EFT and DFT may be due to the introduction of exotic grass subfamilies such as Pooideae and Chloridoideae into the environment.

The current distribution of the Pooideae ($C_3$) grass subfamily in southern Africa indicates that these grasses commonly occur in cool, moist temperate conditions (Rossouw 2009). The $C_3$ Ehrhartoideae grass subfamily is currently observed to grow in forests, on open hillsides and in aquatic environments. The evidence of calcrete that exhibited spring features at both EFT and DFT, and the presence of amphibian fossil samples from DFT, supports the presence of aquatic environments at EFT and DFT. The springs may explain the high diversity and abundance of ungulate fossils at EFT (Klein et al. 2007). Due to the long, hot and dry summers in this winter rainfall region, the presence of underground water would have been vital for the survival of fauna. The Danthonoideae grasses occur in regions that have more than 40% of the rainfall occurring during the winter months (Gibbs Russell *et al*. 1990). This would imply that based on the presence of certain grass types, similar conditions existed in EFT and DFT during the time that their various stratigraphic layers were deposited. However the absence of Cyperaceae type phytoliths in the DFT phytolith samples suggests that DFT was subject to less humid conditions compared to the middle Pleistocene environment of EFT. The presence of this plant family varied across the samples, but the oldest stratigraphic layers sampled at EFT had the highest frequency of these phytoliths and may be interpreted as representative of humid conditions where swampy vegetation grew in the region. Through time it appears that the environmental conditions became more arid and the ancient

mosaic plant community that may have consisted of woody fynbos, grass and swampy-type plants became less diverse.

### 6.6 Comparison To Previous Paleoenvironmental Studies

Previous palaeoenvironmental reconstructions of the South African southwestern coast were based on analyses of fossil fauna from several sites (including EFT, DFT, Hoedjiespunt, Sea Harvest and Swartklip). This phytolith analysis provides direct evidence of local vegetation that grew in the past while these previous fauna studies may have been representative of a broader environmental region. That being said, the results from the study of the EFT and DFT fossil sediment samples, support previous palaeoenvironmental research conducted by Luyt *et al.* (2000), Stynder (2009) and Lehmann *et al.* (2016). In particular, they parallel Luyt *et al.*'s (2000) and Lehmann *et al*.'s (2016) isotopic evidence that indicated that the majority of herbivores at EFT and DFT had pure $C_3$ diets. While there is now strong evidence that a $C_3$-dominated floral community existed along the South African southwestern coast during the middle Pleistocene, results also suggest the presence at times, of small amounts $C_4$ grasses (limited summer rainfall). Luyt *et al*.'s (2000) results also suggested the existence of a cool growing season and persistent winter rainfall. Lehmann *et al.*'s (2016) research indicates that the winter rainfall zone may in fact have been in place for the past 5 million years. Therefore, according to Lehmann *et al*.'s (2016) research, during periods of increased winter rainfall, there would have been an increase in $C_3$ vegetation. In addition, more recent research by Cordova and Avery (2017) sampled opal phytoliths from the dental calculus on three elephants from EFT and suggested that $C_3$ grasses predominated in the broader environment during this time.

This study of different phytolith assemblages within specific stratigraphic layers at EFT supports Luyt *et al*.'s (2000) research, which suggested that, both significant tree/shrub and grassy elements were present during the period in which the Main and Bone Circle assemblages were deposited. Additionally, results are consistent with Stynder's (2009) reconstruction of the EFT middle

Pleistocene vegetation community as one that included a mosaic of grass, shrubs and trees. The combination of tree/shrub and grassy vegetation does not occur in the region today, which suggests that conditions became much harsher and drier over time (Luyt *et al*. 2000). The results of this study suggest that the palaeovegetation would have provided adequate vegetational diversity to account for the extraordinary diversity of EFTM ungulates. The vegetational diversity that had existed in the EFTM environment would have required wetter climatic conditions than those observed today. The relatively high percentage of Cyperaceae phytoliths in the oldest EFT samples provided a good indication of humid conditions and the plausible presence of wetlands and swampy vegetation communities. The observed decrease in Cyperaceae type phytoliths in the phytolith assemblages suggests that the environmental conditions became more aird through time. It is therefore likely that the recorded decrease in ungulate diversity at DFT may have been influenced to some degree by a decrease in the region's vegetation diversity.

The dominance of $C_3$ type grasses observed in the DFT fossil sediment samples do not support previous palaeoenvironmental reconstructions by Klein *et al.* (1999), who suggested a bush-grass mosaic perhaps broadly resembling the extant savanna woodland biome of South Africa. Furthermore, while grass phytoliths dominated the vast majority of the samples, it is apparent that woody plants were better represented in phytolith assemblages from EFT than in the younger DFT samples. Fossil remains of reedbuck, hippopotamus, swamp rat, Saunder's vlei rat and some amphibian taxa (Sampson 2003) had indicated the presence of shoreline lags and interdunal ponds in the area. This study supports the findings of Luyt *et al*. (2000) who suggested that EFT and DFT were located in a winter rainfall zone at least throughout the middle Pleistocene and into the present time. As with the EFT paleoenvironment, the existence of ponds in the DFT region would have required a higher water table than present, and this in turn implies that a high, interglacial sea level may have influenced the vegetational composition of the late middle Pleistocene environment.

The results of the current study provide direct evidence of the prominence of a mosaic vegetation

community in the EFT and DFT palaeoenvironments. However it is clear that based on the variations in the phytolith assemblages, the EFT environment may have been more humid than DFT. Contemporary vegetation surveys in the Cape region have indicated that $C_3$ cool-season grasses (Pooideae, Ehrhartoideae and Danthonioideae) and Restionaceae (restios) are still abundant in the winter rainfall zone (Cordova 2013). It should be noted that, as with some of the fossil sediment samples, a $C_4$ grass component has been recorded in these surveys. It is however not unusual for a small percentage of $C_4$ grasses to be found in modern fynbos and renosterveld vegetation types (Vogel *et al*. 1978; Rebelo *et al*. 2006).

### 6.7 Limitations

There are certain limitations in working with grass silica short cell phytoliths. The only diagnostic features for identification of the distribution of silica phytoliths in soils are their shape and size (Palmer 1976). Contamination and miscalculations may occur in every step from extraction from soil samples to quantitative analysis. It is possible that the sampling method that was used in this study may have lead to a bias in the phytolith analysis. A compound microscope facilitates a 2D-image of the morphotypes and this may shadow the appropriate characterisation of phytolith morphotypes, as the top and base of phytoliths can differ remarkably. The use of a 3D-image allows for a better interpretation of the morphotypes (Pearsall *et al*. 2004). While the phytolith analysis of the samples from EFT and DFT provides important data on the nature of the vegetation at the sites, it is important to note that several factors may have influenced the phytolith deposition. From the EFT and DFT sediments, it is evident that some of the samples selected appear to have undergone some degree of dissolution induced by post-depositional factors. These include the formation of calcareous nodular layers that can induce an increase in pH and therefore the dissolution of phytoliths, noted both in EFT1.2 and DFT1.2. When phytoliths have been preserved in sufficiently high numbers for interpretation, they appear in relatively good condition, allowing for their morphological identification. The microenvironment in which the plants originally grew (e.g. sand,

clay, seasonally wet) may also determine the chances of phytoliths preserving. Generally the preservation of phytoliths in sediments is satisfactory, but phytoliths are susceptible to breakage, damage and decay from movements, weathering and different soil pH levels (Baker 1959; Wilding & Drees 1971). Cabanes *et al.* (2011) noted that if plant materials were rapidly buried, it may enhance their chances of preservation but we would not know if this occurred at the study sites. Grasses produce more phytoliths than woody dicotyledonous plants and as a result these phytoliths may be underrepresented relative to grass phytoliths. In addition, Wilding and Drees (1974) demonstrated that phytoliths from the leaves of deciduous trees are 10 to 15 times more soluble than grass phytoliths. Furthermore, more delicate (less hardy in structure) phytoliths are likely to be under-represented in the fossil record (Bamford 2006). Taking into account the differential production of phytoliths of woody dicotyledonous plants relative to other plant families then, the consistent presence of these "woody dicot" phytoliths in all the samples suggest that woody dicotyledons were an important plant component in the EFT and DFT environment. The presence of trees however, cannot be confirmed because we are unable to distinguish, at this stage, between phytoliths of woody and herbaceous dicots.

### 6.8 Challenges and Future Research

Phytolith analysis is an encouraging method of investigation for broad classifications of vegetation patterns in paleoenvironmental reconstructions, but there are limitations. It should be noted that as suggested by Dunn (1983), researchers should execute more thorough investigations of systematics and depositional contexts of phytoliths before making conclusions based on the size, frequency and presence of phytoliths in archaeological sites. Furthermore, as demonstrated by Esteban *et al.* (2016), accurate vegetation identification can be made more difficult when grassy plants, which produce high quantities of phytoliths, are present in the sediment samples. Esteban *et al.* (2016) observed that phytolith assemblages and concentrations of phytolith types are less likely to be the result of genuine changes in the vegetation but may be due to the abundance of 'good' phytolith producers versus plants which produce fewer or no phytoliths. In addition, as observed in some of

the sediment samples in this study, the preservation of phytoliths is closely related to the surrounding sediment's characteristics, such as pH and mineral composition. Therefore, the conclusions of this study are not without biase. Further in depth research focusing on sedimentology may aid future research into these open-air archeological sites.

There are several suggestions for future research that were highlighted during this project.
More sampling should be done at both EFT and DFT in order to investigate broader environmental changes. In this study, viable samples from DFT were limited and further sampling would therefore be beneficial in providing a more reliable interpretation of the paleovegetation of this site. The implementation of horizontal sampling in this study provided a sediment sample from a particular stratigraphic unit, which represented the average phytolith composition at that time period. In order to precisely interpret each stratigraphic unit, more samples should be taken in smaller intervals within each sediment unit. In addition, it would be ideal if the stratigraphic layers could be more accurately dated, this would enable a clearer interpretation of temporal vegetation changes in the region. In some fossil sediment samples, there was evidence of small amounts of sedges, woody dicotyledonous plants and palms. Future research should look at breaking down the phytolith plant classification categories to distinguish between herbaceous monocots, grasses and sedges and between woody herbs, shrubs and trees by looking for more diagnostic features in these phytolith morphotypes.

In view of the fact that restios (shrubby grasses) are a common feature of the present day EFT and DFT vegetation and Restionaceae are the defining family in the fynbos plant community (Rebelo *et al.* 2006), fynbos was most likely prevalent during the middle Pleistocene. Globular decorated phytoliths have been associated with herbaceous monocots such as Restionaceae (Piperno 2006; Esteban *et al*. 2016). In this study clear identifications of restio phytoliths could not be executed confidently and as a result this phytolith type was classed under the woody dicotyledonous plant

category. Future research should sample a range of restio species currently growing in the region to aid in the identification of these phytolith morphotypes in the sediment samples.

Another aspect that needs to be investigated further is the presence of charcoal and burnt phytoliths in some of the sediment samples. Quantification and analysis of the charred phytolith morphotypes may assist in providing information about past fires.

### 6.9 Conclusions

The phytolith analyses of the older stratigraphic layers from EFT suggest that there was a mosaic of plant types with diverse grass subfamilies growing in this region during the middle Pleistocene. This diversity of vegetation types likely supported a wide range of ungulates. With time, the woody component started to disappear, leaving a mix of grass and fynbos during the late Pleistocene (Stynder 2009). By the beginning of the Holocene it appears that the wide range of grass subfamilies that had been observed in the Pleistocene sediment samples was replaced by fynbos. This may explain the decrease in ungulate diversity as observed in the fossil faunal records of DFT, Hoedjiespunt (HDP1), Sea Harvest and Swartklip.

The existence of standing water associated with the springs and the fossil remains of water-dependent fauna identified at EFT and DFT is confirmed by the presence of one of the dominant grass subfamilies, Ehrhartoideae, which was observed in the fossil sediment samples and is seen today as growing in moist-aquatic environments. This would also have provided an accessible water source for middle Pleistocene human populations. The mixed nature of the vegetational community proposed for EFT and DFT differs markedly from the contemporary situation, where trees are rare and grasses occur in small quantities. The analysis also suggests that there has not been a transition from winter to summer rainfall in the region or the extension of rainfall into summer months as suggested by Klein *et al.* (2007). Overall, the results of this study parallel those of previous isotopic and dental microwear studies, and as such, proves that phytolith analyses is a suitable approach to

reconstruct palaeo-plant communities along the South African southwestern coast.

The present study used phytoliths to demonstrate that the vegetation community that dominated EFT and DFT during the middle Pleistocene did not conform to the global trend of expansive $C_4$ grasslands. Instead, it showed that $C_3$ grasses and other $C_3$ vegetation types where abundant (Luyt *et al*. 2000). Thus in contrast to East Africa where middle Pleistocene human populations occupied $C_4$-dominated environments, those living at EFT and DFT were faced with very different environmental challenges. The results of this study along with other ongoing palaeoenvironmental research in this region may substantially impact the research on middle Pleistocene hominin adaptations in Africa, as comparisons can now be made between the two regions in terms of the observed differences in hominin behaviour.

## REFERENCES:


Adams, J.M. & Faure, H. 1997. QEN Members. *Review and Atlas of Palaeovegetation: Preliminary Land Ecosystem Maps of the World since the Last Glacial Maximum*. Tennessee (USA): Oak Ridge National Laboratory.

Albert, R. M., Tsatskin, A., Ronen, A., Lavi, O., Estroff, L., Lev-Yadun, S. & Weiner, S. 1999. Mode of occupation of Tabun Cave, Mt Carmel, Israel during the Mousterian Period: A study of the sediments and phytoliths. *Journal of Archaeological Science* 26: 1249–1260.

Albert, R. M. 2000. Study of ash layers through phytolith analyses from the Middle Paleolithic levels of Kebara and Tabun caves (Israel). Ph.D. Thesis, Dept. of Prehistory, Ancient History and Archaeology. University of Barcelona.

Albert, R. M. & Weiner, S. 2001. Study of phytoliths in prehistoric ash layers using a quantitative approach. In: Meunier, J. D. & Colin, F. (eds) *Phytoliths, Applications in Earth Science and Human History*: 251–266. Lisse: A.A. Balkema Publishers.

Albert, R. M., Bar-Yosef, O., Meignen, L. & Weiner, S. 2003. Quantitative Phytolith Study of Hearths from the Natufian and Middle Palaeolithic Levels of Hayonim Cave (Galilee, Israel). *Journal of Archaeological Science* 30: 461-480.

Albert, R. M., Bamford, M. K. & Cabanes, D. 2006. Taphonomy of phytoliths and macroplants in different soils from Olduvai Gorge (Tanzania) and the application to Plio-Pleistocene palaeoanthropological samples. *Quaternary International* 148: 78-94.

Albert, R. M., Bamford, M. K. & Cabanes, D. 2009. Palaeoecological significance of palms at Olduvai Gorge, Tanzania, based on phytolith remains. *Quaternary International* 193: 41-48.

Albert, R. M. & Bamford, M. K. 2012. Vegetation during UMBI and deposition of Tuff IF at Olduvai Gorge, Tanzania (ca. 1.8 Ma) based on phytoliths and plant remains. *Journal of Human Evolution* 63: 342-350.

Albert, R. M. & Marean, C. W. 2012. The Exploitation of Plant Resources by Early Homo sapiens: The Phytolith Record from Pinnacle Point 13B Cave, South Africa. *Geoarchaeology: An International Journal* 27: 363-384.

Albert, R. M., Bamford, M. K. & Esteban, I. 2015. Reconstruction of ancient palm vegetation landscapes using a phytolith approach. *Quaternary International* 369: 51-66.

Aleman, J.C., Canal-Subitani, S., Favier, C. & Bremond, L. 2014. Influence of the local environment on lacustrine sedimentary phytolith records. *Palaeogeography, Palaeoclimatology, Palaeoecology* 414: 273-283.

Alexandre, A., Meunier, J.-D., Lézine, A.-M., Vincens, A. & Schwartz, D. 1997. Phytoliths indicators of grasslands dynamics during the late Holocene intertropical Africa. *Palaeogeography, Palaeoclimatology, Palaeoecology* 136: 213–219.

Alexandre, A., Meunier, J. D., Mariotti, A., & Soubies, F. 1999. Late Holocene phytolith and carbon isotope record from a latosol at Salitre, south-central Brazil, *Quaternary Research* 51: 187–194.

Baker, R. G. 1959. Opal Phytoliths in Some Victorian Soils and "Red Rain" Residues. *Australian Journal of Botany* 7: 64-87.

Baker, R. G., Fredlund, G. G., Mandel, R. D. & Bettis, E. A. 2000. Holocene environments of the central Great Plains: multi-proxy evidence from alluvial sequences, southeastern Nebraska. *Quaternary International* 67: 75–88.

Bamford, M. K., Albert, R. M. & Cabanes, D. 2006. Plio-Pleistocene macroplant fossil remains and phytoliths from Lowermost Bed II in the eastern palaeolake margin of Olduvai Gorge, Tanzania. *Quaternary International* 148: 95–112.

Bamford, M. K., Stanistreet, I. G., Stollhofen, H. & Albert, R. M. 2008. Late Pliocene grassland from Olduvai Gorge, Tanzania. *Palaeogeography, Palaeoclimatology, Palaeoecology* 257: 280–293.

Barboni, D., Bonnefille, R., Alexandre, A. & Meunier, J. D. 1999. Phytoliths as paleoenvironmental indicators, West Side Middle Awash Valley, Ethiopia. *Palaeogeography Palaeoclimatology Palaeoecology* 152: 87-100.

Barboni, D., Bremond, L. & Bonnefille, R. 2007. Comparative study of modern phytolith

assemblages from inter-tropical Africa. *Palaeogeography Palaeoclimatology Palaeoecology* 246: 454-470.

Barboni, D. & Bremond, L. 2009. Phytoliths of East African grasses: An assessment of their environmental and taxonomic significance based on floristic data. *Review of Palaeobotany and Palynology* 158(1): 29-41.

Barboni, D., Ashley, G. M., Dominguez-Rodrigo, M., Bunn, H. T., Mabulla, A. Z. P. & Baquedano, E. 2010. Phytoliths infer locally dense and heterogeneous paleovegetation at FLK North and surrounding localities during upper Bed I time, Olduvai Gorge, Tanzania. *Quaternary Research* 74: 344-354.

Basell, L. 2008. Middle Stone Age (MSA) site distributions in eastern Africa and their relationship to Quaternary environmental change, refugia and the evolution of Homo sapiens. *Quaternary Science Reviews* 27: 2484-2498.

Berger, L. R. & Parkington, J. E. 1995. Brief Communication: A New Pleistocene Hominid-Bearing Locality at Hoedjiespunt, South Africa. *American Journal of Physical Anthropology* 98: 601-609.

Berger, L. R., Hawks, J., Dirks, P. H. G. M., Elliott, M. & Roberts, E. M. 2017. Homo naledi and Pleistocene hominin evolution in subequatorial Africa. *eLife*. DOI: 10.755/eLife.24234

Berlin, A. M., Ball, T., Thompson, R. & Herbert, S. C. 2003. Ptolemaic agriculture. ‘‘Syrian Wheat’’ and Triticum aestivum. *Journal of Archaeological Science* 30: 115–121.

Besaans, A. J. 1972. 3217D & 3218 C-st. Helenabaai 3317B & 3318A Saldanhabaai. Geological Survey of South Africa. Department of Mines, Pretoria.

Bishop, L. C. 2010. Suoidea. In: Werdelin, L., Sanders, W. (eds) *Cenozoic Mammals of Africa:* 821-842. Berkeley: University of California Press.

Blinnikov, M. S. 1999. Late Pleistocene history of the Columbia Basin grassland based on phytolith records in loess. PhD Thesis. University of Oregon. Eugene.

Blinnikov, M., Busacca, A. & Whitlock, C. 2002. Reconstruction of the Late Pleistocene grassland of the Columbia basin, Washington, USA, based on phytolith records in loess. *Palaeogeography, Palaeoclimatology, Palaeoecology* 177: 77–101.

Blinnikov, M., Bagent, C. M. & Reyerson, P. E. 2013. Phytolith assemblages and opal concentrations from modern soils differentiate temperate grasslands of controlled composition on experimental plots at Cedar Creek, Minnesota. *Quaternary International* 287: 101-113.

Bowdery, D. 1999. Taphonomy, Phytolith and the African Dust Plume. In: M, J. Mountain & Bowdery, D. (eds) *Taphonomy: the Analysis of Processes from Phytoliths to Megafauna. Research Papers in Archaeology and Natural History*: 3-8. Canberra: Australian National University.

Bozarth, S. R. 1992. Classification of opal phytoliths formed in selected dicotyledons native to the Great Plains. In: Rapp, Jr., G. & Mulholland, S. C. (eds) "*Phytolith Systematics*": 193–214. Plenum: New York.

Braun, D. R., Levin, N. E., Stynder, D., Herries, A. I. R., Archer, W., Forrest, F., Roberts, D. L., Bishop, L. C., *et al*. 2013. Mid-Pleistocene Hominin occupation at Elandsfontein, Western Cape, South Africa. *Quaternary Science Reviews* 82: 145-166.

Brémond, L., Alexandre, A., Peyron, O. & Guiot, J. 2005. Grass water stress estimated from phytoliths in West Africa. *Journal of Biogeography* 32: 311–327.

Brémond, L., Alexandre, A., Wooller, M.J., Hely, C., Williamson, D., Schafer, P.A., Majule, A. & Guiot, J. 2008. Phytolith indices as proxies of grass subfamilies on East African tropical mountains. *Global and Planetary Change* 61: 209–224.

Butzer, K. W. 1973. Re-evaluation of the geology of the Elandsfontein (Hopefield) site, south-western Cape, South Africa. *South African Journal of Science* 69: 234-238.

Butzer, K.W. 2004. Coastal eolian sands, paleosols, and Pleistocene geoarchaeology of the Southwestern Cape, South Africa. *Journal of Archaeological Science* 31: 1743-1781.

Cabanes, D., Weiner, S. & Shahack-Gross, R. 2011. Stability of phytoliths in the archaeological record: a dissolution study of modern and fossil phytoliths. *Journal of Archaeological Science* 38: 2480-2490.

Campbell, B. M. 1985. A classification of the mountain vegetation of the Fynbos Biome. *Memoirs of the Botanical Survey of South Africa* 50: 1–121.

Carter, J. A. 2002. Phytolith analysis and paleoenvironmental reconstruction from Lake Poukawa Core, Hawkes Bay, New Zealand. *Global and Planetary Change* 33: 257– 267.

Cerling T. U., Harris, J. M., MacFadden, B. J., Leakey, M. G., Quade, J., Eisenman, V. & Ehleringer, J. R. 1997. Global vegetation change through the Miocene/Pliocene boundary. *Nature* 389: 153-158.

Chase, B. M. & Thomas, D. S. G. 2007. Multiphase late Quaternary aeolian sediment accumulation in western South Africa: Timing and relationship to palaeoclimatic changes inferred from the marine record. *Quaternary International*, 166(1): 29-41.

City of Cape Town (CoCT). 2011. *Integrated Reserve Management Plan For The Blaauwberg Nature Reserve.* Available Online: http://resource.capetown.gov.za/documentcentre/Documents/City%20strategies,%20plans%20and%20frameworks/Blaauwberg_IRMP_Jun2011v02_Final.pdf [Accessed: February 2016].

Coetzee, J. A. & Rogers, R. 1982. Palynological and lithological evidence for the Miocene palaeoenvironment in the Saldanha region (South Africa). *Palaeogeography, Palaeoclimatology, Palaeoecology* 39: 71–85.

Collura, L. V. & Neumann, K. 2016. Wood and bark of West African woody plants. *Quaternary International* xxx:1-18.

Compton, J. S. 2011. Pleistocene sea-level fluctuations and human evolution on the southern coastal plain of South Africa. *Quaternary Science Reviews* 30: 506-527.

Cordova, C. E. & Scott, L. 2010. The potential of Poaceae, Cyperaceae and Restionaceae phytoliths to reflect past environmental conditions in South Africa. *Palaeontologia Africana* 30: 107–134.

Cordova, C. E. 2013. C3 Poaceae and Restionaceae phytoliths as potential proxies for reconstructing winter rainfall in South Africa. *Quaternary International* 287: 121-140.

Cordova, C. & Avery, G. 2017. African savanna elephants and their vegetation associations in the Cape Region, South Africa: Opal phytoliths from dental calculus on prehistoric, historic and reserve elephants. *Quaternary International* 443: 189-211.

Cowling, R. M. 1984. A syntaxonomic and synecological study in the Humansdorp region of the Fynbos Biome. *Bothalia* 15: 175–227.

Cowling, R. 1992. *Fynbos: South Africa's unique floral kingdom.* Cape Town: University of Cape Town Press.

Cowling, R. M., Richardson, D. M. & Mustart, P. J. 1997. Fynbos. In: Cowling, R. M., Richardson, D. M. & Pierce, S. M. (eds) *Vegetation in South Africa*: 99-130. Cambridge: Cambridge University Press.

Cowling, R. M. & Heijnis, C. E. 2001. The identification of broad habitat units as biodiversity entities for a systematic conservation planning in the Cape Floristic Region. *African Journal of Botany* 67: 15–38.

Cowling, R. M. & Lombard, A. T. 2002. Heterogeneity, speciation/extinction history and climate: explaining regional plant diversity patterns in the Cape Floristic Region. *Diversity and Distributions* 8: 163-179.

Cruz-Uribe, K., Klein, R. G., Avery, G., Avery, M., Halkett, D., Hart, T., Milo, R. G., Sampson, C. G. & Volman, T. P. 2003. Excavation of buried Late Acheulean (Mid-Quaternary) land surfaces at Duinefontein 2, Western Cape Province, South Africa. *Journal of Archaeological Science* 30: 559-575.

Das, S., Ghosh, R. & Bera, S. 2013. Application of non-grass phytoliths in reconstructing deltaic environments: A study from the Indian Sunderbans. *Palaeogeography, Palaeoclimatology, Palaeoecology* 376: 48-65.

Deacon, J. 1976. Report on stone artefacts from Duinefontein 2, Melkbosstrand. *South African Archaeological Bulletin* 31: 21–25.

Deacon, J. & Lancaster, N. 1988. *Late Quaternary Palaeoenvironments of Southern Africa*. New York: Oxford University Press.

Deacon, H. J. 1998. Elandsfontein and Klasies River Revisited. In: Ashton, N., Healy, F. & Pettitt, P.B. (eds) *Stone Age Archaeology: Essays in Honour of John Wymer:* 23-28. Oxford: Oxbow Books.

Dodd, J. R. & Stanton Jr., R. J. 1990. *Paleoecology. Concepts and Applications* (2nd ed.): 502. New York: Wiley.

Drennan, M. R. 1953. The Saldanha skull and its associations. *Nature* 172: 791-793.

Dunn, M. E. 1983. Phytolith Analysis in Archaeology. *Midcontinental Journal of Arhaeology* 8(2): 287-297.

Ehleringer, J. R., Sage, R. F., Flanagan, L. B. & Pearcy, R. W. 1991. Climate change and the evolution of climate change. *Trends in Ecology & Evolution* 6: 95–99.

Ehleringer, J. R., Cerling, T. E. & Helliker, B. R. 1997. C4 photosynthesis, atmospheric CO2, and climate. *Oecologia* 12: 285–299.

Ellis, R. P. 1979. A procedure for standardizing comparative leaf anatomy in the Poaceae. II: The epiderniis as seen in surface view. *Bothalia* 12 (4): 641-671.

Ellis, R. P., Vogel, J. C. & Fuls, A. 1980. Photosynthetic pathways and the geographical distribution of grasses in southwest Africa/Namibia. *South African Journal of Science* 76: 307–314.

Ellis, R. P. 1984. Eragrostis walteri – a first record of non–Kranz leaf anatomy in the sub-family Choloridoideae (Poaceae). *South African Journal of Botany* 3: 380 – 386.

Esteban, I. 2016. Reconstructing past vegetation and modern human foraging strategies on the south coast of South Africa. PhD Thesis, Universitat de Barcelona, Barcelona.

Esteban, I., De Vynck, J. C., Singels, E., Vlok, J., Marean, C. W., Cowling, R. M., Fisher, E. C., Cabanes, D. & Albert, R. M. 2016. Modern soil phytolith assemblages used as proxies for Paleoscape reconstruction on the south coast of South Africa. *Quaternary International* xxx 1-20.

Esteban, I., Vlok, J., Kotina, E. L., Bamford, M. K., Cowling, R. M., Cabanes, D. & Albert, R. M. 2017. Phytoliths in plants from the south coast of the Greater Cape Floristic Region (South Africa). *Review of Palaeobotany and Palynology* xxx.

Fahmy, A. G. 2008. Diversity of lobate phytoliths in grass leaves from the Sahel region, West Tropical Africa: Tribe Paniceae. *Plant Systematics and Evolution* 270: 1-23.

Feathers, J. K. 2002. Luminescence dating in less than ideal conditions: case studies from Klasies River Mouth and Duinefontein, South Africa. *Journal of Archaeological Science* 29: 177–194.

Fishkis, O., Ingwersen, J. & Streck, T. 2009. Phytolith transport in sandy sediment: experiments and modelling. *Geoderma* 151: 27-36.

Fishkis, O., Ingwersen, J., Lamers, M., Denysenko, D. & Streck, T. 2010. Phytolith transport in soil: a laboratory study on intact soil cores. *European Journal of Soil Sciences* 61: 445- 455.

Franz-Odendaal, T. A., Lee-Thorp, J. A. & Chinsamy, A. 2002. New evidence for the lack of C4 grassland expansions during the early Pliocene at Langebaanweg, South Africa. *Paleobiology* 28: 378–388.

Franz-Odendaal, T.A. & Kaiser, T. M. 2003. Differential mesowear in the maxillary and mandibular cheek dentition of some ruminants (Artiodactyla). *Annales Zoologici Fennici* 40: 395–410.

Fredlund, G. G. & Tieszen, L. T. 1994. Modern phytolith assemblages from the North American Great Plains. *Journal of Biogeography* 21: 321–335.

Fredlund, G. G. & Tieszen, L. L. 1997. Calibrating grass phytolith assemblages in climatic terms: application to late Pleistocene assemblages from Kansas and Nebraska. *Paleogeography, Paleoclimatology, Paleoecology* 136: 199–211.

Ganqa, N. M., Scogings, P. F. & Raats, J. G. 2005. Plant factors affecting diet selection by black rhino in the Great Fish River Reserve, South Africa. *South African Journal of Wildlife Research* 35:77-83.

Garnier A., Neumann K., Eichhorn B. & Lespez L. 2012. Phytolith taphonomy in the middle- to late-Holocene fluvial sediments of Ounjougou (Mali, West Africa). *The Holocene* 23: 416–431.

Gibbs Russell, G. E. 1988. Distribution of subfamilies and tribes of Poaceae in southern Africa. Monographs in Systematic Botany, *Missouri Botanical Gardens* 25: 555–566.

Gibbs Russell, G. E., Watson, L., Koekemoer, M., Smook, L., Barker, N. P., Anderson, H. M. & Dallwitz, M. J. 1990. Grasses of Southern Africa. In: *Memoirs of the Botanical Survey of South Africa*, vol. 58. Pretoria: National Botanical Institute.

Gibson, D.J. 2009. *Grasses and grassland ecology*. London: Oxford University Press.
Gobetz, K. E. & Bozarth, S. R. 2001. Implications for Late Plesitocene Mastodon Diet from Opal Phytoliths in Tooth Calculus. *Quaternary Research* 55: 115-22.

Goldblatt, P. & Manning, J. 2002. Plant diversity of the Cape Region of South Africa. *Annals of the Missouri Botanical* 89: 281–302.

GPWG: Grass Phylogeny Working Group 2001. Phylogeny and subfamilial classification of the Grasses (Poaceae). *Annals of the Missouri Botanical Garden* 88: 373 – 357.

Grab, S., Scott, L., Rossouw, L. & Meyer, S. 2005. Holocene palaeoenvironments inferred from a sedimentary sequence in the Tsoaing River Basin, western Lesotho. *Catena* 61: 49-62.

Grine, F. E. & Klein, R. G. 1993. Late Pleistocene human remains from Sea Harvest site, Saldanha Bay, South Africa. *South African Journal of Science* 89: 145-152.

Grunow, J. O. 1980. Feed and habitat preferences among some large herbivores on African veld, Proceedings of the Annual Congresses of the Grassland Society of Southern Africa 15(1): 141-146.

Gu, Y., Pearsall, D. M., Xie, S. & Yu, J. 2008. Vegetation and fire history of a Chinese site in southern tropical Xishuangbanna derived from phytolith and charcoal records from Holocene sediments. *Journal of Biogeography* 35: 325-341.

Halkett, D., Hart, T., Yates, R., Volman, T. P., Parkington, J. E., Orton, J., Klein, R. G. Cruz-Uribe, K. & Avery, G. 2003. First excavation of intact Middle Stone Age layers at Ysterfontein, Western Cape Province, South Africa: implications for Middle Stone Age ecology. *Journal of*

*Archaeological Science* 30: 955-971.

Hare, V. & Sealy, J. 2013. Middle Pleistocene dynamics of southern Africa's winter rainfall zone from δ13C and δ18O values of Hoedjiespunt faunal enamel. *Palaeography, Palaeoclimatology, Palaeoecology* 374: 72-80.

Hendey, Q .B. 1968. The Melkbos site: an Upper Pleistocene fossil occurrence in the South-Western Cape Province. *Annals of the South African Museum* 52: 89–119.

Hendey, Q. B. 1974. The late Cenozoic Carnivora of the southwestern Cape Province. *Annals of the South African Museum* 63: 1-369.

Hetherington, R., Wiebe, E., Weaver, A. J., Carto, S. L., Eby, M. & MacLeod, R. 2008. Climate, African and Beringian subaerial continental shelves, and migration of early peoples. *Quaternary International* 183: 83-101.

Horrocks, M., Deng, Y., Ogden, J. & Sutton, D. G. 2000. A reconstruction of the history of a Holocene sand dune on Great Barrier Island, northern New Zealand, using pollen and phytolith analyses. *Journal of Biogeography* 27: 1269– 1277.

Horrocks, M., Shane, P. A., Barber, I. G., D'Costa, D. M. & Nichol, S. L. 2004. Microbotanical Remains Reveal Polynesian Agriculture and Mixed Cropping in Early New Zealand. *Review of Palaeobotany and Palynology* 131: 147-57.

Horrocks, M. 2005. A combined procedure for recovering phytoliths and starch residues from soils, sedimentary deposits and similar materials. *Journal of Archaeological Science* 32: 1169–1175.

Kealhofer, L., Torrence, R. & Fullager, R. 1999. Integrating Phytoliths within Use-Wear/Residue Studies of Stone Tools. *Journal of Archaeological Science* 26: 527-46.

Khumbulu Indigenous Garden, 2014. Vachellia karoo.[image online] Available at: < http://kumbulanursery.co.za/plants/vachellia-karoo> [Accessed 3 January 2017].

Klein, R. G. 1975. Paleoanthropological implications of the non-archeological bone assemblage from Swartklip 1, south-western Cape Province, South Africa. *Quaternary Research* 5: 275-288.

Klein, R. G. 1976. A Preliminary Report on the 'Middle Stone Age' Open-Air Site of Duinefontein

2 [Melkbosstrand, South-Western Cape Province, South Africa]. *The South African Archaeological Bulletin* 31(121/122), 12-20.

Klein, R. G. 1978. The fauna and overall interpretation of the ‘‘Cutting 10’’ Acheulean site at Elandsfontein (Hopefield), Southwestern Cape Province, South Africa. *Quaternary Research* 10: 69-83.

Klein, R.G., 1983a. The stone age prehistory of southern Africa. *Annual Review of Anthropology* 12: 25-48.

Klein, R. G. 1983b. Palaeoenvironmental implications of Quaternary large mammals in the Fynbos region. *South African National Scientific Programmes Report* 75: 116-138.

Klein, R. G. 1988. Archaeological significance of animal bones from Acheulean sites in southern Africa. *African Archaeological Review* 6: 3-25.

Klein, R. G. & Cruz-Uribe, K. 1991. The bovids from Elandsfontein, South Africa, and their implications for the age, palaeoenvironment, and origins of the site. *African Archaeological Review* 9: 21-79.

Klein, R. G., Avery, G., Cruz-Uribe, K., Halkett, D., Hart, T., Milo, R. G. & Volman, T. P. 1999. Duinefontein 2: an Acheulean site in the Western Cape Province of South Africa. *Journal of Human Evolution* 37: 153-190.

Klein, R. G., Avery, G., Cruz-Uribe, K. & Steele, T. E. 2007. The mammalian fauna associated with an archaic hominin skullcap and later Acheulean artifacts at Elandsfontein, Western Cape Province, South Africa. *Journal of Human Evolution* 52: 164-186.

Klein, R.G. 2009. *The Human Career: Human Biological and Cultural Origins* (2nd ed.) Chicago: University of Chicago Press.

Lancelotti, C. 2010. Fuelling Harappan Hearths: Human Environment Interactions as Revealed by Fuel Exploitation and Use. Unpublished PhD Dissertation. Department of Archaeology. Cambridge: University of Cambridge.

Lee-Thorp, J. A. & van der Merwe, N. J. 1987. Carbon isotope analysis of fossil bone apatite. *South African Journal of Science* 83: 712-715.

Lee-Thorp, J. A. & Beaumont, P. B. 1995. Vegetation and seasonality shifts during the late Quaternary deduced from 13C/12C ratios of gragers at Equus Cave, South Africa. *Quaternary Research* 43: 426–432.

Lehmann, S. B., Braun, D. R., Dennis, K. J., Patterson, D. B., Stynder, D., Bishop, L. C., Forrest, F. & Levin, N. E. 2016. Stable isotopic composition of fossil mammal teeth and environmental change in southwestern South Africa during the Pliocene and Pleistocene. *Palaeogeography, Palaeoclimatology, Palaeoecology* 457: 396-408

Lentfer, C. & Boyd, W. E. 2000. Simultaneous Extraction of Phytoliths, Pollen and Spores from Sediments. *Journal of Archeological Science* 27(5): 363-372.

Linder, H. P. & Ellis, R. P. 1990. A revision of Pentaschistis (Arundineae: poaceae). *Contributions from the Bolus Herbarium* 12: 1-124.

Lu, H. Y., Wu, N. Q., Liu, D. S., Han, J. M., Qin, X. G., Sun, X. J. & Wang, Y. J. 1996. Seasonal climatic variation recorded by phytolith assemblages from the Baoji loess sequence in central China over the last 150,000 a. *Science in China* (Series D) 39: 629– 639.

Luyt, J., Lee-Thorp, J. A. & Avery, G. 2000. New light on middle Pleistocene west coast environments from Elandsfontein, Western Cape, South Africa. *South African Journal of Science* 96: 399-403.

Mabbutt, J. A. 1956. The physiography and surface geology of the Hopefield fossil site. *Transactions of the Royal Society of South Africa* 35: 21-58.

MacLeod, S. B., Kerley, G. I. H. & Gaylard, A. 1996. Habitata and diet of bushbuck *Tragelaphus scriptus* in the Woody Cape Nature Reserve: observations from faecal analysis. *South African Journal of Wildlife Research* 26: 19-25.

Madella, M. 1997. Phytolith analysis from the Indus Valley site of Kot Diji, Sindh, Pakistan. In: Sinclair, A., Slater, E. & Gowlett, J. (eds) *Archaeological Sciences*: 294-302. Oxford: Oxbow Books.

Madella, M., Alexandre, A. & Ball, T. 2005. International Code for Phytolith Nomenclature 1.0. *Annals of Botany* 96: 253-260.

Madella, M. & Lancelotti, C. 2012. Taphonomy and phytoliths: a user manual. *Quaternary International* 275: 76-83.

Manning, J. 2007. *Field Guide to Fynbos*. Cape Town: Struik Publishers.

Maslin, M. A. & Christensen, B. 2007. Tectonics, orbital forcing, global climate change, and human evolution in Africa: introduction to the African paleoclimate special volume. *Journal of Human Evolution*, 53 (5), 443-454.

McLean, B. & Scott, L. 1999. Phytoliths in sediments of the Pretoria Saltpan and their potential as indicators of environmental history at the site. In Partridge, T. C. (ed.) *Tswaing investigations into the origin, age and palaeoenvironments of the Pretoria Saltpan*: 167–171. Pretoria: Council for Geosciences.

Mercader, J., Astudillo, F., Barkworth, M., Bennett, T., Esselmont, C., Kinyanjui, R., Grossman, D. L., Simpson, S. & Walde, D. 2009. Phytoliths in woody plants from the Miombo woodlands of Mozambique. *Annals of Botany* 104: 91–113.

Mercader, J., Astudillo, F., Barkworth, M., Bennett, T., Esselmont, C., Kinyanjui, R., Grossman, D.L., Simpson, S. & Walde, D., 2010. Poaceae phytoliths from the Niassa Rift, Mozambique. *Journal of Archaeological Science* 1953–1967.

Mercader, J., Bennett, T., Esselmont, C., Simpson, S. & Walde, D. 2011. Soil phytoliths from the miombo woodlands in Mozambique. Quaternary Research 75: 138-150.

Messager, E., Lordkipanidze, D., Delhon, C. & Ferring, C. R. 2010. Palaeoecological implications of the Lower Pleistocene phytolith record from the Dmanisi Site (Georgia). *Palaeogeography, Palaeoclimatology, Palaeoecology* 288: 1-13.

Moll, E. J., Campbell, B. M., Cowling, R. M., Bossi, L., Jarman, M. L. & Boucher, C. 1984. A description of major vegetation categories in and adjacent to the Fynbos Biome. *South African National Scientific Programmes Report* 83: 1–29.

Mulholland, S. C. 1989. Phytolith shape frequencies in North Dakota grasses: A comparison to

general patterns. *Journal of Archaeological Science* 16: 489–511.

Mulholland, S. C. & Rapp, G. Jr. 1992. A morphological classification of grass silica-bodies. In: Rapp, G. Jr. & Mulholland, S.C. (eds) *Phytolith Systematic, Emerging Issues: Advances in Archaeological and Museum Science* 1: 65-89. New York: Plenum Press.

Needham, H. D. 1962. Aspects of Quaternary Geology of the Sandveld with Particular Reference to the Hopefield Fossil Site, Geology. Msc. Thesis Geology. Cape Town: University of Cape Town.

Neumann, K., Fahmy, A., Lespez, L., Ballouche, A & Huysecom, E. 2009. The Early Holocene palaeoenvironment of Ounjougou (Mali): Phytoliths in a multiproxy context. *Palaeogeography, Palaeoclimatology, Palaeoecology* 276: 87–106.

Njenga, E. W. 2005. The chemotaxonomy, phylogeny and Biological activity of the genus Eriocephalus l. (Asteraceae). Ph.D. thesis. Faculty of Health Sciences. Johannesburg: University of the Witwatersrand.

Nörström, E., Scott, L., Partridge, T. C., Risberg, J. & Holmgren, K. 2009. Reconstruction of environmental and climate changes at Braamhoek wetland, eastern escarpment South Africa, during the last 16,000 years with emphasis on the Pleistocene-Holocene transition. *Palaeogeography, Palaeoclimatology, Palaeoecology* 271: 240–258.

Novello, A., Barboni, D., Berti-Equille, L., Mazur, J-C., Poilecot, P. & Vignaud, P. 2012. Phytolith signal of aquatic plants and soils in Chad, Central Africa. *Review of Palaeobotany and Palynology* 178: 43-58.

Novello, A., Lebatard, A-E., Moussa, A., Barboni, D., Sylvestre, F., Bourles, D. L., Pailles, C., Buchet, G. *et al.* 2015. Diatom, phytolith, and pollen records from a $^{10}Be/^{9}Be$ dated lacustrine succession in the Chad basin: Insight on the Miocene–Pliocene paleoenvironmental changes in Central Africa. *Palaeogeography, Palaeoclimatology, Palaeoecology* 430: 85-103.

Okubo, A. & Levin, S. A. 1989. A theoretical framework for data analysis of wind dispersal of seeds and pollen. *Ecology* 70: 329–338.

Ollendorf, A. L. 1992. Toward a classification scheme of sedge (Cyperaceae) phytoliths. In: Rapp

Jr., G. & Mulholland, S.C. (eds) *Phytolith Systematics. Emerging Issue. Advances in Archaeological and Museum Science* 1: 91–111. New York: Plenum Press.

Osterrieth, M., Madella, M., Zurro, D. & Alvarez, M. F. 2009. Taphonomical aspects of silica phytoliths in the loess sediments of the Argentinean Pampas. *Quaternary International* 193: 70-79.

Owen-Smith, N. & Cooper, S .M. 1987. Palatability of woody plants to browsing ruminants in a South African savanna. *Ecology* 68: 319 -331.

Palmer, P. G. 1976. Grass cuticles: a new palaeoecological tool for East African lake sediments. *Canadian Journal of Botany* 54 (15): 1725 – 1734.

Parolin, M., Rasbold, G. G. & Pessenda, L. C. R. 2014. Paleoenvironmental conditions of Campos Gerais, Parana, since the Late Pleistocene, based on phytoliths and C and N isotopes. In: Coe, H. H. G. & Osterrieth, M. (eds) *Synthesis of Some Phytolith Studies in South America (Brazil and Argentina):* 149-170. New York: Nova Science Publishers, Inc.

Parr, J.F., Lentfer, C.J. & Boyd, W. E. 2001. A comparative analysis of wet and dry ashing techniques for the extraction of phytoliths from plant material. *Journal of Archaeological Science* 28: 875 – 886.

Partridge, T. C., Wood, B. A. & deMenocal, P. B. 1995. The influence of global climatic change and regional uplift on large-mammal evolution in East and southern Africa. In: Vrba, E. S., Denton, G. H., Partridge, T. C. & Burckle, L. H. (eds) *Paleoclimate and Evolution, with Emphasis on Human Origins*: 331-355. New Haven, CT: Yale University Press.

Patterson, D. B., Lehmann, S. B., Matthews, T., Levin, N. E., Stynder, D., Bishop, L. C. & Braun, D. R .2016. Stable isotope ecology of Cape dune mole-rats (Bathyergus suillus) from Elandsfontein, South Africa: Implications for C4 vegetation and hominin paleobiology in the Cape Floral Region. *Palaeogeography, Palaeoclimatology, Palaeoecolecology* 457: 409-421.

Pearsall, D. M. 1982. Phytoliths analysis: Applications of a new palaeoethnobotanical technique in archaeology. *American Anthropologist* 84: 862–871.

Pearsall, D. M. 2000. *Paleoethnobotany: a handbook of procedures* (second edition). London:

Academic Press, Inc.

Pearsall, D. M., Chandler-Ezell, K. & Zeidler, J. A. 2004. Maize in ancient Ecuador: results of residue analysis of stone tools from the Real Alto site. *Journal of Archaeological Science* 31: 423 – 442.

Pearsall, D. M. 2015. *Paleoethnobotany. A Handbook of Procedures*. Third Edition (1989, 2000). Walnut Creek, CA: Left Coast Press.

Philander, C. & Rozendaal, A. 2015. Geology of the Cenozoic Namakwa Sands Heavy Mineral Deposit, West Coast of South Africa: A World-Class Resource of Titanium and Zircon. *Economic Geology* 110: 1577-1623.

PhytCore DB, 2014. Ellipsoid phytolith. [online] Available at: http://www.phytcore.org/phytolith/index.php?rdm=tWt24kNTSV&action=phytzoom&ID=505 [accessed 2 February 2017].

Pickering, R., Jacobs, Z., Herries, A. I., Karkanas, P., Bar-Matthews, M.,Woodhead, J. D., Kappen, P., Fisher, E. & Marean, C. W. 2013. Paleoanthropologically significant South African sea caves dated to 1.1-1.0 million years using a combination of U-Pb, TT-OSL and palaeomagnetism. *Quaternary Science Reviews* 65: 39-52.

Piperno, D. 1988. *Phytolith analysis — An Archaeological and Geological Perspective*. London: Academic Press.

Piperno, D.R. & Pearsall, D.M. 1998. The silica bodies of tropical American grasses: Morphology, taxonomy and implications for grass systematics and fossil phytolith identification. *Smithsonian contributions to Botany* 85.

Piperno, D.R. & Jones, J. G. 2003. Paleoecological and archaeological implications of a Late Pleistocene/Early Holocene record of vegetation and climate from the Pacific coastal plain of Panama. *Quaternary Research* 59: 79– 87.

Piperno, D. 2006. *Phytoliths: A Comprehensive Guide for Archaeologists and Paleoecologists.* San Diego: AltaMira Press.

PlantZAfrica, 2011. Acacia nigrscens.[image online] Available at: < http://www.plantzafrica.com/plantab/acacianigrescens.htm> [Accessed 3 January 2017].

PlantZAfrica, 2005. Acacia nilotica.[image online] Available at: < http://www.plantzafrica.com/plantab/acacianilot.htm> [Accessed 3 January 2017].

PlantZAfrica, 2012. Acacia tortilis.[image online] Available at: < http://www.plantzafrica.com/plantab/acaciatortilis.htm> [Accessed 3 January 2017].

PlantZAfrica, 2009. Dichrostachys cinera. [image online] Available at: < http://www.plantzafrica.com/plantcd/dichroscinerea.htm> [Accessed 3 January 2017].

PlantZAfrica, 2003. Sutherlandia frutescens. [image online] Available at: < http://plantzafrica.com/plantqrs/sutherfrut.htm> [Accessed 3 January 2017].

PlantZAfrica, 2004. Metalasia muricata. [image online] Available at: < http://plantzafrica.com/plantklm/metalmuri.htm> [Accessed 3 January 2017].

Potts, R. 1998. Variability Selection in Hominid Evolution. *Evolutionary Anthropology* 7(3): 81-96.

Rebelo, A. G., Boucher, C., Helme, N., Mucina, L. & Rutherford, M. C. 2006. Fynbos Biome. In: Mucina, L. & Rutherford, M.C. (eds), *The Vegetation of South Africa. Lesotho, and Swaziland, Strelitzia, vol. 19: 53-219.* Pretoria: South African National Biodiversity Institute.

Retallack, G. J. 1990. *Soils of the past: an introduction to paleopedology*. London: Unwin-Hyman.

Rightmire, G.P. 2001. Patterns of hominid evolution and dispersal in the middle Pleistocene. *Quaternary International* 75: 77–84.

Roberts, D. L. 1996. Geology of the Elandsfontyn fossil site. In: Almond, J.E. (ed.), *Excursion Guide: Fossil Sites in the Southwestern Cape: 1-7.* Stellenbosch: Paleontological Society of South Africa.

Roberts, D. L. & Brink, J. S. 2002. Dating and correlation of neogene coastal deposits in the Western Cape (South Africa): implications for Neotectonism. *South African Journal of Geology*

105: 337-352.

Roberts, D.L., Botha, G.A., Maud, R.R. & Pether, J. 2006. Coastal Cenozoic deposits. In: Johnson, M.R., Anhaeusser, C.R. & Thomas, R.J. (eds) *The geology of South Africa*: 605-628. Johannesburg: Geological Society of South Africa.

Roberts, D. L. 2006a. Langebaan Formation. In: Johnson, M.R. (ed.), *Catalogue of South African Lithostratigraphic Units*: 9-12.

Roberts, D. L. 2006b. Sandveld Group. In: Johnson, M.R. (ed.), *Catalogue of South African Lithostratigraphic Units:* 25-26.

Roberts, D. L., Bateman, M. D., Murray-Wallace, C. V., Carr, A. S. & Holmes, P. J. 2009. West Coast dune plumes: climate driven contrasts in dunefield morphogenesis along the western and southern South African coasts. *Palaeogeography, Palaeoclimatology, Palaeoecolecology* 271: 28–31.

Rosen, A. M. 1992. A preliminary identification of silica skeletons from Near Eastern archaeological sites: an anatomical approach. In: Rapp Jr., G. & Mulholland, S.C. (eds) *Phytolith Systematics. Emerging Issue. Advances in Archaeological and Museum Science* 1: 129–147.

Rossouw, L. 1996. The extraction of opal phytoliths from the fossilized teeth of two bovid species from Florisbad. *Navorsinge van die Nasionale Museum, Bloemfontein 12(8)*: 265-275.

Rossouw, L. 2009. The application of fossil grass-phytolith analysis in the reconstruction of late Cainozoic environments in the South African interior. PhD dissertation. Bloemfontein: University of the Free State.

Rossouw, L., Stynder, D. & Haarhof, P. 2009. Evidence for opal phytolith preservation in the Langebaanweg 'E' Quarry Varswater Formation and its potential for palaeohabitat reconstruction. *South African Journal of Science* 105: 223-227.

Rossouw, L. & Scott, S. 2011. Phytoliths and Pollen, the Microscopic Plant Remains in Pliocene Volcanic Sediments Around Laetoli, Tanzania. In: Harrison, T. (ed.) *Paleontology and Geology of Laetoli, Tanzania: Human Evolution in Context. Volume 1: Geology, Geochronology, Paleoecology*

*and Paleoenvironment, Vertebrate Paleobiology and Paleoanthropology*: 201-215. New York: Springer.

Rossouw, L. 2016. An Early Pleistocene Phytolith Record from Wonderwerk Cave, Northern Cape, South Africa. *African Archaeological Review* 33: 251-263.

Rovner, I. 1971. Potential of opal phytoliths for use in palaeoecological reconstruction. *Quaternary Research* 1: 345–359.

Rovner, I. 1983. Plant Opal Phytolith Analysis: Major Advances in Archaeobotanical Research. *Advances in Archaeological Method and Theory* 6: 225-266.

Rovner, I. 1988. Macro- and Micro-ecological Reconstruction using Plant Opal Phytolith Data from Archaeological Sediments. *Geoarchaeology: An International Journal* 3(2): 155-163.

Runge, F. 1999. The opal phytolith inventory of soils in central Africa —quantities, shapes, classification, and spectra. *Review of Palaeobotany and Palynology* 107: 23-53.

Rutherford, M. C. & Westfall, R. H. 1994. Biomes of southern Africa: an objective characterization. *Memoirs of the Botanical Survey of South Africa:* 63.

Sampson, C.G. 2003. Amphibians from the Acheulian Site at Duinefontein 2 (Western Cape, South Africa). *Journal of Archaeological Science* 30(5): 547-557.

Saul, H., Madella, M., Fischer, A., Glykou, A., Hartz, S. & Craig, O. E. 2013. Phytoliths in Pottery Reveal the Use of Spice in European Prehistoric Cuisine. PLos ONE 8(8): e70583. https://doi.org/10.1371/journal.pone.0070583.

Scheepers, R. & Nortje, A. N. 2000. Rhyolitic ignimbrites of the Cape granite Suite, southwestern Cape Province, South Africa. *Journal of African Earth Sciences* 31: 647-656.

Schubert, B.W., Ungar, P.S., Sponheimer, M. & Reed, K. E. 2006. Microwear evidence for Plio Pleistocene bovid diets from Makapansgat Limeworks Cave, South Africa. *Palaeogeography, Palaeoclimatology, Palaeoecology* 241: 301–319.

Schulze, B. R. 1986. Climate of South Africa. Part 8. *General Survey*. South African Weather Bureau, Pretoria.

Scott, L., Anderson, H.M. & Anderson, J.M. 1997. Vegetation History. In: Cowling, R.M, Richardson, D.M. & Pierce, S.M. (eds) *The Vegetation of Southern Africa*: 62-84. Cambridge: Cambridge University Press.

Scott, L. 2002. Grassland development under glacial and interglacial conditions in Southern Africa: review of pollen, phytoliths, and isotope evidence. *Palaeogeography, Palaeoclimatology, Palaeoecology* 177: 47–57.

Scott, L. & Rossouw, L. 2005. Reassessment of botanical evidence for palaeoenvironments at Florisbad, South Africa. *South African Archaeological Bulletin* 60 (182), 96–102.

Singer, R. 1954. The Saldanha skull from Hopefield, South Africa. *American Journal of Physical Anthropology* 12: 345–362.

Singer, R. & Wymer, J. J. 1968. Archaeological investigations at the Saldanha skull site in South Africa. *South African Archaeological Bulletin* 23: 63-74.

Skead, C. J. 1980. Historical Mammal Incidence in the Cape Province, Vol. 1. Department of Nature and Environmental Conservation of the Provincial Administration of the Cape of Good Hope, Cape Town.

Skinner, J. D. & Smithers, R. H. N. 1990. *The Mammals of the Southern African Subregion*. Pretoria: University of Pretoria.

Sponheimer, M. S., Grant, C. C., De Ruiter, D., Lee-Thorp, J., Codron, D. & Codron, J. 2003. Diets of impala from Kruger National Park: evidence from stable carbon isotopes. *Koedoe* 46 (1): 101–106.

Stromberg, C. A. E. 2004. Using phytolith assemblages to reconstruct the origin and spread if grass-dominated habitats in the great plains of North America during the late Eocene to early Miocene. *Palaeogeography, Palaeoclimatology, Palaeoecology* 207: 239 – 275.

Strömberg, C.A. E. 2009. Methodological concerns for analysis of phytolith assemblages: does count size matter? *Quaternary International* 193: 124–140.

Stromberg, C. A. E. & McInerney, F. A. 2011. The Neogene transition from C 3 to C 4 grasslands in North America: assemblage analysis of fossil phytoliths. *Paleobiology* 37(1): 50-71.

Stynder, D. D. 1997. The use of faunal evidence to reconstruct site history at Hoedjiespunt 1 (HDP1), Western Cape. M.A. Thesis. Department of Archaeology. Cape Town: University of Cape Town.

Stynder, D. D., Moggi-Cecchi, J., Berger, L. R. & Parkington, J. E. 2001. Human mandibular incisors from the Late Middle Pleistocene locality of Hoedjiespunt 1, South Africa. *Journal of Human Evolution* 41: 369-383.

Stynder, D. D. 2009. The diets of ungulates from the hominid fossil-bearing site of Elandsfontein, Western Cape, South Africa. *Quaternary Research* 71: 62-70.

Tankard, A. J. & Rogers, J. 1978. Late Cenozoic palaeoenvironments on the west coast of Southern Africa. *Journal of Biogeography* 5: 319–337.

Tieszen, L.L., Senyimba, M.M., Imbamba, S.K. & Troughton, J.H. 1979. The distribution of C3 and C4 grasses and carbon isotope discrimination along an altitudinal and moisture gradient in Kenya. *Oecologia* 37:337-350

Twiss, P. C., Suess, E. & Smith, R. M. 1969. Morphology classification of grass phytoliths. *Soil Science Society of America Proceedings* 33: 109– 115.

Twiss, P.C. 1992. Predicted world distribution of C3 and C4 grass phytoliths. In: Rapp Jr., G. & Mulholland, S.C. (eds) *Phytolith Systematics: Emerging Issues, Advances in Archaeological and Museum Science:* 113-128. New York: Plenum Press.

Van Oudtshoon, F. P. 1992. *Guide to grasses of South Africa*. Cape Town: Briza Publications.

Van Zyl, J. H. M. 1965. The vegetation of the S. A. Lombard Nature Reserve and its utilisation by certain antelope. *Zoologica Africana* 1:55-71.

Vogel, J. C. 1978. Isotopic assessment of dietary habits of ungulates. *South African Journal of Science* 74: 298-301.

Watling, J., Saunaluoma, S., Parssinen, M. & Schaan, D. 2015. Subsistence practices among earthwork builders: Phytolith evidence from archaeological sites in the southwest Amazonian interfluves. *Journal of Archaeological Science: Reports* 4: 541-551.

Wildflower Nursery, 2015. Grewia flavescens. [image online] Available at: <http://wildflowernursery.co.za/indigenous-plant-database/grewia-flavescens/ >[Accessed 3 January 2017].

Wilding, L. P. & Drees, L. R. 1971. Biogenic opal in Ohio soils. *Soil Science Society of America Proceedings* 35: 1004-1010.

Wilding L. P. & Drees, L. R. 1974. Contributions of forest opal and associated crystalline phases to fine silt and clay fractions of soils. *Clays Clay Miner* 22: 295–306.

Wolde Gabriel, G., Ambrose, S. H., Barboni, D., Bonnefille, R., Bremond, L., Currie, B., DeGusta, D., Hart, W. K., *et al*. 2009 The geological, isotopic, botanical, invertebrate, and lower vertebrate surroundings of *Ardipithecus ramidus*. *Science* 326 (65): 65e1-65e5.

Zurro, D., Garcia-Granero, J. J., Lancelotti, C. & Madella, M. 2016. Directions in current and future phytolith research. *Journal of Archaeological Science* 68: 112-117.

**APPENDICES**

# APPENDIX I:
# Images of plant species processed for modern phytolith reference collection

**FIG. 1**: *Mature specimen of Acacia karroo (Khumbulu Indigenous Garden 2014)*

**FIG 2**: *Left: Mature specimen of Acacia nigrescens. Right: Seed pods from Acacia nigrescens (PlantZAfrica 2011).*

**FIG. 3**: *Left: Mature specimen of Acacia nilotica. Right: Seed pods from Acacia nilotica (PlantZAfrica 2005).*

**FIG**. **4**: *Mature specimen of Acacia tortilis (PlantZAfrica 2012).*

**FIG. 5**: *Mature specimen of Dichrostachys cinerea (PlantZAfrica 2009).*

**FIG. 6**: *Left: Sample of Lessertia (Sutherlandia) frutescens. Right: Mature specimen of Lessertia frutescens (PlantZAfrica 2003).*

**FIG. 7**: *Specimen of Carissa macrocarpa.*

**FIG**. **8**: *Ehrharta villosa var. villosa growing at DFT.*

**FIG. 9**: *Specimen of Eriocephalus punctulatus.*

**FIG. 10**: Left: *Metalasia densa* growing at DFT. Right: Close up of *Metalasia densa.*

**FIG. 11**: *Left: Specimen of Metalasia muricata. Right: Mature specimen of Metalasia muricata. (PlantZAfrica 2004).*

**FIG. 12**: *Left: Specimen of Osteospermum moniliferum subsp. monilifera. Right: Osteospermum (Chrysanthemoides) moniliferum subsp. monilifera growing at DFT.*

**FIG. 13**: *Specimen of Grewia flavescens (Wildflower Nursery 2015).*

**FIG. 14**: *Specimen of Grewia occidentalis.*

**FIG. 15**: *Left: Morella cordifolia growing at DFT. Right: Cutting of Morella cordifolia.*

**FIG. 16**: Left: *Lycium afrum growing at DFT. Right: Cutting of Lycium afrum.*

**FIG. 17**: Left: *Pelargonium spp. growing at DFT. Right: Cutting of Pelargonium spp.*

**FIG. 18**: Left: *Searsia spp. growing at DFT. Right: Cutting of Searsia spp.*

**FIG. 19**: *Left: Thesium spp. growing at DFT. Right: Cutting of Thesium spp.*

**FIG. 20**: *Trachyandra divaricata growing at DFT.*

# APPENDIX II:
## Tables of Raw Data

Elandsfontein:

**Table A:** Raw data for EFT samples

| | Sample IDs: | EFT 1.1 | EFT 1.2 | EFT 1.3 | EFT 1.4* | EFT 2.1 | EFT 2.2 | EFT 2.3* | EFT 3.1 | EFT 3.2* | EFT 4.1 | EFT 4.2 | EFT 4.4 | EFT 4.8 | EFT 4.9 | EFT 4.10 |
|---|---|---|---|---|---|---|---|---|---|---|---|---|---|---|---|---|
| Group of plants | Morphotype Category | | | | | | | | | | | | | | | |
| Woody Dicotyledons | | | | | | | | | | | | | | | | |
| | Blocky facetated | | 1 | | | 1 | 2 | | 1 | 2 | 2 | 1 | 4 | 2 | | |
| | Blocky polyhedron | 52 | 2 | 16 | 2 | 14 | 1 | 5 | 45 | 15 | 5 | 6 | 8 | 8 | 19 | 30 |
| | Globular decorated | 72 | 15 | 33 | 24 | 21 | 15 | 27 | 21 | 42 | 17 | 19 | 57 | 17 | 30 | 56 |
| | Globular small facetated | 11 | | 2 | 2 | | | 3 | | | 6 | | | | 2 | |
| | Parallelepiped blocky | | | | | | | | 8 | | | | | | | 2 |
| | Sclerenchyma | | | | | 2 | 2 | | 4 | | 6 | | | | | |
| | **Total** | **135** | **18** | **51** | **28** | **38** | **20** | **35** | **79** | **59** | **36** | **26** | **69** | **27** | **51** | **88** |
| | % | 31,0 | 34,0 | 30,5 | 24,6 | 18,6 | 6,6 | 12,2 | 26,9 | 19,7 | 18,0 | 15,1 | 27,2 | 17,9 | 20,7 | 16,3 |
| Poaceae, GSSC | | | | | | | | | | | | | | | | |
| | Bilobate V1 | 1 | | | | | | | | | | | | | | |
| | Bilobate V2 | 7 | 2 | 2 | 1 | 1 | 25 | 2 | 11 | 24 | 6 | 1 | 13 | | 12 | 64 |
| | Bilobate V3 | | | | | | | | | | | | | | 2 | |
| | Cross | 6 | 1 | | | | | 5 | | 2 | | | 7 | | 2 | 12 |
| | Oblong | 2 | | 1 | 7 | 6 | 26 | | 3 | 33 | 8 | 11 | 18 | 9 | 10 | 37 |
| | Polylobate | | | | | | 3 | | | | | | 2 | 1 | 1 | 3 |
| | Reniform | 11 | 1 | | | | | | | 6 | 4 | | 5 | | 5 | 16 |
| | Rondel | 33 | 3 | 4 | 3 | 7 | 34 | 22 | 22 | 22 | 11 | 19 | 27 | 3 | 1 | 67 |
| | Saddle 1 | 7 | 2 | 5 | 2 | 2 | 2 | | 4 | 23 | 5 | 1 | 5 | 21 | 6 | 73 |
| | Saddle 2 | 1 | | | | | 2 | | | | 2 | 3 | 5 | 6 | 10 | 12 |
| | Trapezoid | 52 | 4 | 19 | 19 | 27 | 47 | 24 | 13 | 25 | 43 | 27 | 34 | 19 | 29 | 42 |
| | **Total** | **120** | **13** | **31** | **32** | **43** | **139** | **53** | **53** | **135** | **79** | **62** | **116** | **59** | **78** | **326** |
| | % | 27,6 | 24,5 | 18,6 | 28,1 | 21,1 | 46,2 | 18,5 | 18,0 | 45,0 | 39,5 | 36,0 | 45,7 | 39,1 | 31,7 | 60,3 |
| | | | | | | | | | | | | | | | | |
| Family Specific | | | | | | | | | | | | | | | | |
| | Globular echinate **(Arecaceae)** | 3 | 1 | | | 1 | 5 | | 2 | 0 | | | 11 | | | 0 |
| | Cyperaceae | 8 | 1 | 2 | | | | | 21 | 1 | | | | 2 | 20 | 6 |
| | **Total** | **11** | **2** | **2** | **0** | **1** | **5** | **0** | **23** | **1** | **0** | **0** | **11** | **2** | **20** | **6** |
| | % | 2,5 | 3,8 | 1,2 | 0,0 | 0,5 | 1,7 | 0,0 | 7,8 | 0,3 | 0,0 | 0,0 | 4,3 | 1,3 | 8,1 | 1,1 |
| Monocots | | | | | | | | | | | | | | | | |
| | Cylindroid | 29 | 1 | 20 | 8 | 26 | 15 | 50 | 7 | 6 | 15 | 4 | 6 | 8 | 20 | 19 |
| | Parallelepiped elongate psilate | 18 | | | | | | | 21 | | | | | 2 | 6 | 4 |
| | Parallelepiped elongate | | 2 | | | 1 | | | | 1 | | | | | 4 | |

| | | | | | | | | | | | | | | | | |
|---|---|---|---|---|---|---|---|---|---|---|---|---|---|---|---|---|
| | facetated | | | | | | | | | | | | | | | |
| | Stomata cells | | 3 | 2 | | 3 | 9 | | 6 | | 3 | | | 1 | 3 | |
| | Silica skeleton long cells psilate | | | | | 14 | 16 | 7 | | 1 | | 10 | | | | 3 |
| | **Total** | 47 | 6 | 22 | 8 | 44 | 40 | 57 | 34 | 8 | 18 | 14 | 6 | 11 | 33 | 26 |
| | % | 10,8 | 11,3 | 13,2 | 7,0 | 21,6 | 13,3 | 19,9 | 11,6 | 2,7 | 9,0 | 8,1 | 2,4 | 7,3 | 13,4 | 4,8 |
| Poaceae | | | | | | | | | | | | | | | | |
| | Bulliform | 12 | | 5 | 3 | 3 | 4 | 3 | 3 | 4 | 8 | 4 | | 4 | 2 | 5 |
| | Long cell dendriform/echinate | | | | 2 | | | | 31 | 1 | | | | 7 | 4 | |
| | Parallelepiped thin psilate | | | 2 | | | | | | | | | | | | |
| | **Total** | 12 | 0 | 7 | 5 | 3 | 4 | 3 | 34 | 5 | 8 | 4 | 0 | 11 | 6 | 5 |
| | % | 2,8 | 0,0 | 4,2 | 4,4 | 1,5 | 1,3 | 1,0 | 11,6 | 1,7 | 4,0 | 2,3 | 0,0 | 7,3 | 2,4 | 0,9 |
| Non-diagnostic, other | | | | | | | | | | | | | | | | |
| | Blocky | 35 | 3 | 16 | 7 | | 13 | 30 | 28 | 27 | 24 | 14 | 21 | 17 | 33 | 34 |
| | Elongate echinate | 9 | 8 | 16 | | 6 | | | | 8 | 3 | 3 | 4 | 11 | | 6 |
| | Elongate sinuous | | | | 7 | 8 | 4 | 3 | | 2 | | 1 | 2 | | 5 | 3 |
| | Ellipsoid psilate/rugose | | | | | 27 | 1 | | 2 | | 3 | 9 | | | | |
| | Globular psilate | 15 | | 11 | 13 | 12 | 16 | 24 | 21 | 45 | 12 | 14 | 9 | 5 | 7 | 19 |
| | Honeycombed plate | | | | | | | 26 | | | | | | | | |
| | Mesophyll | | | | 6 | 2 | 2 | 2 | | | | | | | 1 | |
| | Perforated platelet | | 1 | | | | 1 | | | | | 2 | | | | 2 |
| | Trichome/ Hair cell | 42 | 2 | 9 | 8 | 16 | 23 | 29 | 16 | 9 | 13 | 5 | 16 | 7 | 12 | 24 |
| | Vessels/Tracheids | 9 | | 2 | | 4 | 33 | 24 | 4 | 1 | 4 | 18 | | 1 | | 2 |
| | **Total** | 110 | 14 | 54 | 41 | 75 | 93 | 138 | 71 | 92 | 59 | 66 | 52 | 41 | 58 | 90 |
| | % | 25,3 | 26,4 | 32,3 | 36,0 | 36,8 | 30,9 | 48,3 | 24,1 | 30,7 | 29,5 | 38,4 | 20,5 | 27,2 | 23,6 | 16,6 |
| | | | | | | | | | | | | | | | | |
| | **TOTAL Phytolith count** | **435** | **53** | **167** | **114** | **204** | **301** | **286** | **294** | **300** | **200** | **172** | **254** | **151** | **246** | **541** |
| | | | | | | | | | | | | | | | | |
| Others | Unclassified | 82 | 8 | 26 | 27 | 23 | 29 | 19 | 43 | 26 | 24 | 24 | 18 | 26 | 34 | 41 |
| | Diatoms | | | | | 2 | 14 | | | 2 | 5 | 5 | | | | 6 |
| | Charred fragments | | | | 13 | 10 | | 1 | | | | | 20 | | | 8 |

**Table B:** *The total counts and diagnostic counts of phytoliths in EFT sediment samples*

| Sample | Total Phytolith Count | Total Diagnostic Phytolith Count |
|---|---|---|
| EFT1.1 | 435 | 340 |
| EFT1.3 | 167 | 124 |
| EFT1.4* | 114 | 86 |
| EFT2.1 | 204 | 168 |
| EFT2.2 | 301 | 225 |
| EFT2.3* | 286 | 172 |
| EFT3.1 | 294 | 246 |
| EFT3.2* | 300 | 264 |
| EFT4.1 | 200 | 156 |
| EFT4.2 | 172 | 129 |
| EFT4.4 | 254 | 211 |
| EFT4.8 | 151 | 115 |
| EFT4.9 | 246 | 195 |
| EFT4.10* | 541 | 470 |

**Table C:** *Percentages of phytoliths (calculated out of total phytolith count) in each phytolith category for EFT samples.*

| | EFT 1.3 | EFT 1.1 | EFT 1.4* | EFT 2.2 | EFT 2.1 | EFT 2.3* | EFT 3.1 | EFT 3.2* | EFT 4.2 | EFT 4.9 | EFT 4.8 | EFT 4.4 | EFT 4.1 | EFT 4.10* |
|---|---|---|---|---|---|---|---|---|---|---|---|---|---|---|
| Woody Dicots | 30,5 | 31 | 24,6 | 6,6 | 18,6 | 12,2 | 26,9 | 19,7 | 15,1 | 20,7 | 17,9 | 27,2 | 18 | 16,3 |
| GSSC | 18,6 | 27,6 | 28,1 | 46,2 | 21,1 | 18,5 | 18 | 45 | 36 | 31,7 | 39,1 | 45,7 | 39,5 | 60,3 |
| Arecaceae | 0 | 0,7 | 0 | 1,7 | 0,5 | 0 | 0,7 | 0 | 0 | 0 | 0 | 4,3 | 0 | 0 |
| Cyperaceae | 1,2 | 1,8 | 0 | 0 | 0 | 0 | 7,1 | 0,3 | 0 | 8,1 | 1,3 | 0 | 0 | 1,1 |
| Monocots | 13,2 | 10,8 | 7 | 13,3 | 21,6 | 19,9 | 11,6 | 2,7 | 8,1 | 13,4 | 7,3 | 2,4 | 9 | 4,8 |
| Poaceae | 4,2 | 2,8 | 4,4 | 1,3 | 1,5 | 1 | 11,6 | 1,7 | 2,3 | 2,4 | 7,3 | 0 | 4 | 0,9 |
| Non-diagnostic, Other | 32,3 | 25,3 | 36 | 30,9 | 36,8 | 48,3 | 24,1 | 30,7 | 38,4 | 23,6 | 27,2 | 20,5 | 29,5 | 16,6 |

**Table D:** *Percentages of phytoliths (calculated out of total phytolith count) in each phytolith category for EFT samples.*
*Grass category includes GSSC and other grass phytoliths.*

| | EFT 1.3 | EFT 1.1 | EFT 1.4* | EFT 2.2 | EFT 2.1 | EFT 2.3* | EFT 3.1 | EFT 3.2* | EFT 4.2 | EFT 4.9 | EFT 4.8 | EFT 4.4 | EFT 4.1 | EFT 4.10* |
|---|---|---|---|---|---|---|---|---|---|---|---|---|---|---|
| Woody Dicots | 30,5 | 31 | 24,6 | 6,6 | 18,6 | 12,2 | 26,9 | 19,7 | 15,1 | 20,7 | 17,9 | 27,2 | 18 | 16,3 |
| Grass | 22,8 | 30,4 | 32,5 | 47,5 | 22,6 | 19,5 | 29,6 | 46,7 | 38,3 | 34,1 | 46,4 | 45,7 | 43,5 | 61,2 |
| Arecaceae | 0 | 0,7 | 0 | 1,7 | 0,5 | 0 | 0,7 | 0 | 0 | 0 | 0 | 4,3 | 0 | 0 |
| Cyperaceae | 1,2 | 1,8 | 0 | 0 | 0 | 0 | 7,1 | 0,3 | 0 | 8,1 | 1,3 | 0 | 0 | 1,1 |
| Monocots | 13,2 | 10,8 | 7 | 13,3 | 21,6 | 19,9 | 11,6 | 2,7 | 8,1 | 13,4 | 7,3 | 2,4 | 9 | 4,8 |
| Non-diagnostic, Other | 32,3 | 25,3 | 36 | 30,9 | 36,8 | 48,3 | 24,1 | 30,7 | 38,4 | 23,6 | 27,2 | 20,5 | 29,5 | 16,6 |

**Table E:** *Percentages of monocot phytoliths, dicotyledonous phytoliths and the 'unclassified' for EFT samples.*

| | EFT 1.3 | EFT 1.1 | EFT 1.4* | EFT 2.2 | EFT 2.1 | EFT 2.3* | EFT 3.1 | EFT 3.2* | EFT 4.2 | EFT 4.9 | EFT 4.8 | EFT 4.4 | EFT 4.1 | EFT 4.10* |
|---|---|---|---|---|---|---|---|---|---|---|---|---|---|---|
| Dicot | 37,1 | 34,5 | 36 | 12,3 | 37,7 | 20,6 | 34,7 | 34,7 | 28,5 | 23,6 | 21,2 | 30,7 | 25,5 | 19,8 |
| Monocot | 37,2 | 43,7 | 39,5 | 62,5 | 44,7 | 39,4 | 49 | 49,7 | 46,4 | 55,6 | 55 | 52,4 | 52,5 | 67,1 |
| Unknown | 25,7 | 21,8 | 24,6 | 25,2 | 17,6 | 39,9 | 16,3 | 15,7 | 25 | 20,7 | 23,8 | 16,9 | 22 | 13,1 |

**Table F:** *Percentages of GSSC phytoliths (calculated out of total phytolith count) for EFT samples.*

| Phytolith morphotype | | | | | | | | | | | |
|---|---|---|---|---|---|---|---|---|---|---|---|
| Sample no. | Lobate Class | | | | | Saddle class | | Trapeziform class | | | |
| | Bilobate Var 1 | Bilobate Var 2 | Bilobate Var 3 | Polylobate | Cross | Saddle Var 1 | Saddle Var 2 | Trapezoid | Rondel | Oblong | Reniform |
| EFT1.3 | 0 | 1,2 | 0 | 0 | 0 | 3 | 0 | 11,4 | 2,4 | 0,6 | 0 |
| EFT1.1 | 0,2 | 1,6 | 0 | 0 | 1,4 | 1,6 | 0,2 | 12 | 7,6 | 0,5 | 2,5 |
| EFT1.4* | 0 | 0,9 | 0 | 0 | 0 | 1,8 | 0 | 16,7 | 2,6 | 6,1 | 0 |
| EFT2.2 | 0 | 8,3 | 0 | 1 | 0 | 0,7 | 0,7 | 15,6 | 11,3 | 8,6 | 0 |
| EFT2.1 | 0 | 0,5 | 0 | 0 | 0 | 1 | 0 | 13,2 | 3,4 | 2,9 | 0 |
| EFT2.3* | 0 | 0,7 | 0 | 0 | 1,7 | 0 | 0 | 8,4 | 7,7 | 0 | 0 |
| EFT3.1 | 0 | 3,7 | 0 | 0 | 0 | 1,4 | 0 | 4,4 | 7,5 | 1 | 0 |
| EFT3.2* | 0 | 8 | 0 | 0 | 0,7 | 7,7 | 0 | 8,3 | 7,3 | 11 | 2 |
| EFT4.2 | 0 | 0,6 | 0 | 0 | 0 | 0,6 | 1,7 | 15,7 | 11 | 6,4 | 0 |
| EFT4.9 | 0 | 4,9 | 0,8 | 0,4 | 0,8 | 2,4 | 4,1 | 11,8 | 0,4 | 4,1 | 2 |
| EFT4.8 | 0 | 0 | 0 | 0,7 | 0 | 13,9 | 4 | 12,6 | 2 | 6 | 0 |
| EFT4.4 | 0 | 5,1 | 0 | 0,8 | 2,8 | 2 | 2 | 13,4 | 10,6 | 7,1 | 2 |
| EFT4.1 | 0 | 3 | 0 | 0 | 0 | 2,5 | 1 | 21,5 | 5,5 | 4 | 2 |
| EFT4.10* | 0 | 11,8 | 0 | 0,6 | 2,2 | 13,5 | 2,2 | 7,8 | 12,4 | 6,8 | 3 |

**Table G:** *Percentages of associated with grass subfamilies for EFT samples.*

| | EFT 1.3 | EFT 1.1 | EFT 1.4* | EFT 2.2 | EFT 2.1 | EFT 2.3* | EFT 3.1 | EFT 3.2* | EFT 4.2 | EFT 4.9 | EFT 4.8 | EFT 4.4 | EFT 4.1 | EFT 4.10* |
|---|---|---|---|---|---|---|---|---|---|---|---|---|---|---|
| **SUBFAMILY** | | | | | | | | | | | | | | |
| Chloridoideae | 3 | 1,8 | 1,8 | 1,4 | 1 | 0 | 1,4 | 7,7 | 2,3 | 6,5 | 17,9 | 4 | 3,5 | 15,7 |
| Danthionoideae | 11,4 | 12 | | 15,6 | 13,2 | 8,4 | 11,9 | 0 | 15,7 | 13,8 | 12,6 | 18,1 | 14,5 | 22,32 |
| Ehrhartoideae | | 10,1 | | 11,3 | 0 | 8,4 | 0 | 9,3 | 11 | 0 | 0 | 0 | 5,5 | 7,86 |
| Panicoideae | 1,2 | 3,2 | 0,9 | 7,6 | 0,5 | 1,7 | 0,7 | 8,7 | 0,6 | 4,45 | 0,7 | 3,6 | 3 | 7,52 |
| Pooideae | 3 | 0,5 | 25,4 | 10,3 | 6,3 | 0 | 1 | 27,3 | 6,4 | 6,95 | 8 | 20,1 | 13 | 6,8 |

Duinefontein:

**Table H:** Raw data for DFT samples

| | Sample IDs: | DFT1.1 | DFT2.1 | DFT2.2 | DFT2.3 | DFT2.5 | DFT2.6 | DFT2.7 |
|---|---|---|---|---|---|---|---|---|
| Group of plants | Morphotype Category | | | | | | | |
| Woody Dicotyledons | | | | | | | | |
| | Blocky faceted | | | 14 | | | | |
| | Blocky polyhedron | 2 | | | 21 | 2 | 6 | 2 |
| | Globular decorated | 6 | 12 | 64 | 23 | 14 | 6 | 27 |
| | Globular small faceted | | | | 14 | 4 | 2 | 4 |
| | Parallelepiped blocky | | | | | 2 | | 14 |
| | Sclerenchyma | | 1 | | | | | |
| | **Total** | 8 | 13 | 78 | 58 | 22 | 14 | 47 |
| | % | 6,5 | 6,5 | 26,0 | 12,1 | 24,4 | 20,3 | 10,2 |
| Poaceae, GSSC | | | | | | | | |
| | Bilobate V2 | | 3 | 1 | 7 | | | 19 |
| | Cross | | | | 4 | | | 4 |
| | Oblong | 5 | 22 | 14 | 17 | 7 | | 67 |
| | Reniform | | | | 3 | | | 16 |
| | Rondel | 8 | | 6 | 34 | 13 | 2 | 106 |
| | Saddle 1 | | 12 | 1 | 22 | 3 | | 18 |
| | Saddle 2 | | | | 6 | | | 12 |
| | Trapezoid | 11 | 25 | 19 | 36 | 23 | 16 | 74 |
| | **Total** | 24 | 62 | 41 | 129 | 46 | 18 | 316 |
| | % | 19,4 | 31,0 | 13,7 | 27,0 | 51,1 | 26,1 | 68,3 |
| | | | | | | | | |
| Family specific | | | | | | | | |
| | Opaque perforated platelet **(Asteraceae)** | | | | 1 | | | 6 |
| | **Total** | | | | 1 | | | 6 |
| | % | 0 | 0 | 0 | 0,2 | 0 | 0 | 1,3 |
| Monocots | | | | | | | | |
| | Cylindroid | 10 | 26 | 26 | 35 | 5 | 1 | 27 |
| | Parallelepiped elongate psilate | | | | 10 | | | |
| | Parallelepiped elongate faceted | | | | 1 | | | |
| | Stomata cells | 6 | | 14 | 17 | | | |
| | Silica skeleton long cells psilate | 4 | | | 39 | | 4 | 4 |
| | **Total** | 20 | 26 | 40 | 102 | 5 | 5 | 31 |
| | % | 16,1 | 13,0 | 13,3 | 21,3 | 5,6 | 7,2 | 6,7 |
| Poaceae | | | | | | | | |
| | Bulliform | 2 | 21 | 17 | 12 | | 4 | |
| | Long cell dendriform/echina | | 8 | 2 | 9 | | | 5 |

| | | | | | | | | |
|---|---|---|---|---|---|---|---|---|
| | te | | | | | | | |
| | **Total** | 2 | 29 | 19 | 21 | 0 | 4 | 5 |
| | **%** | 1,6 | 14,5 | 6,3 | 4,4 | 0,0 | 5,8 | 1,1 |
| Non-diagnostic, other | | | | | | | | |
| | Blocky | 15 | | 42 | 22 | 9 | 10 | 17 |
| | Elongate sinuous | 5 | 20 | | 6 | | | 4 |
| | Ellipsoid psilate/rugose | | | | 15 | | | |
| | Globular psilate | 6 | 33 | 39 | 25 | 3 | 8 | 6 |
| | Mesophyll | 14 | | 9 | 18 | | | |
| | Trichome | 15 | 10 | 32 | 52 | 5 | 10 | 3 |
| | Vessels/tracheids | 15 | 7 | | 29 | | | 28 |
| | **Total** | 70 | 70 | 122 | 167 | 17 | 28 | 58 |
| | % | 56,5 | 35,0 | 40,7 | 34,9 | 18,9 | 40,6 | 12,5 |
| | | | | | | | | |
| | **TOTAL Phytolith count** | **124** | **200** | **300** | **478** | **90** | **69** | **463** |
| | | | | | | | | |
| Others | Unclassified | 18 | 19 | 25 | 40 | 17 | 2 | 39 |
| | Charred fragments | 1 | | 5 | 14 | | | |
| | Diatoms | | | | | | | 80 |

**Table I:** *The total counts and diagnostic counts of phytoliths in DFT sediment samples*

| Sample | Total Phytolith Count | Total Diagnostic Phytolith Count |
|---|---|---|
| DF1.1 | 124 | 60 |
| DFT2.1 | 200 | 163 |
| DFT2.2 | 300 | 217 |
| DFT2.3 | 478 | 351 |
| DFT2.5 | 90 | 76 |
| DFT2.7* | 463 | 411 |

**Table J:** *Percentages of phytoliths (calculated out of total phytolith count) in each phytolith category for DFT samples.*

| | DFT1.1 | DFT2.1 | DFT2.2 | DFT2.3 | DFT2.5 | DFT2.7* |
|---|---|---|---|---|---|---|
| Woody Dicots | 6.5 | 6.5 | 26.0 | 12.1 | 24.4 | 10.2 |
| GSSC | 19.4 | 31.0 | 13.7 | 27 | 51.1 | 68.3 |
| Family Specific | 0.0 | 0.0 | 0.0 | 0.2 | 0.0 | 1.3 |
| Monocots | 16.1 | 13.0 | 13.3 | 21.3 | 5.6 | 6.7 |
| Poaceae | 1.6 | 14.5 | 6.3 | 4.4 | 0.0 | 1.1 |
| Non-diagnostic, Other | 56.5 | 35.0 | 40.7 | 34.9 | 18.9 | 12.5 |

**Table K:** *Percentages of phytoliths (calculated out of total phytolith count) in each phytolith category for DFT samples.*
*Grass category includes GSSC and other grass phytoliths.*

| | DFT1.1 | DFT2.1 | DFT2.2 | DFT2.3 | DFT2.5 | DFT2.7* |
|---|---|---|---|---|---|---|
| Woody Dicots | 6.5 | 6.5 | 26.0 | 12.1 | 24.4 | 10.2 |
| Grass | 21 | 45,5 | 20 | 31,4 | 51,1 | 69,4 |
| **Asteraceae** | | | | 0,2 | | 1,3 |
| Monocots | 16,1 | 13 | 13,3 | 21,3 | 5,6 | 6,7 |
| Non-diagnostic, Other | 56.5 | 35.0 | 40.7 | 34.9 | 18.9 | 12.5 |

**Table L:** *Percentages of monocot phytoliths, dicotyledonous phytoliths and the 'unclassified' for DFT samples.*

| | DFT1.1 | DFT2.1 | DFT2.2 | DFT2.3 | DFT2.5 | DFT2.7* |
|---|---|---|---|---|---|---|
| Dicot | 6.5 | 6.5 | 26.0 | 12.1 | 24.4 | 10.2 |
| Monocot | 37,1 | 58,5 | 33,3 | 52,9 | 56,7 | 77,4 |
| Unknown | 56.5 | 35.0 | 40.7 | 34.9 | 18.9 | 12.5 |

**Table M:** *Percentages of GSSC phytoliths (calculated out of total phytolith count) for DFT samples.*

| Phytolith morphotype | | | | | | | | | | |
|---|---|---|---|---|---|---|---|---|---|---|
| Sample no. | Lobate Class | | | | Saddle class | | Trapeziform class | | | |
| | Bilobate Var 1 | Bilobate Var 2 | Bilobate Var 3 | Cross | Saddle Var 1 | Saddle Var 2 | Trapezoid | Rondel | Oblong | Reniform |
| DF1.1 | 0.0 | 0.0 | 0.0 | 0.0 | 0.0 | 0.0 | 8.9 | 6.5 | 4.0 | 0.0 |
| DFT2.1 | 0.0 | 1.5 | 0.0 | 0.0 | 6.0 | 0.0 | 12.5 | 0.0 | 11.0 | 0.0 |
| DFT2.2 | 0.0 | 0.3 | 0.0 | 0.0 | 0.3 | 0.0 | 6.3 | 2.0 | 4.7 | 0.0 |
| DFT2.3 | 0.0 | 1.5 | 0.0 | 0.8 | 4.6 | 1.3 | 7.5 | 7.1 | 3.6 | 0.6 |
| DFT2.5 | 0.0 | 0.0 | 0.0 | 0.0 | 3.3 | 0.0 | 25.6 | 14.4 | 7.8 | 0.0 |
| DFT2.6 | 0.0 | 0.0 | 0.0 | 0.0 | 0.0 | 0.0 | 23.2 | 2.9 | 0.0 | 0.0 |
| DFT2.7 (Modern soil sample) | 0.0 | 4.1 | 0.0 | 0.9 | 3.9 | 2.6 | 16.0 | 22.9 | 14.5 | 3.5 |

**Table N:** *Percentages of associated with grass subfamilies for DFT samples.*

| | DFT1.1 | DFT2.1 | DFT2.2 | DFT2.3 | DFT2.5 | DFT2.7* |
|---|---|---|---|---|---|---|
| **SUBFAMILY** | | | | | | |
| Chloridoideae | | 6 | 0,3 | 5,9 | 3,3 | 6,5 |
| Danthionoideae | 8,9 | 12,5 | 6,3 | 8,1 | 25,6 | 16 |
| Ehrhartoideae | | | | 7,1 | 14,4 | 26,4 |
| Panicoideae | | 1,5 | 0,3 | 1,88 | | 2,4 |
| Pooideae | 10,5 | 11 | 6,7 | 4,02 | 7,8 | 17,1 |